DESIGN OF A ROBOTIC MANIPULATOR FOR AUTOMATIC APPLICATION OF MILKING CUPS

by

James White, B.Eng

A thesis submitted in fulfilment of the
requirements for the degree of

Master of Engineering

Dublin City University

Under the supervision of Dr. Brian Corcoran, PhD

Second supervisor: Dr. Harry Esmonde, PhD

School of Mechanical and Manufacturing Engineering

Teagasc advisor: Dr. Eddie O'Callaghan, PhD

Dairy Production Research Centre, Teagasc, Fermoy, Co. Cork

2006

I hereby certify that this material, which I now submit for assessment on the programme of study leading to the award of Master of Engineering is entirely my own work and has not been taken from the work of others save and to the extent that such work has been cited and acknowledged within the text of my work.

Signed: 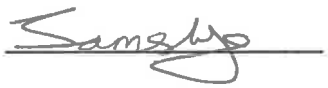

ID No.: 50538507

Date: 25th October 2006

DUBLIN CITY UNIVERSITY

ABSTRACT

DESIGN OF A ROBOTIC
MANIPULATOR FOR AUTOMATIC
APPLICATION OF MILKING CUPS

by James White

The application of milking cups to cow teats has been identified as a significant component of net manual labour on the commercial dairy farm. Several automatic milking systems (AMS) are available commercially, however such commercial AMS have low capacity (typically 7.5 cows/unit/hr) and speed of teat detection and milking cup application is relatively low. Attempts to introduce commercial AMS into pasture-grazing systems have been unsuccessful as maximising milking efficiency in pasture-grazed herds involves optimizing throughput of cows during the milking session. This design project investigated the use of a commercial robot arm for high-speed milking cup application. Operating requirements and workspace parameters were determined from field observation of cows in a milking parlour. An end-effector capable of handling four milking cups simultaneously was developed and interfaced with a 6-axis robot arm to form a robotic milking cup application mechanism. The end-effector profile is sufficiently compact to allow access between the rear legs of the cow while enabling full access to all four teats for application of milking cups. A control system was designed and implemented for the applicator and basic testing was performed to validate operation. Test results indicate that small changes in teat location (<20mm) may be tracked at a position update rate of approximately 200 ms.

ACKNOWLEDGMENTS

The author gratefully acknowledges the assistance and support of Dr. Brian Corcoran in his role as supervisor for this research. The author also wishes to thank Dr. Eddie O'Callaghan (Teagasc Moorepark Dairy Production Centre) and Dr. Harry Esmonde (Dublin City University) for their support, and Teagasc and the Walsh Fellowship programme for providing sponsorship and funding. The professionalism and excellent technical support of the DCU technical staff was much appreciated, particularly that of Mr. Eoin Tuohy and Mr. Liam Domican.

Finally thanks are due to my wife, Julie-Ann, for her patience and encouragement during the preparation of this thesis.

TABLE OF CONTENTS

LIST OF FIGURES

LIST OF TABLES

DESIGN OF A ROBOTIC MANIPULATOR FOR AUTOMATIC APPLICATION OF MILKING CUPS

Dublin City University
Ollscoil Chathair Bhaile Átha Cliath

Chapter 1

INTRODUCTION AND LITERATURE SURVEY

1.1 Background: Challenges in modern Irish dairy farming

Dairy farming is an important section of the Irish agricultural industry, providing rural employment and contributing significantly to export revenue[1]. In 2005, the combined output of milk products in Ireland was 5.33 million tonnes, of which 80% was exported. Milk products accounted for 25% of total Irish agricultural export value in 2004 and represented 4.1% of total European Union milk production in 2005. For the 2005 period, turnover for Irish dairy production was over €1.8 billion, with 23,800 dairy farmers directly employed in milk production and many more employed in related processing and service industries[2][3].

Despite impressive performance figures, the dairy farming industry faces increasing challenges. Dairy farming is classified as labour intensive[4]; the milking process may be classified as light to moderately heavy labour, and feeding and cleaning as moderate to heavy labour[4][5]. The working day on a dairy farm is usually long, typically spanning ten to twelve hours, making farm working conditions less attractive to workers. In an Irish context, the economic successes of the last decade have resulted in rising labour costs and a lower availability of labour in rural areas as the workforce becomes more mobile and wages and conditions in other industrial sectors become more attractive. This presents problems for farmers who wish to increase scale of operation, as labour is more difficult to acquire and the increased cost of such labour may reduce any profits from increase of scale. Changes in environmental regulation have increased the cost of farm management, in particular with regard to waste management. Such costs cannot be offset by increasing milk prices as milk prices are regulated and under current EU policy prices may fall over the next decade[6][7]. Added to these problems is the accession of ten new EU member states, some of whom enjoy lower labour overheads and may eventually compete directly with Irish dairy producers. The Irish dairy farmer thus faces the challenge of maintaining competitiveness in an environment where milk prices are decreasing and production costs are increasing.

1.2 The Milking process and labour

The milking process may be defined as the herding of animals before and after milking, washing and disinfecting of teats, attachment of milking cups, extraction of milk and removal of milking cups[4]. A comprehensive labour study on Irish dairy farms has shown that 33% of net labour on the farm was directly associated with the milking process[4]. Fig. 1 illustrates the breakdown of net labour over a twelve month period. Automated extraction and collection of milk is a mature technology, and milking machines are universally used on dairy farms. The remaining sections of the milking process consist of three general tasks: cow traffic routing, teat preparation (cleaning), and milking equipment attachment/removal. Of the net labour associated with these tasks, 64% is carried out between teat cup application and removal[4][8].

With a large proportion of dairy farm labour tied up in the milking process, much effort has been expended in researching and developing labour-reducing solutions in this area. Successful labour reduction can increase competitiveness through increased output per man-hour and the opportunity for increased scale of operations[9].

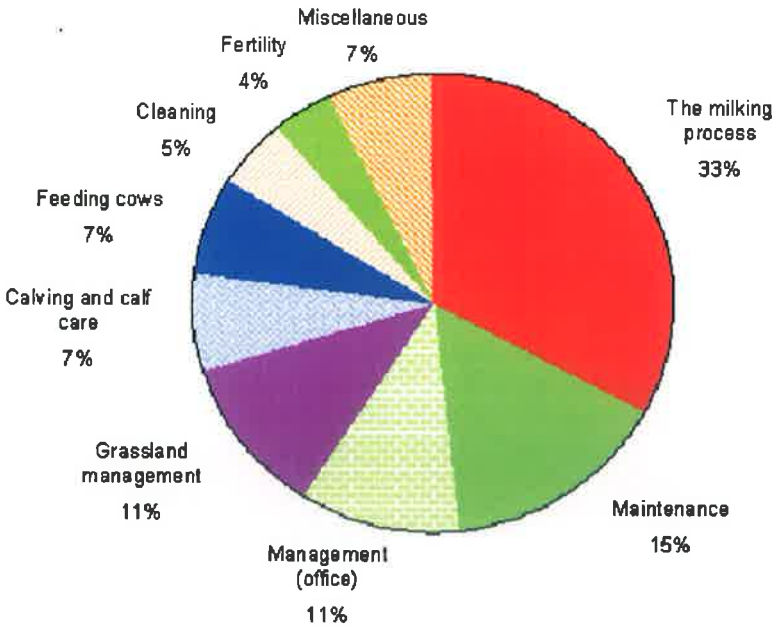

Figure 1. Breakdown of total net labour input associated with dairying over the 12 month period (Courtesy of Teagasc)

1.3 Developments in milking process automation

In the manufacturing industry, reductions in manual labour are often achieved through automation. Similarly, automation techniques have been developed and introduced to reduce labour in the milking process.

1.3.1 Milking machines

At the turn of the 20th century, milking was almost entirely a manual process. During the 19th century many methods for extracting milk were investigated, and several were patented and marketed with varying levels of success. Some systems attempted simple catheterisation of the udder, forcing the teat orifice open and allowing milk to flow freely. Others applied a vacuum to the teats to extract milk. Both systems had disadvantages: catheterisation provided low flow rates and increased the risk of udder infection, while constant vacuum systems caused blood to pool in the teats, damaging udder tissue and causing discomfort to the cow. In the late 1890s a successful milking machine was developed using an intermittent vacuum system to extract milk. The intermittent or pulsating vacuum method interrupted the vacuum at regular intervals to allow the teat surface to return to atmospheric pressure, overcoming the problem of blood pooling in the teat by allowing proper blood circulation. Additionally, the intermittent action was similar to that that of a suckling calf, with the result that the pulsating action assisted in stimulating milk let down by the cow. The pulsating vacuum system is now universally used in modern milking machines [10].

The general design of a teat-cup for use in a pulsating vacuum system is shown is shown in Fig. 2. The cup consists of a rigid cup, or shell, into which a hollow, flexible rubber liner is inserted. The liner separates the cup volume into two chambers: a tapered, flexible-walled cylindrical chamber into which the teat is inserted and an outer annular chamber between the rigid shell and the liner. During the release phase (A), a constant partial vacuum (typically 30-45kPa) is applied to both chambers. There is no pressure differential between the two chambers, so the vacuum acts directly on the teat and milk is extracted into the milk tube. During the 'squeeze' phase (B), the vacuum level in the outer annular chamber is returned to atmospheric pressure, resulting in a differential pressure on the liner. The liner collapses around the teat, cutting off the vacuum from the milk tube and returning

the teat to atmospheric pressure. During both phases the teat is gripped either by direct vacuum or by the collapsed liner, preventing detachment of the cup during milking [11].

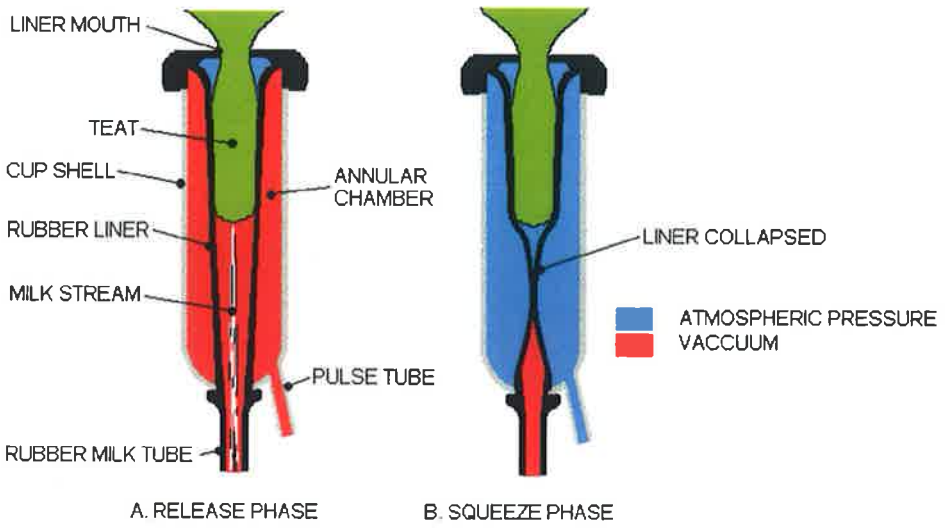

Figure 2. Principle of teat-cup action

A group of four milking cups is termed a cluster (Fig. 3.). The milk and vacuum tubes from each milking cup are attached to a small reservoir, the claw, that provides connection to a common milk and vacuum line and a pulsating vacuum line. Fig. 3 also shows an automatic cluster removal line, which removes the cups when milk flow rate has fallen below a preset level and returns the cluster to the milking machine in preparation for the next cow. Automatic cluster removal eliminates another labour component of the milking process, and improves hygiene by keeping the cluster from contact with the parlour floor.

The task of cleaning teats can be automated to some extent by spraying with disinfectant, although there are some reservations over the efficacy of this method [12].

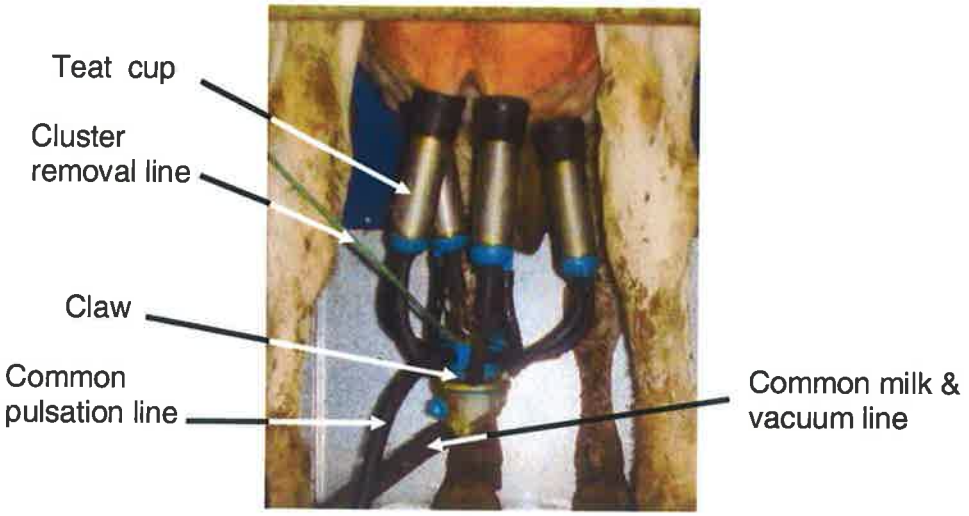

Figure 3. Cluster and claw attached to teats

Early milking systems were operated with manual vacuum pumps; however the growing availability of electric power and the internal combustion engine allowed the introduction of powered vacuum pumps. Milking machine development in the 20th century was slow, but with gradual improvements in reliability and cost, milking machines were in widespread use by the early 1970s.

1.3.2 Milking parlours

Automation of milk extraction significantly reduced labour involved in the milking process, allowing the dairy farmer to increase the scale of operations by installing more milking machines and increasing herd size. With increased operational scales, a need arose for investigation of milking parlour design and workflow to optimise handling of larger herds. A milking parlour is an indoor area in which milking machines and milk collection equipment are housed and in which cows are positioned for milking. The simplest milking parlour is a series of parallel stalls in a barn in which the cows are held. The stall prevents the cow from straying, and allows an operator to access the teats from the rear or side. The stall may be designed with features such as a feed bin to provide concentrated feedstuffs or dietary supplements to the animal and safety features such as an anti-kick rail to protect the operator. With larger herd sizes and the increased capital cost of a multiple milking machine installation, better utilisation of space and equipment was

required. Many variations of parlour design have been investigated [13][14] focusing on optimising milking machine utilisation, improving cow traffic flow and reducing operator labour. The two main parlour styles with potential for high capacity are herringbone and rotary parlours.

1.3.2.1 Herringbone parlours

The herringbone parlour, shown in Fig. 4A, is one of the most common milking parlour arrangements. In the herringbone parlour, the stalls are divided into two parallel rows, separated by a low-level trench or 'pit' which provides a more ergonomic working height for the operator. The cows enter each side of the parlour in single file, and are turned to face outwards at an angle to the pit until the parlour is full. The operator works in the pit, moving from animal to animal to inspect, clean and disinfect teats and attach milking cups. In modern parlours it is usual to have one milking machine per stall, however in "swing-over" parlours a single milking machine serves two cows on opposite sides of the pit. Swing over parlours reduce the number of milking machines required, and are reasonably efficient as the operator can clean and prepare one cow while the other is milked. Herringbone capacity is variable depending on user requirements, however typical sizes range between 12 and 30 stalls. The herringbone parlour is an efficient batch production method, but suffers from the disadvantage that a single interruption (such as a slow-milking cow or dropped cluster) results in a delay for the entire batch [13]. Several designs aimed at reducing batch delays are in use[13], however the normal capacity for a one-man operated herringbone parlour is 50-75 cows/h, with practical limits of 120 cows/h [8][14].

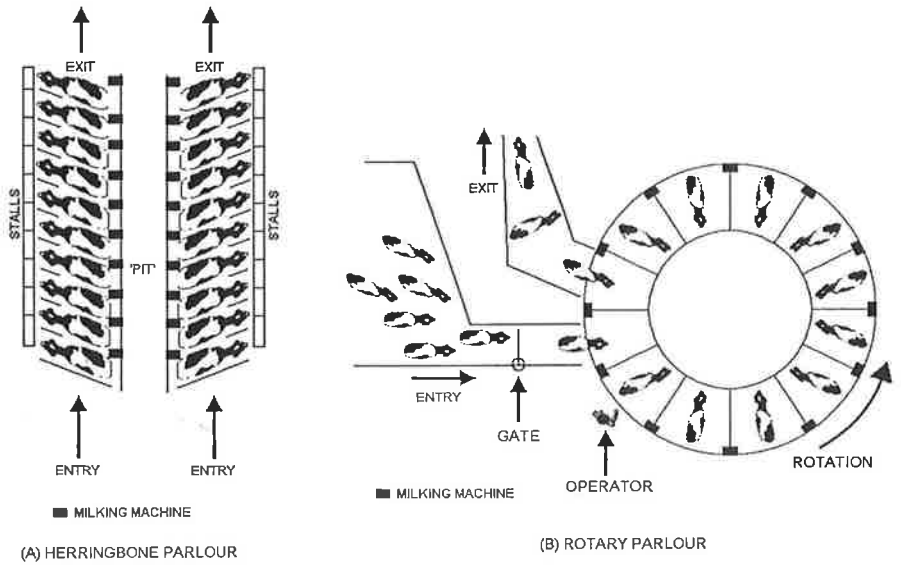

Figure 4. High capacity milking parlour layouts: Herringbone (A) and Rotary (B)

1.3.2.2 Rotary parlours

An alternative to herringbone-style batch milking systems is the rotary milking parlour [15]. Fig. 4B illustrates the layout of a typical abreast (side-by-side stalls) rotary parlour. The parlour comprises a rotating carousel, on which the stalls and milking equipment are mounted. The carousel rotates slowly and in increments of one stall, allowing cows to walk onto the carousel. The cow is rotated past an operator who attaches the milking cluster by reaching between the rear legs of the cow. Milking is performed as the carousel rotates, and when milking is complete the cluster is automatically removed and the cow exits the carousel at the exit station. The number of stalls on the carousel is variable, ranging from 10 to 80 depending on herd size. On the standard abreast rotary parlour (Fig. 4B), the cow must exit by reversing off the platform. Cows quickly become accustomed to reversing, however alternative rotary designs present the cow sideways (tandem rotary) or at an angle (herringbone rotary) to the operator, allowing forward exit but with a less efficient utilisation of space on the carousel [16]. Automated cow traffic control systems are widely available for controlling entry and exit traffic in the parlour. A control panel next to the milking cup application position allows control of automated gates and the rotary carousel, allowing a single operator to perform and supervise the entire milking process, including application of milking cups. Typical capacity for a single-

operator rotary parlour is 120 cows/h, however this can rise to 300 cows/h in a well-managed system[8].

Sequential processing methodology used in the rotary parlour provides excellent utilisation of labour, as a single operator can perform the entire milking process from a single location. Single animal delays have minimal impact on overall milking time as single-cow bottlenecks (due to slow-milking cows or dropped clusters) may be avoided by allowing a cow to remain on the carousel for more than one rotation [8]. Problems with mechanical reliability were experienced with rotary parlours in the 1960s and 1970s[9][13], but these have been resolved through design improvement and rotary parlours are available from many major milking equipment manufacturers[9]. The main disadvantage of the rotary parlour is the increased capital and maintenance costs associated with more complex design and automation; however these extra costs may be offset through labour-saving and increased capacity. Rotary parlours provide significant reduction in milking time for large herds when compared with high-capacity herringbone parlours: a large dairy enterprise in the UK with a herd of 800 cows reported a reduction in milking time from 10 hours per day with a herringbone parlour to 2 hours per day with an 80-stall rotary parlour, with no additional labour input[17].

1.3.3 Robotics application in milking systems

Automation of milking cup application would upgrade semi-automated milking to a fully automated process. Motivation for developing a full automatic milking system (AMS) comes from two sources: elimination of a repetitive, laborious task with associated health risks [18], and provision for increasing parlour throughput without increasing labour input. It would seem that the application of robotics techniques would be appropriate to this task, but automatic attachment of milking cups is a complex problem, requiring a robust and accurate teat position sensor and a dextrous manipulator to work beneath the cow. Natural variation between animals in udder size, shape and colour causes difficulty in consistently sensing teats[19]. This sensing issue, along with the limited application time (less than 20s [8]) for cup application has been the primary obstacle to automated milking cup application in high-capacity parlours, with the result that no research has been reported in the

field. However, robotic techniques have been applied successfully to the milking process in an alternative milking system: voluntary milking.

1.3.3.1 The Voluntary Milking System

To maintain milk yield during the lactation period, cows must be milked at consistent intervals, usually twice daily and with maximum time spacing between milkings. In fact, consistency of milking intervals is so important that all activities must be scheduled around the milking process on the dairy farm. Such a milking routine imposes restrictions on time management and personal life of an individual farmer, as the farmer is committed to milking in the early morning and in the evening for seven days a week regardless of personal health, family responsibilities or social schedule. This time restriction is exacerbated for lone farmers and farm families if extra labour cannot easily or economically be obtained, and is a factor in the decline in small-scale dairy farming. Since the 1970s, much research effort has been expended in investigating methods to alleviate time management constraints in conventional dairy farming [21], culminating in the development of the automated voluntary milking system (VMS).

Voluntary milking allows the cow to decide its own milking time and interval, rather than being milked as part of a group at set milking times. VMS requires complete automation of the milking process, as the cow may elect to be milked at any time during a 24 hour period [20]. A typical VMS layout is shown in Fig. 5. The milking unit (examined in more detail in Section 1.6.1) comprises a milking machine, a teat position sensor, a robotic arm for automatic teat-cup application and removal and a gate system for controlling cow traffic. The cows are permanently housed in a barn, and spend most of their time resting or feeding in the loose-stall area.

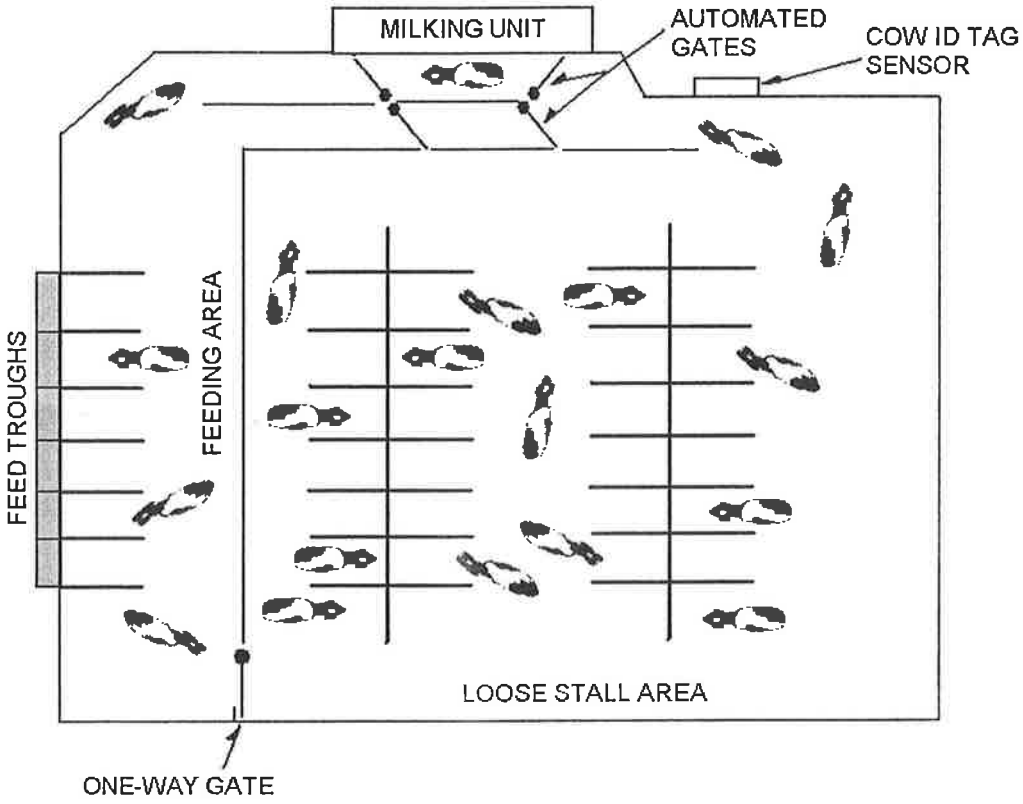

Figure 5. General layout of a VMS barn

When the cow elects to attend the milking unit, due to conditioned habit or udder fullness, a cow ID sensor reads an identification tag on the cow and passes the cow ID to the control system. If the cow has been milked too recently, the automatic gate system routes the cow past the unit. If the cow may be milked, the cow is routed into the milking unit, where automatic teat cleaning, milking cup application and milking takes place. As an incentive to attend the milking unit, concentrated feedstuffs may be fed to the cow in the milking unit, and the barn may be arranged such that access to the main feeding area can only be obtained by passing the milking unit.

The innovative core of the VMS system is the robotic manipulator in the milking unit. This robotic arm automates the tasks of teat cleaning and milking attachment and removes the final elements of manual labour from the milking process. Careful design of the robot arm and associated sensors and controls allows robust unsupervised performance, such that the farmer is only required to attend the cows for condition inspection and when a cow has not attended for milking.

Typical capacity for a VMS is 60-70 cows per milking unit. VMS typically achieves milking frequencies between 2 and 3 times per day [29], so a single milking unit handling 60 cows and milking each cow 3 times per day has a capacity of 7.5 cows/h. This low capacity is convenient for lower-cost design of the robot arm and associated control system, as a window of several minutes is available for each cow and high-speed operation is not required.

VMS units have been available commercially since the early 1990s, and have proved relatively successful in implementing the voluntary milking method. In fact VMS is the only automatic milking system (AMS) available to farmers. The term AMS or "robotic milking" is universally used to describe the VMS systems by the various manufacturers and the dairy industry press, however it can be seen that VMS is a specialised subset of AMS.

1.3.3.2 Limitations of current Automatic Milking Systems

VMS represents complete automation of the milking process, eliminating manual labour from the milking process and freeing the farmer from the strict milking schedule of conventional dairy farming. However the expected benefits in terms of increased productivity and profitability have not materialised for several reasons:

- Capital investment is high compared to conventional parlours; a double-unit AMS handling 120 cows per day is similar in cost to a rotary parlour that can handle 120 cows per hour.

- Capacity is low, typically 7.5 cows/AMS unit/h, compared to 120 cows/h for a standard high capacity parlour.

- Due to low capacity, return on capital investment is low and profitability is similar or lower than conventional milking systems, particularly for larger enterprises [30].

- More complex technology reduces the ability of the farmer to repair faults, increasing reliance on maintenance services.

Additionally, not all cows are suitable for automatic milking. The robot arm and/or sensor mechanism will be unable to apply milking cups to certain cows due to

abnormal udder shape, with incidence of non-conforming animals reported as 5-15% of herd size[18]. The farmer must decide whether to continue to milk non-conforming animals manually or cull (remove for slaughter) the animal. Some animals, particularly older cows, will have difficulty adapting to the VM system. In such cases the farmer must locate the animal and bring it to the milking unit; a decision must be made to cull the animal if it fails to adapt after sufficient training [18]. Advances in control algorithms and robot arm dexterity have improved attachment capabilities, and it would be reasonable to expect these improvements to continue in future AMS.

Finally, VMS is not universally applicable within the dairy industry. VMS functions best in zero-grazing systems, where the cows are permanently housed during the lactation period. On zero-grazing farms, grass is cut during the day and fed to the cows in the barn along with concentrates, rather than allowing the cows to graze at pasture. Zero-grazing is common in countries such as the Netherlands where land is at a premium and all available pasture area is utilised for grass production, with excellent milk yields obtained by this system. However countries such as Ireland, the UK, USA and New Zealand typically operate pasture-grazing systems, in which the cows graze in fields and are brought in groups to the milking parlour for milking. Conversion to zero-grazing would represent a complete and expensive systemic change for the farmer, complicated by the fact that the farmer must maintain normal milk production during the changeover and thus operate two separate milking systems in parallel for a period. A study in the Netherlands [28] indicated that VMS may be used with local pasture grazing up to 400m from the milking unit, however practical attempts (as observed by Teagasc staff in Ireland and New Zealand) to adapt VMS to the pasture-grazing system have been unsuccessful, primarily because grazing is not always available adjacent to the milking parlour and cows would not voluntarily attend the milking unit from remote pasture.

1.4 Benefits of Automating High-Capacity Parlours

A high-capacity rotary or herringbone parlour containing automatic milking machines, cow traffic management devices, cluster removal and teat cleaning, is an efficient, semi-automated milking system. The single remaining manual labour

element in such a system is the application of milking cups to teats. Successful automation of milking cup application in a high-capacity parlour would upgrade the parlour to an AMS with much higher capacity than current systems, and would represent an alternative to the voluntary milking model. Automated high-capacity parlours would be applicable in pasture-grazing systems, and would provide better return on investment for larger dairy enterprises due to economies of scale. Such automation would not interfere with the normal milking routine, so cows would not have to adjust to a new system and cull rates of older cows would be eliminated. Cull rate due to non-conforming udder shapes would be limited by capabilities of the milking cup application mechanism and teat detection system, as with current VMS.

1.5 Literature survey

A survey of available literature was undertaken to determine the current state of the art in automatic attachment of milking cups and the various techniques used by AMS manufacturers. The literature survey focused on manipulator design and methods of milking cup attachment rather than the design of complete automatic milking stalls. The survey attempts to capture the development of AMS, leading to the current state of the art in milking cup attachment. Consideration of each development was divided into a technical description of the design, a brief summary of the operation method and a discussion of the design features relevant to this thesis.

1.5.1 Development of Automatic Milking Systems

Interest in automatic milking began in the 1970s, with patent applications filed by Gabler in 1971 (an East German patent briefly described by Rossing and Hogewerf [18]) and Notsuki and Ueno in 1977 (Japan)[33]. Both designs used milking equipment mounted in the floor of the milking stall, however the 1971 patent describes a single milking bowl to cover the entire udder rather than single milking cups. Notsuki and Ueno used milking cups with independent Cartesian positioning mechanisms as shown in Fig. 6. The four positioning mechanisms were mounted on a horizontal table that was raised through the floor of the stall.

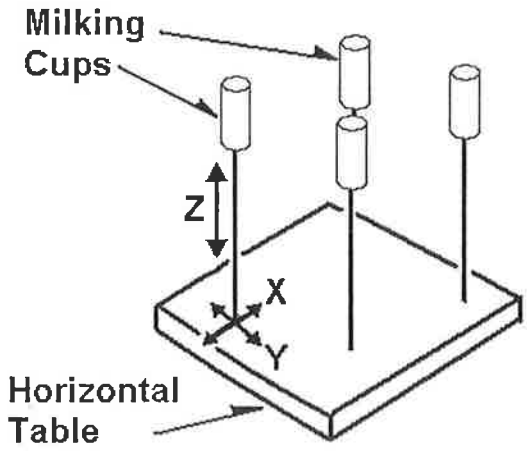

Figure 6. Cartesian milking-cup positioning mechanism (Notsuki and Ueno, 1977)

Cup positioning drive was via stepper motors on all axes. Teat positions were determined from historical data for each cow, rather than through real-time detection. This system was not produced commercially, and it is unlikely that sufficient robustness could be obtained from the historical teat position system, as udder shape and teat position vary with cow age and stage of lactation.

In the 1980s and early 1990s, interest in automatic milking increased. Several research centres in Europe developed prototype AMS and interest from commercial companies led to the development of practical systems. These developments are detailed in the following sections.

1.5.1.1 Silsoe Research Institute/DeLaval

In the UK, the Silsoe Research Institute developed a pneumatically actuated robot arm for teat cup attachment [25]. Two types of manipulator were detailed in the patent application for this device [26], however only the manipulator finally used is shown in Fig. 7.

Description

Teat position sensing was carried out by a laser and photodiode grid mounted on the robot wrist. The robot arm was essentially biomimetic, reproducing the action of a human shoulder and elbow with revolute joints and having a forearm and wrist mechanism driven through small angles with pneumatic actuators. The forearm was telescopic, allowing extra reach under the cow if necessary. A space-frame structure was used to provide a simple and rigid support for the arm. The complete robot arm had five degrees of freedom, four for the arm (including telescoping forearm) and one at the wrist (rotation only). Pneumatic cylinders with full position feedback and differential pressure control were used as actuators. Teat cups were picked up from a magazine using a pneumatically actuated two-fingered gripper, gripping onto a welded bracket on the side of the cup.

Operation

The approach direction was from the side of the animal and cups were attached sequentially. Movement of the animal was discouraged by reducing the dimensions of the stall to closely fit the animal (this type of stall is commonly termed a 'crush').

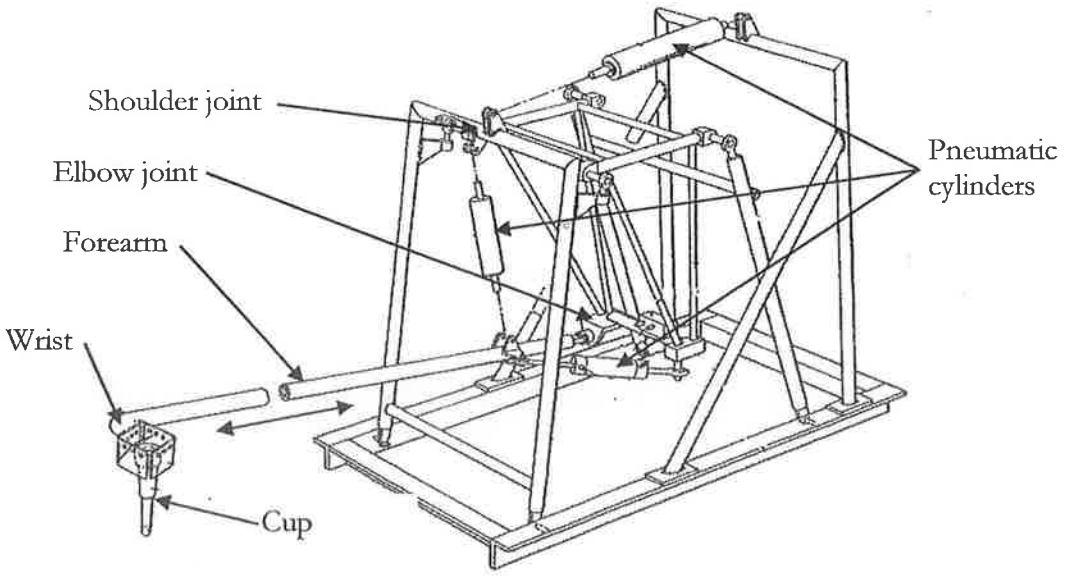

Figure 7. Silsoe Research Institute manipulator (wrist gripper not shown) (Source: esp@cenet database UK patent GBGB2226941 [26])

Discussion

Use of a frame design for this robot arm provided a rigid and robust mechanism at relatively low cost. No special castings or extrusions were required, and the entire mechanism was fabricated from stainless steel stock. On the other hand, the frame design increased the footprint of the robot leaving less room for other elements of the milking unit. The choice of frame and linear actuators restricted the range of movement of the mechanism to small angles in front of the frame and limited the choice of locations for positioning the milking cup magazine. Other than the telescoping forearm bearing, all of the bearings on the mechanism were sealed rotational bearings, providing good resistance to dust and water ingress.

Modelling of the robot arm would have been straight-forward, as the inverse kinematics of revolute-jointed robot arms is well known from literature. However, position control of pneumatic cylinders is made more complex by the compressibility of air, often necessitating slower performance to prevent oscillations about the demand position. Additionally, non-linear friction characteristics of pneumatic seals combined with air compressibility can result in a jerky (stick-slip) motion at low velocity. Despite this control disadvantage, use of pneumatics provides several advantages: the cylinders are simple, light-weight and relatively low-cost, compressed air is simple to generate and environmentally safe, and the compressibility of air lends some compliance to the system in the event of interference with the animal. No mention is made of the control platform used, however it is reasonable to assume that a separate external pneumatic position controller would have been used to drive the actuators as this is a specialised task.

This system operated successfully and was purchased by a Swedish commercial dairy manufacturer, Alfa Laval, now named DeLaval. The DeLaval system is currently in production with several modifications to the original Silsoe design: working volume was increased by dispensing with the support frame; pneumatic operation was eventually changed to low-pressure hydraulics; and the sensing method was altered to use a laser-scanning device mounted on the end-effector.

1.5.1.2 Multinorm/Prolion

Hogewerf (1992) reported on an AMS developed by a Dutch commercial company, Multinorm [23]. Fig. 8 shows the design of the manipulator used as detailed in the patent application [35].

Description

The Multinorm system used an ultrasonic sensing system to locate the teats, with a static sensor mounted at the side of the stall for locating the nearest teat and a fine sensor mounted on the end-effector for locating the other three teats with respect to the first teat. The manipulator had three degrees of freedom, comprised of a two-link arm with revolute joints to cover the horizontal plane, mounted on a parallel linkage to provide vertical motion. The cluster of milking cups was held upright on a tray at the end of a separate support arm, with the milk tubes passing through holes in the tray. This arrangement eliminated the need for an articulated wrist on the manipulator. The support arm could move freely and was spring-counterbalanced so that it would remain at any position to which it was moved. All axes of the manipulator were pneumatically actuated.

Operation

Manipulator approach to the udder was from the side of the cow. Movement of the animal was discouraged by shortening the length of the stall to fit the animal and including a bar to exert light pressure on the opposite rear leg of the cow, forcing a stable stance. In operation, the robot arm gripped the support arm and manoeuvred the cluster under the cow. Cups were attached sequentially, each cup being raised slightly by a small pneumatic cylinder during application. Each cup was released from the tray as the tray moved downwards after each attachment, but remained loosely restrained by the milk tube passing through the tray. Following attachment, the robot arm disconnected from the support arm, leaving the support arm to support the milk tubes and hold dropped milking cups off the floor when milking was complete. This feature allowed the manipulator arm to be decoupled from the cluster tray and travel on a rail to service adjacent stalls. Prolion built this system to service one to four stalls.

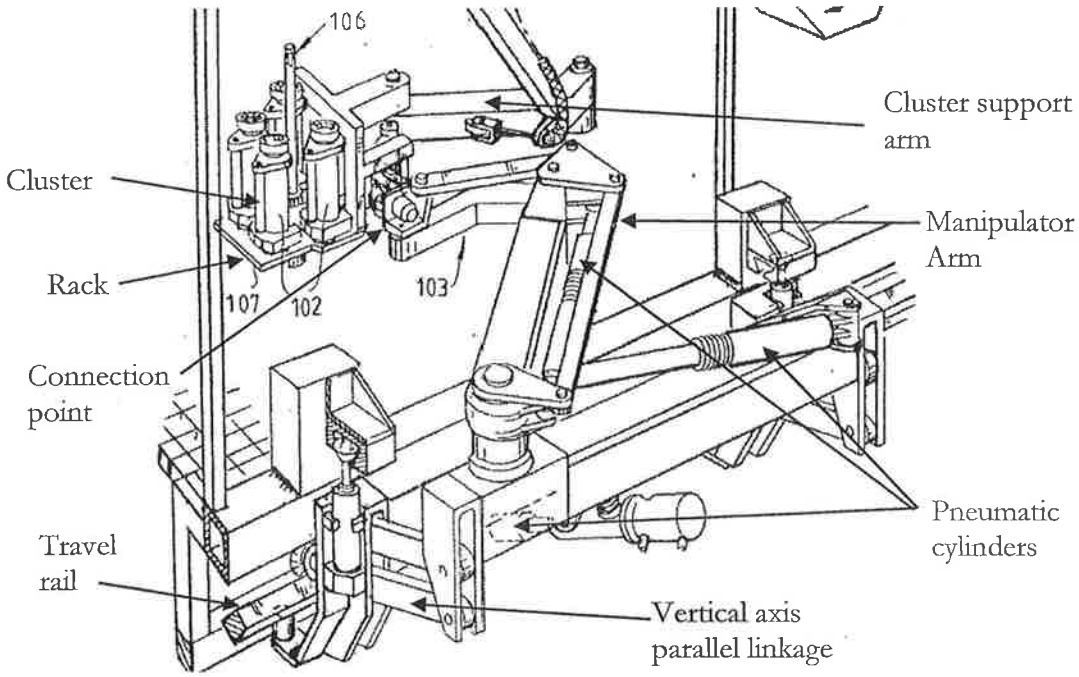

Figure 8. Multinorm/Prolion AMS (Source: esp@cenet database European patent EP0323875 [35])

Discussion

Use of revolute joints significantly reduced the footprint of this manipulator and increased the working envelope compared to the Silsoe design. The parallel linkage avoided the use of linear bearing slides, which are more difficult to seal than standard bearings. Pneumatic actuators provided the advantages mentioned previously, but with the associated slower performance for position control. A key development in this design was the use of a single manipulator to service several stalls. This increased the utilisation of the manipulator, at the expense of a small increase in design complexity.

The Multinorm system was taken over by another commercial company, Prolion, and was produced and used in the Netherlands [20]. The system was also manufactured under the Gascoigne Melotte brand name. Prolion was recently acquired by the Dutch firm Punch Technix, who continue to market an updated version of this system (the Titan RMS).

1.5.1.3. Gascoigne Melotte

An AMS system that attached milking cups between the rear legs of the cow was developed by the commercial company Gascoigne Melotte (the Netherlands) [27].

Description

This design attached all four milking cups simultaneously. Fig. 9 shows the general layout of the robot arm. The arm configuration was Cartesian, with all axes actuated by pneumatic cylinders. A retracting mechanism allowed the entire arm to be withdrawn from beneath the cow, and a separate cleaning arm was provided. Two mobile arms (not shown) were provided at the rear of the stall to spread the legs of the cow and maintain separation during application.

End-effector design was more complex than those examined previously, providing three degrees of freedom for each cup. The design of the cup positioning mechanisms is shown in Fig. 10 (for clarity, only two cups are shown). Each axis was actuated by a small pneumatic cylinder. Guide rails were provided along which each cup was driven, and a special linkage was used to allow a vertically positioned actuator to drive the cup along the lateral (x) axis.

Operation

Teat position was read from historical data, and verified by a local stereovision system. The cups were moved to the horizontal teat positions on the retracted end-effector. The end-effector was then moved underneath the cow, and the vertical axis for each cup was actuated to raise the cups to the teats. A set of arms (not shown on drawings) were used to spread and keep the legs of the cow apart during application. The arm remained under the cow during milking, and retracted the cups once milking was complete. A sensing plate pressed against the rear of the cow detected changes in cow position, allowing the robot arm to compensate for small movements.

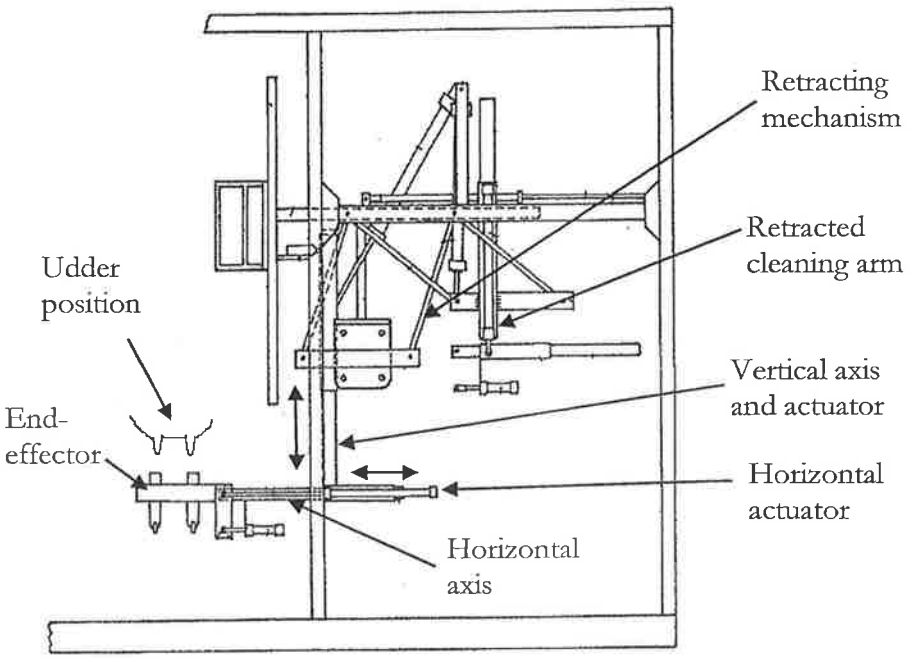

Figure 9. Gascoigne Melotte AMS (Source: esp@cenet database European patent EP0309036 [37])

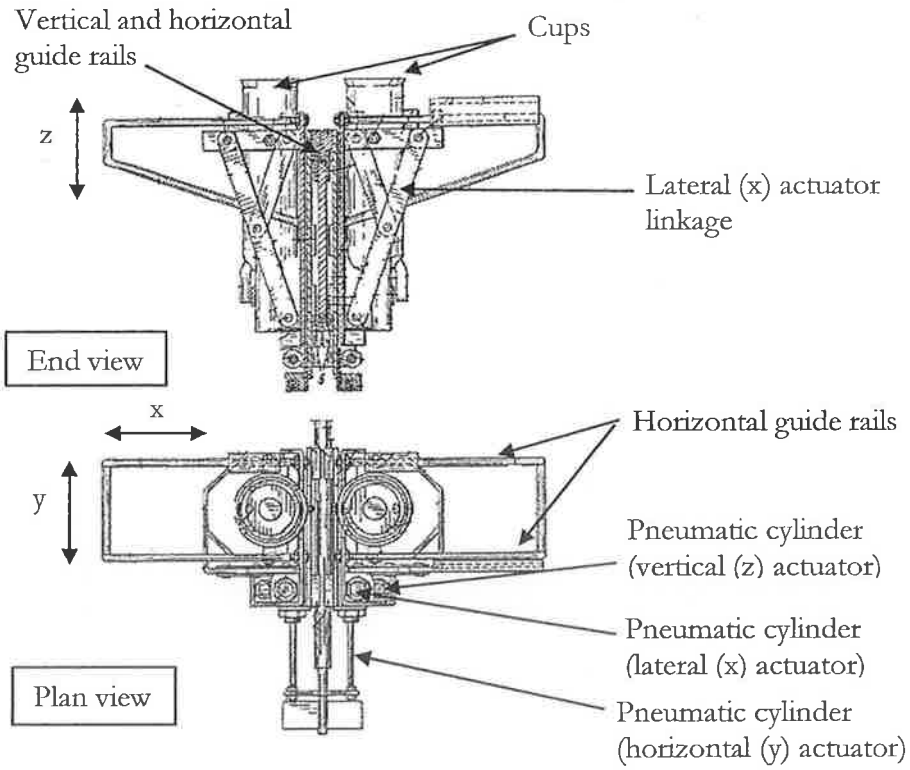

Figure 10. Gascoigne Melotte AMS, cluster detail showing two milking cups (Source: esp@cenet database US patent US4936256 [38])

Discussion

This design was different from the previously considered AMS, in that it approached from the rear of the cow, and applied all four cups simultaneously. Simultaneous application carries a fourfold speed advantage over sequential application methods, due to the elimination of multiple locate-and-place operations. Additionally, the rear-access method is a slightly shorter route to the udder than access from the side, and avoids the area in front of the rear legs in which the leg is most likely to move (noted from observation of cows). All twelve actuators were fitted into the end-effector in a reasonably compact arrangement, however the lateral guide-rail arrangement occupied a significant amount of space. Complexity of the end-effector is a disadvantage, as the additional controls, actuators and mechanisms would increase costs. However use of a Cartesian configuration for all axes allowed for relatively straight-forward construction and control, perhaps offsetting some of the end-effector costs. Soiling of the end-effector by the cow was a serious risk with this design, therefore some means of shielding the end-effector from excrement would be required.

This design was tested on an experimental farm in the Netherlands, however it was not put into commercial production [18][20].

1.5.1.4 Lely

Lely, another Dutch milking equipment manufacturer, developed a milking system that applied milking cups from the side of the cow [34].

Description

Similar to the Prolion system discussed above, the Lely system used a revolute-jointed arm to cover the horizontal plane, coupled to a parallelogram mechanism on the vertical axis. The arm design is shown in Fig. 11. The cluster was held in a manner similar to the Prolion system, each cup being held vertically on the end-effector until applied to the teat, and then released, with the robot arm remaining under the cow to hold the milking lines during milking.

Pneumatic cylinders operated the arm, although the vertical axis used a hydro-pneumatic cylinder (hydraulic fluid on one side of the cylinder) to provide more force when lifting the arm. The end-effector incorporated a laser sensing device for locating the teats and a cleaning brush for cleaning teats prior to cup application.

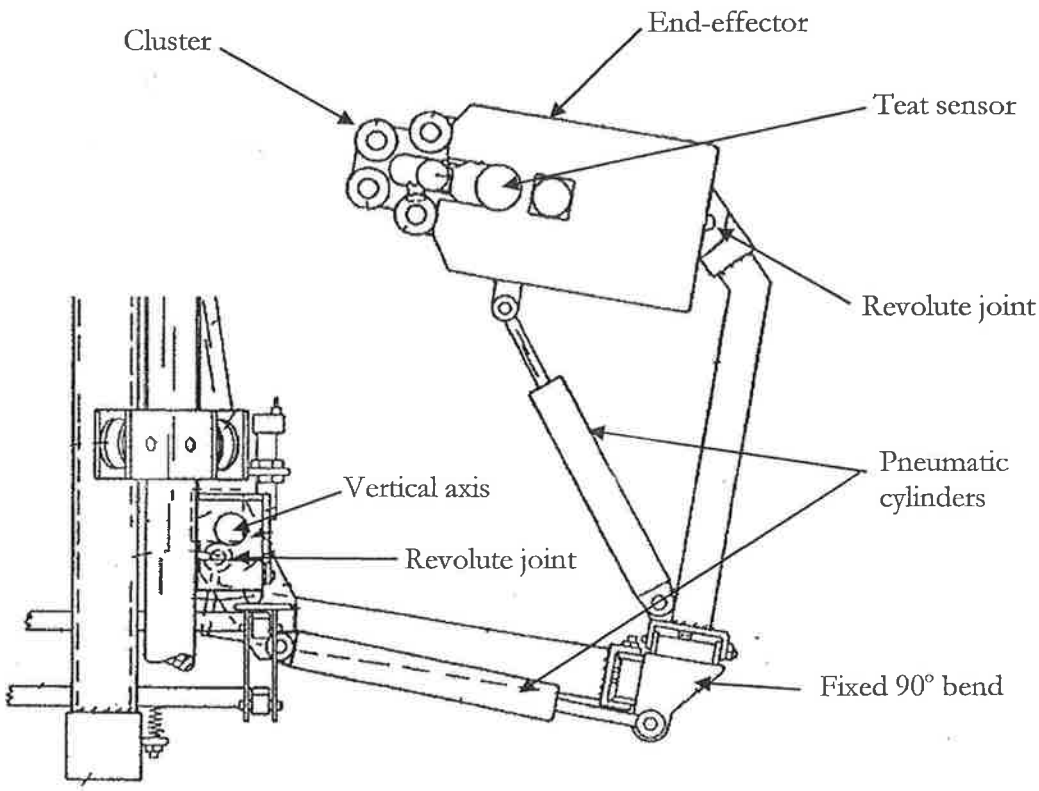

Figure 11. Lely AMS (Source: esp@cenet database German patent DE4293178 [34])

Operation

Operation was the same as the Prolion system, with cups applied sequentially. Approach direction was from the side of the cow. A sensing device pressed lightly against the cow was used to detect motion and allow the robot arm to follow the movements of the cow during milking.

Discussion

The Lely robot was relatively simple in design, utilising linear actuators to drive all axes. Use of revolute joints increased the robustness of the design, while pneumatics provided relatively safe and somewhat compliant actuation. The system

speed was limited by the sequential application method. The 90-degree bend in the arm was used to facilitate approach to the udder along the longitudinal axis of the cow. Approaching the udder in this manner kept the end-effector clear of the area in front of the rear legs, demonstrating that while access from the side gives more manoeuvring space, care is still necessary to avoid interference with the cow.

The Lely design was one of the most successful of all AMS, and is still in production. The design has also been manufactured under licence by Fullwood in the UK.

1.5.1.5 Insentec/Idento/Galaxy AMS

Insentec, Idento and Galaxy, member companies of a Dutch agricultural equipment group, developed an AMS that used a standard industrial robot arm to apply milking cups.

Description

A 5-axis robot arm was mounted on a track system, allowing servicing of several adjacent stalls, as shown in Fig. 12. Teat position was detected using a laser-based sensor mounted on the end-effector. The robot arm joints were electrically actuated, while the two-fingered gripper on the end-effector was operated pneumatically. An additional cleaning device (not shown) was mounted underneath the end-effector and used to clean the teats before application.

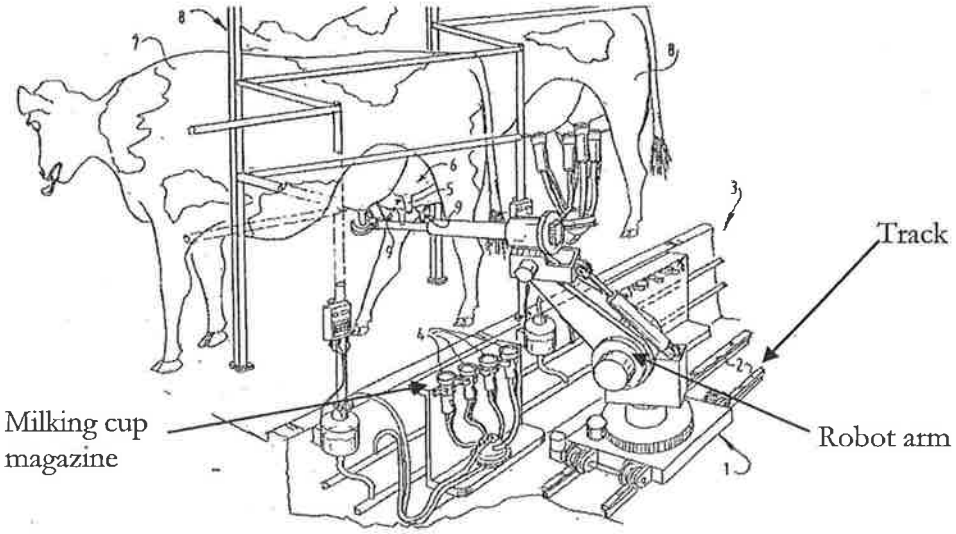

Figure 12. Galaxy AMS (Source: esp@cenet database World patent WO02087316)

Operation

Cups were held in a magazine at the side of the stall and picked up individually by the gripper. Application was sequential, and the udder was accessed from the side of the cow. Cups were automatically retracted back into the magazine once milking was complete.

Discussion

Use of a standard robot arm in this system greatly simplified the design task, as in-house fabrication and control of the robotics was eliminated. A 5-axis arm has excellent dexterity for acquiring and positioning cups, while electrical actuators provide faster operation than pneumatics. A disadvantage of electrical actuation (and the associated electronic sensors) is increased sensitivity to moisture ingress, necessitating careful waterproofing of joints and connections. Operation speed was limited by the sequential application of cups from a magazine, however the speed of the robot arm could compensate for this to some extent. Utilisation of the robot was increased by the track system, allowing the robot to service more than one stall. This design was successfully introduced to the market and is still in production, although the Insentec, Idento and Galaxy companies are now owned by a Danish dairy manufacturer, SAC.

1.5.1.6 CEMAGREF

The French Institute of Agricultural and Environmental Engineering (CEMAGREF) developed a prototype automatic milking system having four robot arms, one for each cup [31][40].

Description

Teat positions were determined using a stereovision system and local laser/photodiode grids on each end-effector. Small revolute-jointed robot arms with four degrees of freedom were used to handle the milking cups. Pneumatic cylinders were used to actuate the robot arms. Two arms were mounted in a space below the floor of the stall, and two arms were mounted at the sides of the stall, each with a permanently attached milking cup. Inflatable air bags at the sides of the stall were used to hold the cow in position during application.

Operation

Cups were applied simultaneously by all four arms, the arms remaining in position until milking was complete and then removing the cups.

Discussion

Simultaneous application of milking cups meant that application speed was high for this system. However the complexity of the design is a disadvantage, due to the requirement for multiple robot arms and major modifications to the floor of the milking stall. In addition, the robot arms were under-utilised, as the arm remained in place under the cow during the entire milking process. The workspace under the cow would have been crowded with four manipulators present, increasing the risk of collisions and necessitating careful control.

The CEMEGREF system operated successfully in prototype form, however it was not produced commercially, possibly due to the complexity of the system.

1.5.1.7 Duvelsdorf

In Germany, the commercial company Duvelsdorf manufactured a prototype Cartesian robot for application of milking cups[41][42].

Description

Teat position was determined using an ultrasonic sensor. The robot consisted of a set of linear sliding arms mounted at the side of the stall, as shown in Fig. 13. All axes were electrically actuated via rack-and-pinion gearing. A two-finger gripper was provided for holding milking cups, which were picked up from a magazine.

Operation

Milking cups were collected individually from a stall-mounted magazine and applied sequentially, after which the robot was retracted and could be used to service adjacent stalls by travelling on an elongated horizontal axis. Approach direction was from the side of the cow.

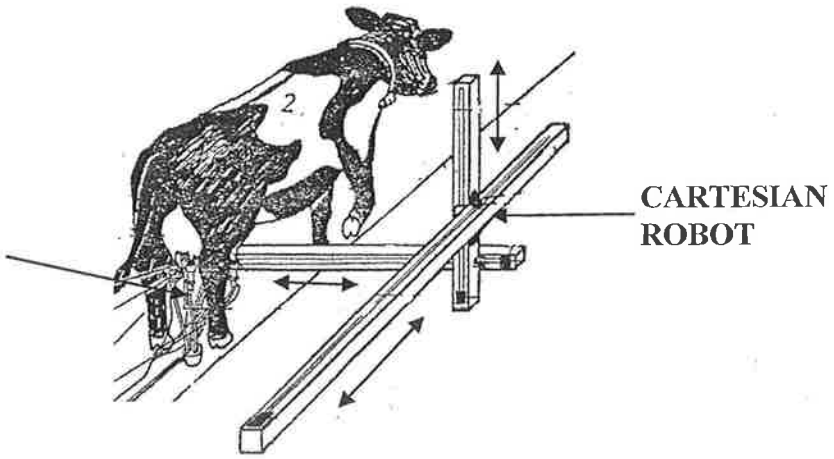

Figure 13. Duvelsdorf Cartesian Robot (Source: esp@cenet database EP300115 [42])

Discussion

Cartesian mechanisms are relatively simple to implement and control, however there is a disadvantage in the space requirements compared to revolute-jointed robots. Dexterity is limited compared to other designs considered, as the robot only has three degrees of freedom. Use of electrical actuators and linear slides would

have provided excellent speed and accuracy, although linear slides are more difficult to seal than rotating bearings. Servicing of additional stalls by elongating the horizontal axis parallel to the stall (mentioned in the patent application [42]) would have been simple to achieve, resulting in improved utilisation of the robot. As noted previously for the Lely design, the space directly in front of the rear legs should be kept free (as the cow may step into this space), so an additional 90° angle at the end of the manipulator was required for optimum access to teats.

The Duvelsdorf system was acquired by a German dairy manufacturer, WestfaliaSurge, and some development was carried out, however the research programme was discontinued in 2004 due to concerns over the low profitability of AMS [43].

1.5.1.8 German Federal Research Institute for Agriculture

The German Federal Research Institute for Agriculture developed a robot similar to the Duvelsdorf Cartesian manipulator, but with an additional revolute joint at the end-effector [32].

Description

Teat positions were detected using a combination of stereovision and ultrasonic sensors. The manipulator had four degrees of freedom, the first three axes being Cartesian and the final axis revolute, with all axes electrically actuated using stepper motors. Cups were picked up and applied using a two-fingered gripper.

Operation

Cup application was sequential and approach direction was from the side of the stall.

Discussion

The system had similar characteristics to the Duvelsdorf device, however addition of an extra axis to the Cartesian robot improved the dexterity of this design with only a small increase in complexity. Use of electrical actuators would have provided excellent accuracy and speed. As far as can be ascertained, this design was not implemented commercially.

1.5.1.9 AUTARI/University of Udine

In Italy, a consortium (AUTARI) at the University of Udine, developed a Cartesian robot for automatic application of milking cups[44].

Description

The design used a Cartesian arrangement similar to the Duvelsdorf system. Teat positions were detected using a laser-based sensor device. All four cups were held in a cluster at the end-effector.

Operation

Access to the udder was from the side of the cow and cups were applied sequentially.

Discussion

While this system has the limitations of Cartesian design described for the Duvelsdorf system, provision for holding all four cups at the end-effector would improve the speed of operation.

This system was used experimentally, but there is no evidence that it has entered commercial production.

1.5.2 Summary and state of the art in automatic milking

Rossing and Hogewerf (1997)[18] summarised the approach and cup handling methods used by the various AM systems:

a) Approach direction from the side of the cow

b) Approach direction from the rear of the cow

c) Approach direction from below the cow

d) Application of cups sequentially with a single robot arm

e) Application of cups sequentially with one robot arm holding all four milking cups on a rack

f) Four independent robot arms, each having a permanently attached cup

Despite much experimentation in milking robotics design in the last two decades, only four manufacturers produce automatic milking systems at present, and their products represent the state of the art in automatic milking devices. All current manufacturers use the side-approach direction (a) for access to the udder. Of the application methods, (d) is currently implemented by the DeLaval VMS [45] and the SAC Galaxy AMS [46], while (e) is used by the Lely Astronaut AMS [47] and Titan RMS (Punch Technix) [48]. It should be noted that both Lely and Punch Technix AMS are manufactured under licence by other companies: Fullwood Merlin (Lely) and Gascoigne Melotte GM3000 (Punch Technix/RMS). Figures 14 and 15 illustrate the layout of two current AMS milking units.

Figure 14. Rear view of current DeLaval VMS showing rear of robot arm at right. Inset: Detail of robot arm and end-effector (Courtesy of DeLaval International AB)

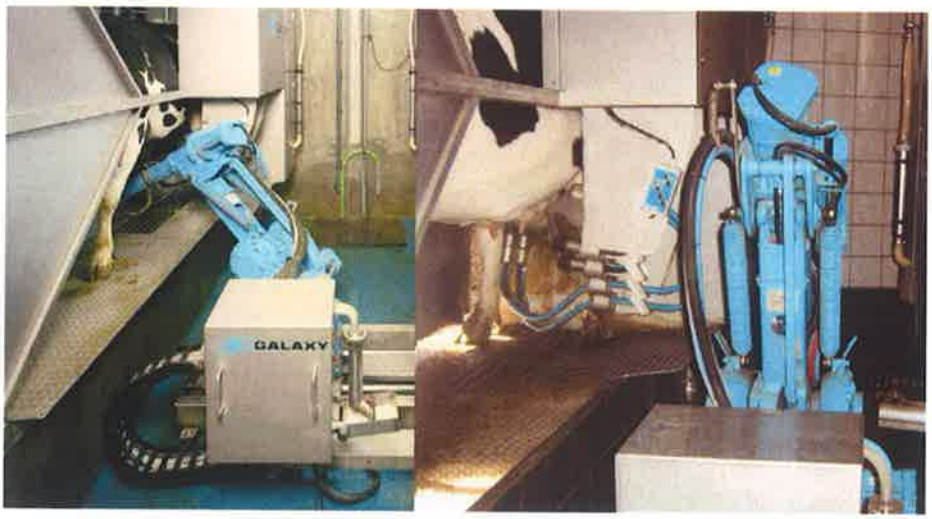

Figure 15. SAC Galaxy AMS. Left: robot arm applying milking cups. Right: retracted robot arm, two cups attached to teats and two cups in magazine (Courtesy of S.A.Christensen & Co.)

The Gascoigne Melotte design for simultaneous application of milking cups, although apparently successful in trials [20], was presumably too complex for production, as the company later produced a version of the Prolion system that applied cups sequentially. In the context of voluntary milking, high application

speed is less important, as the application time is a small proportion of overall milking time for the cow (five to eight minutes). Sequential application with all four milking cups held at the end of the end-effector improves operation speed by eliminating the need to collect individual cups from a magazine.

In most systems considered, the legs of the cow are relatively unrestrained, necessitating sensors to determine if the cow moves significantly during application. Passive devices, such as a grid in the floor of the stall (visible in Fig. 15) or sloped plates in the floor were used to encourage leg separation. The exception to this was the Gascoigne Melotte system, which used two arms inserted between the rear legs of the cow to spread the legs and prevent interference with the robot during cup application. Such an approach seems to have been both effective and acceptable to the cow (Kuipers and Rossing [20] shows an image of the system in operation), perhaps because of the relatively short time for which the device was in contact with the animal. The low-capacity nature of VMS allows the cow to be relatively unrestrained, as there is ample time to withdraw and retry application if the cow moves. However for faster systems, as with the Gascoigne Melotte simultaneous application system, there is obviously a need to constrain the movement of the cow briefly during application. In such a system a small movement of the cow may be sufficient to cause application failure for all four cups.

A feature of the Lely AMS is the ability to detect and compensate for angled teats. The angle of the teat is measured and, if the angle is sufficiently large, applies the cup at this angle (for small angles vertical application is sufficient). Accommodation of teat angles up to 45° is claimed for this method. Teat angle accommodation may reduce application failure incidence for some cows, and would therefore reduce the cull rate due to non-conforming teats. It may be argued however, that this feature reduces motivation to breed cows for good teat presentation (i.e. vertical teats), thus preserving incidence of angled teats in the herd. Therefore teat-angle compensation is most useful for the transitional period when a herd is being adapted to automatic milking. Teat angle compensation requires more complex manipulator control to accurately follow the angled application path.

Each manufacturer has chosen to use revolute joints for the majority of the robot arm axes. This decision is due to the improved dexterity of revolute-jointed arms (giving better workspace coverage in a more compact package) and also for the better sealing characteristics of rotational bearings over sliding bearings.

Actuation methods used are hydraulic (DeLaval), electrical/pneumatic (SAC Galaxy) or pneumatic (Lely, Titan RMS). Use of pneumatics in most early designs is understandable, as the simplicity and robustness of the actuators in damp and dirty conditions is a significant advantage over electrical actuation. However the limited force available at standard pneumatic pressures (mentioned in Section 1.6.1.1) led DeLaval to change from pneumatic to low-pressure hydraulic actuators [45]. It is also possible that hydraulic actuation was chosen to overcome the position control limitations inherent in pneumatics, as this change would have eliminated compressibility effects and allow increased operation speeds. The Galaxy system demonstrated that electrical actuation (as part of a standard robot arm) was viable for use in the milking stall environment, providing excellent precision at reasonable cost.

Manufacturers are understandably reluctant to provide exact control hardware details. However it is reasonable to assume that in all cases an industrial PC platform is used to store the robot arm model, process teat-position data and provide output signals to drive the arm. In the case of pneumatic and hydraulic actuators, a separate specialised position control unit would be necessary to drive the actuators, while the Galaxy robot arm controller would accept position data directly form the control computer. In all cases control software is reported as proprietary, and no operating system is specified.

1.5.3 Robotics application in high-capacity parlours

Without exception, all current AMS are designed for use with the voluntary milking model. As voluntary milking is an inherently low-capacity method, it may be anticipated that the associated techniques and mechanisms may be less suitable for use in high-speed, high capacity parlours. In particular, the large time-window available for teat position detection and cup application would not be present in a high-capacity parlour, where high cow-throughput is the primary goal. Multi-stall

systems in which a single robot services several stalls attempt to increase the throughput per robot, however such increases are small compared to conventional parlours. For example as shown in Figure 16, a 5-stall (box) Titan RMS system, which has the highest capacity of all available AMS, has a capacity of 220cows/day or 27.5cows/h if each cow is milked three times. The vertical axis of Figure 16 shows the possible milk yield, or quotum, in litres for the various stall configurations.

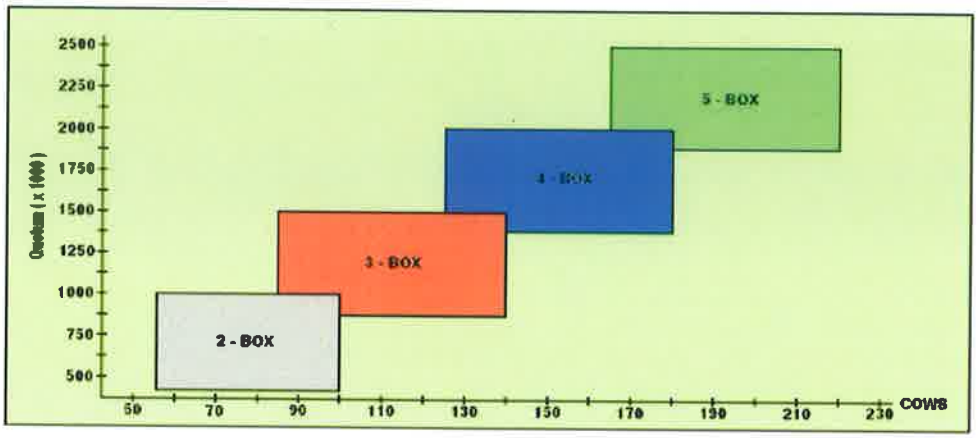

Figure 16. Capacity of Titan system with multiple stalls (Courtesy of Punch Technix N.V.)

Several manufacturers have filed patents for methods to improve robot utilisation (and thus improve capacity), two of which involved rotating stalls past the robot arm [49][50], one having a long double-row of stalls with the robot moving on a rail between stalls [51], and the fourth a mobile unit for attaching milking cups to cows in the field [52]. While each of these systems would (theoretically) increase AMS capacity, the limitations of VMS still apply, and none of these have been released for commercial use to date.

1.6 Objective of this thesis

Having examined both the available literature and systems available from manufacturers it was apparent that, to date, no attempts had been made to automate milking cup application in high capacity parlours. The motivation for such automation was presented in the introduction to chapter 1, and the objective of this thesis is therefore to present a design for a robotic manipulator capable of applying milking cups to cow teats within a high-capacity rotary milking parlour. This thesis thus represents an initial step in a new direction for milking parlour automation.

As part of the overall objective, the following goals were identified:

- An analysis of the working environment and identification of environmental constraints affecting the operation of automated equipment.
- Identification of performance requirements for the manipulator.
- Analysis of various approach strategies for the milking application task, and selection of a suitable approach methodology.
- Characterisation of the workspace in which the manipulator must operate, and parameterisation of the workspace to establish design constraints.
- Design of a suitable end-effector (tooling) for the manipulator to handle and apply milking cups within identified constraints and performance requirements. Use of computer aided engineering techniques to facilitate this design process and provide analytical techniques fro design evaluation.
- Selection of an industrial robotic arm to handle the designed end-effector within identified constraints and performance requirements.
- Development of a control system to integrate and control the manipulator components, and specification of an outline control algorithm for manipulator operation.

- Performance testing of the designed end-effector to ensure conformation with specified requirements. Performance testing of the control interface between control system and the robot arm.

A teat position sensor is required to fully replace a human operator, however teat sensing is not considered in this thesis. Constraints imposed by conventional rotary parlour design will be taken into account with the intention of minimising any required alterations to standard parlour layout and operation.

Chapter 2

ENVIRONMENTAL ANALYSIS AND DEVELOPMENT OF APPROACH METHODOLOGY

2.1 Workspace analysis

Design for robotic automation requires a clear knowledge of the characteristics and parameters of the area in which the robot will operate. This operating region is termed the workspace. For this application, the workspace is a region on a rotary carousel containing static objects with invariant dimensions (stall rails, stall floor) and mobile objects with variable dimensions (cow legs, udder). An analysis was undertaken to characterise the workspace in terms of stall layout, stall dimensions and biometric data for dairy cows.

2.1.1 The rotary parlour stall

Stalls on a rotary parlour are designed to house an individual cow during milking. A conventional stall limits movement without being uncomfortable for the animal. The floor is typically concrete, while the sides of the stall are made from galvanised steel tubing.

Fig. 17 shows the area of the parlour where the operator works during milking. The control panel at the right of the image allows control over various parlour functions, such as carousel speed and gate operation. Cow identification is performed using an aerial mounted at the entry point to pick up ear tag radio signals. Individual cow identifiers are passed to a control computer, and the operator may be alerted to special requirements (e.g. to divert milk from a cow that is being treated with medication) via an audio or visual signal on the control panel.

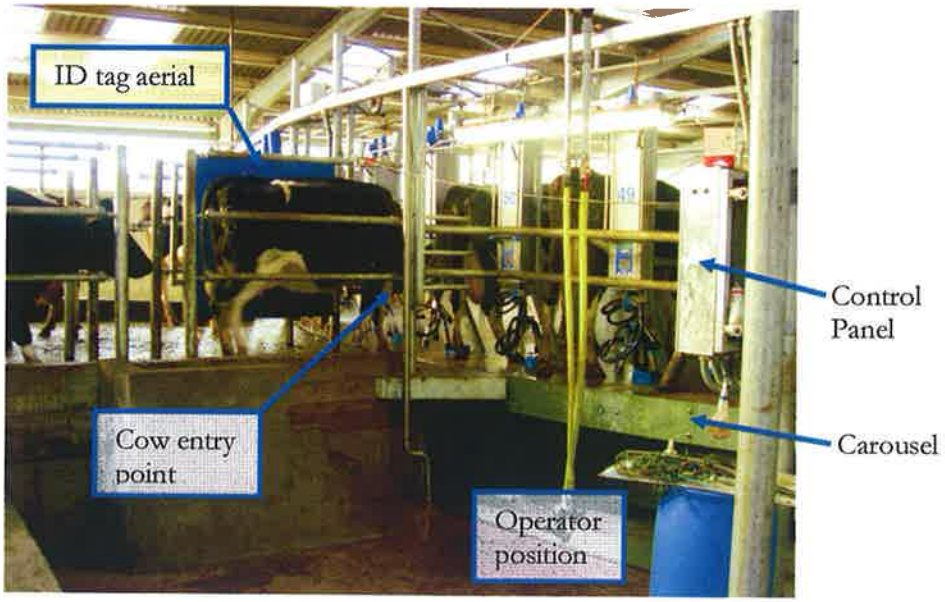

Figure 17. View of rotary parlour showing operator position for milking cup application

Two rails are visible at the rear of the stall: the upper rail is simply a barrier, while the lower rail is an anti-kick rail that discourages the cow from raising its rear legs. Height of the anti-kick rail is important, as it forms the upper limit of the aperture for access to the udder. The floor forms the lower limit of this access aperture, while the legs of the cow form the sides. The operator position is the location at which a robotic manipulator is expected to operate, reaching into the stall through the access aperture. Stall characteristics were observed from the operator position, and measurements were taken to parameterise the stall.

2.1.2 Workspace parameters

Figure 18 shows the parameters of interest in the stall (measured from a Dairymaster Swiftflo Revolver rotary parlour).

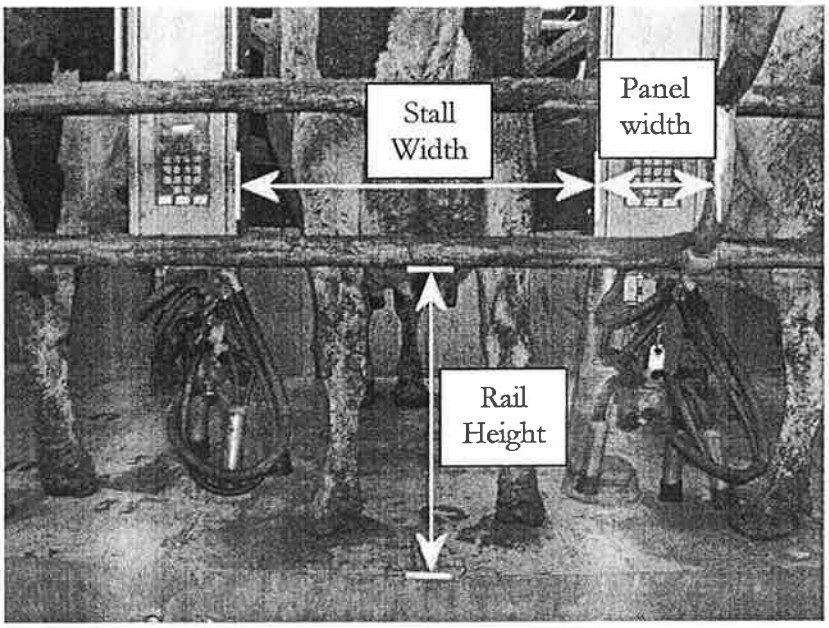

Figure 18. Stall measurements

It was assumed that these parameters were representative of most rotary carousels on the market, as the stall dimensions are based on animal size rather than manufacturer preference. Panel width at the side of the stall was included because this is the approximate area in which milking cups are presented for pick-up and an end-effector should be capable of operating into this area. Relevant dimensions on the stall were measured, as well as the height of the stall floor above the ground. Workspace parameters are shown in Table 1.

	Dimension (mm)
Stall width	740
Rail height	640
Panel width	200
Height of carousel above parlour floor	1200

Table 1. Stall parameters

2.1.3 Biometric data

Biometric data are measurements of physical characteristics of living organisms. Measurements for two areas of the cow were required for design of the manipulator end-effector: the aperture between the rear legs and locations of the teats. Figure 19

and Figure 20 show a solid model of the workspace (to scale) with dimensions of interest highlighted.

In Figure 19, the access aperture formed by the legs is clearly visible as a trapezoid between the hocks ('rear knee') and the hooves. Depending on the animal, the legs may be badly 'hocked-in' with hocks very close together, or straight-legged, with hocks widely spaced at the same width as the hooves. The majority of cows were observed to have slightly hocked-in rear legs, this trait being desirable for animal breeders to produce [53]. Dimensions of interest are the width at the hocks and hooves and the height of teats above the floor.

Figure 20 shows a view (to scale) of the udder from below the cow. The udder is composed of four quarters, each having a single teat: front left, front right, rear left and rear right. In rare cases a fifth teat may be present, although these are not usually functional.

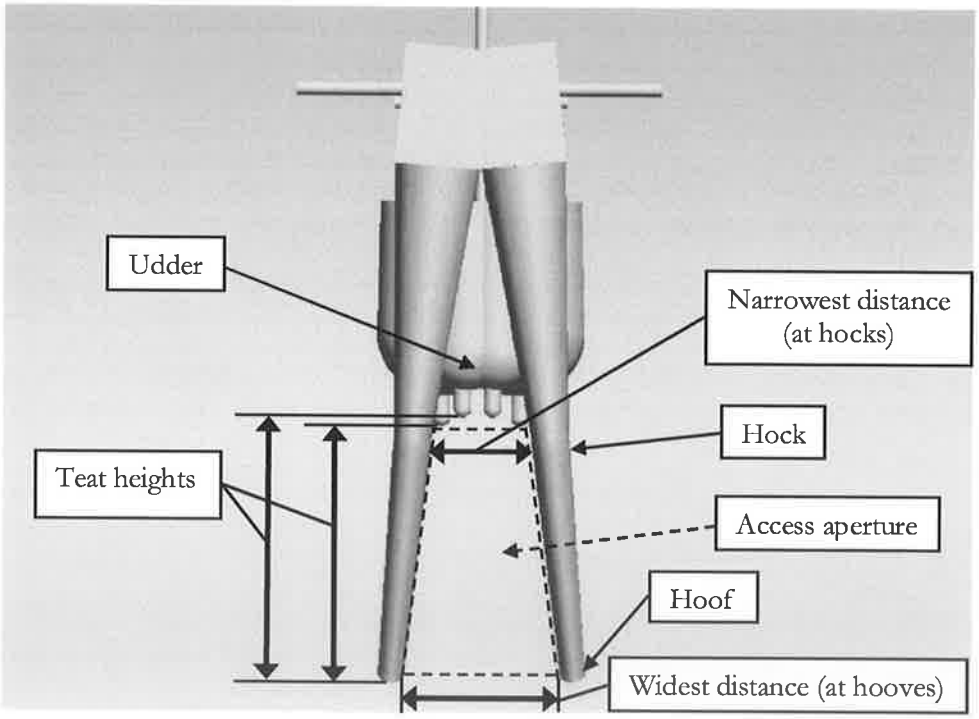

Figure 19. 3D workspace model showing rear view of udder and access aperture

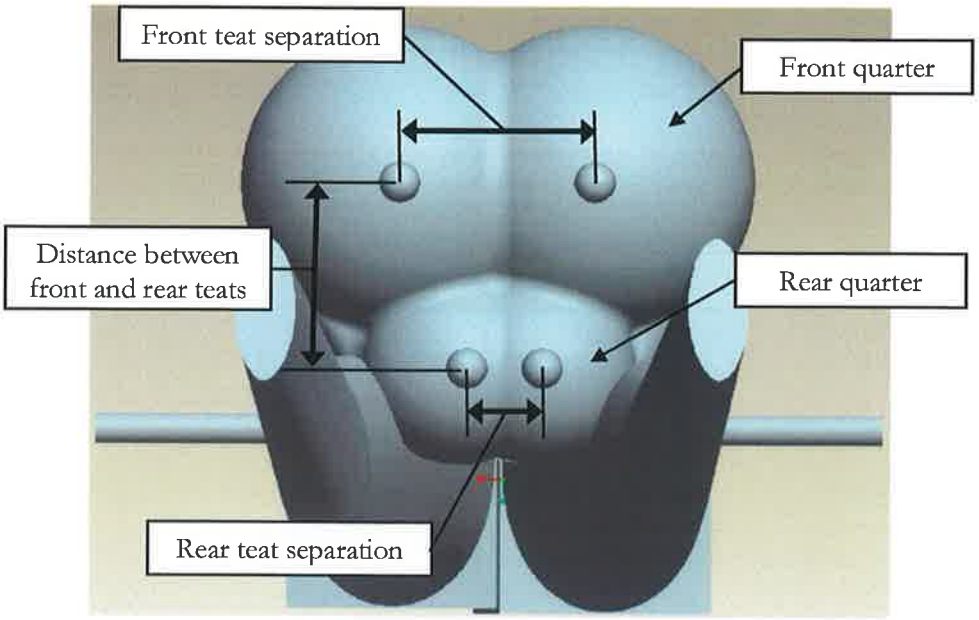

Figure 20. 3D workspace model showing view from below

Important teat dimensions are the distances between teats as shown in Figure 20. Teat positions were assumed to be symmetrical about the centre of the udder; while this is not always the case, the assumption is reasonably sound for design of the end-effector. Much variation was observed in teat positions, ranging from all teats touching together to all teats on the outer extremes of the udder. These extremes are often tolerated but are considered undesirable by dairy breeding associations, and dairy cow breeders aim to produce animals with evenly spaced teats [53]. Regularly spaced teats may therefore be presumed to be the norm, and extreme teat configurations may be ignored for the purposes of this design project.

Compliance of teats is an important characteristic to consider when designing the end-effector, as elasticity of the teats allows movement to accommodate inaccuracies in milking-cup positioning. Observed compliance can be greater than 10mm, and a practical range of up to 4mm was assumed.

From enquiries with Teagasc Moorepark Dairy Research Centre, it was found that biometric data is not usually collected for animals, as such data has little value for animal production. Instead, animal producers use a technique known as condition scoring, where animal characteristics such as udder size or leg straightness are given

a score (e.g from 1 to 10) based on observed conformation to accepted standards. Scores are weighted and combined to give an overall score for the animal. Such a technique is useful in compensating for variations in breed characteristics, but does not contain physical measurements. While it is likely that dairy manufacturers possess biometric data for dairy cows, such information is of a proprietary nature.

Useful biometric data for teat positions were obtained from an agricultural science publication [54]. The data used were measured from a herd of 54 Holstein-Friesian cows in their first lactation. While the sample size is relatively small, such cows are representative of those found in Irish dairy farms and thus the data are suitable for defining end-effector parameters. The data obtained are summarised in Table 2. The maxima and minima of the various traits are important for defining end-effector specifications, while the mean and standard deviation give an indication of the normal operating region. Diameter of teats was also included, as this gives an indication of the positioning accuracy required from the end-effector; for example, a positioning error of +/- 1mm is only 4.5% of minimum teat diameter, which could easily be accommodated by teat compliance.

Trait (mm)	Mean	sd	Minimum	Maximum
Rear teats distance to floor	592	29	520	660
Front teats distance to floor	588	27	530	660
Diameter of front teats	27	2	22	32
Diameter of rear teats	27	2	22	32
Distance between front teats	130	23	80	180
Distance between rear teats	52	15	35	100
Distance between front and rear teats	125	19	75	180

Table 2. Biometric data for teats (extracted from Kuczaj, et. al. (2000)[54])

Biometric data for spacing of hooves and hocks could not be obtained from literature, so measurements were made in a working parlour (model: Dairymaster Swiftflo Revolver) in Co. Cork, Ireland. Distance between hocks, hooves and the distance from lowest rear teat to floor was measured for 35 cows during milking on a rotary carousel. Due to constraints imposed by the working nature of the parlour,

it was not possible to take measurements from the entire herd (approximately 200 cows). Instead, worst-case parameters were established by selection of cows with poor udder presentation, i.e. hocks closer together and low teats. These measurements therefore define the smallest aperture through which the end-effector must operate. Maximum distance from the anti-kick rail to the rear teats was also measured to determine the reach required under the cow. Table 3 shows the results of these measurements.

Trait (mm)	Mean	sd	Minimum	Maximum
Width at hocks	184	40	115	256
Width at hooves	216	58	115	333
Floor to lowest rear teat tip	426	63	291	552
Distance from rear teat to rail				250

Table 3. Biometric data: Leg separation and rear teat height for 34 dairy cows

Measurement of rear teat height was performed for comparison to the data in Table 2. Difference in mean teat height between the two data sets was 166mm, with the Irish herd having lower teats. This difference can be attributed to two factors: the cows in Table 2 were primiparous (first time-calving) so udders would be a little smaller and higher; and these cows were selected imports [54] and would thus be expected to display excellent physical characteristics compared to the Irish herd sample, in which cows were selected for poor presentation. Combination of the two sets of data gives a realistic indication of real-world variation in cow characteristics.

2.1.4 Workspace modelling

Stall parameters and biometric data were combined to generate a three-dimensional model of the workspace. Figure 21 shows workspace volumes constructed from the maximum, minimum and average biometric data. The minimum volume (red) represents a combination of the lowest teat height and narrowest width observed, while the maximum volume (blue) shows the highest teat level and widest leg spacing.

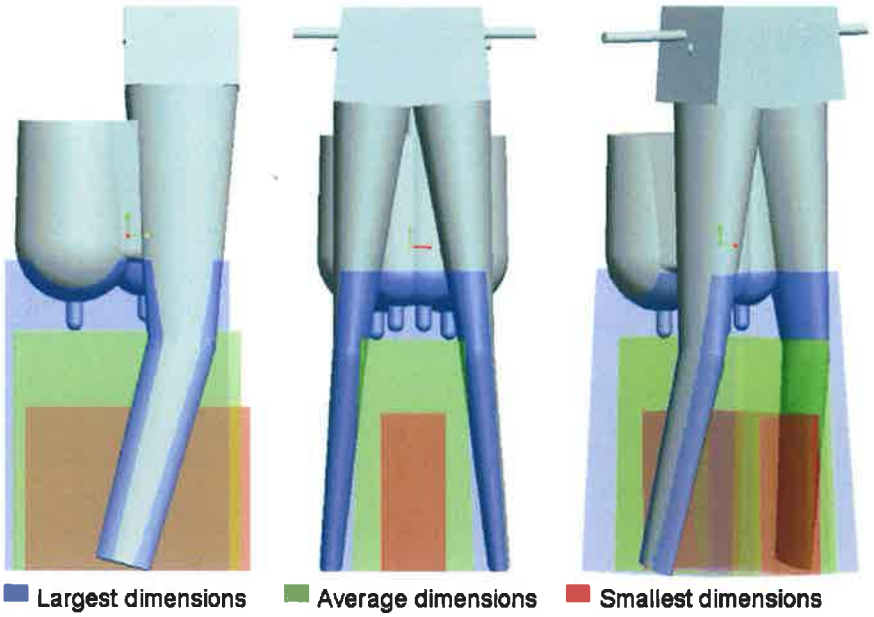

Figure 21. Solid model of maximum, minimum and average workspace volumes beneath cow

Average dimensions are indicated by the green volume, and reference to the standard deviations in Table 3 gives a picture of the typical working region around the boundaries of this volume. End-effector size is constrained such that it must be sufficiently compact to fit through the narrowest aperture, while having sufficient reach to access the widest spaced teats.

A solid model of the region under the udder in which the milking cups must be positioned was constructed from the biometric data in Table 2, as shown in Figure 22. The orange region denotes the area in which teats may be located, while the yellow cross-hair marks the arithmetic averages of the mean teat positions.

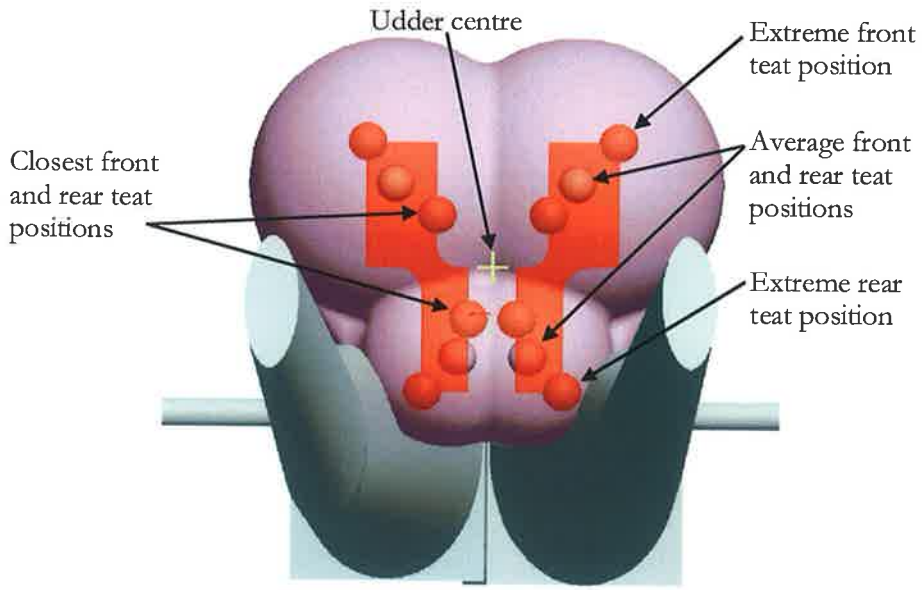

Figure 22. Teat position areas (teat diameter to scale, Ø27mm)

While teat positions are rarely symmetrical about a centre point as in the model, it was assumed that increasing the reach of the end-effector by a small margin would allow access to moderately skewed teat configurations.

Finally, the solid models of biometric data were combined with a solid model of a single stall to form a complete model of the workspace, shown in Figure 23. This solid model contains all parameters of the workspace, allowing visualization and testing of the end-effector design in software.

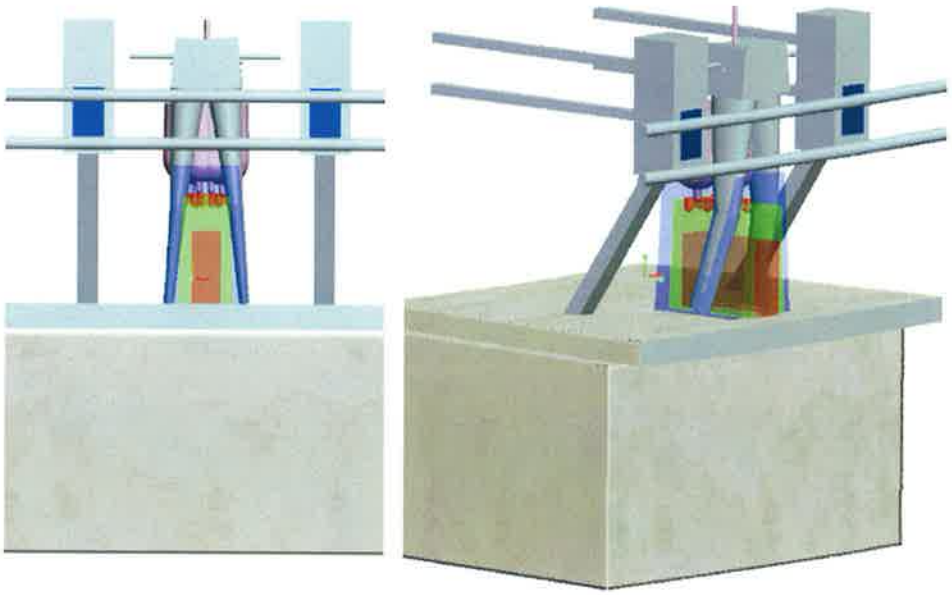

Figure 23. Solid model of complete workspace

2.2 Milking cup types and properties

The payload for the robotic manipulator is a milking-cup cluster so characteristics and measurements of milking-cups were required for end-effector design. Many brands of milking cups are available on the market, leading to some variation in size and style between manufacturers. Certain aspects of milking cup design are governed by international standard for best practice [55], with cup configuration and mode of operation remaining as described in section 1.3.1. Variations in manufacturer design affect cup shell diameter, cup height, liner mouthpiece diameter, liner head diameter and milking line diameter and material (and hence flexibility). Cup shell material is usually stainless steel, due to its toughness and corrosion resistance. Plastic cups are available, however resistance to impact and heavy compression (kicking or stepping by a cow) is lower than with steel and these are less preferable.

Figure 24 shows parameters of the milking cup affecting end-effector design. Overall height of the shell affects access of the end-effector to the teats, with a shorter height being more desirable. Liner head diameter determines the minimum

distance between teats that may be accommodated with automatic application (i.e. one liner head diameter). Cup shell diameter affects parameters of the cup-gripping device on the end-effector, with a smaller diameter contributing to more compact design.

Mouthpiece diameter has an impact on positioning performance of the robotic manipulator: where the teat is narrower than the mouthpiece, a larger degree of positioning error may be accommodated than if the teat is larger than the mouthpiece. Application is therefore more likely to succeed for narrower teats. Unfortunately, choice of mouthpiece diameter is determined by the physical characteristics and by milking process requirements and thus is not variable for application requirements. However it has been observed that due to the negative pressure within the cup liner and compliance of the teat, the teat is sucked strongly into the cup, even when positioning is off by several millimetres. This side-effect of milking cup design is highly favourable for cup positioning, increasing allowable positioning error.

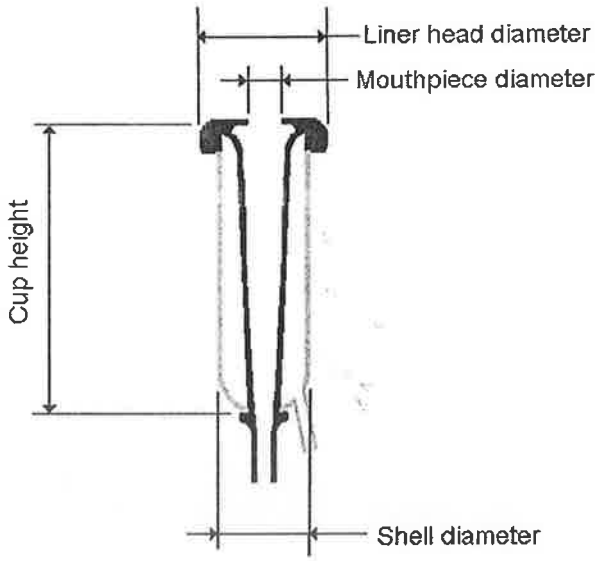

Figure 24. Milking cup parameters

Observed milking lines using rubber materials (nitrile or silicon) tend to have a larger diameter and wall thickness to withstand the milking vacuum, resulting in higher stiffness. Increased stiffness affects the handling characteristics of the cup, as extra force is required for manoeuvring by the end-effector. Use of thick rubber

milking lines has largely been for convenience in manufacturing (as the cup liner and milking line can be fabricated in one piece), however Teagasc Dairy Research Centre has indicated that milking lines may be replaced by lighter lines allowing better flexibility, and this will be assumed.

A single brand of milking cup was used for end-effector design and testing. The milking cup supplied was a Dairymaster acrylic shell with 916S liner. The shell is normally stainless steel for this design, however the acrylic shell is transparent and more useful during testing and experimentation. Properties of this milking cup are detailed in Table 4.

Property	Unit	Value
Cup height	mm	190
Liner head diameter	mm	57
Shell diameter	mm	45
Mouthpiece diameter	mm	22
Mass, including two x 150mm lengths rubber tubing	g	210

Table 4. Milking cup parameters

2.3 Working with Animals – Ethics and the Duty of Care

Application of automation techniques in animal husbandry must be performed in an ethical manner. A duty of care is owed to animals by those who earn profit from their services, in particular farm animals who are often highly dependent on human management. Such duty is enshrined in law at national [56] and European level [57], placing the onus of care on the owner and manager of animals and imposing penalties for those who fail to comply. The European Communities (Protection of Animals Kept for Farming Purposes) Regulations, 2000, states the following:

> *4. (1)* The owner or keeper of animals shall take all reasonable steps to ensure the welfare of the animals under their care and to ensure that such animals are not caused any unnecessary pain, suffering or injury.

An injury sustained by an animal during milking from a robotic manipulator may fall into the category of "unnecessary suffering". Thus, in designing a manipulator to operate in close proximity to an animal, all care must be taken to ensure safety for the animal. "Failure to take reasonable steps to ensure welfare" includes errors of omission in control algorithms that may lead to unpredicted contact with the animal, as well as more obvious dangers such as allowing high-speed operation of the end-effector close to the animal.

To discharge the duty of care in a responsible manner, it is the design policy of this project that system design will keep welfare of the cow clearly in mind and performance will err on the side of cow safety.

2.3.2 Interaction of cow and machinery

Two interviews with experienced dairy farmers indicated that cows adapt quickly and quietly to farm machinery. This was verified by observation of cows in two rotary parlours, where cows walked onto the rotary carousel with its associated moving and noisy machinery without coercion. Noise level of milking equipment did not appear to affect cow comfort, and most cows waited patiently for milking cup attachment with little rear leg movement. In two cases, cows which were being milked for the first time were noticeably uncomfortable, moved agitatedly and kicked the milking cups off the udder. Investigation revealed that such cows should have been trained on the rotary parlour (i.e. passed through a cycle on the carousel without being milked) to accustom them to the process. According to the farmer these cows would become comfortable with the milking parlour after one to two milking sessions. Two conclusions may be drawn from these observations:

Firstly, cows will adapt quickly to new machinery in the parlour and will not experience undue stress as a consequence of introduction of a robot arm. Application of milking cups from the rear of the cow would provide a further advantage in that the manipulator is out of sight of the animal.

Secondly, structured management of new cows in the parlour is vital for automated milking cup attachment, as the risk of injury to a frightened and untrained cow is not permissible. A system whereby cows were introduced to the parlour with

manual application of milking cups would seem suitable. However, with welfare of the animal in mind it seems that some active mechanism, such as a leg-restraint, must be incorporated to prevent the animal from coming into contact with the manipulator during application. Such a device was used by Gascoigne Melotte [27][20] as discussed in Section 1.6.1.3, and passive devices for encouraging leg-spreading (e.g. gratings in the floor (Galaxy) are currently incorporated in AMS.

2.4 Environmental assumptions

There are many variables to consider when incorporating a robotic manipulator into a milking parlour and several additional projects would be necessary for complete integration. As this is a proof of concept design, several assumptions were made about the working environment:

2.4.1 Animal behaviour and control assumptions

- Cows are managed and trained so as to be comfortable and docile on the carousel
- Some form of active leg restraint is employed to prevent cow contact with the manipulator during milking cup application
- A sensor is provided to detect unusual movement of the cow and provide a signal to abort application
- Teat positions are detected separately and provided to the manipulator control system in real-time
- The cow tail is held aside by some device

2.4.2 Parlour assumptions

- The rotary carousel control system provides a signal to indicate when a stall is in front of the manipulator
- The rotary carousel may be halted by a signal from the manipulator control system until application is complete
- Some means of preventing fouling of the manipulator by the cow is provided

2.4.3 Milking equipment assumptions

- Milking cluster is provided for pick-up at a known location (the cluster does not have to be detected and assembled by the manipulator)

- Milking tubes are of sufficient length and flexibility to accommodate all movements of the manipulator
- The milking equipment incorporates a sensor to determine when the teat is in the cup, and provides a signal to this effect

2.4.4 End-effector assumptions

- As a consequence of the preceding assumption that a signal is provided when the teat is in the cup, a common z-axis for all teat cups is assumed, i.e. individual cups will not have independent z-axis movement.

2.4.5 Design philosophy

- Modular design with off-the shelf components will be preferred, rather than custom designed and manufactured parts

2.5 Analysis of approach methods

Approach to the animal for application of milking cups was broken down into three areas: direction of approach, sequence of application and speed of application cycle. Approach methods for milking cup application were selected for minimal interference with the conventional rotary parlour layout.

2.5.1 Application cycle and timing

The application cycle consists of collecting the milking cups, detection of teat positions, application of cups and exit from under the cow. Operation of the manipulator in a high-speed parlour requires minimisation of application cycle time. Speed of application was established using existing manual methods as a benchmark: a recent study on Irish farms [4] and a previous study [58] showed that manual application time for a complete cluster is approximately 20 seconds, while measurements taken in a working rotary parlour showed that application time could be as low as ten seconds.

While a 20 second application time would be ideal, practical difficulties in sensing teat position and concern for safety dictated a higher target time. An initial target time of 30 seconds was chosen for the cycle time, allowing for slower operation of the manipulator and more time for teat position verification.

2.5.2 Direction of access and application sequence

Minimising cycle time requires that the shortest approach route and fastest application sequence be determined. As described by Rossing and Hogewerf [18], milking cups may be attached from the side, rear or underneath the cow and either sequentially, two-at-a-time or with all four applied simultaneously.

Approach from directly underneath the cow would require significant modifications to the floor of the stall, so such a method was ruled out.

Current AMS approach from the side of the cow, avoiding the risk of fouling present at the rear of the cow, but without providing a significantly larger access aperture to the udder. From Figure 25 it is clear that to avoid the movement regions of the legs the end-effector must approach the udder in a longitudinal direction (L_s), with practically the same constraints experienced as for application from the rear (L_r).

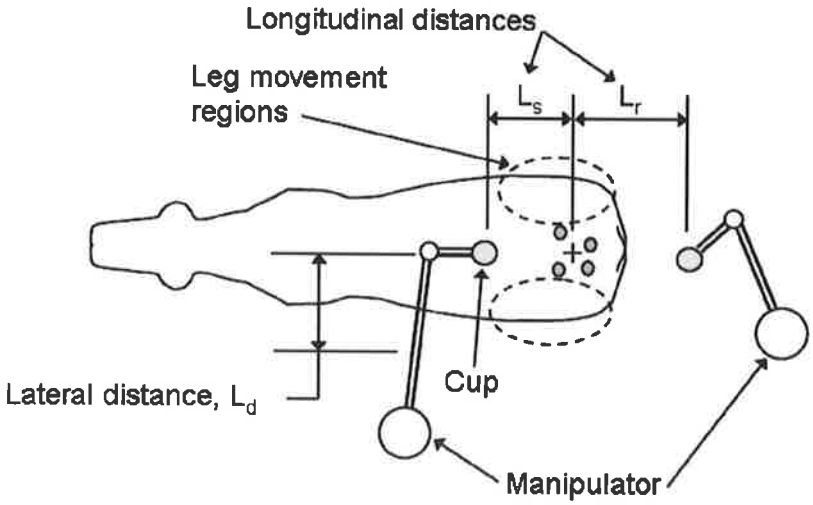

Figure 25. Comparison of approach distances from side and rear

2.5.1 Motion analysis

A motion analysis was performed to determine the travel time for application from the side or rear with various cup application sequences. With reference to Figure 25, equations 1-3 show times for sequential application from the side with a single cup at the end-effector, t_{ss1}, all four coups held at the end-effector, t_{ss4}, and simultaneous

application of all four cups, t_{sc}. Small movements underneath the udder (from udder centre to each teat) are designated l_t.

$$t_{ss1} = 8t_{L_d} + 8t_{L_s} + 3t_{l_t} \quad \text{eqn. 1}$$

$$t_{ss4} = 2t_{L_d} + 2t_{L_s} + 3t_{l_t} \quad \text{eqn. 2}$$

$$t_{sc} = 2t_{L_d} + 2t_{L_s} \quad \text{eqn. 3}$$

From these three equations, it is clear that simultaneous application provides the fastest application tine, while holding four cups at the end-effector greatly increases the speed of application for sequential application. For single-cup acquisition, t_{ss1}, the time taken to acquire each cup from a magazine was neglected. The difference in application speed between t_{ss4} and t_{sc} depends on time for small movements between teats, t_{lt}. In turn, t_{lt} is limited by the speed with which teat positions can be sensed after each milking cup application. Observation of current AMS (using manufacturer demonstration videos) has shown that detection time is high and thus t_{ss4} would be significantly longer than t_{sc}.

Equations 4-6 show the application time for application from the rear for sequential application with a single cup in the end-effector, t_{rs1}, all four cups held at the end-effector, t_{rs4}, and simultaneous application of all four cups, t_{rc}.

$$t_{rs1} = 8t_{L_r} + 3t_{l_t} \quad \text{eqn. 4}$$

$$t_{rs4} = 2t_{L_r} + 3t_{l_t} \quad \text{eqn. 5}$$

$$t_{rc} = 2t_{L_r} \quad \text{eqn. 6}$$

Again, it is clear that simultaneous application is the fastest technique.

Assuming distances L_r and L_s to be of similar magnitude, then travel distance for side application will always be greater by the lateral distance L_d. Comparison of

equations 6 and 3 shows that application from the rear provides a time advantage of $2t_{1,d}$.

Based on this motion analysis simultaneous application of milking cups from the rear of the cow was selected as the most suitable application technique. Such an approach has the advantages of reducing cycle time by minimising access distance to the teats and improving safety by minimising manipulator travel under the cow. In the event of an emergency in which rapid exit of the end-effector is necessary, a rear approach provides a shorter and safer exit path from the workspace. Risk of equipment fouling is present at the rear of the cow, however it has been assumed that some shield will be in place to minimise this risk and observation in rotary parlours has shown that fouling during milking cup application is infrequent is infrequent.

Simultaneous application has the disadvantage that manoeuvring space for the manipulator is restricted by the presence of the entire cluster, as illustrated in Figure 26. Design of the end-effector and choice of robot arm should provide maximum dexterity in this limited workspace.

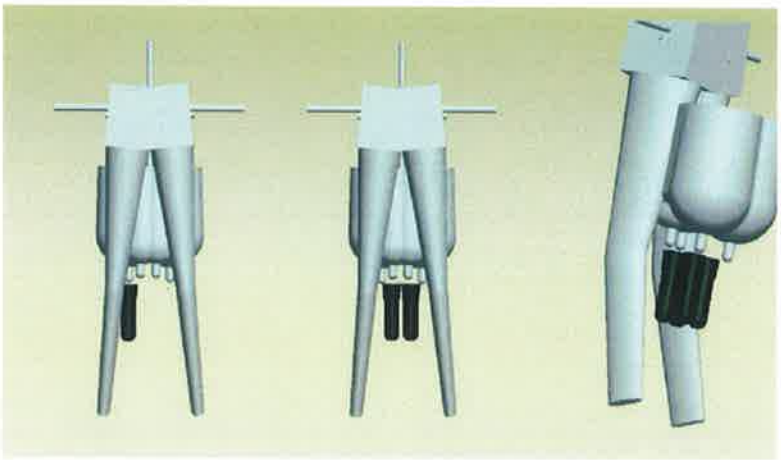

Figure 26. Workspace with single cup (left), two cups (centre) and four cups (right)

2.5.4 Exit strategy

Post-application exit strategy must be considered to avoid interfering with applied milking cups. Simultaneous application results in a complete cluster and associated

milk and vacuum lines occupying the workspace, reducing the exit aperture for the end-effector. End-effector design must take this into account, providing for an exit that does not dislodge applied cups or catch the milking lines.

2.5.5 Positioning performance

Real-time teat position detection was presumed for this design, however some knowledge of the limitations of teat detection speed and coordinate output frequency was required, as these affect the performance requirements of the end-effector. A teat-detection system tested at Dublin City University was found capable of outputting all four teat coordinates at 10Hz, but with robust performance achievable only under highly controlled lighting conditions. Assuming that a reduction in output frequency to 5Hz would increase robustness, then positioning response time for milking cups should be less than 200ms to ensure that small movements of the teats during application can be accurately tracked.

As the udder of the cow has no internal motive muscles, it was reasoned that significant movement of teats (neglecting miniscule movements due to breathing, pulse, etc.) must be caused by skeletal movement and hence movement of the legs. As part of an overall safety algorithm, large movements in teat position would therefore be interpreted as abnormal motion of the cow and some delay or escape strategy would be executed to allow teat position to stabilise. Therefore the range of 'small movements' of teats that must be tracked during the 200ms interval was arbitrarily defined as +/-20mm, with a more accurate value to be determined by later trial and observation.

As mentioned in section 2.1.3, teat compliance coupled with the vacuum inside the teat cup can compensate for a significant misalignment between the centre of the cup and the centre of the teat. This was observed as up to 10mm, while a figure of 4mm was assumed to be a reasonable average for misalignment. With this in mind, positioning accuracy was specified as +/-2mm. Within this region there is a high likelihood of application success.

2.6 Summary

Workspace parameters were determined and characteristics peculiar to working with live dairy cows were analysed. A solid model of the workspace was constructed containing stall and biometric data to allow software visualisation and concept testing during the design process. Measurements of milking-cups were made to determine manipulator payload and provide parameters for design of an end-effector gripping method. Ethical considerations affecting introduction of automation to animal husbandry were reviewed leading to a design policy for ensuring welfare of the animal, while observation of the interaction between animal and machinery was carried out to determine the effects of machinery presence and noise on the cow in a parlour environment.

Application cycle was defined and a target application time was selected based on automation requirements and safety considerations. Additionally, a motion analysis was carried out to determine the most suitable approach direction to the cow and application sequence for milking cups. It was determined form this analysis that approach from the rear of the cow would minimise manipulator travel under the cow, thus reducing cycle time and improving safety. Simultaneous cup application was shown to be the fastest application method, providing a significant decrease in application cycle time.

Chapter 3

END-EFFECTOR CONCEPTUAL DESIGN AND DETAILED DESIGN

3.1 End-effector product design specification

A product design specification (PDS), shown in Table 5, was generated for the end-effector based on established constraints and known parameters. The PDS establishes discrete design goals and is the reference for evaluating the final design.

Table 5. End-effector PDS

Performance
1. Independent positioning of each cup in the horizontal plane shall be provided within respective positioning region under the teats
2. Positioning response time of each cup for small movements of +/-20mm shall be less than 200ms
3. Cups shall be positioned with an accuracy of +/-2mm with respect to the centre of the teat tip
4. Sufficient force shall be available to handle each milking cup mass of 0.21kg, and associated milking lines
5. A gripping device for each cup must be provided capable of holding the cup securely and rigidly during manoeuvring
6. The gripping device shall have rapid acquisition and release times
7. As common z-axis motion is assumed, cups shall be released independently as each teat is acquired
8. Each axis shall have a home sensor to provide an accurate positional reference
9. Where applicable limit switches shall be used to prevent axis over-travel
Economy
1. As a prototype design end-effector costs may be high, but components, materials and processes shall not be prohibitively expensive
Quantity
1. One end-effector is required
2. Analysis and recommendations for improvements on subsequent design shall be made
Manufacturing facilities
1. Dublin City University mechanical engineering workshop

Table 5 (cont.). End-effector PDS
Customers
1. The manipulator will be used by skilled research staff at Dublin City University and Teagasc Moorepark Research centre
Service life
1. Service life suitable for non-intensive research activities lasting 1-2 years
Environment
1. Ambient temperature: +5° to 45° C (sheltered indoors) 2. Pressure: normal atmospheric 3. Humidity: damp environment, up to 85%RH 4. Dust and dirt (including cow excrement) may be present 5. Environment may be wet or contain spray due to washing
Size
1. The end-effector with attached payload must be capable of fitting through an minimum aperture 291mm tall and 184mm wide 2. Individual teat cup movement range must be a minimum of 45mm (longitudinal axis) by 90mm (lateral axis) for front teats 3. Individual teat cup movement range must be a minimum of45mm (longitudinal axis) by 50mm (lateral axis) for rear teats 4. Reach under the cow must be 250mm
Weight
1. End-effector weight shall be minimised to reduce size and cost of the robot arm 2. Weight distribution shall be as close as possible to the robot arm attachment point to reduce moment of inertia and improve positioning performance
Maintenance
1. Low-maintenance design is preferred, however for prototype design higher maintenance such as regular greasing or oiling is acceptable
Materials
1. Materials used must be readily obtainable locally and machineable by DCU workshop or readily available contractors 2. Where possible, materials that do not require additional treatment or coating for corrosion resistance shall be utilised
Finish
1. Aesthetic appearance is not overly important. Finish may be as-machined/supplied for all components
Testing
1. End-effector dimensions will be checked for compatibility with the access aperture model 2. End-effector positioning accuracy and precision will be tested 3. Positioning response time will be tested for small movements

Table 5 (cont.). End-effector PDS
Safety
1. Limit sensors will be incorporated to prevent axis over-travel
2. Sharp corners shall be removed or padded to reduce severity of contact injury with animal
3. Wires and air lines (if used) shall be protected from abrasion or impact damage

3.2 Concept generation and solid modelling

Based on the outline PDS and workspace analysis, several conceptual designs were generated for the end-effector as detailed in the following sections. Cartesian axis arrangements as illustrated in Figure 27B, were used in the Gascoigne Melotte design described in the literature survey[27][38]; however this method was observed to be much less compact and required complex mechanisms and component arrangements to reduce end-effector size. The Gascoigne Melotte end-effector was not designed for removal after application of milking cups due to its large size, and remained in position until milking was complete. Various configurations of double-revolute axis arms as shown in Figure 27A were also considered. This configuration is used on industrial SCARA robots, but the designs required significant mechanical complexity for incorporating actuators, were less dimensionally compact and thus unsuitable for the confined workspace of this application. All four concepts detailed in the following sections utilise a compact wrist-forearm mechanism (described in section 3.2.1). This mechanism combines features of both revolute and Cartesian mechanisms, exhibiting several advantages in terms of actuator configuration and dimensional compactness. The wrist-forearm mechanism was thus selected as the basis for creating further solid-model conceptual designs.

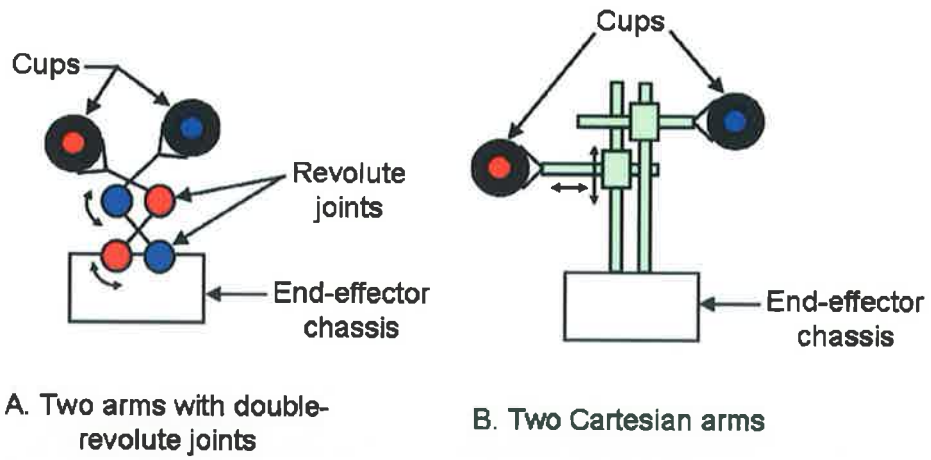

Figure 27. Double-revolute (A) and Cartesian (B) arm configurations

3.2.1 Concept 1

Figure 28 shows a conceptual design for an end-effector with four positioning arms mounted on a chassis. Each arm comprises a linear axis formed by a linear slide running on support bearings, and a revolute arm attached at the end of the linear slide that can be rotated through 90°. The arms are stacked in pairs, with the lower pair used for manipulating the front cups and the upper pair for the rear cups. The front pair of grippers face to the rear, while the rear grippers face to the front, allowing all four cups to be picked up as a single group using a clamping action between front and rear grippers. Gripper design was not specified at this stage, so grippers were represented by simple v-shapes. Linear actuators are shown for each axis, with the revolute arm actuated via a short crank mechanism. Attachment to a robot arm may be provided at mounting flanges A or B.

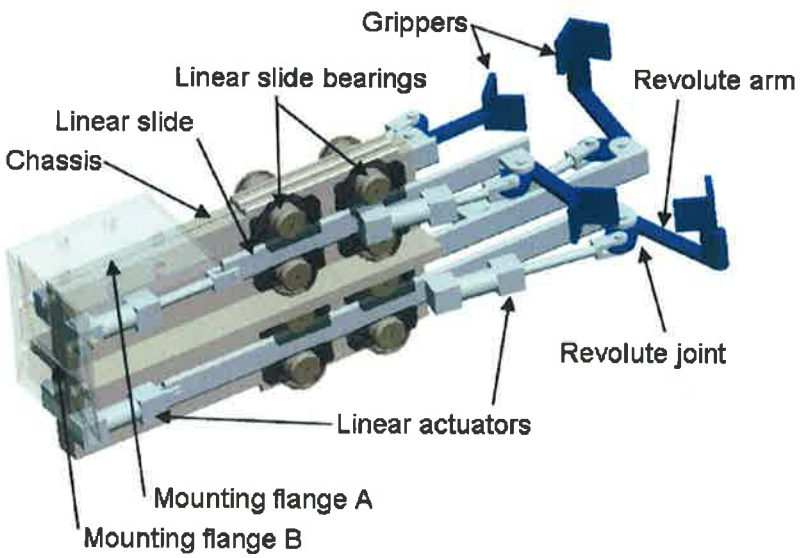

Figure 28. Concept 1

Use of a linear axis coupled to a revolute axis in this manner forms a mechanism that mimics a human wrist and forearm, providing coverage of a horizontal area as shown in Figure 29. A solid green outline indicates the boundary of an area covered with a linear travel distance and an angular travel (in this case 90°), while the hatched green area shows the practical rectangular area that can be utilised. The two

sections outside of this rectangular area may be used, but insufficient reach is provided in the lateral direction to reach all possible teat configurations.

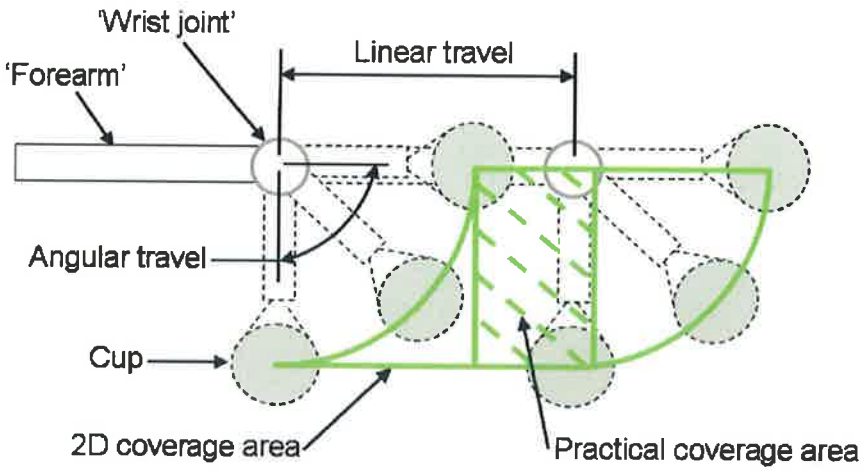

Figure 29. 2D area covered using a wrist-forearm mechanism

This wrist-forearm mechanism requires a longer linear axis travel than an equivalent Cartesian system, but its primary advantage is the narrow frontal profile provided when the revolute arm is in line with the linear axis as demonstrated in Figure 30.

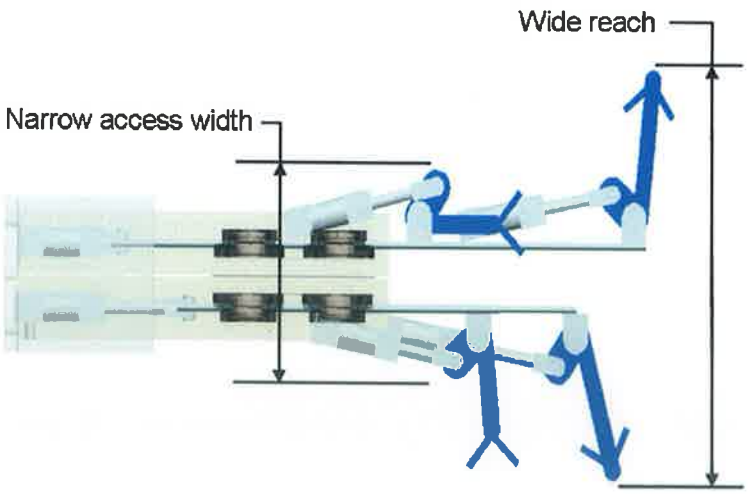

Figure 30. Access width and reach for wrist-forearm mechanism

When inserted into the workspace as shown in the left image in Figure 31, it can be seen that the narrow access profile allows access through the narrowest access aperture (the red volume). At the same time, the reach of the revolute arms allows the cups to move behind the legs if necessary for teat access as shown in the right image in Figure 31.

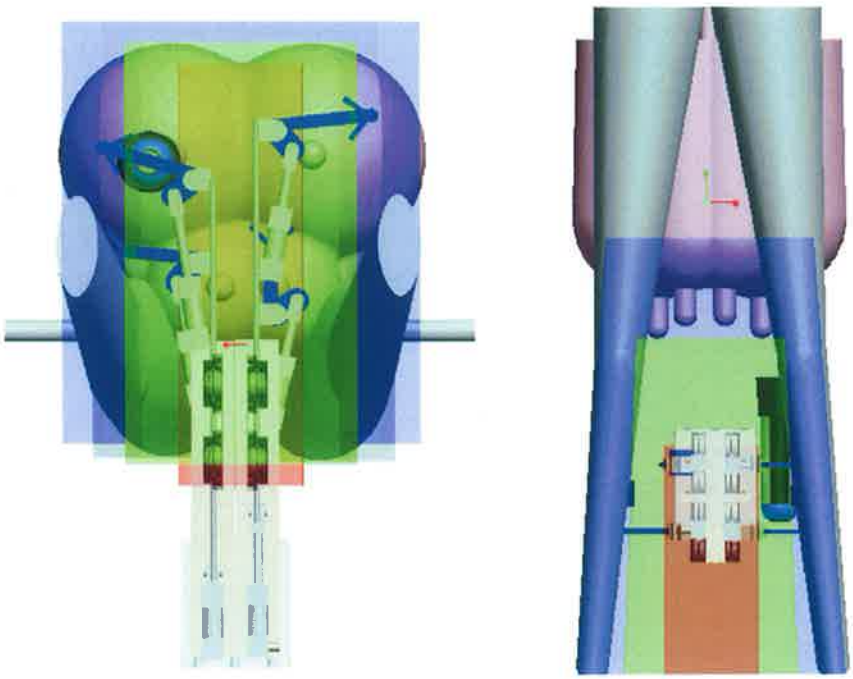

Figure 31. Concept 1 inserted into workspace (to approximate scale)

Use of stacked pairs of arms in this concept results in a taller end-effector, reducing freedom of movement in the workspace, however some improvement may be obtained by careful positioning of the linear slide bearings to minimise distance between upper and lower arms.

Weight distribution for this concept is around the centre of the end-effector, resulting in a larger moment of inertia and increasing the required robot arm capacity. Some improvement might be obtained through repositioning of the linear actuators. Use of linear actuators would allow direct actuation and simple control; however linear actuators and linear position sensors tend occupy a larger volume than equivalent capacity rotational actuators. Use of a linear actuator for the

revolute axis limits the movement range available to approximately 90° (while 180° of motion is theoretically obtainable, torque is greatly reduced at extremes of travel).

3.2.2 Concept 2

A second conceptual design using four parallel arms and rotational actuators was developed as shown in Figure 32. As for Concept 1, grippers are represented by simple v-shapes.

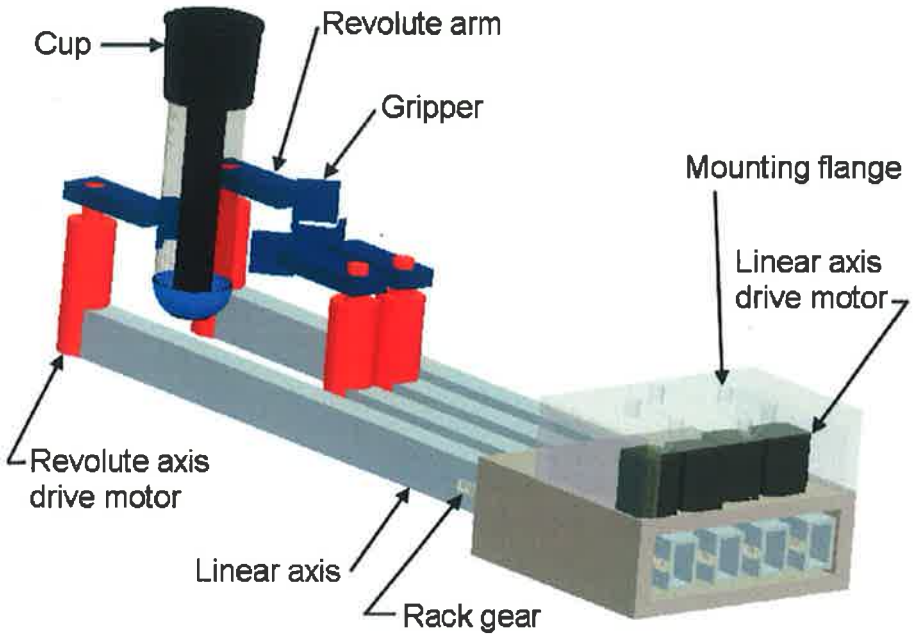

Figure 32. Concept 2

By placing the arms in parallel, the height of the end-effector was reduced to provide better vertical clearance in the workspace. Use of rotational drives for all axes avoids the dimensional and cost disadvantages of linear actuators, allowing a more compact and economic design. The linear axes are driven via rack and pinion gearing, with motors positioned at the rear of the end-effector to bias mass distribution towards the rear. The revolute axes are driven directly by motors, eliminating the need for mechanical linkages, but adding more mass at the end of the end-effector. A mounting flange for the robot arm is provided at the top of the end-effector chassis, allowing room for the linear axes to protrude from the rear if

necessary. Linear axis bearings are not shown, but could be of similar style to those of concept 1.

Figure 33 shows two views of concept 2 inserted in the workspace model. The left image shows that while vertical clearance is good, the end-effector is slightly wider than the narrowest access aperture (the red volume). This width could be reduced somewhat by careful design; however lateral manoeuvring space would still be reduced, particularly during exit when it may be desirable to rotate the end-effector to one side to avoid tangling with milking lines. The right image in Figure 33 shows that the weight distribution is improved over concept 1, with a large proportion of the mass near the flange mount.

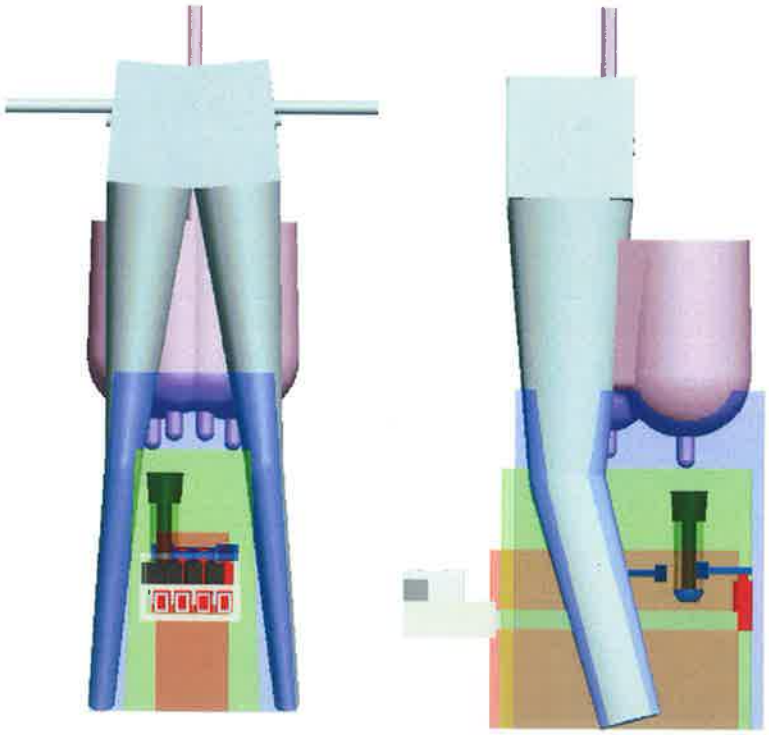

Figure 33. Concept 2 inserted in workspace (to approximate scale)

The advantages of the wrist-forearm mechanism were preserved in this design, however because the front and rear gripper sets are not aligned, it would be more difficult to pick up a cluster of four cups using a clamping action between front and rear grippers. Additionally, the unsupported length of the longer linear axes would

reduce torsion and bending stiffness of the design, requiring larger and heavier arm sections.

Use of rotational actuators simplifies position sensing, as rotary position encoders may be attached or built-in to the motor casing. Having electrical motors and associated sensors mounted at the end of the end-effector carries a risk of increased exposure to damage, however such a risk may be managed by careful design and shielding of components.

3.2.3 Concept 3

A third concept was developed combining rotational actuators for all axes with the stacked arm feature of concept 1. As shown in Figure 34, the design has a compact frontal profile, with relatively low height and narrow width.

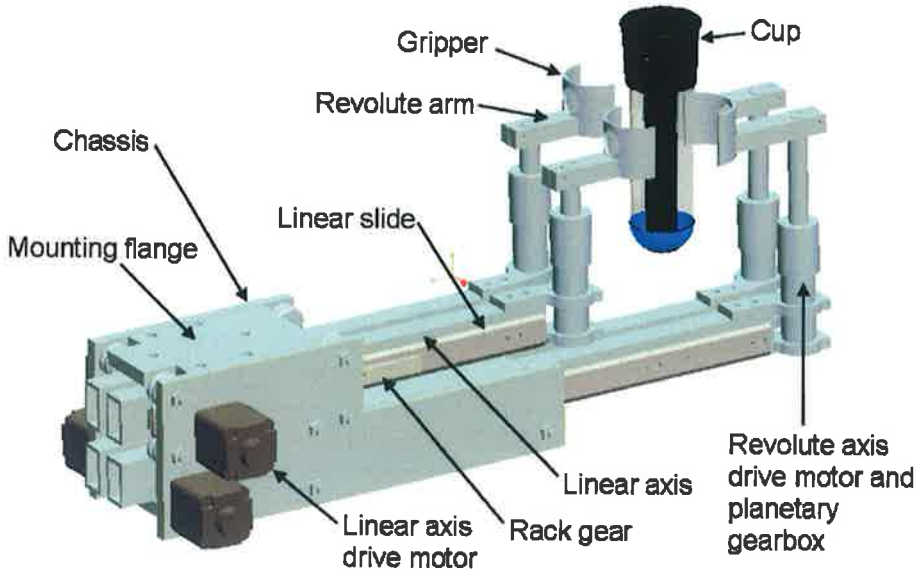

Figure 34. Concept 3

Torsional and bending stiffness for the longer linear axes is improved in this design by extending the chassis forward to provide bearing support for the lower arms. Revolute drive via rack and pinion gearing is used for the linear axes, as with concept 2. The linear axes are supported by a compact arrangement of linear slides and grooved roller bearings. Mass of the revolute axis drive motors has been

reduced by adding gearboxes to improve torque and allow smaller, lighter motors to be used but at the expense of a small increase in height of the revolute axes.

Figure 35 shows concept 3 inserted into the workspace model. The end-effector chassis fits inside the narrowest access aperture, while maintaining sufficient reach to access teats. Vertical height is slightly greater than for concept 2, however sufficient space is available for operation. Mass distribution is biased towards the rear, with much of the distributed near the mounting flange, and mass at the end of the end-effector reduced by use of smaller revolute axis motors.

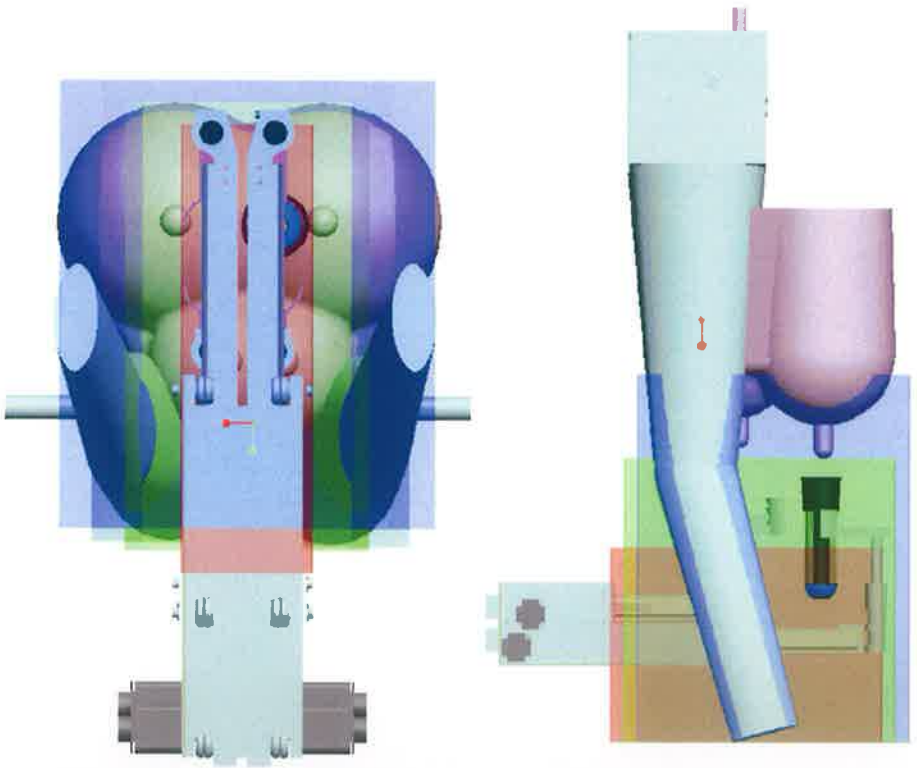

Figure 35. Concept 3 inserted into workspace (to approximate scale)

3.2.4 Concept 4

A modification of concept 3 was considered in which the revolute axis actuators were positioned at the rear end of the linear arm, with the driving force transmitted through the centre of the linear arm either by drive shaft or push-rod. A solid model of this concept is shown in Figure 36 (with only two arms shown).

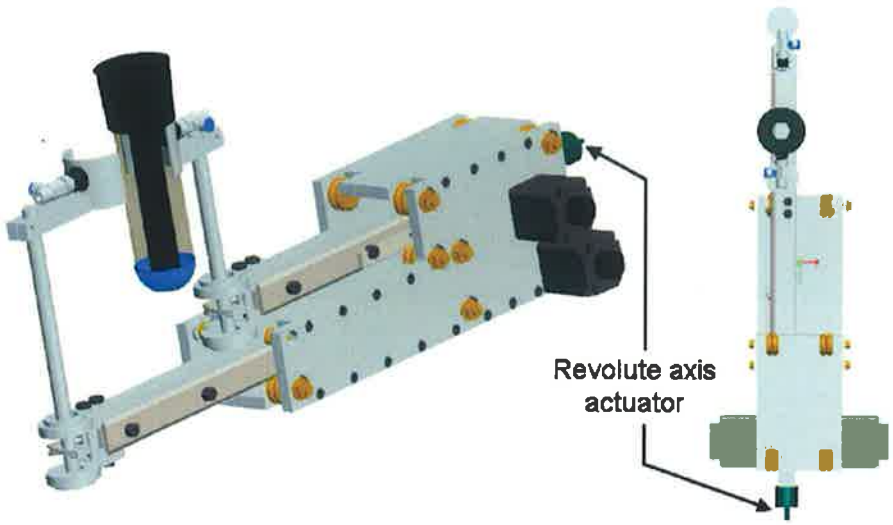

Figure 36. Concept 4

This concept provides excellent mass distribution, having all actuators situated close to the rear and serving to counter-balance some of the extended mass of the arms. Mass at the revolute axes is reduced in this design, reducing the moment of inertia of the end-effector about the mounting point and reducing exposure of the revolute drive actuators to damage. However transmission of force through the centre of the arms presents some design problems. In the case of a rotational drive, the linear arm cross-sectional area would be limited by the diameter of the drive-shaft, which must have good torsional stiffness. The linear arm section would therefore likely be larger than for concept 3, in which only electrical, signal and air/vacuum lines need be routed through the arm. A similar limitation would apply if a push-rod were used to actuate the revolute axis via a crank mechanism, as the push-rod must be sufficiently stiff to resist bending. Additionally, a crank mechanism would limit the range of angular motion available, similar to concept 1. This latter limitation could

be overcome by using a rack-and pinion mechanism, but such a mechanism is more complicated than and not as compact as a crank mechanism. Use of thin cables to drive the revolute axis would be possible, although difficulties can arise from thermal expansion and elasticity over long lengths and a larger arm section would be required. Overall, concept 4 would provide excellent balance and actuator protection for a production model; however the lack of movement range for the revolute axes limits its flexibility as a test platform and the additional complexity of the revolute actuation linkage would increase complexity and cost.

3.3 Concept weighting

A weighting method was used to select the most suitable design from the design concepts, shown in Table 6. Weights from 1 to 3 were assigned to design attributes according to their significance for operation, while the attributes were scored from 1 to 5 with 5 representing the best score. From the weighting process, concepts 2 and 4 were shown to be closely matched. Concept 3 scored higher primarily due to narrower width, allowing better manoeuvrability within the workspace, and better arm support to improve stiffness and allow reduced arm mass. Concept 2 would have slightly lower overall mass due to a smaller chassis, while concept 4 provides optimal mass distribution. The majority of other attributes for concepts 2 to 4 had similar scores, but with concept 4 losing out due to increased design complexity and associated costs. Concept 1 was scored lower due to higher mass and increased design complexity associated with use of linear actuators.

			Score (1-5) x Weight			
Attribute	**High score criterion**	**Weight (1-3)**	**Concept 1**	**Concept 2**	**Concept 3**	**Concept 4**
Reach to teats	large reach area	3	15	15	15	15
Height	low height	3	9	12	12	15
Width	narrow width	3	12	9	15	15
Arm stiffness	higher stiffness	2	10	8	6	10
Mass	low mass	2	4	10	10	10
Mass distribution	toward flange	2	6	8	10	10
Mechanism complexity	low complexity	2	6	12	12	4
Materials cost	low cost	2	6	8	8	6
Ease of manufacture	easier manufacture	2	4	8	8	4
Actuator cost	lower cost	2	4	8	8	8
Actuator complexity	lower complexity	1	2	5	5	5
Total score			78	103	109	102

Table 6. End-effector concept weighting matrix

3.4 Final design selection

Due to the closeness between scoring of the final three concepts, careful selection was made based on the product design specification. Concept 4, while certainly worthy of consideration for a production version of the end-effector, has limited flexibility for testing and experimentation (i.e. the revolute arm cannot rotate 360 degrees without provision of a complex mechanism at the revolute joint) and would require larger linear arm sections. The extended chassis of concept 3 could be incorporated in concept 2 to increase stiffness and allow reduced arm mass. However, from a performance perspective the more compact frontal profile of concept 3 allows better manoeuvrability within the workspace for access and exit, decreased likelihood of collision with the animal and thus improved safety. Increased clearance from the animal would also allow higher operating speed, resulting in improved performance. For this reason, concept 3 was selected as the most suitable design for further development.

3.5 End-effector coordinate system and kinematic analysis

This section describes the assignment of a coordinate system for the end-effector and analysis of the forward and inverse kinematics of the wrist-forearm mechanism. A basic forward kinematic analysis is used to isolate and define control variables, allowing the type and location of feedback sensors to be specified for the end-effector design. The inverse kinematics of the wrist-forearm mechanism provides the mathematical basis for position control of the end-effector cups.

3.5.1 End-effector coordinate system

A coordinate system for the end-effector was chosen based on the international standard for revolute robot coordinate systems (RCS). Figure 37 illustrates the RCS: a right-handed coordinate system with the origin located at the base of the robot, the positive z-axis in the vertical direction and the positive x-axis pointing away from the origin. Alignment of the end-effector coordinate system with the RCS as shown in the diagram simplifies control system transformations between coordinate systems. Thus the end-effector longitudinal axis was defined as the x-axis, the end-effector lateral axis was defined as the y-axis, and vertical movement of the end-effector is therefore along the z-axis.

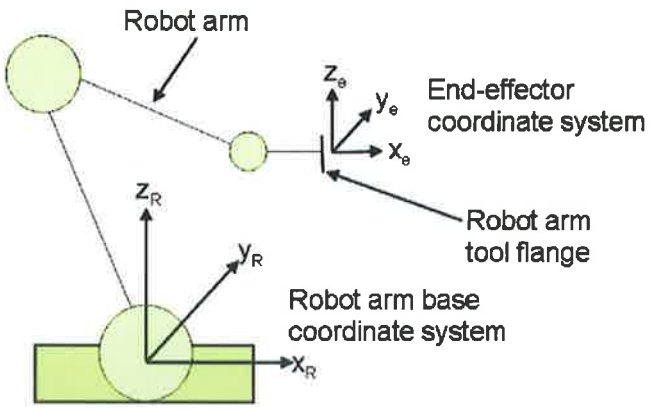

Figure 37. End-effector coordinate system relative to robot coordinate system

3.5.2 End-effector kinematic analysis

A kinematic analysis describes the motion of objects without reference to the forces causing motion. The general layout for the wrist forearm mechanism is shown in Figure 38. The cluster origin is defined as a central point at which all four milking cups are closest together and is located on the end-effector central (x) axis at a constant offset distance, c_O, from the robot arm flange centre (the centre of the tool-flange on the robot wrist to which the end-effector is attached, see Figure 58).

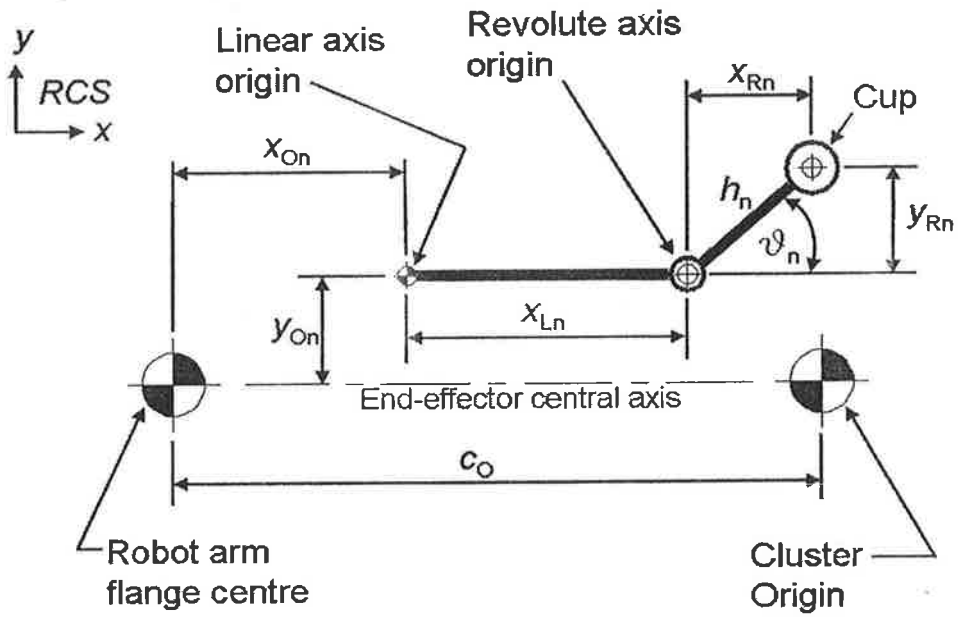

Figure 38. Wrist-Forearm Diagram

As a common z-coordinate was assumed (see section 2.4.4), the z-axis motion is provided by -3the robot arm, and the z-axis position of each cup is equivalent to the robot tool flange z-position plus some constant offset. Table 7 details the end-effector variables and constants for the horizontal plane in Figure 38. The individual arms are labelled from 1 to 4, with odd-numbered arms serving the rear teats and even numbered arms serving the front teats (e.g. x_{L1} = arm holding the rear left teat-cup). The linear axis origin is a reference point on the end-effector chassis from which linear axis extension, x_{Ln}, is measured, while the revolute axis origin is the point about which the revolute arm rotates.

Variable (n = 1,2,3,4)	Definition
x_{Ln}	The linear axis displacement
ϑ_n	Angle of the revolute axis relative to the tool central axis
x_{Rn}	x-component due to angle ϑ_n
y_{Rn}	y-component due to angle ϑ_n
Constant	
x_{On}	A constant offset in the x-direction from the flange centre
y_{On}	A constant offset in the y-direction from the flange centre
h_n	Length of revolute arm (from revolute axis to cup centre)
c_O	Cluster origin offset from robot arm flange centre

Table 7. End-effector variables and constants

The general position vector for the cup, $\vec{s}$, with respect to the robot arm flange centre is:

$$\vec{s}_n = x_n\vec{i} + y_n\vec{j} + z\,\vec{k} \qquad \text{eqn. 7}$$

where displacement of the cup in the x-direction w.r.t. the robot arm flange centre, x_n, is calculated by:

$$x_n = x_{On} + x_{Ln} + x_{Rn} = x_{On} + x_{Ln} + h_n \cos\vartheta_n \qquad \text{eqn. 8}$$

and displacement of the cup in the y-direction, y_n, w.r.t. the robot arm flange centre is found by:

$$y_n = y_{On} + y_{Rn} = y_{On} + h_n \sin\vartheta_n \qquad \text{eqn. 9}$$

In the normally envisaged operating mode each of the four revolute arms has a different operating range for ϑ_n : arm 1 =0 to $\pi/2$, arm 2 = 0 to - $\pi/2$, arm 3 =$\pi/2$ to π, arm 4 = - $\pi/2$ to – π (rads). The value of ϑ_n determines the sign of x_{Rn} and y_{Rn}, e.g for the front two arms x_{Rn} will be negative as the revolute arms face towards the cluster origin and for the right two arms y_{Rn} will be negative as they are on the negative side of the central axis.

Provided that the end-effector coordinate system is maintained parallel to the RCS, the cup position in the RCS is determined by simple addition of coordinates. If the position vector for the tool flange centre, $\vec{f}$, is

$$\vec{f} = a\vec{i} + b\vec{j} + c\vec{k} \qquad \text{eqn. 10}$$

then the position of the cup in the RCS, $\vec{p}$, is obtained by adding eqn.7 and eqn.10:

$$\vec{p} = \vec{f} + \vec{s} = (a+x)\vec{i} + (b+y)\vec{j} + (c+z)\vec{k} \qquad \text{eqn. 11}$$

From the kinematic analysis it was determined that feedback requirements from the end-effector are linear distance, $x_{l,n}$, and angle of rotation, ϑ_n, for each arm. Additionally, the constant values must be accurately known and sensors must be provided to indicate reference (home) positions for each axis. Travel limit sensors are desirable for prevention of over-travel of axes, however in the case of the revolute axes this may not practicable as full rotation may be required for some test configurations; in such cases it may be adequate to provide software travel limits based on angular position feedback.

3.5.3 End-effector inverse kinematics

A forward kinematic analysis is useful for isolating geometric parameters of the end-effector, however for control purposes it is necessary to perform an inverse kinematic analysis. The inverse kinematic analysis is used to determine joint and axis parameters that will achieve a required cup position, and thus forms the basis of the end-effector control model.

Referring again to the general layout for the wrist forearm mechanism shown in Figure 38, the cluster origin is the centre point of the cluster, located on the tool central axis at a constant offset distance, c_O, from the robot arm tool flange centre. During operation, an average of the horizontal teat coordinates may be calculated to provide a single reference point under the udder. The robot arm then positions the end-effector such that the cluster origin coincides with this average teat coordinate and the cluster is thus centred between the four teats. If necessary a weighted average of teat coordinates may be used to bias the cluster origin towards the front

or rear teats. Use of this method allows decoupling of cup motion from horizontal motion of the robot during application of milking cups, as once the cluster origin is positioned at the average teat coordinate under the udder, horizontal motion of the robot is not required, and positioning of cups is achieved by movement of the end-effector arms only.

The notation used in the following section uses a bold italic case for vectors, e.g. $\boldsymbol{q}$, while a leading superscript, e.g. ^{F}, indicates the reference frame for the vector. Superscript R denotes the RCS with origin at the base of the robot, while superscript F denotes the end-effector coordinate system with origin at the robot arm tool flange (as illustrated in Figure 37).

During operation, the tool is moved such that the cluster origin coincides with the average of the teat coordinates, $^{R}\boldsymbol{q}_{AV}$, and the tool central axis is parallel to the x-axis of the RCS:

$$^{R}\boldsymbol{q}_{AV} = (x_{AV}, y_{AV}) \qquad \text{eqn. 12}$$

The required position of the Robot Arm Flange Centre, $^{R}\boldsymbol{q}_{F}$, is then determined by:

$$^{R}\boldsymbol{q}_{F} = {}^{R}\boldsymbol{q}_{AV} - {}^{F}\boldsymbol{q}_{Co} \qquad \text{eqn. 13}$$

where $^{F}\boldsymbol{q}_{Co} = (c_o, 0, 0)$, i.e. the cluster origin is located at a constant positive offset from the tool flange and collinear with the x-axis.

Individual teat coordinates, $^{R}\boldsymbol{q}_{n}$, (n = 1, 2, 3, 4) relative to the RCS are shifted to the Robot Arm Flange Centre coordinate frame, $^{F}\boldsymbol{q}_{n}$, by

$$^{F}\boldsymbol{q}_{n} = {}^{R}\boldsymbol{q}_{n} - {}^{R}\boldsymbol{q}_{F} \qquad \text{eqn. 14}$$

y_{Rn} (defined in Table 7 and Figure 38) is calculated by subtracting the y-offset, y_{On}, from ${}^{F}y_{n}$:

$$y_{Rn} = \left({}^{F}y_{n} - y_{On}\right) \qquad \text{eqn. 15}$$

The absolute value of x_{Rn} is calculated from the h_n and y_{Rn} parameters:

$$|x_{Rn}| = \sqrt{h_n^2 - y_{Rn}^2}$$

To avoid redundant solutions, the sign of x_{Rn} may be assigned per-axis based on the intended geometric configuration, i.e. for the rear teat arms x_{Rn} positive, and for the front teat arms is x_{Rn} negative.

ϑ_n may be calculated using the inverse sine function:

$$\vartheta_n = \sin^{-1}\left(\frac{h_n}{y_{Rn}}\right) \qquad \text{(rad)}$$

However, the sine function becomes inaccurate around 90^0. This problem can be overcome using the atan2 algorithm. The atan2 algorithm handles indeterminacies due to sine and cosine functions at zero crossing points ($x = 0, y = 0$), and avoids the sine and cosine function inaccuracies (close to 90^0 and 0^0 respectively) by evaluating signs separately and calculating the inverse tangent.

$$\vartheta_n = \text{atan2}\left(\frac{y_{Rn}}{x_{Rn}}\right) \qquad \text{(rad)} \qquad \text{eqn. 16}$$

The linear axis displacement, x_{Ln}, is calculated by subtracting x_{On} and x_{Rn} from ${}^{F}x_{n}$:

$$x_{Ln} = \left({}^{F}x_{n} - x_{Rn} - x_{On}\right) \qquad \text{eqn. 17}$$

Equations 12 to 17 allow joint positions on the end-effector and the position of the robot wrist to be specified to achieve desired cup positions. These equations were used in formulating the software control model described in Section 5.

3.6 Torque Requirements Analysis

For this application, the positioning performance parameter of interest each arm is the time taken to move a cup a specified distance. This performance was defined in Section 2.5.5 as a movement of 20mm within 200ms. Rotational actuators were required for all axes of the selected design, therefore torque specifications were specified for each actuator to provide the specified positioning performance.

3.6.1 Linear axis drive theory

Figure 39 shows a schematic of a linear axis driven with a rotational actuator via rack and pinion gearing. The actuator torque, T, produces a force F and is opposed by a net resistive force, R, comprised primarily of bearing and gear friction, electrical cable and milking line drag. Windage resistance may be neglected as the operating speed is low. The linear force produced by a given input torque is determined by the pitch circle diameter (PCD) of the pinion gear.

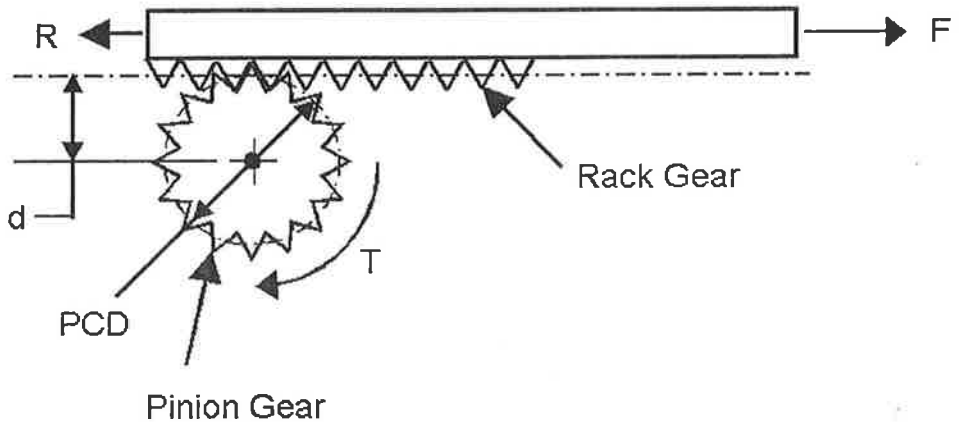

Figure 39. Force and torque for a rack and pinion drive

Assuming rotational inertia of the actuator to be much less than that of the linear axis, the net force required to accelerate the linear axis against the inertia, ma, and the resistive force is given by

$$F - R = ma \Rightarrow F = ma + R \qquad \text{(N)} \qquad \text{eqn. 18}$$

where m is the mass of the complete arm and a is the acceleration.

The torque required to produce F is given by

$$T = Fd \qquad \text{(Nm)} \qquad \text{eqn. 19}$$

where $d = \frac{PCD}{2}$

For DC and stepper motors torque tends to decrease as speed increases, however for lower speed ranges constant torque may be assumed. Therefore if the load on the axis does not change during motion, constant acceleration may be assumed for the linear axis.

The acceleration required to travel a distance, s, within a time interval, t, with zero initial velocity is calculated by

$$s = \frac{1}{2}at^2 \Rightarrow a = \frac{2s}{t^2} \qquad \text{eqn. 20}$$

Assuming a triangular velocity profile, i.e. constant acceleration for t/2 and constant deceleration for t/2 as shown in Figure 40, the maximum required linear actuator torque to travel a distance s in time t may be calculated by combining equations 18, 19 and 20 to give

$$T = d\left(\frac{2m\left(\frac{s}{2}\right)}{\left(\frac{t}{2}\right)^2} + R\right) = d\left(\frac{4ms}{t^2} + R\right) \qquad \text{(Nm)} \qquad \text{eqn. 21}$$

During deceleration the resistive force R will act as a braking force, so the deceleration torque required would be less (by a factor of dR) than that required for acceleration. Because of this effect it could be assumed that R will be cancelled out, but for the sake of completeness and assumption of worst-case conditions R was retained in this equation. Assumption of a triangular velocity profile is valid for short moves, but for longer moves practical limitations of actuator velocity may result in a trapezoidal velocity profile, illustrated by the dashed line in Figure 40.

The associated acceleration profiles, A for the triangular profile and B for the trapezoidal profile, are also illustrated to show the contrast between a short move within the speed limits of the actuator and a long move at which velocity limit is reached. Practical design limitations of the chosen actuators will of course result in some deviation from these idealised profiles, especially as torque tends to reduce at higher speeds.

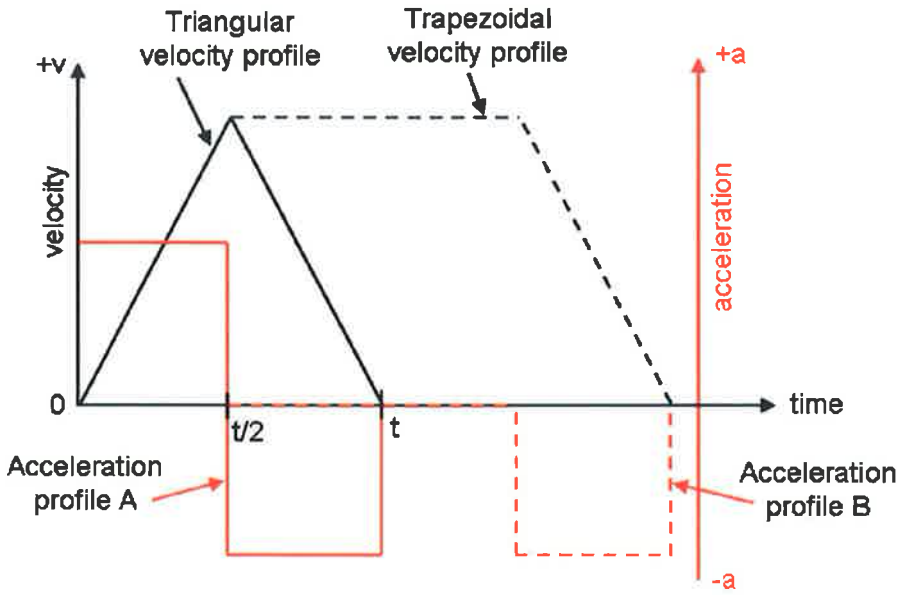

Figure 40. Velocity and acceleration profiles for positioning

3.6.2 Revolute axis drive theory

Figure 41 illustrates the parameters affecting the torque requirements for the revolute actuator. The torque, T, supplied by the motor and gearbox is opposed by the inertia of the revolute arm, gripper and cup, as well as resistance due to the milking line attached to the cup. Rather than attempt to predict milking line resistance forces, it was assumed that these were low and could be modelled as extra mass added to the revolute arm and gripper.

Moment of inertia, I, of the arm components is determined by both the mass of the component and distance from the revolute axis. As the gripper and cup will be close

together during operation, mass of the gripper and mass of the cup may be combined, so only two radial measurements, a and c, are required.

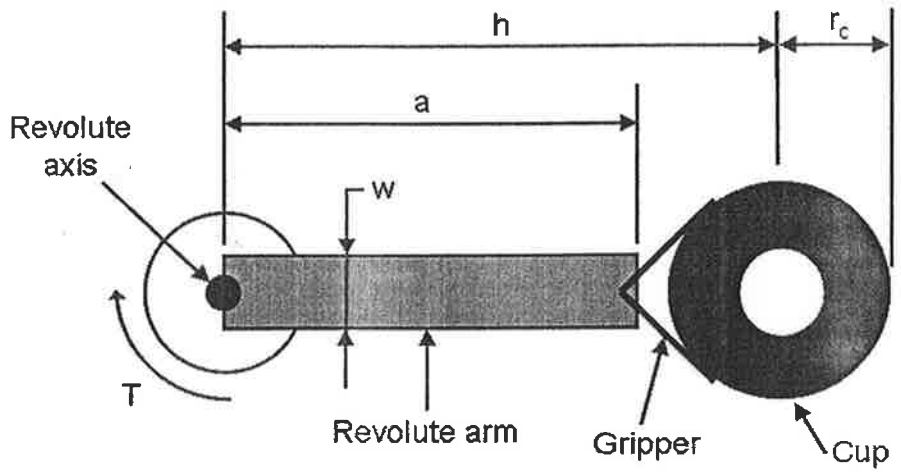

Figure 41. Revolute arm parameters

Torque, T, is given by

$$T = I\alpha \qquad \text{(Nm)} \qquad \text{eqn. 22}$$

where I is the moment of inertia of the arm and α is angular acceleration required.

Treating the milking cup as an upright cylinder of mass m_c and radius r_c, the moment of inertia about the centre of the cup, I_c, is given by

$$I_c = \frac{1}{2} m_c {r_c}^2 \qquad \text{(kg m}^2\text{)} \qquad \text{eqn. 23}$$

and the moment of inertia I_a about the centre of the revolute arm (modelled as a rectangular section bar) is given by

$$I_a = \frac{1}{12} m_a \left(a^2 + w^2\right) \qquad \text{(kg m}^2\text{)} \qquad \text{eqn. 24}$$

These moments of inertia are specified about the component centres, but for torque calculation these must be specified with respect to the revolute axis. This can

be achieved using the parallel axis theorem: if an object of mass m has a moment of inertia about its centroid of I_{xc} ,then the moment of inertia about some parallel axis, I_x , at a distance x from the centroid is given by

$$I_x = I_{xc} + mx^2$$

Therefore I_c about the revolute axis is given by

$$I_c = \frac{1}{2} m_c r_c^{\,2} + m_c h^2 \qquad (\text{kg m}^2) \qquad \text{eqn. 25}$$

and I_a about the revolute axis is given by

$$I_a = \frac{1}{12} m_a \left(a^2 + w^2\right) + m_a \frac{a^2}{4} \qquad (\text{kg m}^2) \qquad \text{eqn. 26}$$

The total inertia of the revolute arm is given by the sum of I_a and I_c :

$$I = I_a + I_c \qquad \text{eqn. 27}$$

Assuming constant torque and hence constant acceleration, the time taken to cover ϑ degrees from rest at a constant angular acceleration α is given by

$$\vartheta = \frac{1}{2} \alpha t^2 \Rightarrow t = \sqrt{\frac{2\vartheta}{\alpha}} \qquad (\text{s}) \qquad \text{eqn. 28}$$

But from eqn.22

$$T = I\alpha \Rightarrow \alpha = \frac{T}{I}$$

Therefore substituting for α in eqn.28 gives

$$t = \sqrt{\frac{2I\vartheta}{T}} \Rightarrow T = \frac{2I\vartheta}{t^2} \qquad \text{eqn. 29}$$

As for the linear axis, the angular velocity profile was assumed to be approximately triangular, so substituting $\frac{t}{2}$ and $\frac{s}{2}$ as before gives

$$T = \frac{2I\left(\frac{\vartheta}{2}\right)}{\left(\frac{t}{2}\right)^2} = \frac{4I\vartheta}{t^2} \qquad \text{(Nm)} \qquad \text{eqn. 30}$$

As required, ϑ may be calculated from the trigonometric relationships:

$$\vartheta = \sin^{-1}\frac{y_n}{h_n} \quad \text{and} \quad \vartheta = \cos^{-1}\frac{x_n}{h_n}$$

3.6.3 Provisional parameter calculations for end-effector and actuator sizing

Based on the teat position data in Table 2 and the end-effector design concept, several precision 2D drawings were constructed to evaluate the geometric layout and required dimensions of the arm mechanisms. Two of these drawings are shown in Figure 42 and Figure 43 which display the 2D working area and arm travel details respectively. A margin of 40mm was added to the maximum teat-spacing distances of Table 2 to allow for asymmetrical teat configurations. From these initial drawings the arm length and arm travel parameters were accurately calculated, in turn allowing component masses to be estimated and consequential torque estimation for actuator specification.

Table 8 shows the calculated parameters for revolute arm length and linear arm travel. These parameters established essential design constraints to be incorporated during solid modelling.

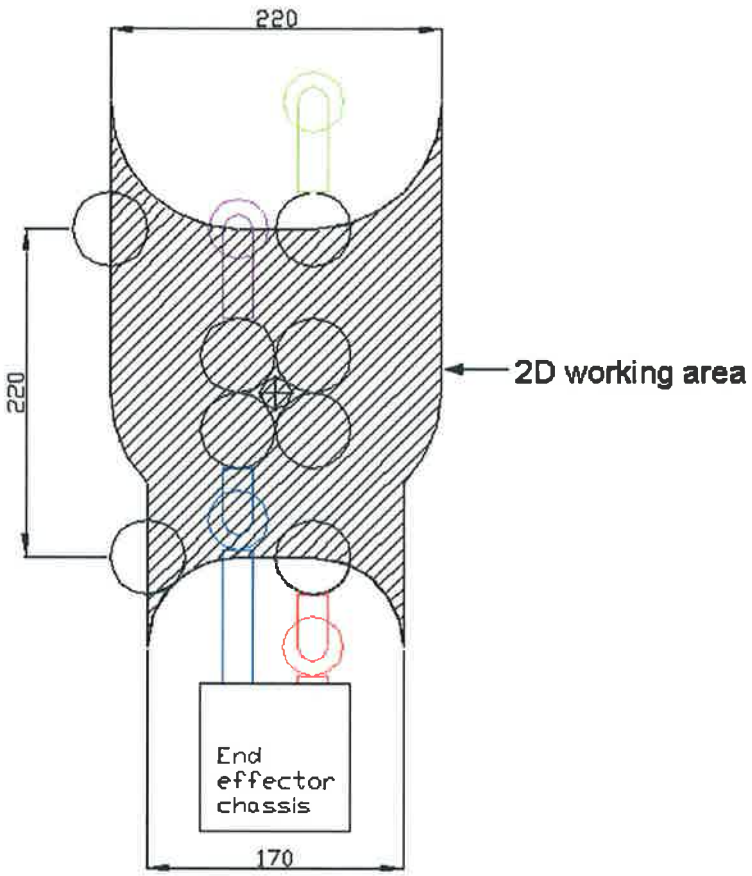

Figure 42. End-effector 2D working area

Parameter	Unit	Value
Front revolute arm length	mm	85
Rear revolute arm length	mm	60
Front linear arm travel	mm	195
Rear linear arm travel	mm	170

Table 8. Arm length and travel parameters

From the parameters in Table 8 simple volumetric models of the arms were constructed and masses estimated for the revolute and linear arms, giving a preliminary indication of actuator torque requirements. Masses were estimated from simple 3D solid models, using the material property function available in Pro/Engineer which allows density values to be assigned to modelled components and calculates mass based on component volume. Aluminium (at standard density

of 2700 kg m^{-3}. Source: Miko Metals Ireland) was presumed for most components, with mild steel (density 7.8 kg m^{-3}. Source: Miko Metals Ireland) presumed for a linear slide bearing on the linear arms.

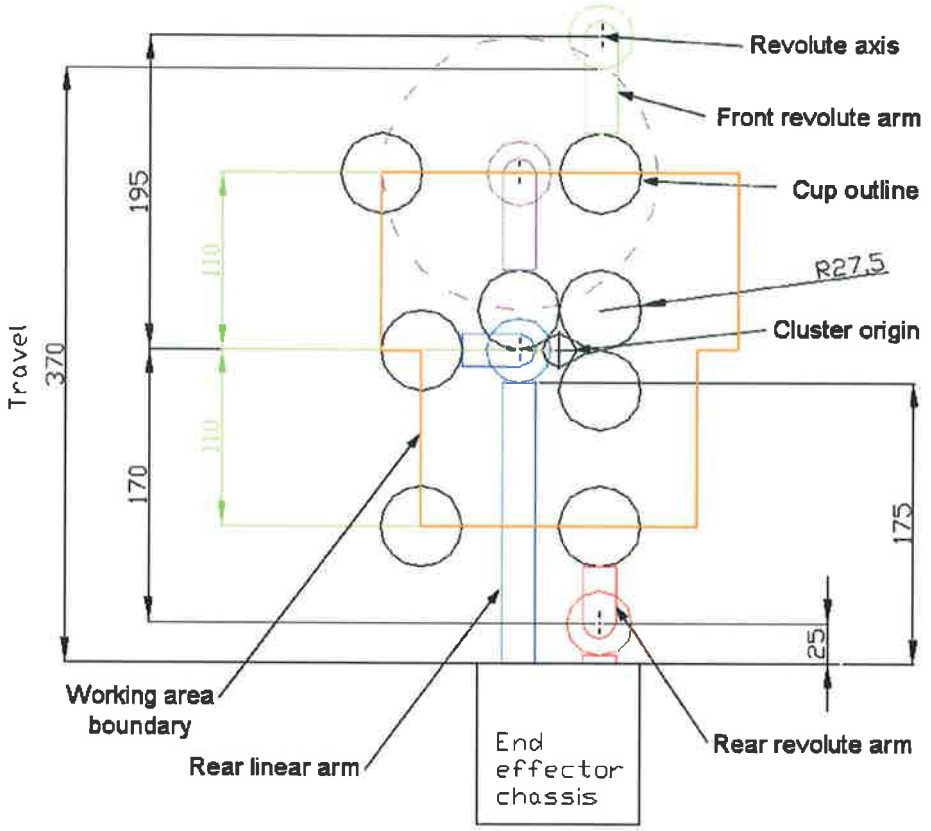

Figure 43. 2D working area travel dimensions

Using the theory outlined in sections 3.6.1 and 3.6.2, the parameters shown in Table 9 were assembled and an estimated torque requirement was obtained for the linear and revolute axis actuators. In each case parameters of the longer revolute and linear arms were chosen for calculations, as these have the greater mass.

For estimation of the linear axis resistance parameter, *R*, reference was made to manufacturers catalogues for friction from linear bearings. As this value was found to be low (coefficient of <0.01), a lumped estimation of friction and milking line resistance of 10N was made. This value was expected to provide a suitable operating margin for the linear actuator. Similarly, mass for the revolute arm and

cup gripper was overestimated (by an approximate factor of 2) to allow margin for resistance of milking lines.

An approximate required velocity was calculated for each arm as an average of displacement over time. This parameter was used for determining actuator suitability through verification that adequate torque was available in the required speed range.

Front revolute arm parameters	**Unit**	**Value**
Length, c	m	0.085
Length , a	m	0.06
Cup radius, r	m	0.0225
Arm width, w	m	0.015
Cup mass	kg	0.21
Gripper mass	kg	0.2
Revolute arm mass	kg	0.25
Max. travel angle, ϑ, to cover 20mm on x or y-axis	rad	0.8172
Moments of inertia about revolute axis:		
Cup and gripper	kg m^2	0.0030
Arm about revolute axis	kg m^2	0.0003
Total moment of inertia	kg m^2	0.0033
Actuator torque required	**Nm**	**0.55**
Approximate revolute actuator speed [(ϑ*60)/(2π*0.2)]	rpm	39
Long linear arm parameters		
Estimated mass of arm + payload	kg	2
Estimated resistive force, R	N	10
Approximate PCD of pinion gear	m	0.015
Approximate linear arm velocity [0.02/0.2]	ms^{-1}	0.1
Approximate linear arm actuator angular velocity	rpm	128
Actuator torque required	**Nm**	**0.135**

Table 9. Approximation of actuator torque requirements

3.7 Actuators and drives investigation and specification

With guideline actuator torque requirements established, an investigation of available actuator types and configurations was performed. Actuators were investigated before detailed design on the rest of the end-effector, as the range and type of available actuator may constrain the mechanical design.

For small rotating electrical actuators, stepper motors or DC servo motors are the primary options. AC servo motors, while available, are generally too large for this application. Electronically-commutated servo-motors, while technically AC motors, are generally considered in the brushless DC servo-motor category.

Table 10 shows a comparison of the major attributes of stepper and DC servo motors.

3.7.1 Properties of stepper motors

Stepper motors differ from normal servo motors in that rotation occurs in discrete steps. This discrete 'stepping' motion is due to the construction of the stepper motor: a number of magnetic poles are provided on the rotor (by positioning of permanent magnets) and by switching stator coils on or off in sequence the poles are forced to rotate. As the rotor poles are fixed, only a finite number of positions or 'steps' may be adopted by the rotor. This property is utilised for open-loop control of stepper motors, as sending a certain number of step pulses to the stator coils of the motor results in a proportional angular displacement of the rotor. A typical resolution for a stepper motor is 200 steps/rev, giving an angular displacement resolution of 1.8°. Additionally, advances in control and drive systems have allowed half-stepping and micro-stepping techniques to be used. As the name suggests, half-stepping allows the rotor to be incremented by half a step by switching the two stator coils on at the same time and thus causing the rotor pole to adopt a position in between steps. Micro-stepping is a more recent development in which precise control of the stator currents is used to smooth out the transition between steps and allow very small increments to be obtained, but at the expense of increased complexity and cost for control hardware. Open-loop control lacks robustness and was not considered for this position control application, however closed loop control of stepper motors may be achieved simply by attaching a

feedback encoder to the motor. As shown in Table 10, stepper motors are less expensive than equivalent DC servo motors, due to simplicity of construction and control circuitry. They also provide maximum torque when stalled, allowing the rotor to act as a brake, and good torque in the lower speed range.

The main disadvantage of stepper motors is the discrete motion range, a limiting value for some positioning applications. The stepping motion of the motor can also cause some vibration and noise when driving geared transmissions.

3.7.2 Properties DC of servo motors

DC servo motors give excellent smoothness of operation and positioning performance due to an infinitely variable rotor position that is only limited by feedback resolution. Unlike stepper motors, torque is reasonably constant across the operating range and does not reduce significantly at high speed. The stall torque capability of a servo motor is zero, i.e. it cannot act as brake, and must wait for a disturbance before reacting with opposing torque. This limitation is of less importance, as modern drive systems provided rapid response. Unlike stepper motors, servo motors must always operate with feedback, however for this application this is not a limitation. The service life of brush-commutated servo motors is limited by the life of the carbon brushes. Modern designs have extended brush life, however brushless electronically commutated servo motors are available with very long service life and at significantly higher cost. Due to the increased complexity of control and drive hardware, control using servo motors tends to be much more expensive than with stepper motors.

Attribute	Stepper Motor	DC Servo Motor
Low speed torque	Excellent	Excellent
High speed torque	Average	Excellent
Stall torque	Excellent	Poor
Smoothness	Poor	Excellent
Mass	Average	Average
Rotor Inertia	Medium	Low
Cost	Low-Medium	Medium-High

Table 10. Comparison of Stepper and DC servo motor attributes

3.7.3 Linear arm actuator selection

The larger mass of the linear arm made the positive braking action of a stepper motor more desirable. Additionally, the larger inertial mass would serve to damp vibration (although not noise) caused by a stepper motor. From evaluation of stepper and servo motors available from several manufacturers, it was determined that the stepper motors and associated drive hardware were four to eight times less expensive than equivalently sized servo motors and drives. Masses for each type actuator were similar, although stepper motors had slightly lower mass overall, due to the lack of an integrated feedback encoder.

The limiting factor for use of a stepper motor was whether the step resolution was sufficient to achieve the target positioning resolution of +/-2mm specified in the PDS (Table 5). A pinion gear PCD of 15mm was assumed (refer to Table 9), giving a pitch circle length (PCL) of 47.1mm. If the number of steps/rev of the stepper motor is N, the minimum incremental movement of the linear axis, dL, is given by

$$dL = \frac{PCL}{N} \qquad \text{(mm/step)} \qquad \text{eqn. 31}$$

A common step resolution is 200 steps/rev, thus from eqn. 31 the minimum linear axis increment would be 0.24mm. With half-stepping this would be reduced to 0.12mm, an acceptable resolution.

Following investigation and quotations from various manufacturers, a McLennan Size 17 hybrid stepper motor was selected. This motor had suitable performance, a relatively high torque-to-mass ratio and was available at low cost. Full-step resolution was 200 steps per revolution, with 400 steps available using half-stepping. The speed range across which the torque of 0.135Nm was available was excellent (up to 1500rpm, equivalent to linear arm velocity of $1.1 ms^{-1}$), while the stall torque (also called holding torque) was quoted as 0.29Nm. The inertia of the rotor is much less than the inertia of the linear arm and therefore does not appreciably affect positioning performance. Matched drive hardware was available from the same manufacturer to ensure compatibility and good performance. The motor was

available with a projecting shaft from the rear on which a feedback encoder could be mounted. The specification for this motor is included in Appendix A.

3.7.4 Revolute actuator selection

Conceptual design of the end-effector called for use of a compact gearbox with the revolute motor to reduce mass and size. Of the stepper and servo motors investigated from various manufacturers, a much broader range of servo motors was available with specifically designed gearboxes for low-torque (0.5-1Nm) applications. The available selection of stepper motors in this torque capacity range was also limited, while gearboxes tended to be larger and heavier than those available for small servo motors. From this investigation, it became clear that servo motors were the most suitable for the revolute actuator drive.

Use of a gearbox limits positioning performance to some extent, as multiple gears increase the backlash (free-play) in the gearbox and consequentially reduce accuracy and precision. Also, frictional losses in the gearbox can reduce efficiency by a significant amount, often up to 60% for small gearboxes. Backlash can be eliminated by use of a harmonic drive gearbox, however upon investigation these proved to be prohibitively expensive.

Through investigation of various DC servo drives available on the market, a Maxon Motors A-max 22 6-Watt DC servo motor with built-in rotational feedback encoder was selected. This motor was available with silver commutating brushes for low electrical noise, or carbon brushes for improved service life under high-current loading conditions. Carbon brushes were selected, as positioning requires intermittent high-current drive. This manufacturer provided a range of planetary and spur gearboxes for direct attachment to the A-max 22 motor, greatly simplifying integration of the motor and gearbox. The motor selected had a continuous torque rating of 0.00743Nm at up to 8000rpm, while the torque requirement was 0.55Nm at approximately 39rpm. By examination of the available gearboxes a gear ratio of 128:1 was selected. Efficiency of this planetary gearbox was quoted as 59%, therefore the available torque from the motor-gearbox combination was

$$(0.00743) * (128) * (0.59) = 0.561\,\text{Nm}$$

at a maximum output speed of 62.5rpm This value met the preliminary torque and speed specification and was therefore acceptable. Peak torque rating for the planetary gearbox was 1Nm which exceeded the application requirements. The average backlash for the gearbox was quoted as 0.8°, giving a worst-case uncertainty of +/-0.59mm on the longer revolute arm and +/-0.42mm for the short revolute arm. These figures were within the required +/-2mm specified in the PDS, and the motor and gearbox were therefore adequate for inclusion in the preliminary design.

A further advantage of the chosen servo-motor type was that a complete position controller and servo-drive unit was available. The footprint of this unit was very small (50mmx50mm) but possessed powerful and flexible control software, along with additional programmable I/O ports. As servo motor tuning can be complex, use of the manufacturers proprietary tuning algorithms offers a time advantage for set-up and also guarantees compatibility.

3.8 Feedback Sensors investigation and specification

Feedback sensors are a requirement for closed-loop control. In the case of the servo motor, a built-in encoder was available from the manufacturer, and this was preferred as it occupies little extra volume when integrated into the motor housing. An encoder resolution of 512cpr (counts per revolution) was available, however the final resolution output is 2048cpr, as the encoder provides two square-wave outputs that are 90° out of phase, resulting in four edges (two rising two falling) that can be counted by the control software.

For the stepper motor encoders several products were available, with the final encoder selected for low-cost and ease of attachment to the stepper motor. A Hewlett-Packard/Agilent encoder of 500cpr was selected with a bore suitable for fixing to the rear shaft of the motor. Similar to the servo encoder, this unit has an actual resolution of 2000cpr, which provides five counts per half-step of the stepper motor.

3.9 Mechanical components investigation and specification

For the conceptual design, the main prefabricated mechanical components were associated with the linear bearing slide mechanism which supports the linear arms. A second area in which investigation was necessary was the gripping mechanism for holding the cups. These were examined and suitable products selected for preliminary design.

3.9.1 Linear bearing slide system

Linear bearing slides are alternatives to recycling ball slides, which although popular and widely used, are difficult to seal in a dirty or moist environment. Figure 44 shows the essential components of a v-groove slide system. While the term 'slide' is used, in fact the entire system relies on rolling components, a feature that provides very low friction and wear characteristics. Sealed roller bearings with a precision-ground v-groove in the outer housing mate closely with precision-ground v-profiles on a linear slide. The v-surface provides a larger contact area compared to spherical roller contact, reducing surface pressure and thus wear. The spherical rolling elements inside the roller bearing are robustly sealed against dirt and moisture ingress, while the v-groove shape tends to force dirt and moisture off the v-bearing surface rather than collecting it.

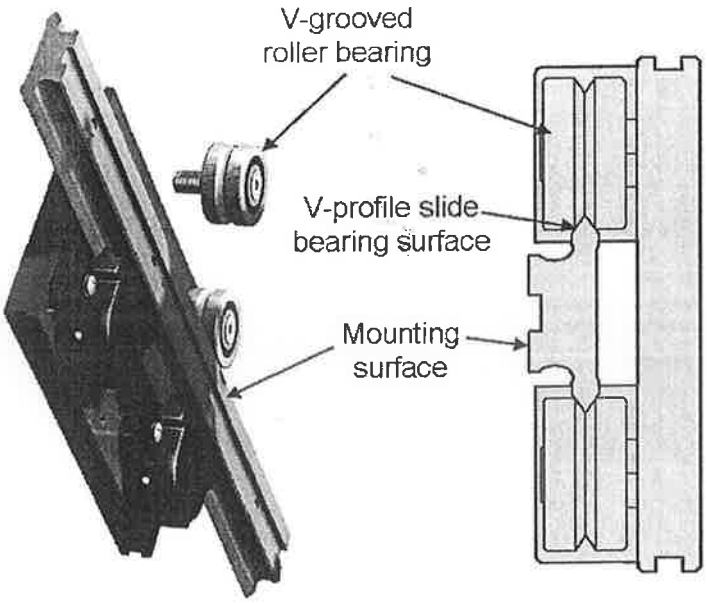

Figure 44. V-groove slide system

Several manufacturers produce v-groove slide systems, and these were investigated and compared. The Hepco SL2 stainless steel slide system was selected for the end-effector. This system uses stainless steel for exposed metallic components, adding dirt and moisture resistance at only a small increase in cost. The size of the slides and v-bearings were selected based on the technical data provided by the manufacturer and the estimated mass and dimensional parameters of the linear arms. To reduce mass, a flat slide without an integral raised mounting surface was specified, with the mounting surface replaced by an aluminium spacer.

3.9.2 Gripper investigation and specification

The gripping device for holding the milking cup must be sufficiently strong to retain the cups during acquisition and motion, as well as having low mass and a compact profile. Several methods of holding cups were observed from the literature survey. These methods are summarised in Figure 45.

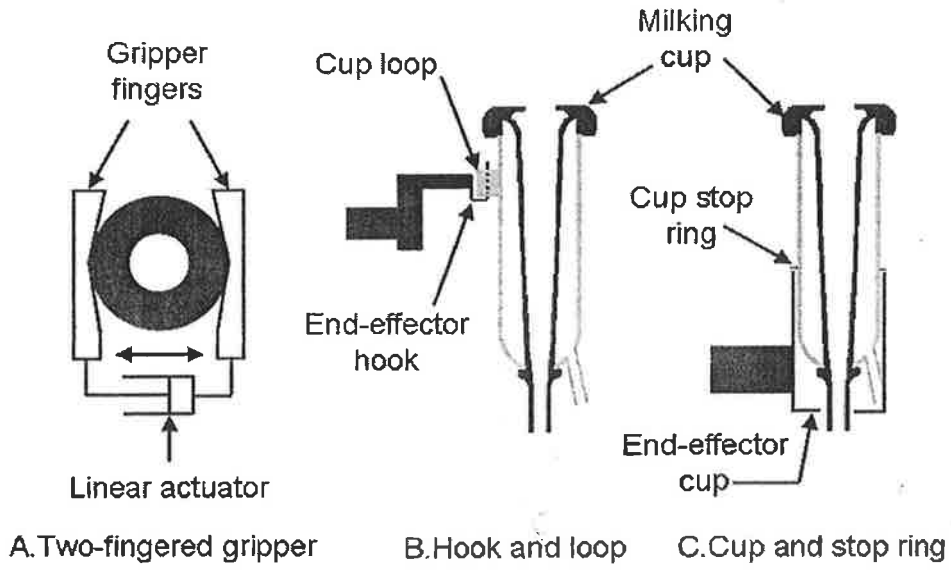

Figure 45. Gripper styles

The two-fingered gripper style Figure 45(A) is commonly used in commercial robotics and has been successfully used in two AMS. Fingered grippers have the advantage of accommodating small variations in cup position during acquisition, depending on the opened width of the fingers, while providing excellent rigidity for positional accuracy during application. The disadvantages of this method are the

side-clearance required for the width of the fingers and the need for an electrical or pneumatic actuator which adds complexity and mass to the end-effector. This method is therefore the most bulky of the observed designs.

A simple and successful method used by one AMS manufacturer is the hook and loop gripper Figure 45(B). This method requires a metal loop incorporated in the shell of the milking cup, into which a hook on the end-effector fits during cup acquisition. Simplicity of design with this gripping method resulted in low mass and a very compact profile. The disadvantages of this design are the modifications required to the milking cup shell, the limited range of positions in which the cup can be acquired (the cup must be presented with the loop facing outwards), and the need to keep the cup vertical during motion. Additionally, positional accuracy is lowered due to clearance required between the hook and loop.

The final gripping method, used by AMS that hold four cups simultaneously, uses a cup-shaped holder into which the milking cup fits Figure 45(C). A stop ring mounted on the milking cup holds the cup at the required height, while a hole in the base of the holder allows milking and vacuum lines to pass through. This method is relatively simple, compact and requires only a small modification to the milking cup shell; however it is primarily design for situations where the end-effector remains under the cow during application. The disadvantages for this application are the difficulty in acquiring and releasing milking lines, and the need to keep the cup vertical during motion.

For this application it was desirable to have the ability to fully invert the end-effector to increase flexibility in acquiring the cup cluster. Of the three methods considered above, only the two-fingered gripper was suitable for this function. However the increased complexity, mass and operating room required by a fingered gripper would be difficult to accommodate in the design. A magnetic gripping device has been proposed by an AMS manufacturer [58], however this device either presumes use of a magnetic material for the cup shell or requires fitment of a ferromagnetic sleeve. In either case modification of the cup shell would be required, as the stainless steel commonly used is not necessarily magnetisable. These

limitations were addressed by introducing a fourth gripper design: a vacuum gripper.

Use of a vacuum gripper would allow for simple acquisition and release of the milking cup with no moving parts required. Digital electronic control of the vacuum can readily be achieved using inexpensive off-the-shelf vacuum controllers, giving fast control response without complex interfacing equipment. Figure 46 (A) shows the original concept for a vacuum gripper. The design called for a gripper shell with a radius shaped to match the milking cup shell and lined with a butyl rubber lining to form an air-tight seal. A vacuum attachment was provided as shown, and a vacuum chamber in the face of the gripper provided an area over which the gripping force was developed. As this design was untested, a test rig was set up and two test grippers were constructed. During testing, it was found that vacuum chamber of area 45mm x 40mm gave a breakaway force of 85N at -50kPa (gauge), and a narrower chamber of 40mm x 30mm gave a breakaway force of 57N. Both breakaway forces corresponded closely to the theoretically calculated forces of 90N and 60N respectively for this design, obtained by

$$F = PA \qquad \text{eqn. 32}$$

where F is the gripping force, P the applied pressure (negative gauge) and A the surface area of the vacuum chamber.

It was discovered however that a lack of compliance in the design made compensation for minute misalignment of the cup and gripper impossible. This problem was solved by revising the design to that shown in Figure 46 (B).

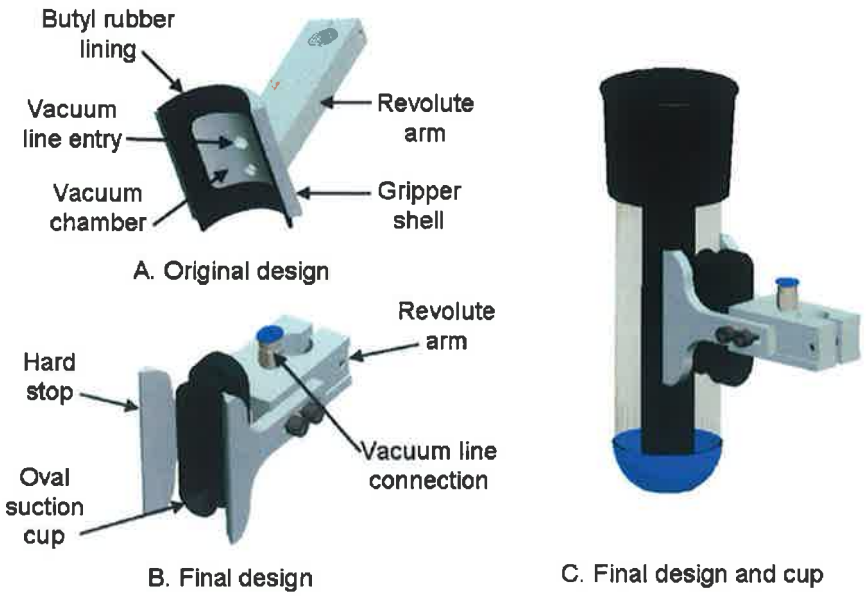

Figure 46. Vacuum gripper original and final designs

The revised design used a commercially available rectangular suction cup with a flexible rubber lip, giving 3 to 4 mm of compliance. To retain the positional accuracy of the original design, hard stops were added on either side of the suction cup, against which the cup could be drawn by the suction force. Although this design was more complex than the original design, involving two extra components, testing showed it to be capable of accommodating misalignment of several degrees between cup and gripper. The breakaway force for this suction cup was quoted as 62.8N at -50kPa, and tests confirmed this to be accurate. This is equivalent to holding a static weight of 6kg and, given that the mass of the payload is only 0.21kg, provides a large margin for accommodating forces experienced during cup handling. To improve compactness, the vacuum line was routed through the centre of the revolute arm, exiting via a push-in connection threaded into the top of the revolute arm.

3.9.3 Linear arm extruded section selection

The material selected for the linear axis arms was hollow rectangular section aluminium tube. The hollow section served two purposes, allowing a light but stiff construction and at the same time facilitating routing of signal cables through the arm. The internal cross-sectional area was constrained to facilitate at least two Ø9mm cables and one Ø4mm vacuum line, as well as allowing access to internal fixing screws for attaching the linear slide and rack gear.

A 30x20x2mm (height x width x wall thickness) section tube was selected from available catalogue sizes. This size was sufficiently compact for the end-effector design while providing sufficient internal cross-sectional area (26x16mm) to accommodate cable and tubing. A simple beam analysis was then performed to verify that the tube possessed sufficient strength and stiffness for the predicted loading conditions.

The unsupported length of the beam was modelled as a simple cantilever. This model is reasonably accurate, presuming that the stepper motor can prevent horizontal motion. The support point of the cantilever is thus the contact point with the last v-groove bearing. It was assumed that the linear slide was self-supporting and stiff, such that if the aluminium tube alone could support the operating load, then the addition of the linear slide would improve stiffness and strength of the entire arm. Material and geometric properties of the beam are shown in Table 11. Proof stress at 0.2% elongation was used rather than yield strength as this is the lower of the two values.

Table 11. Properties of linear axis tube (source: Miko Metals catalogue 2005)

Material	Aluminium 6060-T6	
Dimensions (h x w x thickness)	mm	30x20x2
Second moment of inertia, I	m^4	3.61253×10^{-08}
Material properties	**Unit**	**Value**
Proof stress 0.2%	MPa	160
Shear strength	MPa	153
Tensile modulus, E	GPa	69
Mass per unit length	kg/m	0.5

The second moment of inertia of a beam section is a geometric property affecting stiffness. The second moment of inertia about the horizontal centroid of a solid rectangular section is calculated by

$$I_x = \frac{bd^3}{12} \qquad \text{eqn. 33}$$

where b is the width and d the breadth of the section. To calculate the second moment of inertia for a hollow rectangular section, the second moment of inertia of the hollow area is subtracted from that of the entire area.

Figure 47 (top) shows the forces on the longest linear arm at maximum extension, with dimensions and forces obtained by reference to Figure 43 and Table 9 respectively. Acceleration due to gravity was taken as $10ms^{-2}$. The distributed load represents the mass of the aluminium tube, while the mass of the revolute actuator, arm, gripper and cup were lumped as a single mass at the maximum extension of the revolute arm.

From basic beam theory the shear force and bending moment diagrams for the arm were constructed, as shown in Figure 47 (centre and bottom). The maximum shear force was calculated as 8.95N, and the shear stress, SF, is therefore given by

$$\text{shear stress} = \frac{\text{shear force}}{\text{cross - sectional area}} = \frac{8.95}{(0.03 * 0.02) - (0.026 * 0.016)} = 0.049\text{MPa}$$

This value is well within the shear strength of the material.

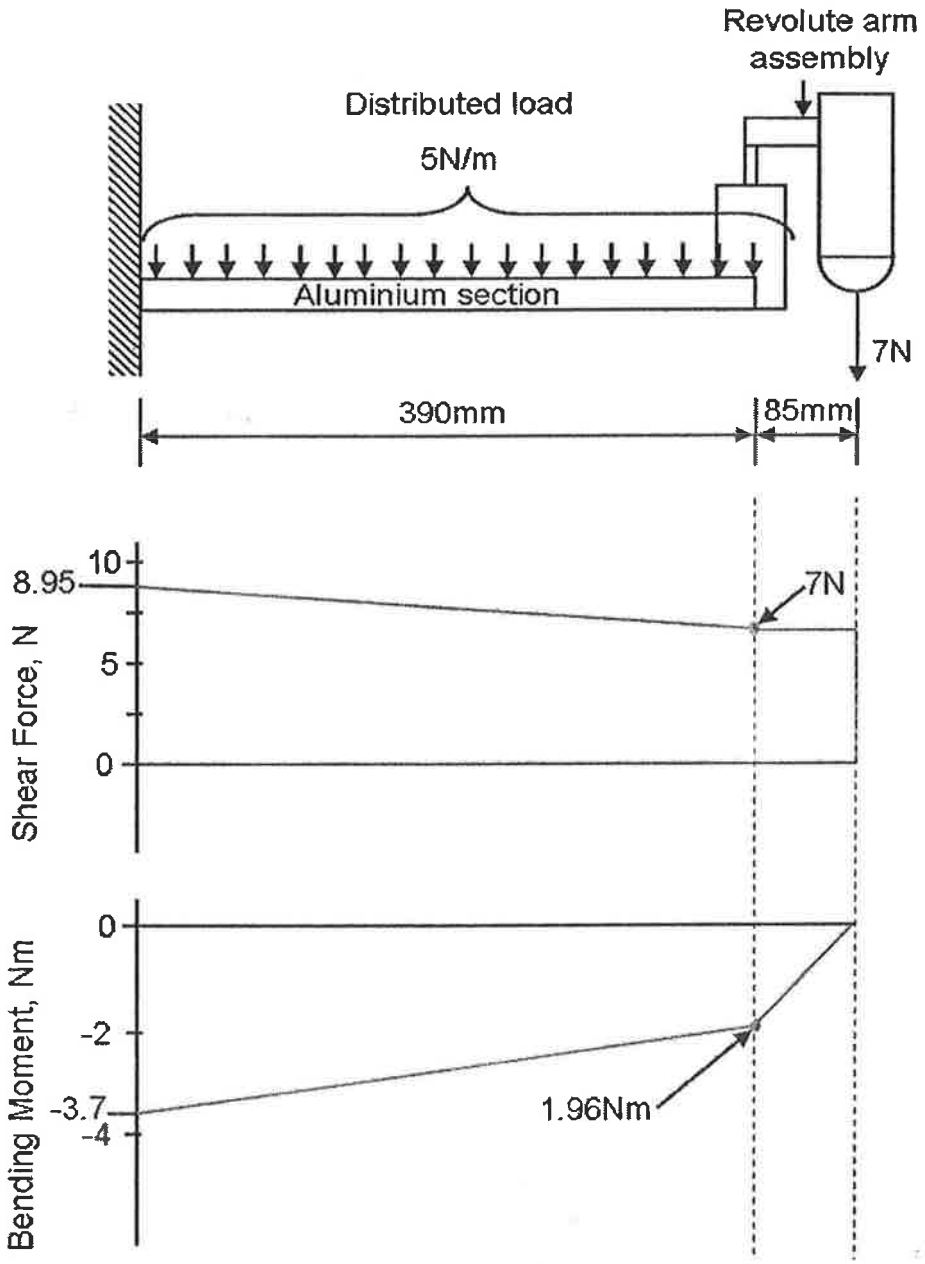

Figure 47. Diagram of forces on unsupported linear arm (top) and associated shear force (centre) and bending moment diagrams (bottom)

Stiffness of the arm assembly was determined by predicting the deflection of the beam using classical Euler-Bernoulli beam theory.

Classical beam theory makes several assumptions about beam conditions:

- The beam is long and slender
- The beam cross-section is constant along its axis
- The beam is loaded in its plane of symmetry
- Deformations remain small.
- The beam material is isotropic
- Plane sections of the beam remain plane

Each of these assumptions may be considered approximately accurate for this application, so the theory is applicable. Solutions for common beam configurations are widely available in literature and were used to obtain deflections for the linear arm. Using the superposition method for beam deflection, the deflection of the arm with the point load and deflection of the arm with the distributed load were calculated separately and then summed to obtain overall deflection:

The formula for maximum deflection of a cantilever beam with a point load (in this case the force due to the revolute axis assembly, 7N), y_p, is

$$y_p = \frac{FL^3}{3EI} \quad \text{m} \qquad \text{eqn. 34}$$

where F is the point load, L the distance of the load from the beam support, E the tensile modulus of the material and I the second moment of inertia of the beam section.

The maximum deflection of a cantilever beam with a uniform distributed load (in this case the force due to the mass of the linear arm,), y_d, is given by

$$y_d = \frac{wL^4}{8EI} \quad \text{m} \qquad \text{eqn. 35}$$

where w is the distributed load in mass per unit length.

Using equations 34 and 35, the maximum deflection, y_{max}, was calculated as

$$y_{max} = y_p + y_d = 1.003 \times 10^{-4} + 5.8 \times 10^{-7} = 1.001 \times 10^{-4} \text{ m}$$

This result represents a deflection of 0.1mm under a worst-case load condition. The deflection is sufficiently small to be acceptable, as it indicates good stiffness for the aluminium tube. It can be observed from the above equation that the load at the end of the arm has a far greater contribution to deflection than the mass of the aluminium tube. It was assumed that the rigid attachment of the linear slide will add to this stiffness and thus produce an assembly that will not deform unacceptably under normal operating conditions. This assumption was verified using the deflection equation provided by the linear slide manufacturer:

$$y_s = \frac{FL^2(3L-k)}{6EI} + FLkR_c \qquad \text{mm}$$

R_c is a constant relating to the stiffness of the cantilever clamp, however as R_c is very small (in the order of 10^{-7}) clamping stiffness was assumed to be infinite. This assumption holds true as long as the linear slide roller bearings are adjusted to provide minimum vertical play. The linear slide deflection, y_s, is thus given by

$$y_s = \frac{FL^2(3L-k)}{6EI} = 0.152 \quad \text{mm}$$

where EI is the product of tensile modulus and second moment of inertia for the slide obtained from manufacturers tables, L is the length of the slide in mm, k is the distance of the point load from the beam support and F is the point load in Newtons.

Comparison of the worst-case deflection estimates for the aluminium tube and linear slide under the same loading condition shows similar deflection for both components. As these components are connected rigidly in parallel the vertical stiffness will be maintained for the entire arm assembly. The increased width of the arm section caused by bolting the linear slide to the aluminium tube also serves to improve lateral and torsional stiffness.

These calculations verified that the selected aluminium tube section size was capable of operating under the anticipated loading conditions without undue deformation.

3.9.4 Revolute axis support

The specified revolute actuator gearbox was provided with a ball-bearing supported shaft capable of supporting a radial load of 70N at 10mm from the bearing (approx. 7kg static load) and an axial load of 100N (approx. 10kg static load). These values were sufficient to meet the anticipated load; however the shaft diameter was only 4mm, presenting difficulty in robust attachment of the revolute arm and other components. A larger diameter shaft was thus required. This shaft was provided by fabrication of a housing that fitted onto the servo-motor and gearbox assembly and contained two additional bearings supporting a Ø14mm aluminium shaft, as shown in the section in Figure 48. The additional bearings relieved non-torsional loads on the gearbox shaft, transmitting these through the housing to the linear arm and thus minimising stress on the revolute actuator assembly.

The bearings selected were 6801-2RS (synthetic rubber sealed) ball bearings, with an internal diameter of 12mm and an external diameter of 21mm. The quoted static load capacity (radial and axial) for these bearings was quoted as 1040N, far in excess of the anticipated loading conditions for the actuator. However, as the bearing was only 5mm wide a radial load at any distance from the bearing would likely cause excessive deflection of the shaft. This problem was solved by specifying two bearings separated by spacer to provide a stiffer assembly, as shown in Figure 48. The new larger shaft was rigidly coupled to the gearbox shaft via a grubsrew. There was no need for a flexible coupling, as the sufficient precision was obtainable form the manufacturing process to ensure accurate alignment of the shafts.

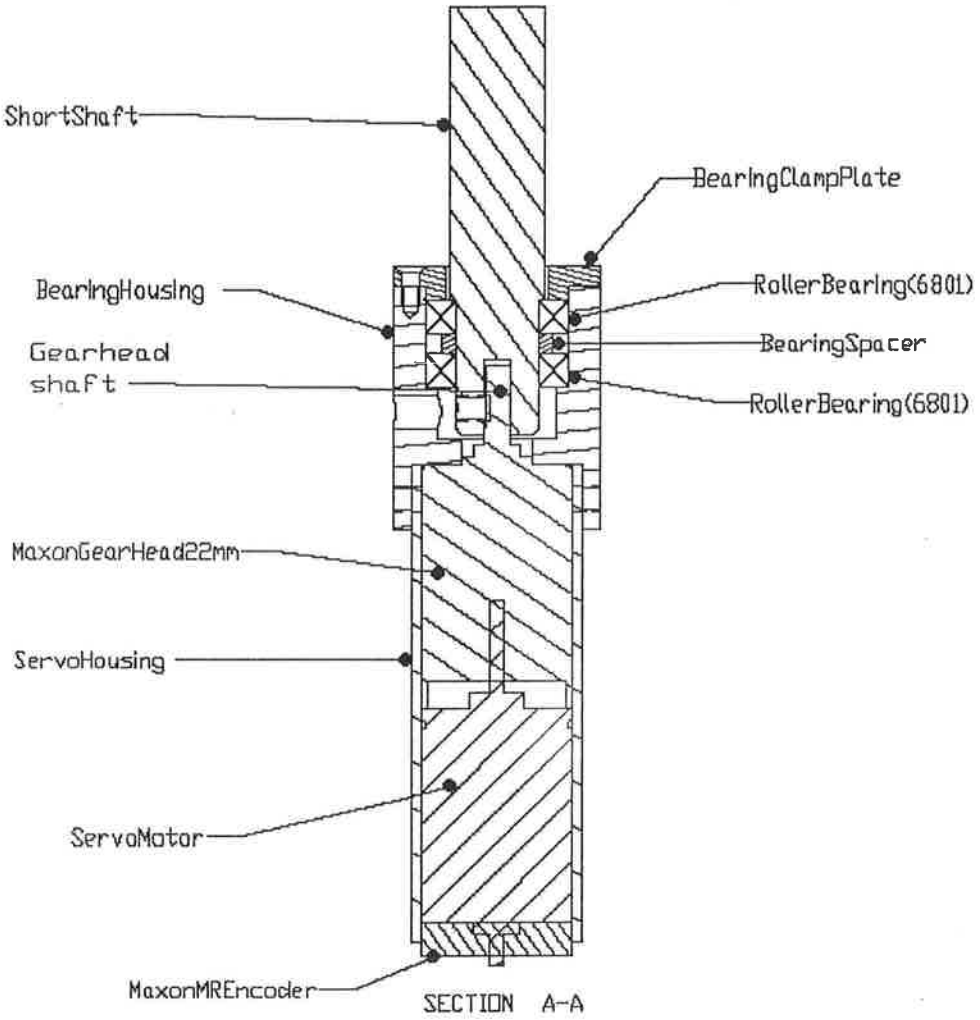

Figure 48. Section of revolute axis actuator, shaft and bearing housing

3.10 End-effector solid modelling and analysis

Following preliminary specification of actuators and mechanical components, a software solid model was constructed, as shown in Figure 49. The model displays the arms at full extension, with the right-hand set of cups close together and the left-hand set of cups rotated. The design was adjusted through an iterative process until the PDS specifications were met and the various components were successfully integrated. Interference analysis was carried out by manipulation of the solid model to ensure that sufficient clearances were provided between components.

The attachment plate on the top of the end-effector was extended (following robot-arm specification as described in Chapter 4) and multiple holes provided to allow some flexibility in mounting position along the x-axis.

Material types and densities were identified and assigned to the model components, allowing mass properties to be incorporated. Choice of material for each manufactured component was a compromise between several design demands: 1) minimise mass, 2) maintain structural strength and stiffness, 3) keep fabrication requirements within the available workshop capabilities. Aluminium was preferred for chassis components due to relatively low density, good stiffness and excellent machinability.

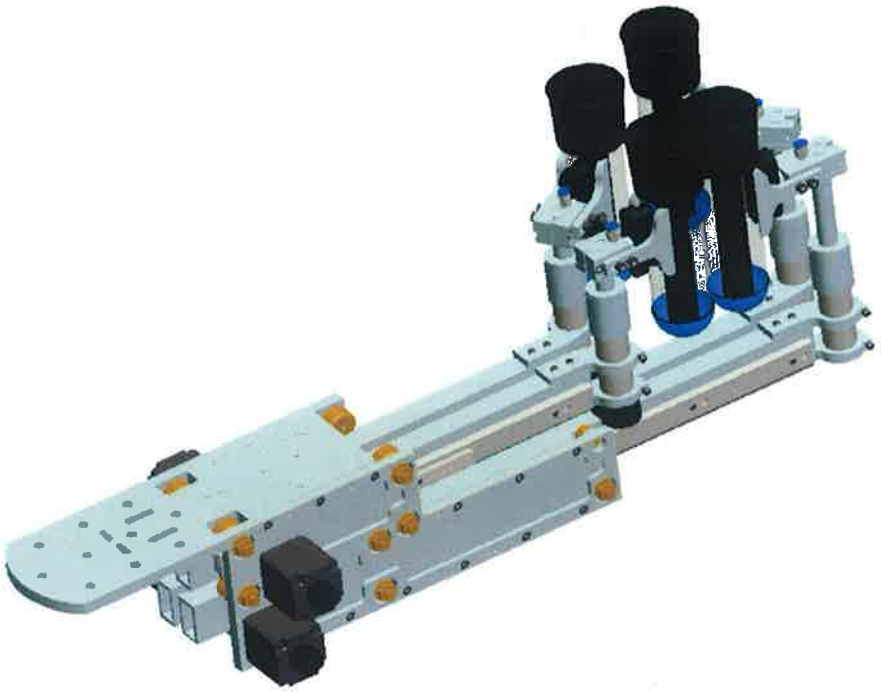

Figure 49. End-effector solid model

3.10.1 Mass properties computational analysis

Mass properties of the entire end-effector were determined using the mass properties analysis function in the solid modelling software. Relevant densities were obtained for each material by reference to supplier datasheets. In cases where density was not available, for example for the milking cup (composed of three separate polymer materials) and drive motors (multiple components and materials), the material volume of the component was extracted from the solid model and an average density was assigned by dividing the known mass by the volume. The computed values extracted from the analysis are shown in Table 12. It is clear from Table 12 that the preliminary estimate of 2kg for the entire longest arm was reasonable, as the total computed mass was 1.45kg. Substituting this mass into eqn. 21 gives a required actuator torque of 0.119Nm, so the provisionally calculated torque value gave a margin of 1.13. This margin was a little low to give confidence in the actuator selection, as the actual resistance value for the linear axis was approximated. To increase the margin the PCD of the pinion was reduced to 10.19mm (a standard manufacturer size), giving a required torque of 0.079Nm and a margin of 1.71. This reduction in PCD also served to decrease the linear increment

per half-step to 0.08mm and increase operating smoothness, as stepper motor vibration effects are diminished at higher rotational speeds.

Component	Quantity	Calculated mass (kg)	Total mass (kg)
Chassis	1	4.40	4.40
Long Arm	2	1.31	2.62
Short Arm	2	1.14	2.28
Revolute Arm Short	2	0.12	0.23
Revolute Arm Long	2	0.14	0.28
Cup	4	0.21	0.84
Total			10.64

Table 12. Computed end-effector mass properties

3.10.2 Moments of Inertia

The material properties analysis tool included in the solid modelling software also returned the moments of inertia about any specified coordinate system. Four coordinate systems of interest were assigned as illustrated in Figure 50: ACS0, ACS1 and ACS2 (where ACS denotes Auxiliary Coordinate System) on the mounting plate and RCS1 at the revolute axis origin. The computed moments of inertia about these coordinate systems are tabulated in Table 13.

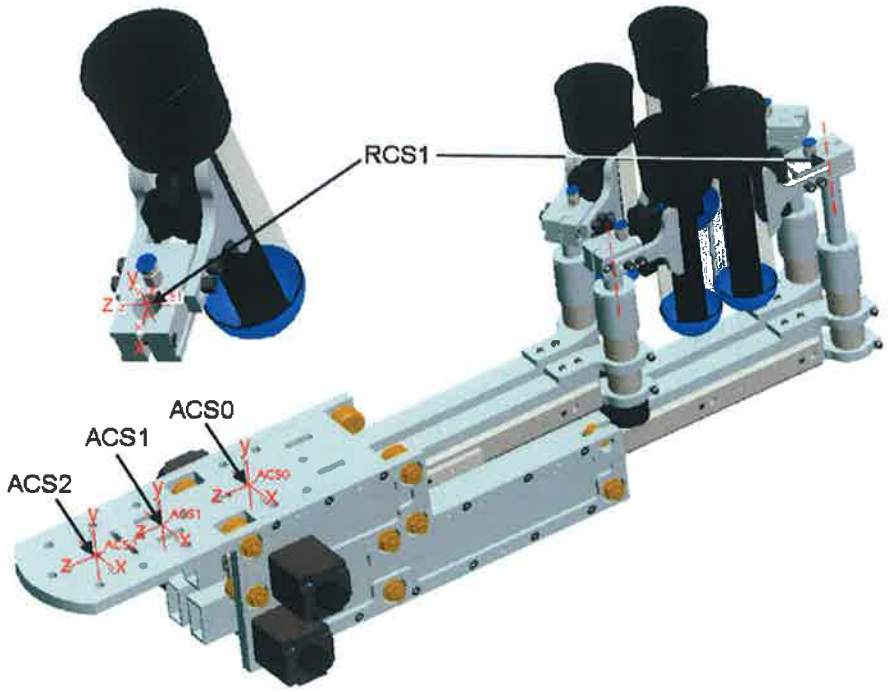

Figure 50. Solid model coordinate systems for moment of inertia calculations

For practical reasons during the solid modelling process the axes of these coordinate systems were parallel with but in different directions to the end-effector coordinate system defined in section 3.5.1 (e.g. for ACS0 the vertical axis is the y-axis instead of the z-axis). Therefore it was necessary to rotate the solid model coordinates systems to obtain the correct moment of inertia in the end-effector coordinate system, and thus in the robot coordinates system (RCS), as these values (about ACS0, ACS1 and ACS2) were necessary for determining the capacity of the robot arm. In Table 13 the original moment of inertia values are shown in square

brackets, while the values without brackets are the corrected moments about the end-effector coordinate system origin. I_{xx}, I_{yy} and I_{zz} refer to the moment of inertia about the x-axis, y-axis and z-axis respectively. In the case of RCS1, only the moment of inertia about the vertical axis, I_{zz}, was of interest. The greatest distance of the centre of gravity from the tool flange was also included, as this was required for robot arm specification.

Coordinate system origin	Moment of inertia in end-effector coordinate system [Moment of inertia about coordinate system origin] (kg m^2)			Centre of gravity along x-axis (mm)
	I_{xx} [I_{zz}]	I_{yy} [I_{xx}]	I_{zz} [I_{yy}]	
ACS0	0.0794	0.8112	0.7719	189
ACS1	0.0794	1.2076	1.1684	269
ACS2	0.0794	1.5956	1.5564	329
RCS1	-	-	0.0019	-

Table 13. Moments of inertia about various coordinate system origins on end-effector

Using the theory outlined in section 3.6.2, the actual component masses and moments of inertia for the longer revolute arm were calculated from the computed inertia value and tabulated in Table 14.

Component	Unit	Computed	(Approximated)
Gripper	kg	0.0641	(0.21)
Cup	kg	0.2100	(0.21)
Arm	kg	0.0737	(0.25)
Total mass	**kg**	**0.3478**	**(0.67)**
Moments of inertia about revolute axis			
Cup and gripper	kg m^2	0.0018	(0.0030)
Arm about revolute axis	kg m^2	0.0001	(0.0003)
Total moment of inertia	kg m^2	0.0019	(0.0033)
Actuator torque required	**Nm**	**0.349**	**(0.55)**

Table 14. Computed moment of inertia and torque requirement vs. originally approximated values for long revolute arm

From the comparison in Table 14 between the computed and originally approximated masses and moments of inertia it is clear that sufficient margin was allowed when assigning provisional mass values to the revolute arm components. This resulted in a higher predicted torque value of 0.55Nm compared to the computed value of 0.349Nm. The revolute actuator thus had a torque margin of 1.58 over the provisionally calculated value in Table 9.

To validate the computational result for the revolute arm moment of inertia, an approximate value for I_{zz} was calculated using a point-mass approximation:

$$I_{zz} = mk^2 \qquad (\text{kg m}^2) \qquad \text{eqn. 36}$$

where m is the total mass of the revolute arm and milking cup and k the approximate radius of gyration. Approximating the radius of gyration as 80mm, and assuming the computed mass of 0.348kg to be accurate, then an approximate value of 0.002kg m^2 was obtained for the moment of inertia. This was sufficiently close to the computed value to give confidence in the accuracy of the computation.

3.10.3 Actuator testing

The solid modelling and computational analysis process gave confidence in the end-effector design before physical construction was commenced. For certainty however, a sample of each actuator was purchased and tested to ensure that they were capable of producing the required torque. A simple test using a weight attached via a string to each actuator shaft was performed, and based on the mass and the diameter of the shaft the torque outputs were calculated. In both cases the stall torque was found to be greater than quoted by the manufacturer, so the actuators were deemed suitable for the application.

3.11 Sensor location and wire routing

The PDS required home position sensors for all axes and travel limit sensors where possible. For the revolute axes, fitting of travel limit sensors would prevent rotation through more than one revolution, limiting the flexibility of the end-effector for testing various manipulation strategies. Software limits can serve the same purpose

without limiting rotation and are suitable for the revolute axes, as even in the event of over-travel failure is unlikely to be catastrophic (the worst-case failure mode is collision with another revolute arm, and actuator torque is sufficiently low to prevent major mechanical damage). In the case of the linear arms, over-travel would be much more catastrophic, as the rack may run off the drive pinion and the linear arm may leave its bearings. The additional mass of the linear arms and the inability to recover make this a critical failure mode, and should be prevented by hardware limit sensors.

Following investigation of suitable sensors for the travel limit switches, hinged roller-lever micro-switches, as shown in Figure 51(B) were selected. The chosen micro-switch features a curved section at the end of the hinge arm that can follow an undulating surface but without additional moving parts, and hence is termed a simulated roller switch. A simple raised tab bonded to the surface of the linear was used to activate the switch, with the switch lever following the tab to close the switch as shown in the illustration.

While micro-switches are robust and inexpensive they can exhibit poor switching point precision as the mechanical response of the lever arm and internal components varies with input force, which in turn depends on the velocity of the arm. To ensure good precision for the home position sensors, slotted optical switches were used, as shown in Figure 51(A). These optical switches incorporate an optocoupler comprised of an infra-red emitting LED that emits infra-red light across a slot to a phototransistor. If the infra-red light is interrupted by blocking the slot, the phototransistor is biased off and internal circuitry (an amplifier and Schmitt trigger) drives the output high. A tab bonded to the linear arm was used to interrupt the beam as illustrated in Figure 51(B). This sensor ensured excellent precision as the sensor is non-contact light-based and the response is extremely fast (in the order of 10μs).

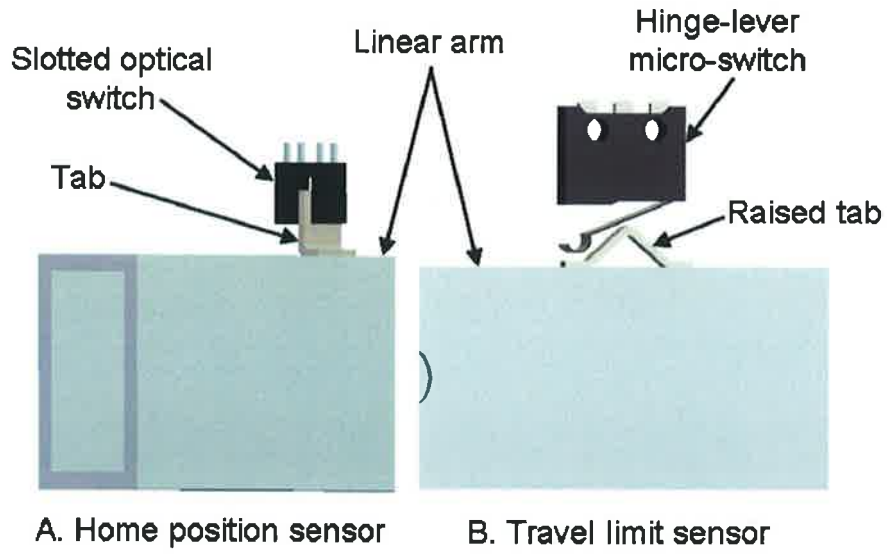

Figure 51. Details of home position (A) and travel limit (B) sensors

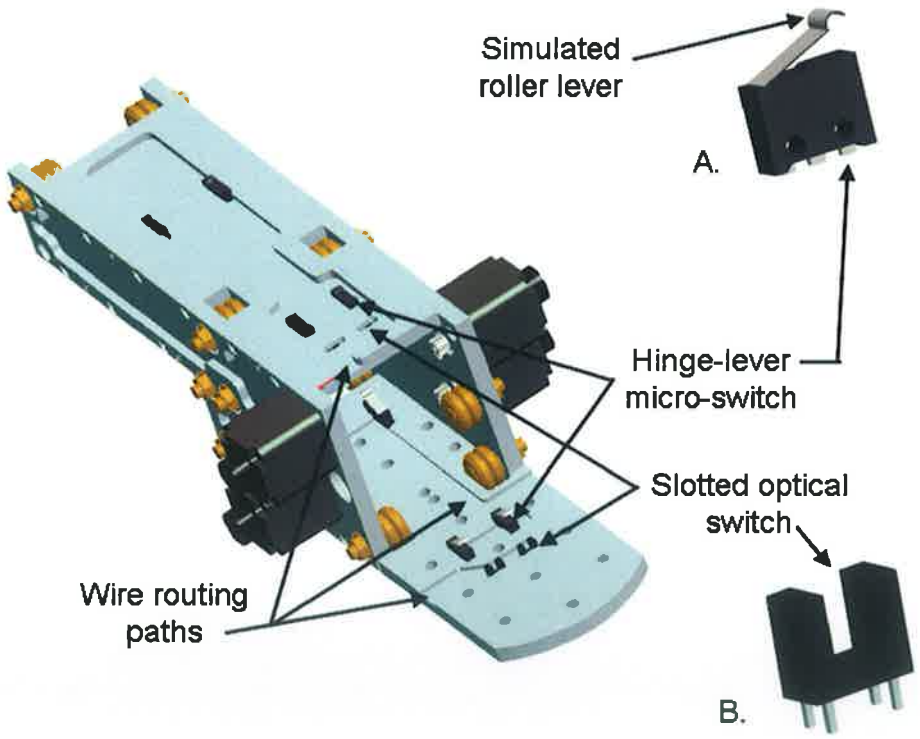

Figure 52. Home and limit sensor positions and wire routing paths and sensor details

The arrangement of the sensors is illustrated in Figure 52. Slots were machined in the upper and lower plates of the chassis to accommodate the sensors, and wire routing paths were cut into the plates to accommodate the necessary signal wires. The lateral spacing of the sensors was designed to prevent interference between the home position and linear limit tabs.

For the revolute axis home position sensor, a photoreflective sensor was used. This sensor contains an infra-red diode and a phototransistor positioned in parallel. In normal operation no infra-red light reaches the phototransistor, but if a surface is brought close enough to the front of the sensor and reflects sufficient infra-red light then the phototransistor will bias on. This sensor features a very compact package (4mm diameter) and was suitable for fitting into a small hole in the side of the revolute actuator bearing housing facing the revolute axis shaft. The reflective nature of the aluminium used in the shaft was utilised to keep the phototransistor biased on, with a small dark strip used to mark the home position. When the dark strip moved past the sensor, the infra-red light was absorbed, and the transistor was biased off. The comprise with using such a small package was the lack of internal signal conditioning circuitry (as available for the linear axis position sensor), so external amplification and thresholding was required to produce a suitable output signal. The photoreflective sensor and mounting location are shown in Figure 53.

Control and signal wiring and vacuum tubing for the revolute arms was routed through the centre of the linear arms to provide protection for the cables.

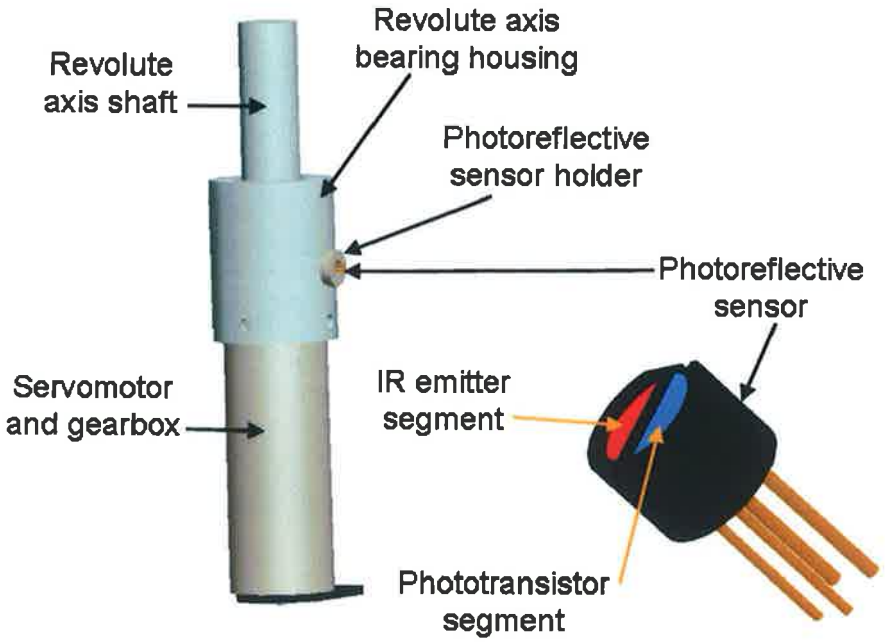

Figure 53. Revolute axis home position sensor and mounting location detail

3.11 Wiring connections

A connection system was necessary to facilitate attachment and detachment of signal and power cables to the end-effector. The original end-effector configuration required 114 connections, with some additional capacity desirable for future use. There are many types, configurations and sizes of connector available, however as this is a prototype design it is possible that the wiring may require alterations or additions during testing. It was thus decided that the connection system should be basic and low-cost, allowing for future modifications without incurring significant expense. D-type connectors are widely available at low cost, provide good connection density, can carry sufficient current for this application and may be installed without specialist tools. To prevent cables becoming detached during operation the connector plugs and sockets may be screwed together using screw terminals.

Four 25-pin D-type (DB25) male connectors and four 9-pin D-type (DB25) male connectors were selected for the signal connections. This provided a capacity of 136 connections, allowing for future expansion needs. Support for the connectors was provided by two stainless steel mounting plates mounted on either side of the end-

effector, as shown in Figure 54. The openings for the connectors were precision laser-cut, along with four holes for cable grommets. The signal cables travelling to the linear arms pass through these rubber grommets which grip the cable and prevent fatigue damage to the wiring connections due to motion of the arms. As shown in Figure 54, the mounting plates were designed to mount onto the threaded ends of the linear bearings, saving space and providing for convenient assembly.

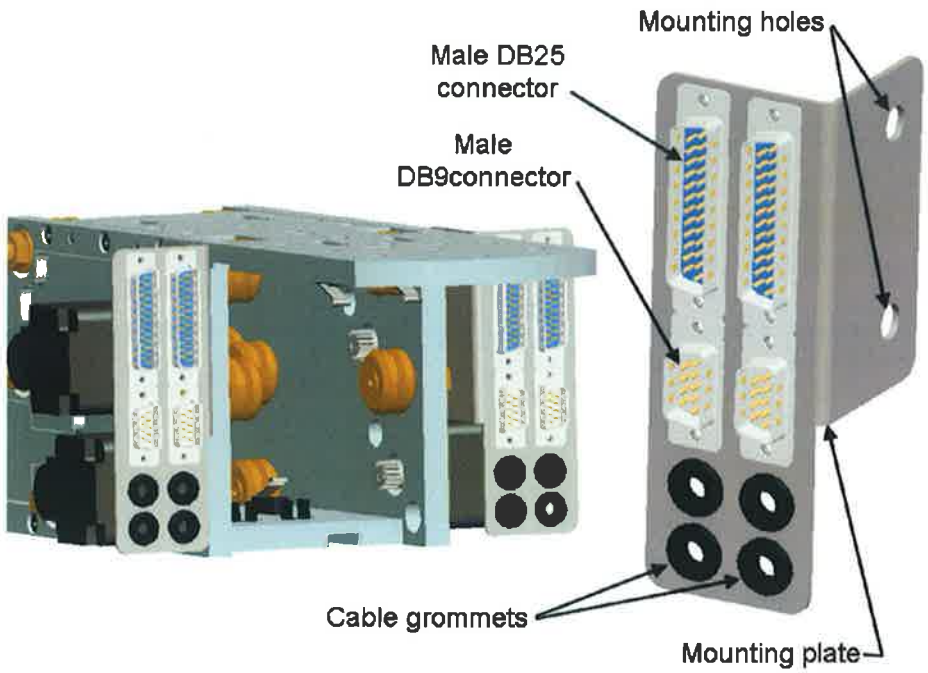

Figure 54. Connector mounting details

3.11 Final design

The complete solid model was assembled as shown in Figure 55. Figure 55(A) shows the end-effector without cups, while Figure 55(B) shows the cups assembled in the cluster origin position. This is the intended acquisition position for the cluster, making use of the clamping action available between the front and rear arm-sets to reduce the precision required by an external cluster assembly mechanism.

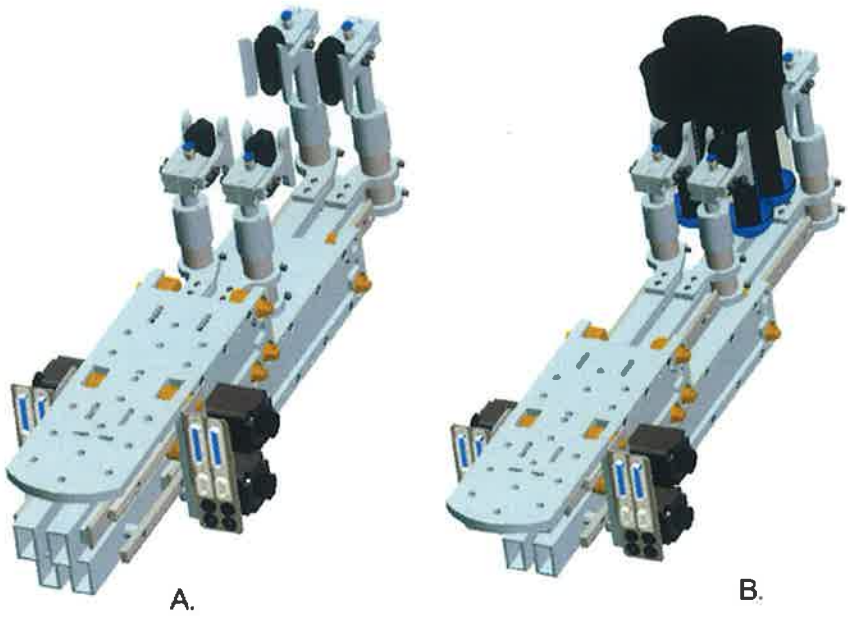

Figure 55. Complete end-effector with cups (A) and without cups (B)

The cup positioning method is demonstrated in Figure 56, in which the wide reach of the end-effector is contrasted with the narrow profile of the chassis.

Flexibility of the design is illustrated in Figure 57, in which two possible configurations are shown. In Figure 57(A) the arms are rotated to one side, allowing cup acquisition from a suitably profiled magazine. Figure 57(B) shows an application configuration in which only the front two cups are used to apply cups, with the rear arms used as cup holders. Several other configurations are possible, providing an adaptable prototyping platform that allows for approach modification during testing.

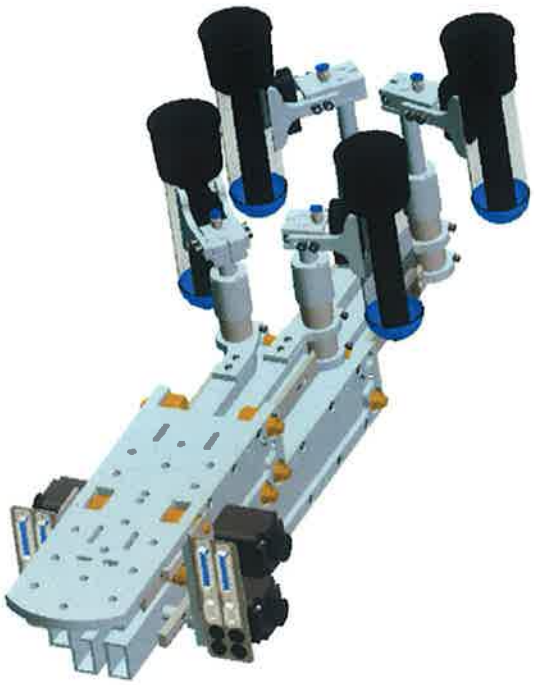

Figure 56. Complete end-effector with cups in various positions

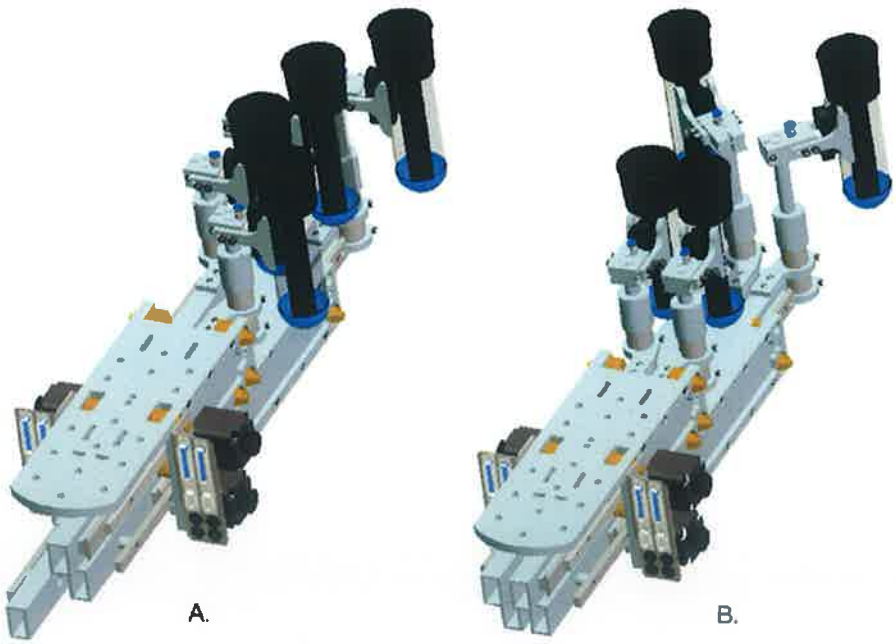

Figure 57. Possible test configurations: (A) side orientation for aquisition from a magazine rack and (B) use of only front two arms for cup application

3.12 Engineering drawings and construction

The solid modelling and evaluation process provided confidence that the final design was capable of performing the required operations within identified constraints. Engineering drawings were generated from the solid model and the end-effector was fabricated and assembled by the DCU workshop facility. The end-effector drawings are included in Appendix B.

Chapter 4

ROBOT ARM SPECIFICATION, INSTALLATION AND COMMISSIONING

4.1 Robot arm specification and selection

Industrial robot arms are commonly applied in current manufacturing systems, replacing human labour for a variety of repetitive, dangerous or unpleasant tasks. Use of industrial robots can significantly improve speed, accuracy and repeatability over manual labour, but severe restrictions in control flexibility (compared to a human worker) require that robot tasks must be well defined with limited deviation in environmental and task variables. Milking cup application is a suitable task for robotic automation, given that the task requires speed and accuracy, the environment is unpleasant for human labour and the workspace and control task are well-defined.

While many robot manipulator types are available, investigation was focused on standard 6-axis industrial robot arms as these are produced in sufficient quantities to allow economies of scale with associated reduction in costs, and the technology is mature and well-understood.

4.1.1 6-axis robot arm description and terminology

A 6-axis robot arm is illustrated in Figure 58. The robot arm design is analogous to a human arm, having a shoulder joint, upper arm, elbow joint, forearm and wrist, as shown in the illustration. The use of revolute joints for all axes simplifies the mechanical design and increases robustness as rotating joints are easier to seal than sliding joints. Figure 59 shows the robot coordinate system (RCS) and labelling convention for the robot axes, starting with axis 1 (or joint 1) at the base of the robot. In the model shown, the elbow motor is mounted on the shoulder and actuates the elbow axis via a pushrod, reducing mass at the elbow and thus reducing the required motor torque. Use of direct drive for axis 1 and 2 and a pushrod for axis 3 increases accuracy by eliminating backlash experienced with gears. It is generally infeasible to provide direct drive at the wrist as the increased mass would require increase in size of the first three axis motors. Instead, the wrist drive is

provided via drive shafts and gears through the forearm, with the motors mounted on the opposite side of the elbow joint to counterbalance the mass of the wrist, forearm and payload. The use of gears reduces positioning accuracy due to inevitable backlash and also limits the torque capacity of the wrist to a level that can be accommodated by the gear teeth. Increasing wrist torque capacity thus requires a corresponding increase in wrist size to accommodate larger gears.

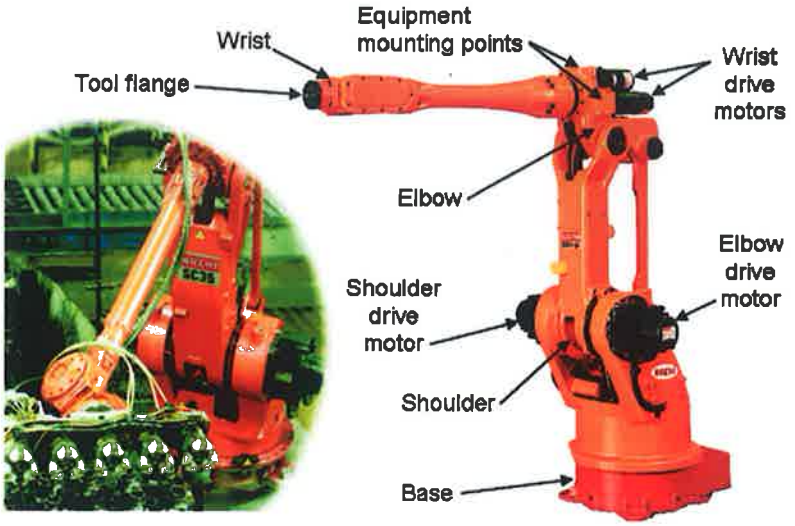

Figure 58. 6-axis robot arm and (inset) robot arm in operation

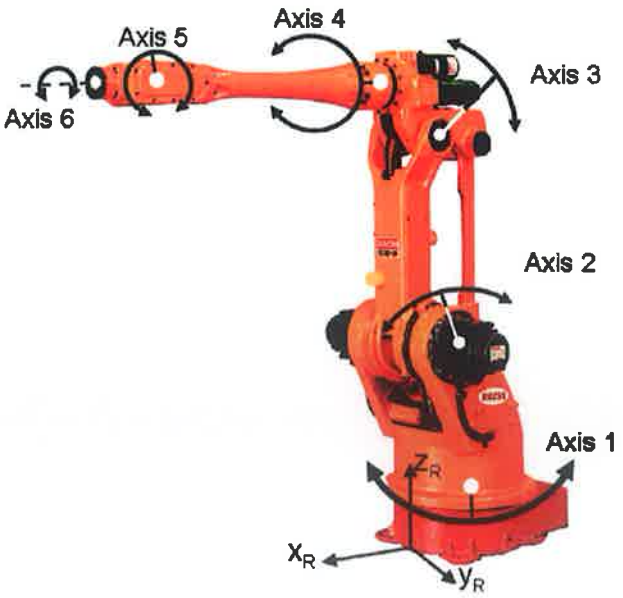

Figure 59. Axis locations for 6-axis robot arm

4.1.2 Robot arm specification

The solid-model analysis of sections 3.10.1 and 3.10.2 provided the payload and torque capacity requirements for the robot arm (Table 12 and Table 13 and Fig 50). These are summarised in Table 15 along with the reach distances necessary for access to the workspace. The centre of gravity (COG) measurement is required as in some cases the calculated moment of inertia of the payload may be within the capacity of the robot arm, but static torque due to the mass at the COG may still exceed permissible limits for the robot arm design.

Table 15. Robot arm torque and payload requirements

Coordinate system origin	**End-effector moment of inertia (kg m^2)**		
	I_{xx} Axis 4	**I_{yy} Axis 5**	**I_{zz} Axis 6**
ACS2	0.0794	1.5956	1.5564
Total payload mass			10.64kg
Minimum required reach (x-axis)			500mm
Minimum required reach (y-axis)			400mm
Minimum required reach (z-axis)			1200mm
Max. end-effector COG distance from wrist			329mm

In addition to these physical requirements, the robot controller was required to accept external commands and position data, and to provide return status signals to an external control system.

From an environmental point of view, sealed water-spray resistant robots were found to be 3 to 5 times more expensive than standard robot arms, and only a restricted range was available. Therefore it was decided that a standard robot would be specified (normally dust-proof but not moisture-proof), with some suitable shielding method applied (such as rubber gaiters) at a later development stage.

4.1.3Vendor investigation and selection

Based on these requirements, suitable robot arm models were investigated from five manufacturers. These were compared under the following headings:

- Payload capacity
- Torque capacity
- Reach
- External communications capability
- Cost

The static payload of 10.64kg was approximated as 11kg to allow margin for additional fittings and cable on the end-effector. While robot arms with capacities in the 11kg to 16kg range (a common payload range) would appear suitable, these payloads are specified at the wrist tool-flange, with the payload reducing as the centre of gravity of the tooling moves away from the tool-flange centre (due to the additional torque load on wrist-axis drive motors and the wrist drive gears). Knowledge of the centre of gravity of the end-effector (specified in Table 15) allowed comparison with manufacturers' wrist axis torque maps to determine whether the payload could be accommodated at the COG offset from the tool-flange.

While most of the product ranges examined contained a robot arm suited to the above requirements, there was significant variation in cost and availability. From the products examined, a Nachi SC35F-01 robot arm with AX-Controller was specified. This robot was available at the lowest cost, while satisfying all requirements for the application. Basic specifications for the SC35F-01 are included in Appendix C, while further reference may be found in the Nachi service manual. The 35kg payload of this arm, while exceeding the requirements for handling the end-effector by a significant margin, was necessary due to the offset nature of the end-effector mass. The next smaller sized robot in the Nachi range is the SC15F-02 (or SR15A-01 long-reach), however to allow this robot to be used the end-effector payload would have to be reduced by a minimum of 3kg, while the centre of gravity offset would have to be reduced to within 250mm from the tool-flange (feasible at attachment points ACS0 and ACS1, Table 13 , but not ACS2).

4.2 Installation and safety

Robot arms are powerful machine tools requiring careful positioning and installation to ensure stable and safe operation, and provision of appropriate safety measures to prevent injury and damage to personnel, fixtures and payload. The installation procedure specified by the manufacturer was studied and implemented, comprising the following steps:

- Identification of installation site
- Review of installation site for suitability and safety
- Provision of appropriate services
- Provision of appropriate safety measures

4.2.1 Installation site

A laboratory installation site was identified for the robot. Accurate architectural floor plans for the site were obtained, and following consultation with the school safety officer and senior technician a plan view of the required working area was developed. The plan included a suitable working region, sufficient rear clearance to avoid collision with fixtures or fittings, access to single and 3-phase power, positioning for the robot controller and other control equipment, and necessary safety fences. The details of this final layout are included in Appendix D. The working region comprises an angle of approximately 100° at a radius of 2m (the maximum reach of the robot arm, 2003mm). It was determined that this angle includes the expected working area in which the robot will operate. The safety fences were installed at a distance of 2.5m from the robot centre to ensure that robot contact was avoided during testing. The robot was prevented from travelling outside the working angle by adjusting mechanical stops on the base of the robot chassis.

Also included in Appendix D are the electrical supply specification for the robot and single-phase electrical supply and compressed air requirements for auxiliary equipment. These were extracted form the robot documentation and used to verify that the existing services were sufficient for the robot installation.

4.2.2 Safety

The power, speed and dexterity of a robotic manipulator raise important safety issues for autonomous operation. During automatic motion, it may be difficult for an operator to predict, anticipate or avoid motion of the robot arm, and thus the following safety steps are necessary:

- exclude access to the robot during operation
- warn personnel that the robot is active (even though it may be stationary)
- interrupt an operation if an intrusion occurs
- train relevant personnel who will work in proximity to the robot arm

Exclusion of personnel was achieved by installing safety fencing around the robot working area with a lockable access door and posting of warning notices on the enclosure. A warning lamp was provided to indicate when the robot arm was in operation, and provision was made for attachment of an interlock switch to the access door to interrupt operation when the door was opened. Training was provided via the relevant safety sections in the installation and operations manuals provided by the manufacturer, and operating procedure and signals were described to those who would work in proximity to the enclosure. In addition to emergency stop buttons on the robot controller and teach pendant, an external emergency stop switch was already in place in the laboratory to allow 3-phase power to be interrupted without entering the robot enclosure.

4.2 Robot Arm Installation

The robot arm installation was carried out according to the instructions provided by the manufacturers. It was verified that the installation surface (concrete floor) was of suitable composition, thickness and flatness, the installation location holes were measured out and marked as per Fig. D1 in Appendix D, and a contractor was employed to install appropriately sized threaded studs in the floor. The arm was lowered onto the studs and secured with bolts and washers tightened to the manufacturers' torque specification.

4.3 Robot Arm Commissioning

Commissioning of the robot arm involved the following steps:

- Familiarisation with manufacturers' safety instructions and commissioning procedure
- Familiarisation with manufacturers' operations manual
- Visual verification that all safety components were in place and operational
- Visual inspection of the robot working area to ensure readiness for operation
- Visual inspection of robot wiring and routing
- System power up and self-diagnostic
- Basic moves of all axes under manual control to verify correct operation

The robot operated as expected, with no unexpected behaviour. The robot may be operated in one of several operating modes: welding, material handling or palletising. The controller was configured in software for materials handling mode, which is closest to the intended milking-cup handling application.

4.4Elbow Mounted Equipment

End-effector tooling usually requires some additional control wiring, as well as air or hydraulic piping. These cables must be routed along the robot arm with appropriate protection from abrasion, pinching and flexure damage, and without interfering with arm movement. The robot arm was supplied with an internal cable loom consisting of 12 shielded twisted-pair signal lines (24 wires in total), 4 power lines and two air lines. These cables are accessed via connectors at the base of the robot and exit at a utility plate mounted in the side of the elbow. However the end-effector required at least 114 signal lines, as well as vacuum connections, so the robot cable provision was insufficient. Additionally, use of the internal cable loom would limit the end-effector cabling to one specific robot arm model, as connectors are not necessarily interchangeable between robot arm makes and models. It was therefore decided to attach the end-effector wiring loom externally, allowing the entire cabling assembly to be lifted off the robot if necessary. This design approach allows portability between robot arms (if necessary) and also eases disassembly for future transport or remodelling.

As the end-effector revolute arm position controllers were controlled via serial cable, positioning of these controllers on the elbow would greatly reduce the required cable count (from 40 to 12). Also, provision of power terminals for the necessary 24V and 5V at the elbow would reduce the cable count from base to elbow. Therefore, as commonly used on industrial robots, an equipment and terminal housing box was mounted at the robot elbow, as shown in Figure 60. Reference to Figure 58 shows the mounting points provided for mounting equipment on the robot elbow. Mounting in this position takes advantage of the greater torque available from the shoulder-mounted drives and proximity to the third axis minimises moment of inertia about that axis. The SC35F model has a payload of 294 N or approximately 29kg, providing ample capacity for the current requirements.

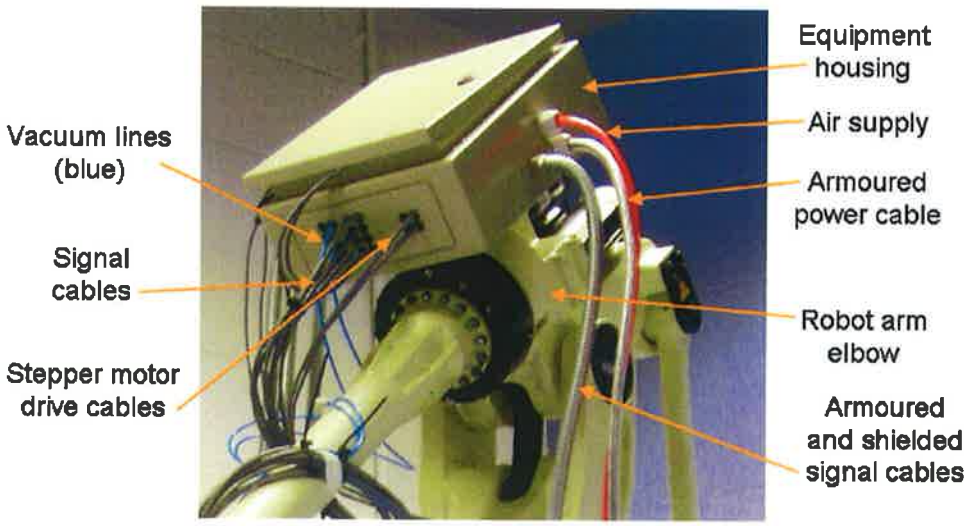

Figure 60. Elbow equipment housing detail

Proximity of the housing to the wrist-axis motors carried a risk of electromagnetic interference to components and signal cables, so a sheet metal electrical housing was chosen for the equipment housing, providing both mechanical strength and excellent shielding when grounded to the electrical supply earth. Figure 60 shows a detail of the housing mounted on the elbow, with a common power cable (24V, 5V and Ground), air supply line and signal cables from the robot base to the housing,

and signal, vacuum and power cables from the housing to the end-effector (note: not all cables are shown in this image, as the picture was taken during assembly).

The equipment housing internal layout is shown in Appendix E, Fig. E1.

Chapter 5

CONTROL SYSTEM DESIGN

5.1 Control system definition

The entire robotic manipulator for milking cup application incorporates a robot arm, end-effector tool and control system. The control system is the most critical and consequentially most complex component of these three elements, as it integrates the robot arm, end-effector and teat location information and implements a control strategy to perform the application task.

The control system for the manipulator comprises three primary layers:

- Control strategy – a high-level definition of how the application task is performed, based on known parameters, inputs and desired performance

- Software layer – the software system on which control strategy is implemented, the manipulator model is stored, inputs are processed and control outputs provided to the hardware layer

- Hardware layer – the physical electronic and electrical components that provide a platform for the software and a means of processing, conditioning and transferring signals between various system elements

In general a control system is defined in the above order, with the required strategy determining the necessary software and the software in turn determining the hardware layer. In practise however, as many of the hardware requirements were specified during the end-effector design, it was more natural to define the hardware requirements first and then determine suitable software to meet these requirements. The control system was specified around a basic high-level definition of the control strategy, as more in-depth algorithm design will be the subject of future work.

5.2 High level control system design

The control task and basic strategy were determined and defined in Chapter 2 as part of the environmental analysis and development of approach method. However the untested nature of the application will likely result in several modifications to the initial approach. The need for control flexibility was thus a requirement for the control system. The basic control algorithm extracted from the approach methodology of Chapter 2 is summarised in Figure 61.

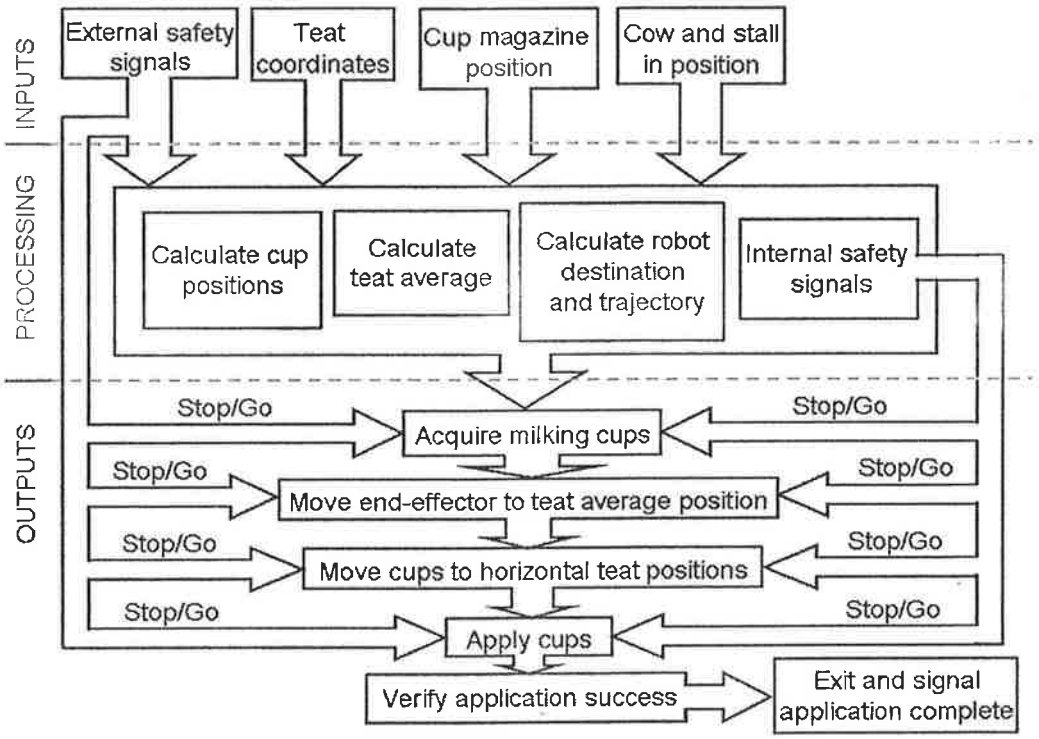

Figure 61. Basic control algorithm

The algorithm is divided into three distinct sections: inputs from external devices; processing of inputs based on stored models and procedures; and generation of outputs to drive the manipulator and provide necessary output signals to external devices. The role of both external and internal safety signals is clearly shown to the left and right of the output motion stages. The assumption was made that external safety signals are absolute and must always interrupt the process, while internal safety signals may also be generated based on teat position processing or manipulator performance monitoring. While necessary for final design, this safety layer can not be defined in detail until further external systems have been

investigated and designed (such as cow leg restraints, rotary parlour angular position control), and various operating strategies have been tried and tested (identifying possible failure modes). This safety design therefore remains to be performed in future development work. Similarly, the other input stages require inputs from external systems or devices that are not yet fully developed. Rather than attempting to pre-empt future design work on these stages, it was necessary to provide the capacity to receive and process these inputs without explicitly defining type or number of signals.

The control system arrangement to implement the above basic algorithm is shown in Figure 62. This high-level map shows the primary controller, the controlled elements and the necessary data flow for control.

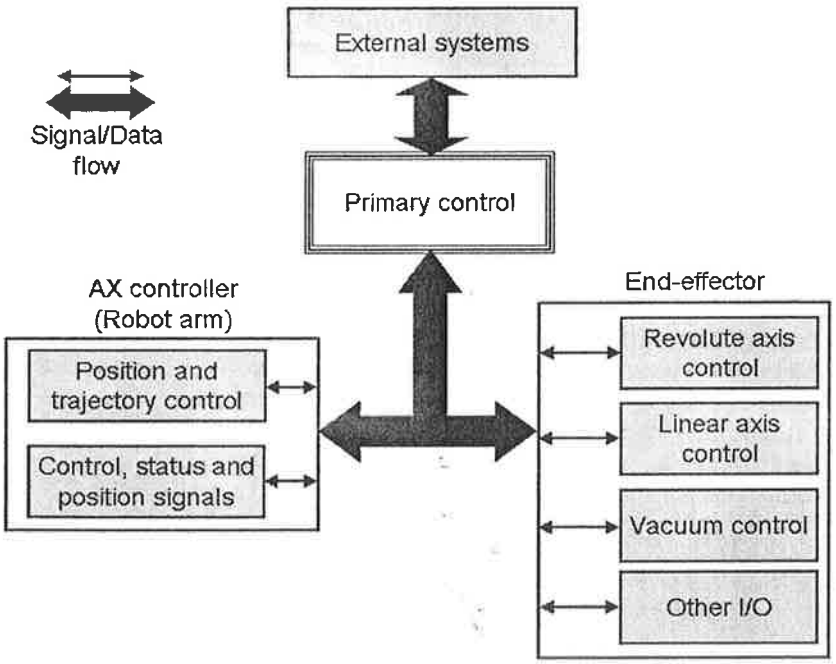

Figure 62. Control system map and data flow

This high-level definition was resolved into a lower level block-diagram containing known control elements (such as the servo motor and stepper motor controllers) and necessary signal conditioning, as shown in Figure 63.

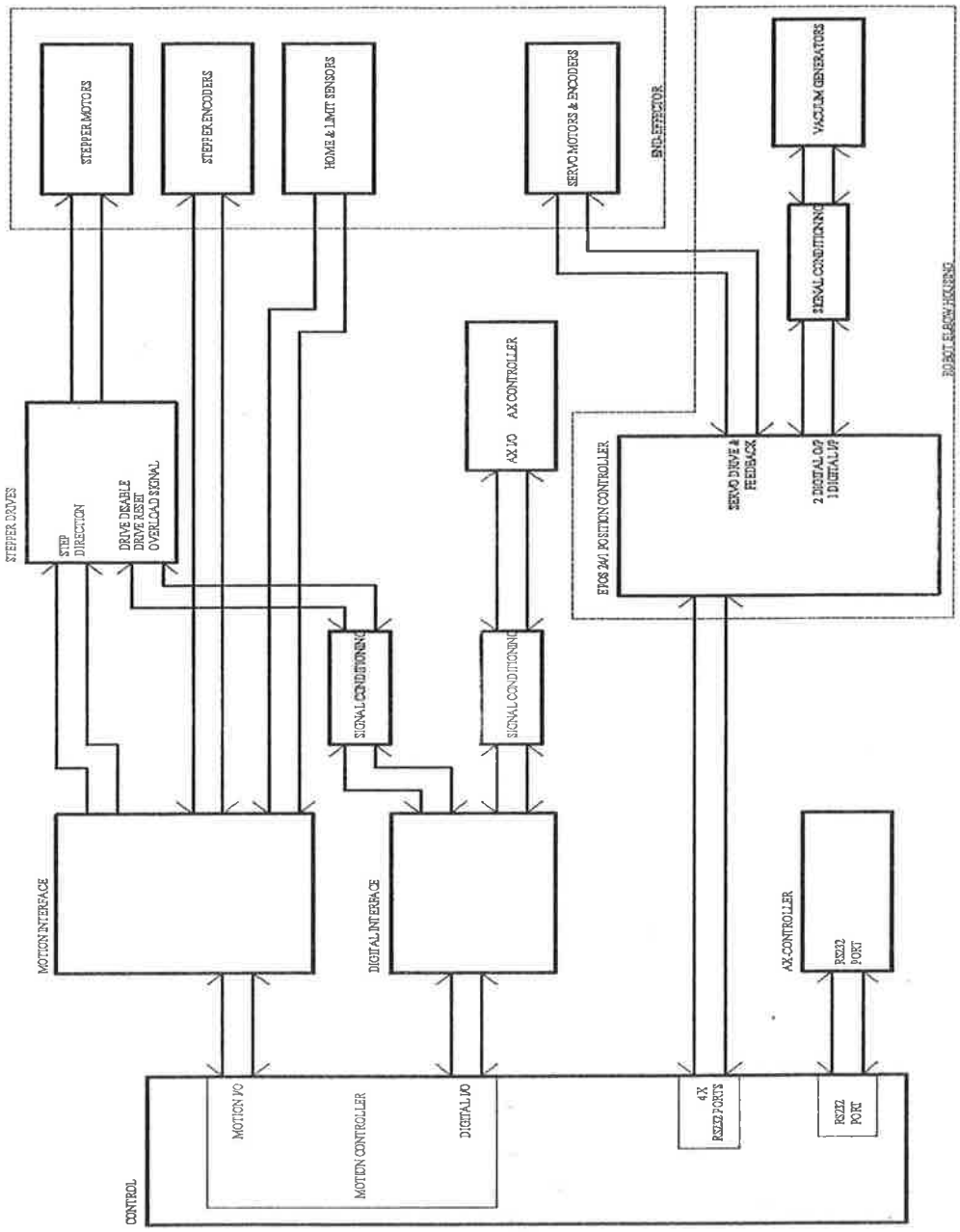

Figure 63. Control block diagram

It can be seen from Figure 63 that much of the hardware was already defined and known by the end-effector design and robot-arm interface requirements. The remaining control hardware element to be defined at this stage was the primary control platform.

5.2 Control Hardware

The control hardware comprises the electronic devices required to host the control software, accept and output signals and provide power drives to actuators.

Three basic hardware topographies are possible: centralised control, in which all signals are received and generated at a single unit; distributed control, in which several controllers control various aspects of the process and communicate on a peer level; and master-slave control, in which several distributed controllers handle sub-tasks but are controlled by a master control unit. The design of the manipulator follows the latter topography, with the robot arm controller, end-effector revolute axis and end-effector linear axis position controllers comprising the slave controllers and a central primary controller coordinating all three. This approach has the advantage of reducing the processing load of the primary controller, as processing-intensive tasks such as real-time position control are handled externally by the slave controllers, but at the allows overall system coordination from a central point. The control system topography is illustrated in Figure 64, showing the master controller, slave controllers, and controlled elements.

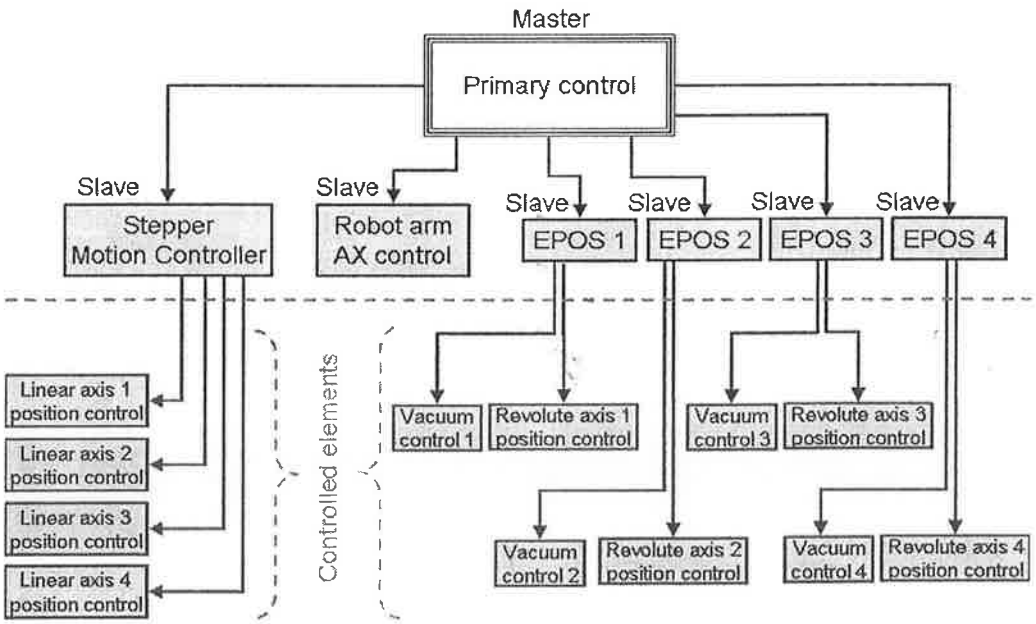

Figure 64. Control system topography

To specify the hardware, an input/output (I/O) definition was drawn up based on known requirements, and a suitable primary control platform was then specified.

5.2.1 Hardware I/O definition

The hardware I/O definition is included in Fig. F1, Appendix F. The definition is specified with respect to the primary controller, i.e. the Input table represents inputs to the primary controller and therefore outputs form the slave controllers. I/O were grouped by group (e.g. end-effector) and sub-group (e.g. servo drive), with each individual signal defined at high level in terms of the signal name and low-level in terms of the signal type (e.g. TTL, serial).

5.2.2 Slave control hardware

Distributed control hardware was already defined for the end-effector revolute axes as these were purchased as matched position controllers for the servo-motors. These EPOS 24/1 (brand name) position controllers feature a proprietary onboard real-time operating system that can provide closed-loop position and velocity control. PID control is implemented for angular position control of the motor and a self-tuning routine is provided to automatically select suitable parameters for the PID controller. The EPOS controller also has several digital I/O ports that may be used to accept additional sensor signals or control other equipment. External communications is via 3-wire RS232 serial connection. Further details of this controller may be found by reference to the manufacturers' literature [61].

For control of the stepper motors, a National Instruments PCI-7344 motion controller was available. This controller is supplied as a PCI card for fitting into a PC, but contains dual onboard processors (a microprocessor and digital signal processor) to process feedback signals and generate control signals independently of the primary control platform. This card can control four stepper motors, as well as all necessary travel limit and home sensor signals, and was therefore suitable for the control task. Additionally, the controller provided 32 digital I/O lines that could be utilised for control or monitoring of additional equipment. These additional I/O lines, although physically part of the motion controller, may be set and read directly by the primary control platform.

The stepper motion controller only provides step and direction output signals for stepper motor control, requiring an intermediate stepper drive to convert these signals into correctly phased drive currents for the stepper motors. As mentioned in section 3.7.3, suitable stepper drives were available at low cost from the stepper motor manufacturer. Four of these MSE-570 stepper drives were required. The stepper drives feature pre-selectable current control, allowing motor torque to be adjusted to match the application. Additional control inputs and outputs were provided on the drives, of which the stepper Overload output was used to monitor drive condition and the Reset and Output disable inputs were used to allow resetting of the drive after an overload condition and disabling of the stepper output. Disabling of the stepper output is necessary to allow the stepper motor shaft to rotate freely (e.g. for manual movement of the linear axis); when the stepper output is enabled and the motor shaft is stationary, current still flows in the motor phase coils and provides a braking or holding torque equal to the maximum torque available from the motor (in the case 0.29Nm).

The robot arm AX controller is the third slave controller. The AX controller is capable of operating as a stand-alone control unit or under external control. In either mode, the controller handles all aspects of manipulator control and requires only position and trajectory data, timing and start/stop control signals. Position data may be sent via the RS232 serial interface from the primary controller, and a programme written for the AX controller to process this data and move the end-effector to the target position. In addition, to the serial interface, a 32 input and 32 output signal lines are provided for input of control signals and output of status signals.

5.2.2 Primary control platform

Having defined the required I/O for the system and identified the slave controllers, the primary control platform could be specified. The primary control system is required to process teat positioning coordinates and provide control signals to slave controllers in approximate real-time, as well as handling additional processing tasks such as safety monitoring. Sufficient capacity must be provided for handling all input and output signals.

Use of the National Instruments motion controller for stepper motor control restricted choice of the control platform to one suitable for PCI cards. Normal PCs are readily and cheaply available, although they are not designed for robust control applications. Industrial PC platforms are available, but at considerable cost. As the application was for development and research however, a normal PC platform was deemed suitable. For the reasons specified in the next section, a high-speed, high memory PC was specified to facilitate fast processing performance for software applications. As five serial ports were required and only one was available on the PC, a serial port expander was installed to provide the additional capacity. Using the additional general I/O capacity on the stepper motor and servo motor controllers, sufficient signal lines were available for the entire manipulator. However if necessary a further I/O card may be added at a later date to expand the capacity of the PC.

5.3 Software platform selection

The software platform comprises two parts, the operating system and the control software. The operating system has a significant impact on real-time performance, as this controls all event timing on the PC. In the context of computer control 'real-time' refers to a deterministic response, such that the processing time for any task may always be determined in advance, allowing explicit timing of control operations (therefore 'real-time' does not necessarily imply high processing speed). Real-time operating systems are available from several vendors, however these are expensive and may require proprietary software for software development. The Windows XP operating system was available at relatively low cost and many software packages for control and development are available, however this operating system is not designed for real-time applications. It was assumed that the high-speed of the PC hardware would be sufficient to allow Windows XP to provide approximate real-time output even if not strictly deterministic, at least compared to the response requirements of the overall manipulator (i.e. sub-200ms positioning time). This assumption was deemed reasonably safe, as all time-critical motion control is handled by genuine real-time operating systems embedded in the slave controllers (the AX controller and servo and stepper controllers).

The second software element was the control software. While the software could have been developed using a language such a C, this is a time-consuming task, especially as many revisions would be necessary throughout the prototyping stage. For this reason Labview 8.0, an integrated graphical development environment, was selected for control software development. The software was available at DCU, and allows rapid software prototyping at high level by providing pre-defined software modules for programming and access to peripheral hardware. The software contained all mathematical functions anticipated for the control programme, and also allows development of code modules in other languages such as C. Finally, this package provides the option to compile developed graphical code into stand-alone programs to allow portability and take advantage of additional speed available by operation independent of the Labview environment.

5.4 Low-level schematic capture and cable specification

Following I/O definition and hardware and software specification, low-level schematics were developed for the various electronic circuits and wiring diagrams required to complete integration of the system elements.

Signal conditioning was necessary in some cases to convert signal types:

In the case of the revolute axis home sensors a comparator was used to threshold, buffer and amplify the high-impedance output from the optocoupler phototransitor, providing a 5V digital signal suitable for the EPOS controller input.

The interface between the 24V robot arm AX controller digital I/O and the 5V TTL digital I/O on the National Instruments motion controller card was constructed using opto-couplers. This optical isolation eliminated the need to link the grounds of the power supplies in each system together and reduced risk of damage to the control PC by accidental connection of the 24V supply to the PC 5V supply.

Amplification and signal conditioning was required to drive the vacuum generators from the EPOS controllers, converting the EPOS 24V high-impedance signal to a 24V current to operate the vacuum controller solenoids. This was achieved using a transistor stage to buffer the EPOS signal.

The cables required to carry signals and power were also specified on the schematics. Shielded cable was used in all cases to avoid electromagnetic interference from the robot arm drive motors and the end-effector signals. Groups of small diameter multi-cored cables were preferred to a single large cable, as smaller cables are easier to route, tend to have better flexibility and are available at lower cost. For differential signals (used for the position encoders) in which an inverted and non-inverted signal is provided for each output, shielded twisted pair (STP) cable was specified to take advantage of the additional interference rejection of this arrangement. Differential signals are subtracted at the receiving location, so if the non-inverted signal (A) is 0V, then the inverted signal (B) is 5V, and the resulting value (A-B) is -5V. If any noise has been superimposed on this signal, it should appear at the same voltage and phase on each line, due to the close proximity (twisted together) of the two signal wires. Thus if a noise spike of 3V appears on both lines, it will be attenuated by the subtraction (i.e. 3V-3V = 0). The twisted pair method also serves to reduce radiated interference, as any electromagnetic radiation from the pair will be comprised of opposing phases at similar amplitudes. The stepper motors require currents of up to 2.3A at frequencies up to 10kHz, resulting in significant radiated interference from the supply cables. To minimise this effect, shielded twisted pair cable was also specified for the stepper drive to stepper motor cables.

These schematics are included in Appendix G, along with the wiring allocation tables for the end-effector and stepper drives.

5.5 End-effector low-level control programming

While the robot arm is fully controlled via its control unit, the designed end-effector required a set of low-level control functions to operate and coordinate each of its axes and signals. These functions are identified in Table 16. Combinations of these functions were then used to implement control of the end-effector as a single unit, incorporating the inverse kinematics developed in Chapter 3.

Function name	Description	Inputs	Outputs
EPOS INIT	Initialise the EPOS controller with necessary parameters (assigned using manufacturer configuration utility), obtain EPOS ID ('KeyHandle') for all subsequent communications	Baudrate, timeout	KeyHandle
EPOS MOVE	Convert angle input to counts/rad and move revolute axis by number of counts	KeyHandle, theta	Position reached
EPOS HOME	Find revolute axis HOME position	KeyHandle	Home found
EPOS CLOSE	Release EPOS communications	KeyHandle	Closed
Linear Axis INIT	Initialises NI PCI-7344 controller with necessary parameters (assigned using manufacturer configuration utility)	-	-
Linear MOVE	Move linear axis to a target position (distance measured in encoder counts from home)	Axis ID, Target position	Move complete
Linear axis HOME	Find linear axis HOME position	Axis ID	Home found

Table 16. End-effector low-level control functions

5.5.1 Inverse kinematics programming

The inverse kinematic analysis developed in section 3.5.3 was incorporated into function blocks to control the position of the milking cups. The constant values identified in Table 7 were measured and tabulated in Table 17. These measurements were taken using a coordinate measuring probe, accurate to +/- 0.1mm, and Vernier callipers.

Constant	Definition	Measured values (mm)			
c_O		390			
		Axis 1	**Axis 2**	**Axis 3**	**Axis 4**
x_{On}	A constant offset in the x-direction from the flange centre	219.4	383.9	212.5	382
y_{On}	A constant offset in the y-direction from the flange centre	23.8	25	-28.4	-27.2
h_n	Length of revolute arm (from revolute axis to cup centre)	60.3	81.8	60	83

Table 17. End-effector constants

Figure 65 show the inverse kinematics function developed in Labview, with inputs at the left and outputs at the right of the diagram. The teat coordinates (q) are input as a three-element array (x, y, z), of which the x and y coordinates (elements 0 and 1 respectively) are extracted for use in the function. The average teat coordinate, qAV-1, is provided (calculated by another function block) along with the end-effector constants, and the inverse kinematic equations for each variable are calculated using mathematical and logic functions. Figure 65 also illustrates the Labview graphical programming method, in which function blocks are linked together to form a program. This program was in turn defined as a function block for reuse in other programs.

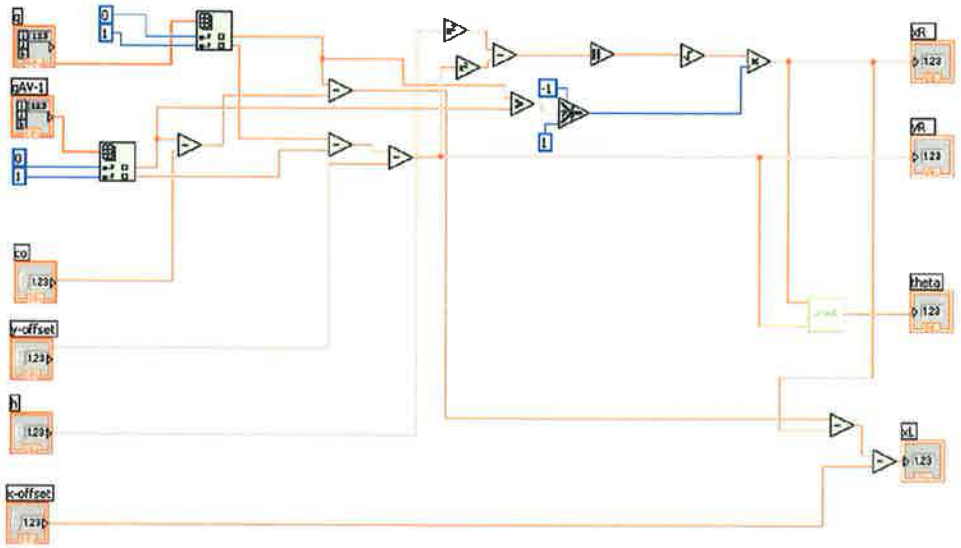

Figure 65. Labview inverse kinematics function

5.6 Robot control programming

A control programme was necessary to provide external control of the robot arm. Low-level control (start, stop, motors on, motors off) of the robot is achieved by setting specific AX controller inputs to the correct levels and in the correct sequence. For position control it was also necessary to write an internal programme for the AX controller to accept inputs and position data from the control PC.

5.6.1 External AX controller control programming

Under external control the AX controller cannot self-start, but must wait for an external start signal. The AX controller then executes a specific program from memory. Up to 1000 programs may be stored in the controller, and the programs may be selected by the external controller using binary code over a specific input range. Due to I/O limitations at the control PC, five input lines were assigned for program selection, allowing selection of 32 programs (2^5). The sequence and timing of program selection and start signals is important and these are explicitly defined in the robot arm operating manual.

A series of control functions were developed to allow external operation of the AX controller via the control PC digital I/O. These are summarised in Table 18.

Function name	Description
EXTERNAL STOP	Halt all robot arm activity and apply brakes to all axes. This signal overrides all other input signals
EXTERNAL MOTORS ON	Start robot motors and remove brakes from all axes (does not move robot arm)
EXTERNAL MOTORS OFF	Apply brakes and shut off all robot motors
PROGRAM SELECT	Selects a robot programme via the external selection inputs
EXTERNAL PLAY START	Starts the selected program, robot motion is possible after this signal
GENERIC SET 7344 PORT	Allows the control PC to SET an output signal to the AX controller high or low
GENERIC READ 7344 PORT	Allows the control PC to READ a signal from the AX controller

Table 18. Labview AX control functions

5.6.2 Internal AX controller programming

The AX controller is programmed in SLIM (Standard Language for Industrial Manipulators), a language similar to BASIC. The following code segment illustrates a typical AX program:

```
REM "program waits for shift signal from control pc'"
REM "when shift input is received, SREQ is issued and
move performed'"
WAIT I26,0,999
SREQ R1,1
SET O3
WAITR R1,3,10000
GETSFT V1!,R1
LETPOSE 1,V1!
MOVEX M1X,L,P1,S= 100.0,MS
RSCLR 1
END
```

In the above code, the AX controller is set to WAIT indefinitely (0=infinite time) until an external input, I26, is set high by the external control PC. The AX controller then sends a shift request, SREQ, to the control PC via the serial port to

request position coordinates, and output O3 is SET to alert the control PC that a request has been sent. The AX controller then waits (WAITR) until a response is received at the serial port and placed into internal register R1. The received position coordinates are then transferred from R1 into real number variables using the GETSFT command, starting at V1 (i.e. V1 = x, V2 = y, etc.). These real number variables are then converted to a Pose variable, P1, using the LETPOSE command. A Pose variable describes a complete robot arm toolplate position using 6 variables, x, y, z, r, p, y, where the first three terms describe position in Cartesian space and the last three terms describe the angles of the wrist axes. Finally a MOVEX command causes the robot arm to move to position P1, at speed, S, of 100mm/s. At the end of this operation, the serial port register R1 is cleared (RSCLR) and awaits another position input.

5.7 Supervisory Control programming

A supervisory control layer is required to coordinate all low-level control, monitor safety signals and implement suitable responses based on developed algorithms. The control layer should also incorporate the teat-position processing functions and control algorithms for implementing desired manipulator performance. This programming task is the subject of future work. For the present system, a basic control layer was assembled to test operation and allow basic coordination of the manipulator. The Labview control panel for this programme is shown in Figure 66. The control panel provided the ability to manipulate the various end-effector constants (top right), button controls to initialise the end-effector axes and robot arm (right and bottom right), and cycle control buttons to start a programmed cycle (right). At the top left of the panel a series of input boxes allowed artificial teat coordinates to be inserted, and below this the average teat coordinates (qAV) and calculated teat cup positions were displayed (Q1-Q4). The qAV-1 value represents the average teat position from the previous iteration, used to determine if the teat locations have moved beyond the reach of the end-effector axes. At the lower right of the panel emergency stop buttons were provided to interrupt operations in the event of malfunction. The emergency stop button simply stops operation, while the emergency escape button signals the robot to return to a known safe position at low speed. While it was desirable for the entire control panel to function as a single unit,

at present only some parts are fully functional, and more work is required to fully integrate all aspects.

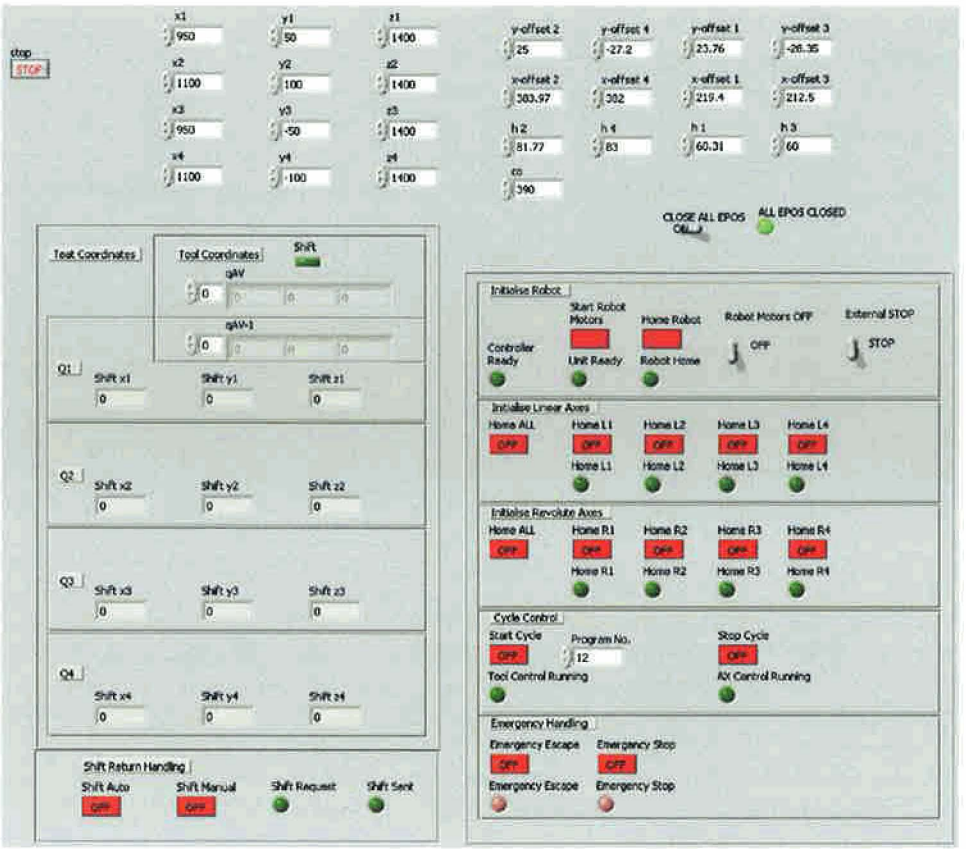

Figure 66. Labview test control panel

5.8 Control algorithm

A basic high-level control algorithm for the manipulator was outlined in section 5.2 and illustrated in Figure 61. There are numerous variations on this algorithm to be investigated and refined before a suitable operating method may be specified for the manipulator, and these form the basis for future work. As a starting point, a single cycle control loop algorithm was developed, as shown in Figure 67. Following initiation of the cycle, the steps within the dashed outline are performed subject to the status of the safety status signals, both internal and external.

Each step of this algorithm contains further sub-algorithms, for example the 'calculate end-effector axis positions' is an algorithm implemented in the Labview function shown in Figure 65.

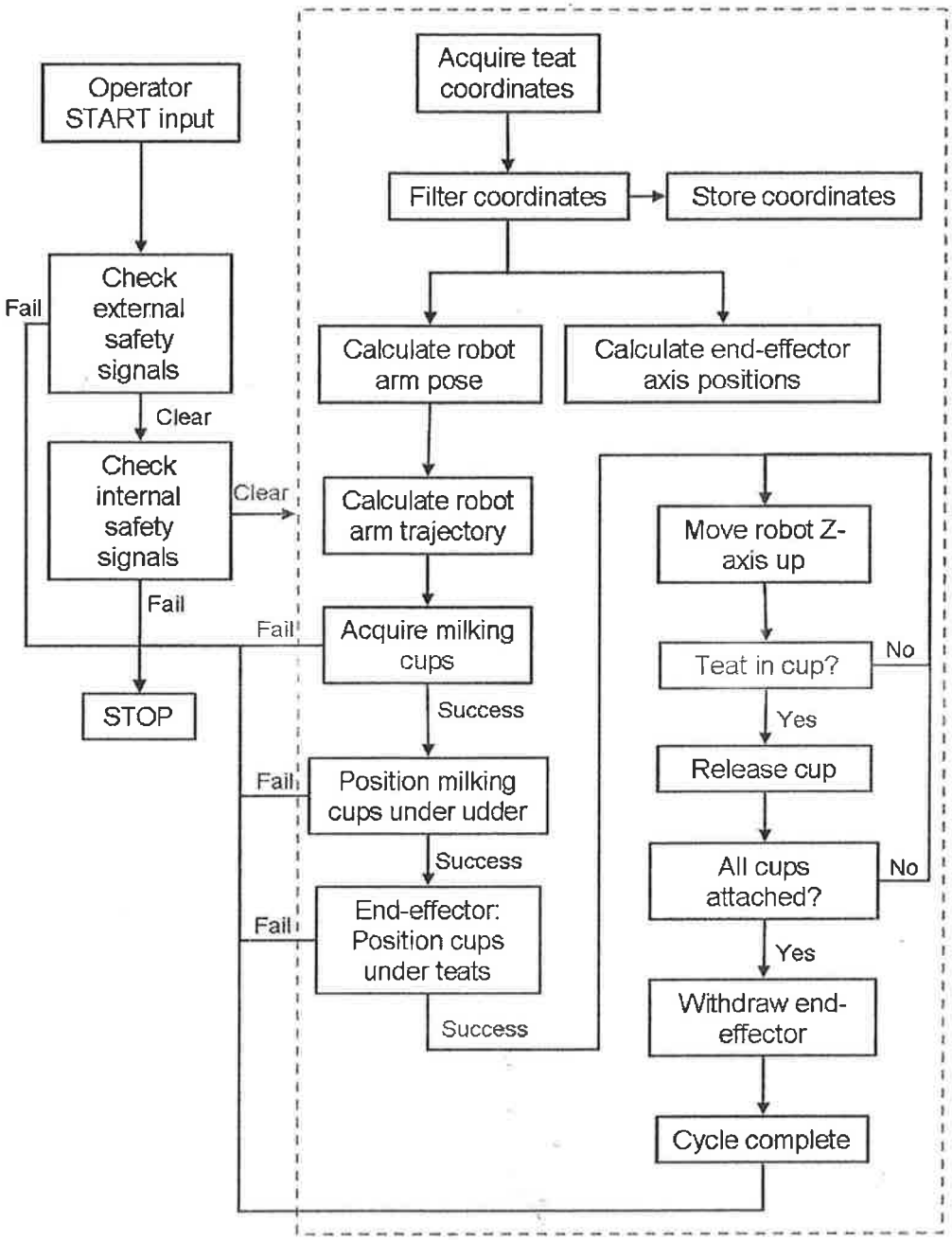

Figure 67. Basic cycle algorithm

5.9 Performance Testing

End-effector performance was tested to evaluate whether design goals stated in the end-effector PDS (Table 5) were met. The two test requirements were:

1. End-effector positioning accuracy and precision shall be tested
2. Positioning response time shall be tested for small movements

Tests were set up and performed to evaluate these requirements as described in the following sections.

5.9.1 End-effector accuracy

For position testing, a coordinate measuring probe (Microscribe) was set up with axes parallel to those of the end-effector and calibrated to provide measurements relative to the end-effector origin (the attachment point to the robot arm tool flange). The stated accuracy of the measurement probe was +/-0.1mm, and this was verified by taking manual linear measurements with a Vernier callipers and comparing to measurements taken with the probe. A milking cup was then sent to a position and the actual position was measured using the measuring probe. These measurements were taken for a single short axis (Q1) and a single long axis (Q2). 23 position measurements were taken for Q1 and 26 measurements were taken for Q2.

Position plots for the short and long arms are show in Figure 68 and Figure 69 respectively. These plots show the test path, describing a figure 'X' in the horizontal plane and extending to the limits of displacement for each axis. For each plot, it can be seen that the actual measured position tracks the demand position with reasonable accuracy. The error between demand and measured positions appears constant, suggesting small geometric misalignments in the end-effector construction or small errors in measurement of end-effector constant parameters.

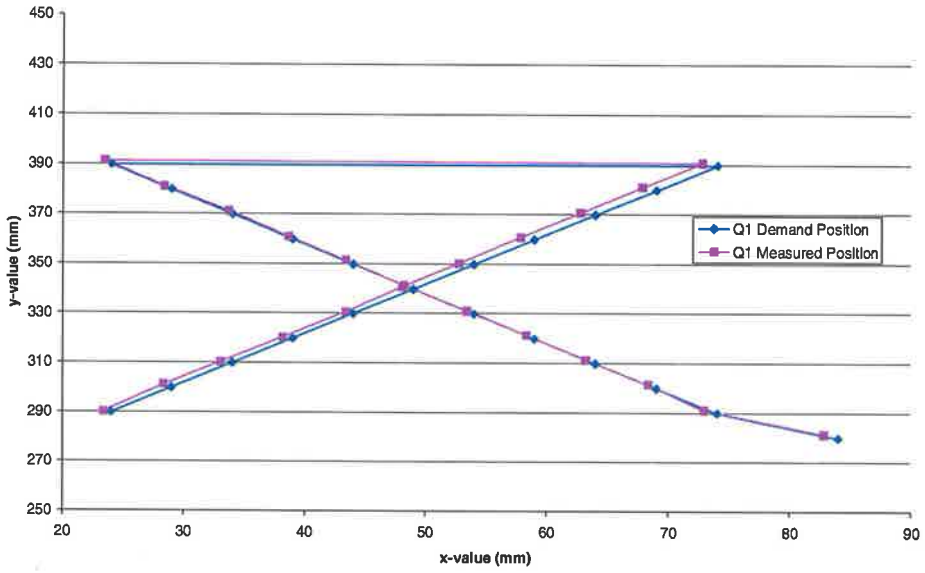

Figure 68. Q1 position plot, demand position and measured position

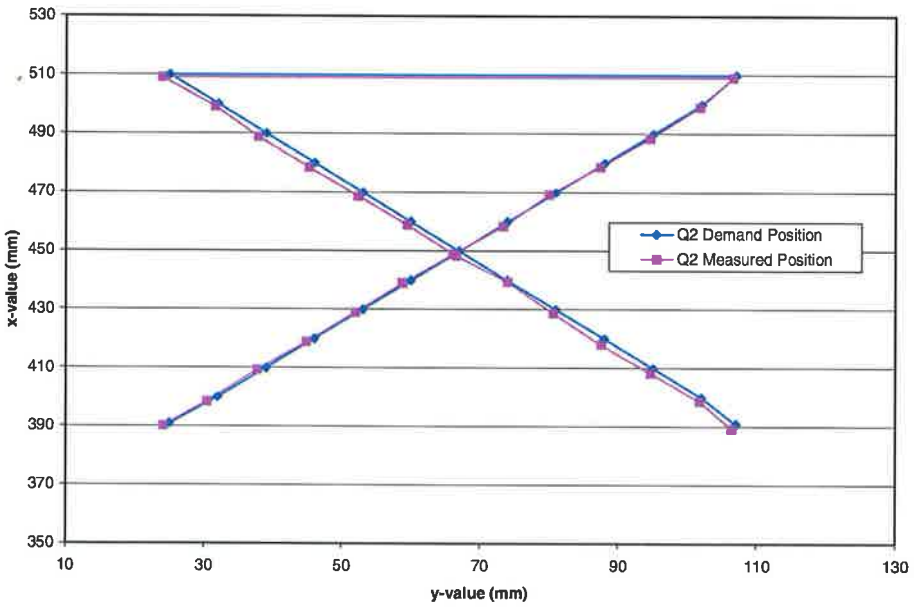

Figure 69. Q2 position plot, demand position and measured position

The position tests were examined more closely by plotting the x and y position errors, as shown in Figure 70 and Figure 71. For both arms it can be seen that the position error about the mean is inside the required +/-2mm position accuracy, with worst-case error ranges of 1.3mm (x) for Q1 and 1.5mm (y) for Q2 (rounded to one decimal place, as the resolution of the measuring probe was +/-0.1mm). The constant offset of the mean value from zero is due to two effects:

1. Small geometric inaccuracies in the end-effector and small errors in measurement of end-effector constants

2. The spring-effect of the vacuum tubing connected to the revolute axis arm

The first effect is expected and may be compensated for in software by subtracting the mean from calculated x and y coordinates.

The anticipated backlash for the revolute axis backlash should produce a small randomly distributed error about the mean, but the spring effect due to the vacuum tubing tends to hold the revolute arm against one side of the backlash, depending on which way the revolute arm is turning. This is observed in the plots of Figure 70 and Figure 71 as a bias above the mean for half of the tests and below the mean for the other half of the tests. Compensation for this second effect in software is impossible, as the effect may not be constant; however it usefully forced the measurements to the extremes of backlash in either direction, ensuring that the error range was well-identified.

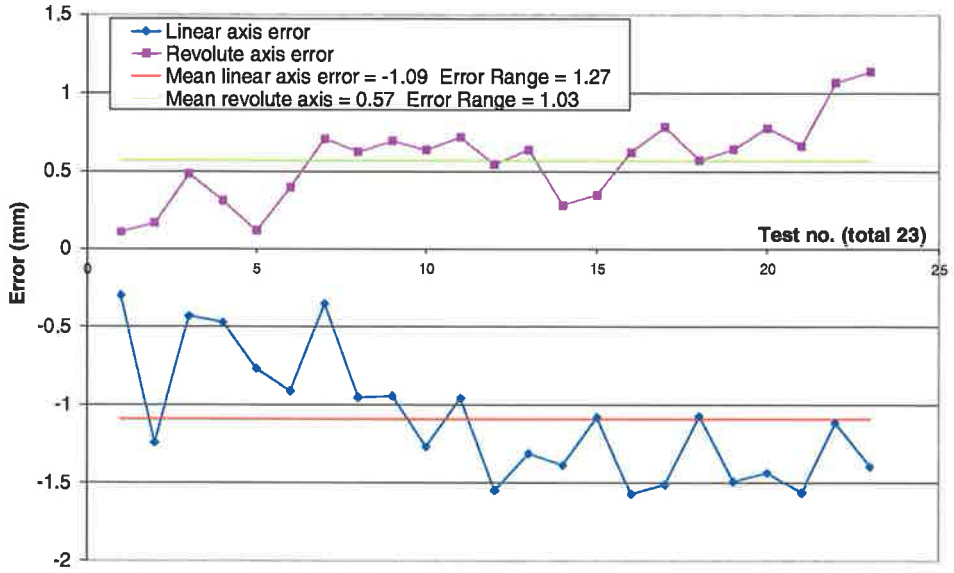

Figure 70. Plot of Q1 linear and revolute axis position errors and mean errors

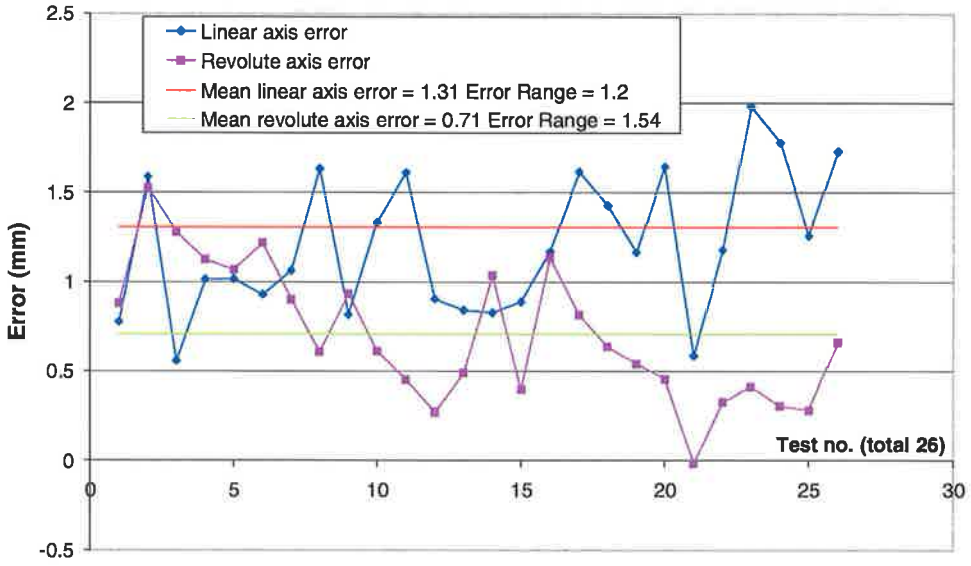

Figure 71. Plot of Q2 linear and revolute axis position errors and mean errors

5.9.2 End-effector axis precision

Precision for the long and short arms was tested by sending the arm to a target position 10 times and measuring the position error for each test. Three trials of 10 tests were conducted for each arm, with a different target position for each trial. In each test both arm axes were sent to the home position before being sent to the target position. The standard deviation was then calculated for each trial, as a measure of precision about the mean. The results of these tests are shown in Table 19.

Table 19. Precision tests

Arm	Trial (10 tests per trial)	Standard deviation (mm)	
		x	y
	1	0.3	0.6
Q1	2	0.1	0.4
	3	0.9	0.1
	1	0.1	0.1
Q2	2	0.1	0.5
	3	0.5	0.1

From Table 19 it can be seen that precision varied significantly between trials, with a worst case result of 0.9mm. The observed precision for both arms was well within positioning requirements (+/-2mm), however the test was too small to provide a complete characterisation of end-effector precision. A more extensive test is therefore recommended for future work.

5.9.3 End-effector positioning time

The target positioning time specified in the end-effector PDS was 200ms for moves within a range of +/-20mm. This performance was tested by measuring the time taken for each axis to achieve a required target position. For practical reasons, the linear and revolute axis travel times were measured separately: each axis position controller provided internal move timing measurement functions which were utilised to simplify the measurement operation, as the short time intervals would be difficult to measure using external equipment. Depending on axis angle, the revolute axis contributes to both x- and y- displacement, so measurement of time to cover an angle provides sufficient information to calculate both x- and y-displacement due to the revolute arm.

Tests were performed on a single long arm (Q2), as the longer arm has the longest travel and thus limits positioning time performance for the whole end-effector. For the linear axis, positioning trials were performed at eight points across the operating range of the linear axis. Each trial comprised 10 tests, with each test requiring travel to the target position from rest at the home position.

For the revolute axis positioning trials were performed at eight points across the operating range of the revolute axis (90°). Again, each trial comprised 10 tests, with each test requiring travel to the target position from rest at the home position. Revolute angles were converted to linear distances at an arm length of 83mm.

The results of these trials are graphed in Figure 72.

Comparison of the two curves in Figure 72 shows that the linear positioning velocity of the linear axis is far higher than that of the revolute axis. As linear and revolute axis travel can occur simultaneously, the revolute axis positioning time is the limiting factor for positioning performance. The linear axis can cover the entire travel range of 170mm in an average of 290ms, while the revolute axis can cover a linear distance of 83mm in an average of 454ms. For the +/-20mm region, average positioning time for the revolute axis was approximately 160ms and approximately 100ms for the linear axis. This is comfortably below the target time of 200ms.

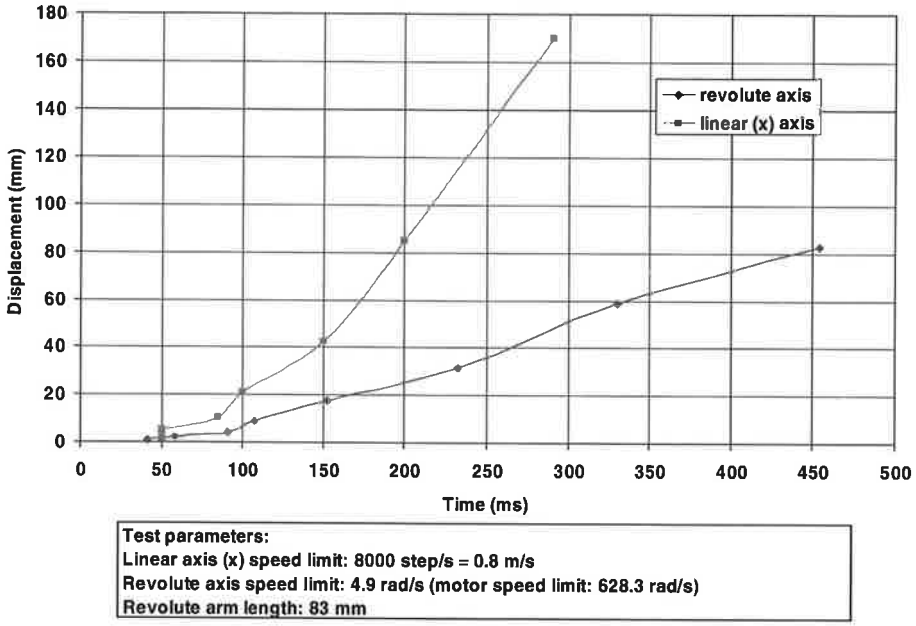

Figure 72. Positioning time performance for end-effector x and y axes

The cluster of trial points at 50ms for the linear axis curve are due to sampling limitations on the linear axis motion controller, as sample times below 50ms could not be achieved. It is also notable that the linear axis velocity curve becomes steeper and straighter as distance increases due to the linear axis achieving maximum velocity. At lower distances, maximum velocity is not reached, and thus positioning time is lower than theoretically possible. Small-displacement positioning time could be improved by increasing acceleration (acceleration was limited to 5000 step s^{-2}), but at the expense of higher gear wear and more vibration.

The performance limit of the revolute axis was due to the velocity limit of 628.3 rad s^{-1} (6000 rpm) assigned to the motor, giving a peak output angular velocity of 4.9 rad s^{-1} (47 rpm). This is the operating limit recommended by the manufacturer for the gearbox at 100% duty cycle; however as the duty cycle for the revolute axis is much lower than 100% it is possible that the motor speed limit could be raised to 837.3 rad s^{-1} (8000rpm, the operating limit for the motor at 100% duty cycle). According to the manufacturers' datasheet this increase would not reduce available torque and would thus provide a 33% increase in angular velocity, bringing the revolute axis linear positioning time close to that of the linear axis.

5.10 Vacuum gripper testing

The vacuum grippers were designed to hold the cup securely and rigidly during application, providing accurate positioning of the cup on the end-effector and thus allowing accurate positioning under the teat. In addition, some compliance was required during the acquisition operation to allow some misalignment between the cup vertical axis and the gripper. Adding compliance to the gripper would seem to reduce positioning accuracy by allowing some flexibility in the gripper, but this problem was solved by allowing a compliant-lipped vacuum cup to pull the milking cup back against a hard-stop. It was necessary to test that this method operated successfully.

The break-away force of the gripper vacuum cup was tested and verified for suitability during the design phase as noted in section 3.9.2. Acquisition performance was tested by arranging two milking cups in an approximately vertical position (+/- 3°), and programming two end-effector axes to grip the cups in a pinching motion between front and rear grippers as illustrated in Figure 73. A small spacer was necessary to keep the lower section of the cups separated, due to the larger diameter of the cup lips. This test was repeated five times, and in each test the cups were acquired successfully. The gripping method was thus verified for correct operation and ability to accommodate milking cup misalignment below 3°.

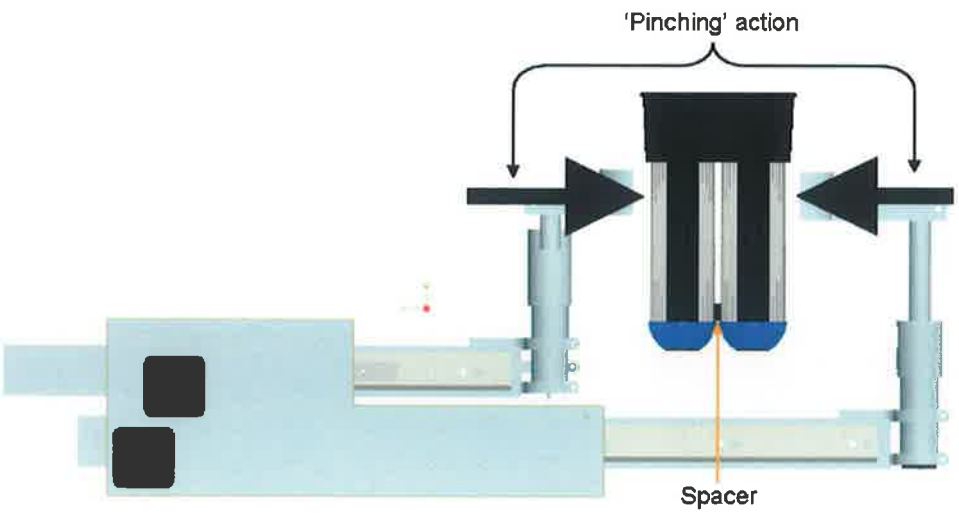

Figure 73. Gripper test - Cup acquisition between front and rear grippers

5.11 Robot arm interface testing

The robot arm is supplied in complete operational state, with test certification to verify that the robot arm functions within the manufacturers' specification. Thus performance testing of the robot arm was limited to verifying that all necessary functions could be controlled from the control PC and that position data could be sent to the AX controller and position movements executed.

The required control inputs and status signals are contained in the hardware I/O definition in Appendix F. The AX controller allows display of all I/O status, thus it was verified that each of these signals could be written to or read from the AX controller as necessary by the control PC.

A timing issue was discovered for the starting input signal for the AX controller. According to the manufacturers' specification, the start signal should have a duration of at least 200ms, however in practice it was found that a duration of at least 500ms was necessary to ensure consistent starting. This is likely due to the fact that the start signal is a relay contact on a power relay (unlike all other signals which are optically isolated digital inputs), and thus the physical switching time of the relay is a limiting factor. As the start signal only occurs once during an operating cycle, this timing limitation should not significantly affect performance.

A Labview programme was written to test position control of the robot arm using serial communications from the control PC. The front panel for this programme is shown in Figure 74. The programme allowed control over the AX controller via STOP, MOTORS ON/OFF and PLAY START/STOP switches. An internal programme was written for the AX controller to accept serial data from the control PC and perform a move (described in section 5.6.2).

The destination position was entered into the test programme as a text string ('SHIFT', top left of panel) in the format x, y, z, r, p, y, where x, y, z are the Cartesian coordinates for the centre of the tool flange, and r, p, y, are the roll, pitch and yaw angles of the robot wrist which determine the orientation of the tool-flange surface. Wrist roll, pitch and yaw correspond to the rotations of axes 4, 5 and 6 in Figure 59. By setting the tool-flange default position as horizontal, and keeping the

r, p, and y variables constant, the robot arm controller keeps the tool flange horizontal and the tool parallel to the x-axis for all moves. The -180 value for yaw shown in Figure 74 was necessary as the default wrist pose was taught with the z-axis rotated in the opposite direction.

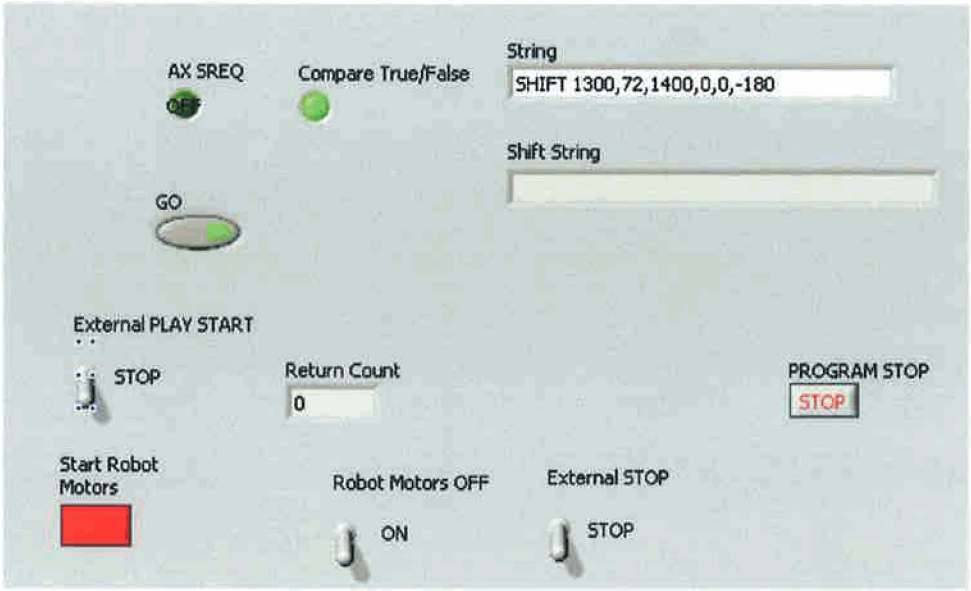

Figure 74. Labview control panel for AX position control testing

This test was successful in allowing coordinates to be sent to the AX controller, the coordinates were converted into a pose variable, and the robot arm moved the end-effector to the required position, with the end-effector x-axis maintained parallel to the RCS x-axis and in a horizontal orientation. In the test panel shown, the actual position was 1300mm in front of the RCS origin (x), 72mm to the left of the RCS origin (y) and 1400mm above the RCS origin (z, the floor in this case).

Chapter 6

CONCLUSIONS AND FUTURE WORK

6.1 Conclusions

The objective of this thesis was to design and build a robotic manipulator capable of applying milking cups to cow teats. This objective was fulfilled by accomplishing the following tasks:

- Analysis of the operating environment and parameterisation of the robot workspace
- Development of an approach methodology for operating in the workspace
- Conceptual and detailed design of a robotic end-effector capable of simultaneously handling four milking cups and suitable for operating within the identified workspace constraints
- Specification and selection of a suitable industrial robot arm and to carry the designed end-effector and capable of working in the identified workspace
- Definition of control system hardware and software requirements
- Specification and construction of control hardware
- Development of low-level control functions for end-effector and robot arm control
- Development of a basic control algorithm for control of the entire manipulator as a basis for future development
- Testing of end-effector performance and identification of areas for improvement

The thorough investigation, analysis and parameterisation of the working environment and workspace have established a well-defined basis for the current design and future development work.

Analysis of possible approach methods allowed a simultaneous cup application strategy to be adopted that should provide optimum application speed. However investigation of other approach strategies, such as two-at-a time application revealed that some testing of these would be warranted, and the end-effector has been

designed to facilitate testing of such methods. This approach fits well with the developmental nature of the manipulator, allowing several methods and strategies to be considered in future work.

Extensive application of computer-aided engineering (CAE) techniques in the design of the end-effector saved both time and material, with all of the iterative development work being carried out in software on a 3D solid model. This approach also accelerated robot arm specification by allowing mass and inertia properties to be determined before construction. The resulting end-effector design is capable of the simultaneous handling of four milking cups, having a profile that is sufficiently compact to allow access between the rear legs of the cow while enabling full access to all four teats. Measurement of the positioning response of the end-effector showed that performance is satisfactory for accommodating small changes in teat position during milking cup application. Positioning accuracy and precision were well within design specification, as demonstrated by system testing. The vacuum-based cup-gripper system proved capable of acquiring, retaining and releasing cups, and provided sufficient compliance to accommodate small misalignments between gripper and cup during acquisition.

Compared to the initial design goals outlined in the product design specification, the end-effector meets or exceeds all requirements with the exception of spray/dampness resistance for electronic components. The components specified during the design are sufficient for laboratory and limited field-testing, and may be modified or enclosed after the initial testing phase when the final requirements become clearer.

The component modules of the robotic manipulator were demonstrated to meet the requirements of a platform suitable for developing and testing application algorithms for high-capacity AMS. Although control functions were developed allowing complete control of all aspects of the manipulator, within the time constraints of the project testing was limited to modular level testing of the individual robotic manipulator and end-effector. Therefore complete integrated system testing remains for future work as outlined in the following section.

6.2 Recommendations for future work

The work performed as part of this thesis represents a starting point for development of high-capacity automatic milking. There are several additional investigative and design tasks to be performed, and numerous operating modes and strategies to be investigated before a final system is presented for autonomous operation in a rotary milking parlour. Several recommendations arising from work performed in these areas to date are provided in the following sections.

6.2.1 Future design work

Of future design tasks, the following are necessary:

1. *Design of a mechanism to encourage spreading of the rear legs and prevent interference with the end-effector during application*

Successful leg-spreading devices were encountered during the literature survey, and review of these devices is recommended as a basis for design work.

2. *Design of a mechanism to collect and assemble milking cups into a cluster suitable for acquisition by the end-effector*

It was assumed that milking cups could be presented in a known orientation and position for acquisition by the end-effector. Such component arrangement tasks are relatively common in industrial automation systems, and it may be expected that this can be achieved in a relatively simple manner. Two instances were noted in the literature survey of devices for retrieval and magazine presentation of milking cups, and these may be of value in developing a suitable design.

3. *Design of a control system to coordinate rotary parlour motion, the above two mechanisms, the milking parlour, and the robotic manipulator.*

Full automation of the milking process can only be obtained through coordination of the separate system elements: milking machine, rotary carousel, milking cup application robot, leg control device and other sensors. A governing control system, perhaps PLC or PC based, will eventually be required to provide interface between

system elements, manage system timing and, most importantly, monitor safety signals and provide appropriate response.

6.2.2 Future control tasks

Control strategy and implementation algorithms will require much analysis and development work. The basic algorithm defined in section 5.8 may serve as an initial foundation, however significant modification is expected and encouraged. Two aspects affecting control strategy are described below:

1. *Handling of milking lines*

The current end-effector design ensures straight-forward acquisition of cups and associated trailing milk lines, however following application of milking cups the trailing milking lines must be avoided. The revolute arms and grippers present a risk of entanglement and milking cup detachment during withdrawal of the end-effector, and careful consideration must be given to avoiding this failure mode. A relatively simply strategy is to ensure that all milking lines trail to one side of the end-effector, and that during withdrawal the end-effector is rotated about the central axis and away from the milking lines. Such a motion would use the side or bottom of the end-effector to push the milking lines to one side, away from the revolute axes and thus minimising risk of entanglement. Further risk reduction may be achieved by rotating the revolute axes in a direction that prevents entanglement with the lines. A second strategy involves using a separately actuated guide rod to hold milking lines to one side, clear of the end-effector during withdrawal, although this would add complexity and cost to the design.

In any event, it is required that milking line diameter be reduced to improve flexibility, and the external surface finish of the milking lines be rendered sufficiently smooth to promote sliding over guide surfaces (the nitrile rubber lines currently used are bulky and do not slide well). Such milking lines are already available at low cost and are expected to be available for future testing.

2. Vision system interface and error handling

During testing simulated teat position coordinates were entered manually, however it is intended that a teat detection system using computer stereo vision be interfaced with the robot manipulator. For future development, it is recommended the following be incorporated:

- Coordinates provided in Cartesian form (x, y, z)
- Coordinates referenced to the robot coordinate system (RCS)
- The coordinate stream is smoothed and error-checked

The first two requirements simply reduce the processing load on the control PC, and may be better implemented on the vision system platform where transformation software functions will be more readily available and in optimised form. The third requirement reduces processing load, but is also an important part of the safety layer, as inevitable interruptions or transient variations (e.g. discovery of a 'phantom teat') in the stream of coordinates may result in unpredicted motion of the manipulator. In the event of a single coordinate being 'lost' (e.g. due to transient noise), smoothing of the coordinate stream based on previous values is necessary to prevent sudden movements of the end-effector. Provided that this smoothing takes place, the manipulator control system can monitor the coordinate stream history for changes with safety implications; for example large changes in average teat position may be due to either position sensor failure or drastic movement by the animal and require immediate arrest of operations.

White, J., O'Callaghan, E.J., Corcoran. B., and Esmonde, H., (2006), "Design of a robotic manipulator for automatic application of milking cups" in *Summary of papers presented at the Agricultural Research Forum 2006, Tullamore, Co. Offaly, Ireland, March 15-16 2006*, Teagasc, pp.71

[1] Irish Dairies Board Annual Report 2004, Ireland, [online], http://www.idb.ie/ar2004/annual-report-2004-pdfs/complete.pdf (Accessed 20th March 2006)

[2] Irish Dairies Board, Ireland, [online], http://www.idb.ie/facts/facts7.htm (Accessed 21st March 2006)

[3] Compendium of Irish Agricultural Statistics 2005, Department of Agriculture and Food, Ireland, [online], http://www.agriculture.gov.ie/publicat/compendium2005/individuallist/O1.xls (Accessed 21st March 2006)

[4] O'Brien, B., et. al., (2001). "Profiling the working year on Irish dairy farms - identification of some work areas towards improvement in efficiency", in *Proceedings of Irish Grassland Association Dairy Conference, Cork, September 11-12, 2001*, pp.112-124

[5] Perkio-Makela, M., Hentila, H., (2004), "Physical work strain of dairy farming in loose housing barns", International Journal of Industrial Ergonomics, Vol. 35, pp.57–65

[6] Breen, J., Donnellan, T., and Hennessy, T., (2003), "A Future for Dairy Farmers after Fischler?", in *Proceedings of the National Dairy Conference 2003, Cork, Ireland, 12th November 2003,* [online], http://www.teagasc.ie/publications/2003/20031112/paper11.htm

[7] Dillon, P., Horan, B., and Shalloo, L., (2003), "Pathways to Increase Profit", in *Proceedings of the National Dairy Conference 2003, Cork, Ireland, 12th November 2003,* [online], http://www.teagasc.ie/publications/2003/20031112/paper8.htm (Accessed 22nd March 2006)

[8] O'Callaghan, E., et. al., "Milking facilities and labour", *Teagasc National Dairy Conference 2001, Cork, Ireland,* [online],

http://www.teagasc.ie/publications/2001/ndc/ndc-callaghan.htm, (Accessed 22nd March 2006)

[9] O'Callaghan, E., "Minimising Labour in Milking", in *Proceedings of the National Liquid Milk Conference 2000,* [online], http://www.teagasc.ie/publications/nlmc2000/paper1.htm, (Accessed 22nd March 2006)

[10] Bramley, A. J., et. al., (1992), *Machine Milking and Lactation,* Insight Books, Vermont, USA

[11] Culpin, C., (1981), *Farm Machinery,* (10th Ed.), Granada Publishing, London, pp. 316-317

[12] Mottram, T., (1997), "Requirements for teat inspection and cleaning in automatic milking systems", *Computers and electronics in agriculture*, Vol. 17, pp. 63-77

[13] Culpin, C., (1981), *Farm Machinery,* (10th Ed.), Granada Publishing, London, pp. 319-323

[14] Bomford, P. H., (1984) "Farm Machinery", in *R. J. Halley, ed., The Agricultural Notebook,* (17th ed.), Butterworths, London, p. 521

[15] Culpin, C., (1981), *Farm Machinery,* (10th Ed.), Granada Publishing, London, pp. 321-322

[16] Culpin, C,. (1975), *Profitable farm mechanization*, Granda Publishing, London, p.274

[17] Waikato Milking Systems newsletter, Issue 12, (2004), [online], http://www.waikatomilking.co.nz/files/Newsletter_June04.pdf, (Accessed 27th March 2006)

[18] Rossing, W. and Hogewerf, P. H., (1997), "State of the art of automatic milking systems", *Computers and electronics in agriculture*, Vol. 17, pp. 1-17

[19] Artmann, R., (1997), "Sensor systems for milking robots", *Computers and electronics in agriculture*, Vol. 17, pp. 19-40

[20] Kuipers, A., and Rossing, W., (1996), "Robotic milking of dairy cows", in *C. J. C. Phillips, ed., Progress in Dairy Science*, CAB International, Wallingford, pp. 263-280

[21] Ordolff, D., (2001), "Introduction of electronics into milking technology", *Computers and electronics in agriculture*, Vol. 30, pp. 125-149

[22] Ordolff, D., (1983), "Investigations on a system for automatic teat cup attaching", in *Proceedings of the National Conference for Agricultural Electronics Applications*, Chicago, December 1983, ASAE Publication 9-84, pp. 501-508.

[23] Hogewerf, P.H., et. al., (1992), "Observation of automatic teat cup attachment in an automatic milking system", in *A. H. Ipema, A. C. Lippus, J. H. M. Metz and W. Rossing, eds., Proc. Int. Symp. Prospects for Automatic Milking, Wageningen, November 1992,* European Association for Animal Production, Wageningen, Netherlands, Vol. 65, pp. 80-90.

[24] Armstrong, D. V., et. al., (1992), "Analysis of capital investment in robotic milking systems for US dairy farms", *Proceedings of the International Symposium on Prospects for Automatic Milking, Wageningen, November 1992,* European Association for Animal Production, Wageningen, Netherlands, Vol. 65, pp. 432-439

[25] Street, M. J., et. al., (1992), "Design features of the Silsoe automatic milking system", in *A. H. Ipema, A. C. Lippus, J. H. M. Metz and W. Rossing, eds., Proceedings of the International Symposium on Prospects for Automatic Milking, Wageningen, 23-25 November 1992,* European Association for Animal Production No. 65, Wageningen, Netherlands, pp. 40-49.

[26] Street, M. J., et. al., (1989), "Automatic Milking System", UK patent GB2226941

[27] van der Linden, R. and Lubberink. J., (1992), "Robot milking system (RMS): design and performance" in *A. H. Ipema, A. C. Lippus, J. H. M. Metz and W. Rossing, eds., Proceedings of the International Symposium on Prospects for Automatic Milking, Wageningen, 23-25 November 1992,* European Association for Animal Production No. 65, Wageningen, Netherlands, pp. 55-63.

[28] Ketelaar-de Lauwere, C. C. , Metz, J. H. M. (2000), "Behavioural aspects of grazing of dairy cows in combination with voluntary automatic milking" in *Gagnaux, D. , Poffet, J. R., eds., Proceedings of the fifth international symposium on livestock farming systems, Posieux, Fribourg, Switzerland, 19-20 August, 1999, 2000,* pp. 381-383.

[29] Hogeveen, H.,W., et. al., (2001) "Milking interval, milk production and milk flow-rate in an automatic milking system", *Livestock Production Science,* Vol. 72, pp. 157–167.

[30] Meskens, L., Vandermersch, M. and Mathijs, E., (2001), "Implication of the introduction of automatic milking on dairy farms: Literature review on the determinants and implications of technology adoption", EU project Automatic Milking Deliverable D1, [online], http://www.automaticmilking.nl/projectresults/Reports/DeliverableD1.pdf, (accessed 20th April 2006)

[31] Marchal, P., et. al., (1992) "Mains Project-Automatic Milking", in *A. H. Ipema, A. C. Lippus, J. H. M. Metz and W. Rossing, eds., Proceedings of the International Symposium on Prospects for Automatic Milking, Wageningen, 23-25 November 1992,* European Association for Animal Production No. 65, Wageningen, Netherlands, pp. 22-33.

[32] Artmann, R., (1992), "Status, results and further developments of automatic milking systems", in *A. H. Ipema, A. C. Lippus, J. H. M. Metz and W. Rossing, eds., Proceedings of the International Symposium on Prospects for Automatic Milking, Wageningen, 23-25 November 1992,* European Association for Animal Production No. 65, Wageningen, Netherlands, pp. 40-48.

[33] Notsuki, I. and Ueno, K., (1977) "System for Managing Milking Cows in Stanchion Stalls", US Patent US4010714

[34] Van den Berg, K., and Fransen, R., (1993), "Verichtung und Verfahren zur Nachbehandlung der Zitzen eines gemolinien Tieres", German Patent DE4293178

[35] Aurik, E. A., et. al., (1989), "Ultrasonic detector, methods for searching for a moving object, ultrasonic sensor unit, element for positioning an animal, terminal apparatus for an automatic milking system, and method for automatically milking an animal", European patent EP0323875

[36] Snijders, B., and Dieleman, P., (1998), "Automated milking parlor for dairy cattle uses optical sensors to detect positions of teats and attach suction pipes, requires minimal human labor", Netherlands patent NL1009631C

[37] Pera, A, (1989), "Milking Machine", European patent EP0309036

[38] Pera, A, (1988), "Milking Machine", US patent US4936256

[39] Cöp, J., and Petrus, H., (2001), "Milking system with three-dimensional imaging", World patent WO0200011

[40] Montalescot, J. B., (1987), "Installation de traite automatique", European patent EP0306579

[41] Duck. M., (1992), "Evolution of Duvelsdorf milking robot", in *A. H. Ipema, A. C. Lippus, J. H. M. Metz and W. Rossing, eds., Proceedings of the International Symposium on Prospects for Automatic Milking, Wageningen, 23-25 November 1992,* European Association for Animal Production No. 65, Wageningen, Netherlands, pp. 49-55.

[42] Duvelsdorf, A., and Duck, M., (1989), "Method and device for the mechanical attachment of one teat cup at a time", European patent EP300115

[43] WestfaliaSurge press release, (2004), "WestfaliaSurge: clear statement for the future of AMS", [online], http://www.westfalia.com/hq/en/what_is_new/news/2004/ams.aspx, (accessed 24th May 2006)

[44] Cosmi, F., et. al., (1997), "Automation in Dairy Farms: a Robotic Milking System", in *Proceedings of the 8th IEEE-ICAR'97 International Conference on Advanced Robotics, 7-9 July 1997,* Monterey, California, USA, IEEE, pp. 33-37

[45] DeLaval International AB information website, [online], http://www.delaval.com/Products/Automatic-Milking-Robotic-milking/DeLaval_VMS/default.htm, (accessed 24th May 2006)

[46] S. A. Christensen & Co. (SAC) information website, [online], http://www.sac.dk/showpage.php?pageid=695356&displayid=695495, (accessed 24th May 2006)

[47] Lely West N.V. information website, [online], http://195.162.136.141/Lely_COM_EN/agri/prodDisplay.jsp?PID=4625&PARID=4624, (accessed 24th May 2006)

[48] RMS Benelux B.V. information website, [online], http://www.robotmilking.com, (accessed 24th May 2006)

[49] Van der Lely, C., (1996), "An implement for automatically milking animals", European patent EP0689761

[50] Oosterling, P. A., (2000), "Method and device for the automatic milking of animals in milking positions which move in a revolving path", World patent WO0074472

[51] Snijders, B., and Dieleman, P., (1998), "Automatische milkinrichting met lichtsensor", Netherlands patent NL1009632

[52] Fransen, R. I. J, van den Berg, K., and van der Lely, A, (2001), "A construction for automatically milking animals", European patent EP1188367

[53] Kirk, J., (1984) "Cattle", in *R. J. Halley, ed., The Agricultural Notebook,* (17th ed.), Butterworths, London, p. 365

[54] Kuczaj, M., et. al., (2000), "Relations between milk performance and udder dimensions of black-white cows imported from Holland", *Electronic Journal of Polish Agricultural Universities, Animal Husbandry,* Vol. 3, Issue 2, [online], http://www.ejpau.media.pl/series/volume3/issue2/animal/art-01.html, (accessed 16th August 2004)

[55] ISO 5707:1996, Milking machine installations - Construction and performance, International Organisation for Standardisation

[56] Acts of the Oireachtas, No. 13/1984: Protection of Animals Kept for Farming Purposes Act, 1984, Section 4(1)(ii), [online], http://www.irishstatutebook.ie, (accessed 25th April 2005)

[57] Statutory Instrument No. 127 of 2000: European Communities (Protection of Animals Kept for Farming Purposes) Regulations, 2000, Section 4, (1), [online], http://www.irishstatutebook.ie, (accessed 25th April 2005)

[58] Whipp, J. I., (1992), "Design and performance of milking parlours", in *A. J. Bramley, F. H. Dodd, G. A. Mein and J. A. Bramley, eds, Machine Milking and Lactation*, Insight Books, Berkshire, UK, Pp.285–310

[59] Wase, L., et. al, (2005), "Gripper device, robot arm and milking robot", World patent WO2005122753

[60] Nachi Maintenance Service Manual SC/SR series [AX], 1st edition, Nachi-Fujikoshi Corp.

[61] EPOS 24/1 Positioning Controller documentation, maxon motor ag, Sachsein, August 2004 edition

APPENDICES

Index to Appendices

Appendix A - Actuator specifications

Appendix B - Engineering drawings

Appendix C - Robot arm specifications

Appendix D - Robot arm installation drawings and specifications

Appendix E - Elbow equipment housing layout

Appendix F - Hardware I/O definition

Appendix G - Electronics schematics

APPENDIX A - Actuator specifications

A1. Stepper motor datasheet

(reproduced courtesy of McLennan Servo Supplies Ltd.)

Size 17 high performance hybrid stepper motor 17HS-240E

The high performance size 17 hybrid stepper motor provides 200 steps /rev when used with full step drives or 400 steps per revolution in the preferred half step drive mode. The motor utilises advanced high energy magnet technology to provide increased torque while the low inductance windings provide excellent high speed performance. Consequently the unit is ideally suited to applications that require high dynamic performance where space is at a premium.
Where increased torque and resolution is required at reduced speed the motor may be fitted to the IP43 gearhead. The 17HS-240E motor is designed specifically for use with Bi-polar drive circuits such as the MSE570. Despite the high quality of the 17HS-240E, the units remain competitively priced and will therefore appeal to both small & medium volume OEM users.

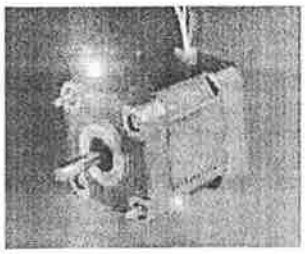

Dimensions mm

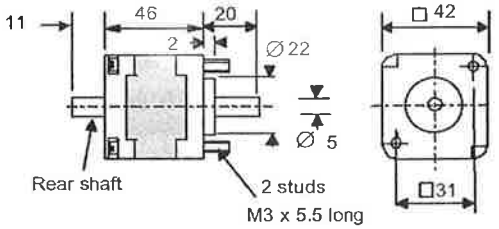

17HS –240E

Specification: 17HS –240E 1.8 degree hybrid stepper motor

motor type	length mm	holding torque Ncm	rotor inertia $Kgcm^2$	resistance per phase ohms	current per phase amps	inductance per phase mH	number of leads	mass Kg
17HS-240E	46	29	0.036	0.72	2.3	0.83	4	0.3

Connections

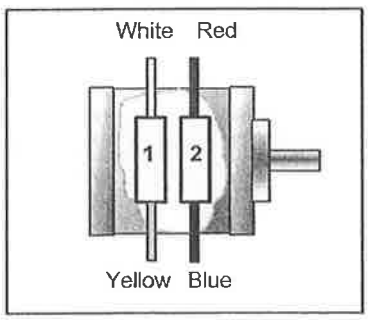

Performance using MSE570 drive

36 Volt rail: 2.3 Amps per phase

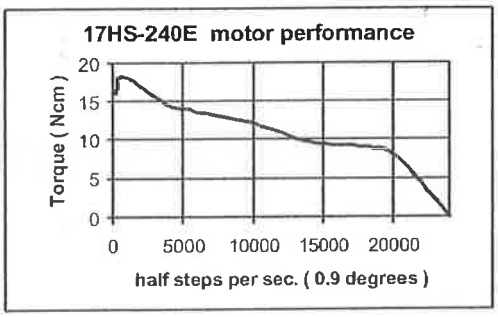

A2. Stepper motor position encoder datasheet – Part no. 110516
(reproduced courtesy of maxon motors UK Ltd.)

maxon tacho

Encoder HEDL 5540, 500 CPT, 3 Channels, with Line Driver RS 422

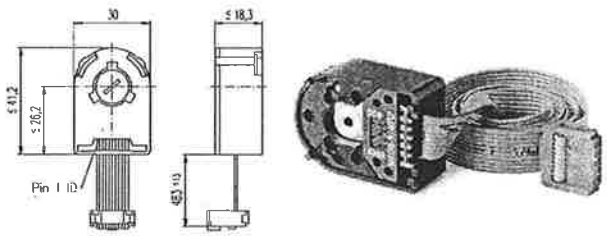

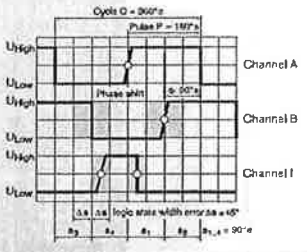

Stock program
Standard program
Special program (on request)

Order Number	110512	110514	110516
Type			
Counts per turn	500	500	500
Number of channels	3	3	3
Max. operating frequency (kHz)	100	100	100
Shaft diameter (mm)	3	4	6

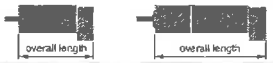

Combination

+ Motor	Page	+ Gearhead	Page	+ Brake	Page	Overall length [mm] / • see: + Gearhead		
RE 25, 10 W	77					75.3		
RE 25, 10 W	77	GP 26, 0.5 - 2.0 Nm	224			•		
RE 25, 10 W	77	GP 32, 0.4 - 2.0 Nm	226			•		
RE 25, 10 W	77	GP 32, 0.75 - 6.0 Nm	227/229			•		
RE 25, 20 W	78					75.3		
RE 25, 20 W	78	GP 26, 0.5 - 2.0 Nm	224			•		
RE 25, 20 W	78	GP 32, 0.4 - 2.0 Nm	226			•		
RE 25, 20 W	78	GP 32, 0.75 - 6.0 Nm	227/229			•		
RE 25, 20 W	78			AB 40	289	105.7		
RE 25, 20 W	78	GP 26, 0.5 - 2.0 Nm	224	AB 40	289	•		
RE 25, 20 W	78	GP 32, 0.4 - 2.0 Nm	226	AB 40	289	•		
RE 25, 20 W	78	GP 32, 0.75 - 6.0 Nm	227/229	AB 40	289	•		
RE 26, 18 W	79					77.2		
RE 26, 18 W	79	GP 26, 0.5 - 2.0 Nm	224			•		
RE 26, 18 W	79	GP 32, 0.4 - 2.0 Nm	226			•		
RE 26, 18 W	79	GP 32, 0.75 - 6.0 Nm	227/229			•		
RE 35, 90 W	81						91.9	
RE 35, 90 W	81	GP 32, 0.75 - 6.0 Nm	228/229				•	
RE 35, 90 W	81	GP 42, 3.0 - 15 Nm	232				•	
RE 35, 90 W	81			AB 40	289	124.1		
RE 35, 90 W	81	GP 32, 0.75 - 6.0 Nm	228/229	AB 40	289	•		
RE 35, 90 W	81	GP 42, 3.0 - 15 Nm	232	AB 40	289	•		
RE 36, 70 W	82						92.2	
RE 36, 70 W	82	GP 32, 0.4 - 2.0 Nm	225				•	
RE 36, 70 W	82	GP 32, 0.75 - 6.0 Nm	228/229				•	
RE 36, 70 W	82	GP 42, 3.0 - 15 Nm	232				•	
RE 40, 150 W	83						91.7	
RE 40, 150 W	83	GP 42, 3.0 - 15 Nm	232				•	
RE 40, 150 W	83	GP 52, 4.0 - 30 Nm	235				•	
RE 40, 150 W	83			AB 40	289	124.2		
RE 40, 150 W	83	GP 42, 3.0 - 15 Nm	232	AB 40	289	•		
RE 40, 150 W	83	GP 42, 4.0 - 30 Nm	235	AB 40	289	•		

Technical Data

Supply voltage	5 V ± 10 %
Output signal	EIA Standard RS 422
drivers used:	DS26LS31
Phase shift Φ (nominal)	90°e
Logic state width s	min. 45°e
Signal rise time (typical at C_L = 25 pF, R_L = 2.7 kΩ, 25°C)	180 ns
Signal fall time (typical at C_L = 25 pF, R_L = 2.7 kΩ, 25°C)	40 ns
Index pulse width (nominal)	90°e
Operating temperature range	0 ... +70°C
Moment of inertia of code wheel	≤ 0.6 gcm²
Max. angular acceleration	250 000 rad s⁻²
Output current per channel	min. -20 mA, max. 20 mA
Option	1000 counts per turn, 2 channels

Pin Allocation

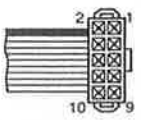

1	N.C.
2	V_{CC}
3	GND
4	N.C.
5	Channel $\overline{A}$
6	Channel A
7	Channel $\overline{B}$
8	Channel B
9	Channel $\overline{I}$ (Index)
10	Channel I (Index)

Pin type Berg 245770
flat band cable AWG 28

Connection example

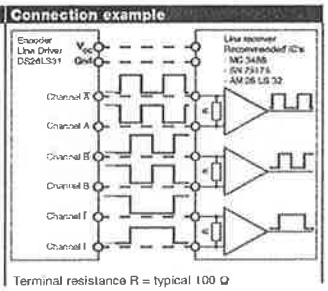

Terminal resistance R = typical 100 Ω

April 2006 edition / subject to change

A3. Servomotor datasheet – Part no. 110160

(reproduced courtesy of maxon motors UK Ltd.)

maxon DC motor

A-max 22 Ø22 mm, Graphite Brushes, 6 Watt

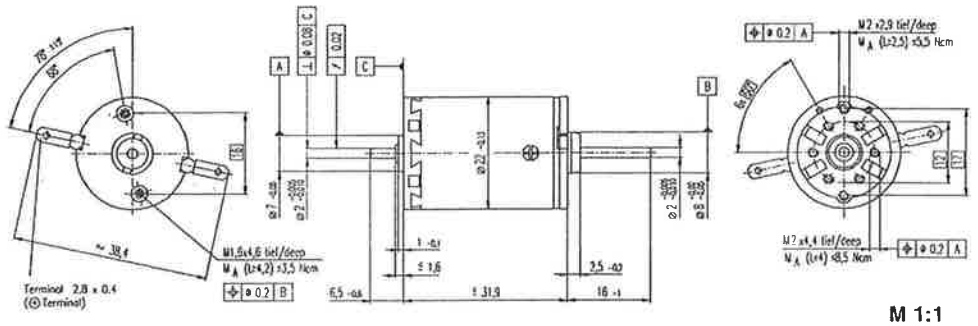

Stock program
Standard program
Special program (on request)

Order Number		110156	110158	110159	110160	110161	110162	110163	110164	110165	110166	110167	110168
Motor Data													
Values at nominal voltage													
1 Nominal voltage	V	6.0	9.0	9.0	12.0	12.0	15.0	18.0	24.0	24.0	36.0	48.0	48.0
2 No load speed	rpm	9250	9710	8530	10200	9200	10100	9800	10500	8500	9650	9130	8220
3 No load current	mA	83.2	57.9	49.7	45.9	40.5	36.0	29.0	23.7	18.4	14.2	10.0	8.85
4 Nominal speed	rpm	5550	6370	5240	6990	5960	6880	6630	7430	5340	6500	5920	5020
5 Nominal torque (max. continuous torque)	mNm	5.82	6.52	6.76	6.77	6.82	6.87	6.94	6.97	7.07	7.00	6.91	7.02
6 Nominal current (max. continuous current)	A	1.00	0.816	0.741	0.664	0.602	0.529	0.433	0.350	0.287	0.214	0.150	0.138
7 Stall torque	mNm	16.1	20.4	18.7	22.8	20.4	22.7	22.3	24.3	19.5	21.9	20.1	18.5
8 Starting current	A	2.73	2.38	1.92	2.09	1.69	1.64	1.30	1.14	0.745	0.631	0.411	0.340
9 Max. efficiency	%	65	70	60	72	71	72	72	73	71	72	71	70
Characteristics													
10 Terminal resistance	Ω	2.20	3.78	4.69	5.74	7.12	9.15	13.8	21.0	32.2	57.1	117	141
11 Terminal inductance	mH	0.105	0.222	0.288	0.362	0.445	0.584	0.890	1.37	2.10	3.68	7.29	8.95
12 Torque constant	mNm / A	5.90	8.55	9.73	10.9	12.1	13.9	17.1	21.2	26.2	34.8	48.9	54.3
13 Speed constant	rpm / V	1620	1120	981	875	790	689	558	450	364	274	195	176
14 Speed / torque gradient	rpm / mNm	604	494	473	461	465	455	451	445	447	450	466	456
15 Mechanical time constant	ms	25.2	21.8	21.2	20.6	20.3	19.9	19.4	19.1	19.0	18.9	18.9	18.8
16 Rotor inertia	gcm²	3.98	4.22	4.28	4.26	4.17	4.17	4.11	4.11	4.07	4.00	3.88	3.92

Specifications

	Thermal data	
17	Thermal resistance housing-ambient	20 K / W
18	Thermal resistance winding-housing	6.0 K / W
19	Thermal time constant winding	10.1 s
20	Thermal time constant motor	540 s
21	Ambient temperature	-30 ... +85°C
22	Max. permissible winding temperature	+125°C
	Mechanical data (sleeve bearings)	
23	Max. permissible speed	9800 rpm
24	Axial play	0.05 - 0.15 mm
25	Radial play	0.012 mm
26	Max. axial load (dynamic)	1 N
27	Max. force for press fits (static)	80 N
	(static, shaft supported)	440 N
28	Max. radial loading, 5 mm from flange	2.8 N
	Mechanical data (ball bearing)	
23	Max. permissible speed	9800 rpm
24	Axial play	0.05 - 0.15 mm
25	Radial play	0.025 mm
26	Max. axial load (dynamic)	3.3 N
27	Max. force for press fits (static)	45 N
	(static, shaft supported)	440 N
28	Max. radial loading, 5 mm from flange	12.3 N
	Other specifications	
29	Number of pole pairs	1
30	Number of commutator segments	9
31	Weight of motor	54 g

Values listed in the table are nominal.
Explanation of the figures on page 49.

Option
Ball bearings in place of sleeve bearings
Pigtails in place of terminals

Operating Range

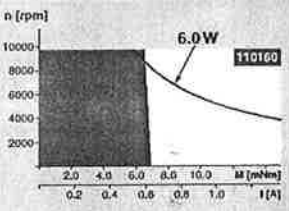

Comments

Continuous operation
In observation of above listed thermal resistance (lines 17 and 18) the maximum permissible winding temperature will be reached during continuous operation at 25°C ambient.
= Thermal limit.

Short term operation
The motor may be briefly overloaded (recurring).

Assigned power rating

maxon Modular System Overview on page 17 - 21

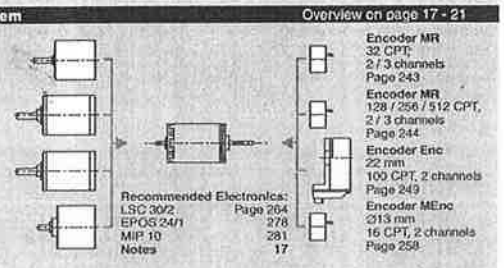

A4. Servomotor gearbox datasheet – Part no. 134170
(reproduced courtesy of maxon motors UK Ltd.)

Planetary Gearhead GP 22 A Ø22 mm, 0.5-1.0 Nm
Metalversion

maxon gear

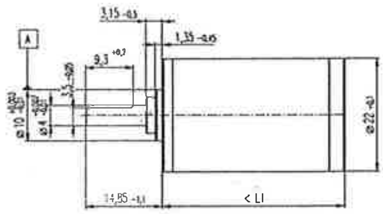

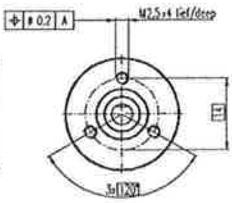

Technical Data

Planetary Gearhead	straight teeth
Output shaft	stainless steel, hardened
Bearing at output	ball bearings*
Radial play, 10 mm from flange	max. 0.2 mm
Axial play	max. 0.2 mm
Max. perm. radial load, 10 mm from flange	70 N
Max. permissible axial load	100 N
Max. permissible force for press fits	100 N
Recommended input speed	< 8000 rpm
Recommended temperature range	-15/+80°C

*Sleeve bearing on request

Stock program
Standard program
Special program (on request!)

Order Number		134156	134158	134163	134168	134172	110340	134183	134186	134190	134195	134203
Gearhead Data												
1 Reduction		3.8 : 1	14 : 1	53 : 1	104 : 1	198 : 1	370 : 1	590 : 1	742 : 1	1386 : 1	1996 : 1	3189 : 1
2 Reduction absolute		15/4	225/16	3375/64	[illegible]	[illegible]	[illegible]	[illegible]	[illegible]	[illegible]	[illegible]	1594323/500
Order Number		110337	134159	134164	134169	134173	134178	134184	134187	134193	134198	134204
1 Reduction		4.4 : 1	16 : 1	62 : 1	109 : 1	231 : 1	389 : 1	690 : 1	867 : 1	1460 : 1	2102 : 1	3728 : 1
2 Reduction absolute		57/13	[illegible]	[illegible]	2187/20	[illegible]	[illegible]	[illegible]	[illegible]	[illegible]	[illegible]	[illegible]
Order Number		134157	110338	134165	134170	134174	134180	134185	134188	134196	134200	134205
1 Reduction		5.4 : 1	19 : 1	72 : 1	126 : 1	270 : 1	410 : 1	850 : 1	1014 : 1	1538 : 1	2214 : 1	4592 : 1
2 Reduction absolute		27/5	3249/169	[illegible]	[illegible]	[illegible]	[illegible]	531441/625	[illegible]	98415/64	177147/80	[illegible]
Order Number			134160	134166	134171	134176	134179		134191	110341	134199	
1 Reduction			20 : 1	76 : 1	157 : 1	285 : 1	455 : 1		1068 : 1	1621 : 1	2458 : 1	
2 Reduction absolute			81/4	1215/16	19683/125	[illegible]	[illegible]		273375/256	[illegible]	[illegible]	
Order Number			134161	110339		134175	134181		134189	134194	134201	
1 Reduction			24 : 1	84 : 1		316 : 1	479 : 1		1165 : 1	1707 : 1	2589 : 1	
2 Reduction absolute			[illegible]	185193/2197		[illegible]	[illegible]		[illegible]	[illegible]	[illegible]	
Order Number			134162	134167		134177	134182		134192	134197	134202	
1 Reduction			29 : 1	89 : 1		333 : 1	561 : 1		1249 : 1	1798 : 1	3027 : 1	
2 Reduction absolute			729/25	4617/52		[illegible]	[illegible]		[illegible]	[illegible]	[illegible]	
3 Number of stages		1	2	3	3	4	4	4	5	5	5	5
4 Max. continuous torque at gear output	Nm	0.5	0.5	0.8	0.8	1.0	1.0	1.0	1.0	1.0	1.0	1.0
5 Intermittently permissible torque at gear output	Nm	0.8	0.8	1.2	1.2	1.6	1.6	1.6	1.6	1.6	1.6	1.6
6 Sense of rotation, drive to output		=	=	=	=	=	=	=	=	=	=	=
7 Max. efficiency	%	84	70	59	59	49	49	49	42	42	42	42
8 Weight	g	42	55	68	68	81	81	81	94	94	94	94
9 Average backlash no load	°	0.5	0.6	0.8	0.8	1.0	1.0	1.0	1.0	1.0	1.0	1.0
10 Mass inertia	gcm²	0.5	0.4	0.4	0.4	0.4	0.4	0.4	0.4	0.4	0.4	0.4
11 Gearhead length L1*	mm	25.4	32.2	39.0	39.0	45.8	45.8	45.8	52.6	52.6	52.6	52.6

*for A-max 19 and A-max 22 is L1 + 2.8 mm

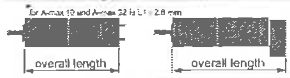

Combination:

+ Motor	Page	+ Tacho / Brake	Page	Overall length [mm]										
S 2322, 6.0 W	81/82			73.4	80.2	87.0	87.0	93.8	93.8	93.8	100.6	100.6	100.6	100.6
S 2322, 6.0 W	82	Digital Encoder 22	202	87.4	94.2	101.0	101.0	107.8	107.8	107.8	114.6	114.6	114.6	114.6
S 2322, 6.0 W	82	Digital Encoder HED_ 55_	204/206	94.2	101.0	107.8	107.8	114.6	114.6	114.6	121.4	121.4	121.4	121.4
A-max 19	109-112			51.5	58.3	65.1	65.1	71.9	71.9	71.9	78.7	78.7	78.7	78.7
A-max 19	109/111	Digital Magnetic Encoder 13	212	59.0	65.8	72.6	72.6	79.4	79.4	79.4	86.2	86.2	86.2	86.2
A-max 19	110/112	Digital Encoder 22	203	68.7	75.5	82.3	82.3	89.1	89.1	89.1	95.9	95.9	95.9	95.9
A-max 22	113-116			54.5	61.3	68.1	68.1	74.9	74.9	74.9	81.7	81.7	81.7	81.7
A-max 22	113-115	Digital Magnetic Encoder 13	212	61.6	68.4	75.2	75.2	82.0	82.0	82.0	88.8	88.8	88.8	88.8
A-max 22	114/116	Digital Encoder 22	203	69.0	75.8	82.6	82.6	89.4	89.4	89.4	96.2	96.2	96.2	96.2
RE-max 21	137-140	MR Encoder on request		51.5	58.3	65.1	65.1	71.9	71.9	71.9	78.7	78.7	78.7	78.7

A5. Servomotor position encoder datasheet – Part no. 201940
(reproduced courtesy of maxon motors UK Ltd.)

maxon tacho

Digital MR Encoder with Line Driver 5 mA, Type M

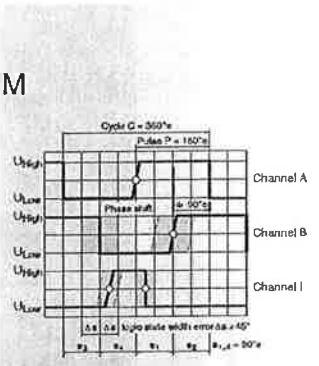

Stock program
Standard program
Special program (on request!)

Order Number	228179	228177	228181	228182	201937	201940
Type						
Counts per turn	128	128	256	256	512	512
Number of channels	2	3	2	3	2	3
Max. operating frequency (kHz)	80	80	160	160	320	320

Combination

+ Motor	Page	+ Gearhead	Page	+ Brake	Page	Overall length [mm] / ▸see: + Gearhead					
RE 16, 3.2 W	73					45.4	45.4	45.4	45.4	45.4	45.4
RE 16, 3.2 W	73	GP 16, 0.1 - 0.3 Nm	200			•	•	•	•	•	•
RE 16, 3.2 W	73	GP 16, 0.06 - 0.18 Nm	201			•	•	•	•	•	•
RE 16, 4.5 W	75					48.4	48.4	48.4	48.4	48.4	48.4
RE 16, 4.5 W	75	GP 16, 0.1 - 0.3 Nm	200			•	•	•	•	•	•
RE 16, 4.5 W	75	GP 16, 0.06 - 0.18 Nm	201			•	•	•	•	•	•
A-max 16	102/104					30.4	30.4	30.4	30.4	30.4	30.4
A-max 16	102/104	GS 16, 0.015 Nm	196			•	•	•	•	•	•
A-max 16	102/104	GS 16, 0.01 - 0.1 Nm	197-199			•	•	•	•	•	•
A-max 16	102/104	GP 16, 0.1 - 0.3 Nm	200			•	•	•	•	•	•
A-max 16	102/104	GP 16, 0.06 - 0.18 Nm	201			•	•	•	•	•	•
A-max 19	106					34.0	34.0	34.0	34.0	34.0	34.0
A-max 19	106	GP 19, 0.1 - 0.3 Nm	202			•	•	•	•	•	•
A-max 19	106	GP 22, 0.5 - 2.0 Nm	206/207			•	•	•	•	•	•
A-max 19	106	GS 24, 0.1 Nm	209			•	•	•	•	•	•
A-max 19	108					35.8	35.8	35.8	35.8	35.8	35.8
A-max 19	108	GP 19, 0.1 - 0.3 Nm	202			•	•	•	•	•	•
A-max 19	108	GP 22, 0.5 - 2.0 Nm	206/207			•	•	•	•	•	•
A-max 19	108	GS 24, 0.1 Nm	209			•	•	•	•	•	•
A-max 22	110/112					36.9	36.9	36.9	36.9	36.9	36.9
A-max 22	110/112	GP 22, 0.1 - 0.6 Nm	204/205			•	•	•	•	•	•
A-max 22	110/112	GP 22, 0.5 - 2.0 Nm	206/207			•	•	•	•	•	•
A-max 22	110/112	GS 24, 0.1 Nm	209			•	•	•	•	•	•
RE-max 17	132/134					30.4	30.4	30.4	30.4	30.4	30.4
RE-max 17	132/134	GP 16, 0.1 - 0.3 Nm	200			•	•	•	•	•	•
RE-max 17	132/134	GP 16, 0.06 - 0.18 Nm	201			•	•	•	•	•	•
RE-max 21	136					34.0	34.0	34.0	34.0	34.0	34.0
RE-max 21	136	GP 22, 0.5 - 2.0 Nm	206/207			•	•	•	•	•	•
RE-max 21	136	GS 38, 0.1 - 0.6 Nm	217			•	•	•	•	•	•
RE-max 21	138					35.8	35.8	35.8	35.8	35.8	35.8
RE-max 21	138	GP 22, 0.5 - 2.0 Nm	206/207			•	•	•	•	•	•
RE-max 21	138	GS 38, 0.1 - 0.6 Nm	217			•	•	•	•	•	•
RE-max 24	140/142					36.9	36.9	36.9	36.9	36.9	36.9
RE-max 24	140/142	GP 22, 0.5 - 2.0 Nm	207			•	•	•	•	•	•
RE-max 24	140/142	GS 38, 0.1 - 0.6 Nm	217			•	•	•	•	•	•

Technical Data

Supply voltage V_{CC}	5 V ± 5 %
Output signal	TTL compatible
Index pulse width (nominal)	90°e
Operating temperature range	-25 ... +85°C
Moment of inertia of code wheel	≤ 0.09 gcm²
Output current per channel	max. 5 mA

Attention: The index signal I is synchronised with channel A or B.

Pin Allocation

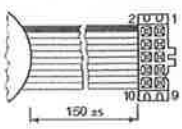

1 Motor +
2 V_{CC}
3 GND
4 Motor –
5 Channel $\overline{A}$
6 Channel A
7 Channel $\overline{B}$
8 Channel B
9* Channel $\overline{I}$ (index)
10* Channel I (index)

DIN Connector 41651
Flat band cable AWG 28
* version with 3 channels

Connection Example

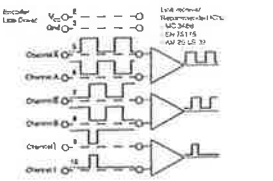

July 2004 edition / subject to change

Appendix B – Engineering Drawings

Bill of Materials for ENDEFFECTOR:			Cutting List			
			Material	Unit Size	Total (rounded) for parts	Total (rounded) for material
Qty	Type	Name	**Cast Tooling Plate**			
1	Part	BOTTOMPLATE	Aluminium, MIC6	196x85x10	196x85x11	X
1	Part	LEFTSIDE	Aluminium, MIC6	343x124x10	343x124x10	X
1	Part	RIGHTSIDE	Aluminium, MIC6	343x124x10	343x124x10	X Depends on
1	Part	TOPPLATE	Aluminium, MIC6	143x85x10	143x85x11	X stock sizes
1	Part	CENTREPLATE	Aluminium, MIC6	146x85x10	146x85x11	X for MIC6
2	Part	SERVOHOUSINGBRACKETUPPERLEFT	Aluminium, MIC6	74.5x40.5x8	149x40.5x8	X
4	Part	SERVOHOUSINGBRACKETLOWER	Aluminium, MIC6	74.5x40.5x8	298x40.5x8	X
2	Part	SERVOHOUSINGBRACKETUPPERRIGHT	Aluminium, MIC6	74.5x40.5x8	149x40.5x8	X
			Round Bar			
4	Part	BEARINGHOUSING	Aluminium F22 or similar	Ø30x36	Ø30x144	
4	Part	BEARINGCLAMPPLATE	Aluminium F22 or similar	Ø30x5	Ø30x20	**Ø30x164**
4	Part	BEARINGSPACER	Aluminium F22 or similar	Ø16x3	Ø16x12	
2	Part	SPACER	Aluminium F22 or similar	Ø16x3.54	Ø16x8	**Ø16x20**
2	Part	LONGSHAFT	Aluminium F22 or similar	Ø14x110	Ø14x220	
2	Part	SHORTSHAFT	Aluminium F22 or similar	Ø14x63	Ø14x126	**Ø14x346**
2	Part	RACKSPACER	Aluminium F22 or similar	Ø12x10.7	Ø12x22	**Ø12x22**
			Flat Bar			
2	Part	LONGSPACER	Aluminium F22 or similar	410x15x6	820x15x6	
2	Part	SHORTSPACER	Aluminium F22 or similar	336x15x6	672x15x6	**746x15x6**
			Tube: Rectangular/Round			
1	Part	SHORTARMRIGHT	Aluminium Tube Rect. F22	365x35x20x2.5	365x35x20x2.5	
1	Part	SHORTARMLEFT	Aluminium Tube Rect. F22	365x35x20x2.5	365x35x20x2.5	
1	Part	LONGARMRIGHT	Aluminium Tube Rect. F22	560x35x20x2.5	560x35x20x2.5	
1	Part	LONGARMLEFT	Aluminium Tube Rect. F22	560x35x20x2.5	560x35x20x2.5	**1850x35x20x2.5**
4	Part	SERVOHOUSING (two materials to be tested)	Aluminium Tube Round F22 SS Tube Round AISI 304	Ø25x1.5x71 Ø25x1.5x71	Ø25x1.5x284 Ø25x1.5x284	**Ø25x1.5x284** **Ø25x1.5x284**

(continued) Bill of Materials for ENDEFFECTOR:				
Qty	**Type**	**Name**	**Source**	**Material**
22	Part	4MMDOWEL	DCU SUPPLY	Pref. Stainless Steel, w/air relief for blind holes
8	Part	M4X30SOCKETSCREW	DCU SUPPLY	All Stainless Steel. 304 or similar
18	Part	M6X14SOCKETSCREW	DCU SUPPLY	
44	Part	6MMWASHER	DCU SUPPLY	
10	Part	M6X20SOCKETSCREW	DCU SUPPLY	
8	Part	M6X10SOCKETSCREW	DCU SUPPLY	
8	Part	M6X14HEXSCREW	DCU SUPPLY	
24	Part	M5X20HEXSOCKETSCREW	DCU SUPPLY	
2	Part	SHORTRACK	HPC IRELAND SUPPLY	
2	Part	LONGRACK	HPC IRELAND SUPPLY	
4	Part	PINION2MMCPX15T	HPC IRELAND SUPPLY	
2	Part	LONGSLIDE	HEPCO SUPPLY	
2	Part	SHORTSLIDE	HEPCO SUPPLY	
2	Part	SSLJ13C	HEPCO SUPPLY	
14	Part	SSLJ25C	HEPCO SUPPLY	
8	Part	BEARING21X12X5(6801DDU/2RS)	TEAGASC SUPPLY	
4	Part	MAXONGEARHEAD22MM	TEAGASC SUPPLY	
4	Part	MAXONSERVOMOTOR	TEAGASC SUPPLY	
4	Part	MAXONMRENCODER	TEAGASC SUPPLY	
4	Part	STEPPERMOTOR	TEAGASC SUPPLY	

Sub-Assembly Components

Sub-Assembly LONGARMRIGHT contains:		
1	Part	LONGARMRIGHT
1	Part	LONGSPACER
1	Part	LONGSLIDE
1	Part	LONGRACK
1	Part	SERVOHOUSINGBRACKETUPPERRIGHT
1	Part	SERVOHOUSINGBRACKETLOWER
1	Sub-Assembly	LONGROTARYLINK
1	Part	RACKSPACER
5	Sub-Assembly	M6X14ANDWASHER
3	Sub-Assembly	M6X20ANDWASHER
3	Part	4MMDOWEL
2	Part	M4X30HEXSOCKETSCREW
2	Sub-Assembly	M6X10ANDWASHER
2	Sub-Assembly	M6X10HEXSCREWANDWASHER

Sub-Assembly SHORTARMLEFT contains:		
1	Part	SHORTARMLEFT
1	Part	SHORTSPACER
1	Part	SHORTSLIDE
1	Part	SERVOHOUSINGBRACKETLOWER
1	Part	SHORTRACK
1	Part	SERVOHOUSINGBRACKETUPPERLEFT
1	Sub-Assembly	SHORTROTARYLINK
4	Sub-Assembly	M6X14ANDWASHER
2	Sub-Assembly	M6X20ANDWASHER
2	Sub-Assembly	M6X10ANDWASHER
2	Sub-Assembly	M6X10HEXSCREWANDWASHER
2	Part	M4X30HEXSOCKETSCREW
2	Part	4MMDOWEL

Sub-Assembly SHORTARMRIGHT contains:		
1	Part	SHORTARMRIGHT
1	Part	SHORTSPACER
1	Part	SHORTSLIDE
1	Part	SERVOHOUSINGBRACKETUPPERRIGHT
1	Part	SERVOHOUSINGBRACKETLOWER
1	Sub-Assembly	SHORTROTARYLINK
1	Part	SHORTRACK
2	Sub-Assembly	M6X20ANDWASHER
4	Sub-Assembly	M6X14ANDWASHER
2	Part	M4X30HEXSOCKETSCREW
2	Part	4MMDOWEL
2	Sub-Assembly	M6X10ANDWASHER
2	Sub-Assembly	M6X10HEXSCREWANDWASHER

Sub-Assembly SHORTROTARYLINK contains:		
1	Sub-Assembly	BEARINGHOUSINGANDSHORTSHAFT
1	Part	SERVOHOUSING
1	Sub-Assembly	SERVOMOTOR

Sub-Assembly BEARINGHOUSINGANDSHORTSHAFT contains:		
1	Part	BEARINGHOUSING
2	Part	BEARING21X12X5 (6801)
1	Part	BEARINGSPACER
1	Part	SHORTSHAFT
1	Part	BEARINGCLAMPPLATE

Sub-Assembly LONGROTARYLINK contains:		
1	Sub-Assembly	BEARINGHOUSINGANDSHAFT
1	Part	SERVOHOUSING
1	Sub-Assembly	SERVOMOTOR

Sub-Assembly BEARINGHOUSINGANDLONGSHAFT contains:		
1	Part	BEARINGHOUSING
2	Part	BEARING21X12X5
1	Part	BEARINGSPACER
1	Part	LONGSHAFT
1	Part	BEARINGCLAMPPLATE

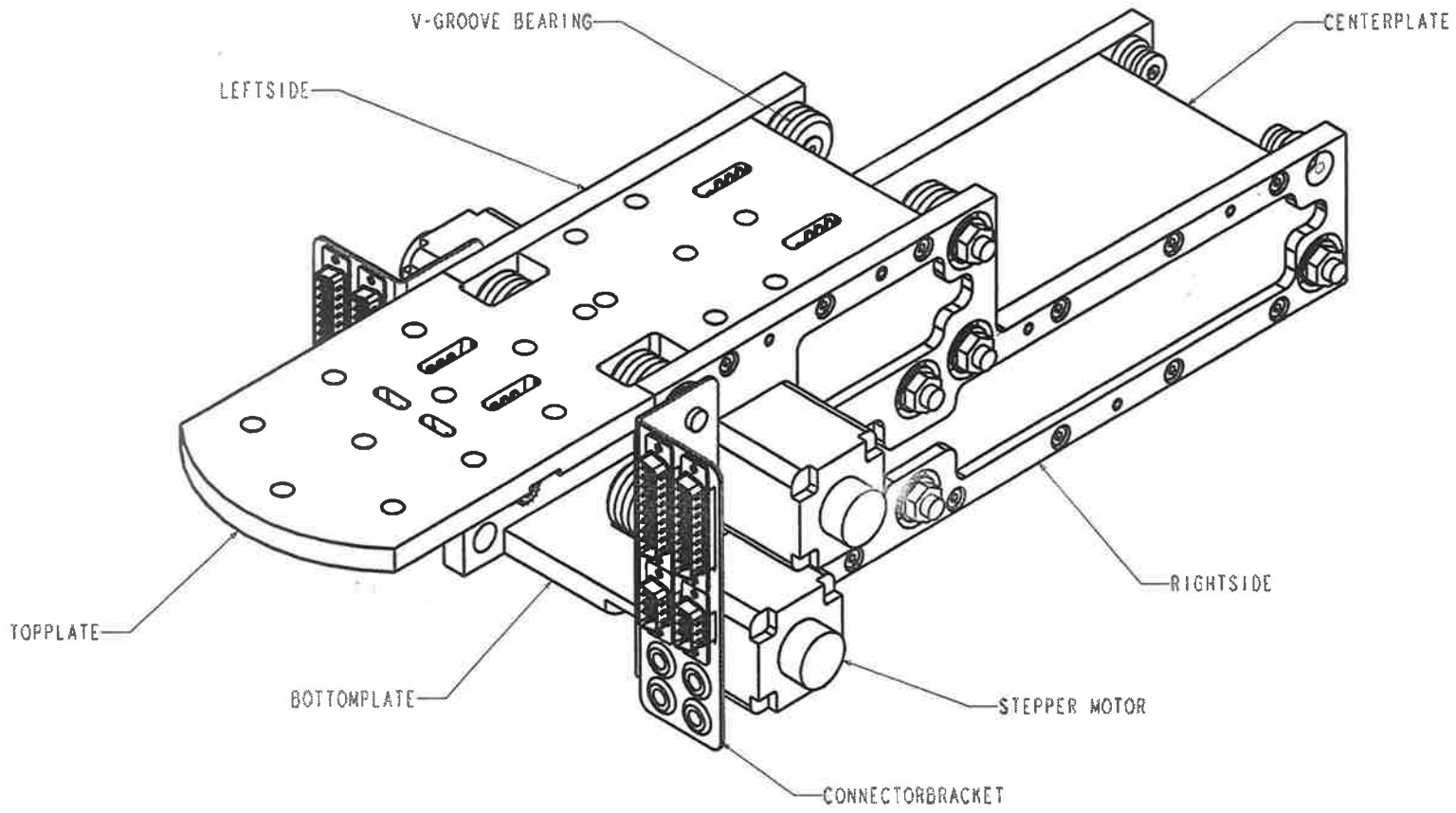

Notes: Housing Assembly	Drawing Name: HOUSINGASSEMBLED	Version:
	File:	Scale: 0.500
	Date: 16-May-05	Material:
	Drawn By:	Sheet No: 1 of 1

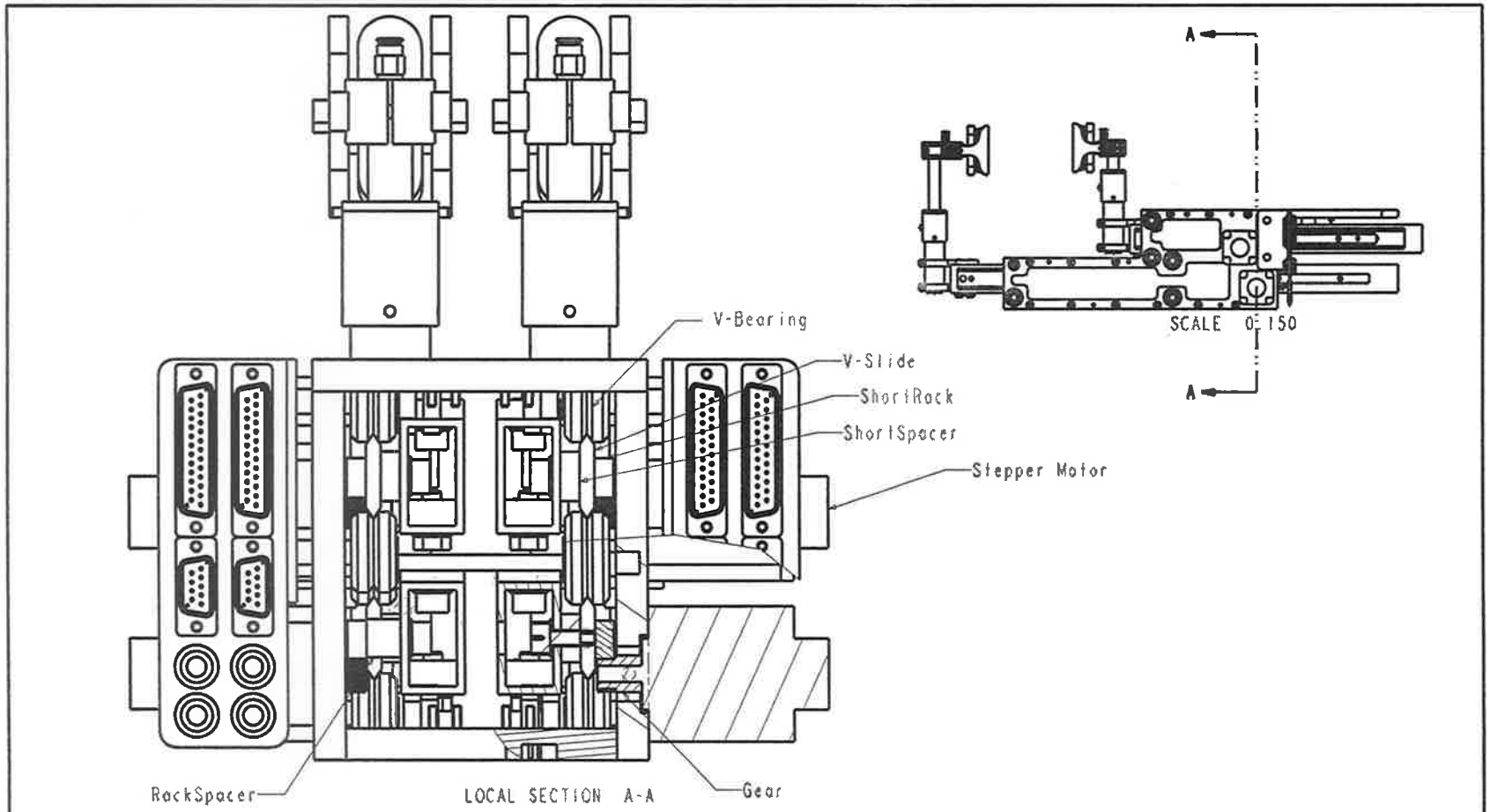

Notes: END VIEW WITH LOCAL SECTION	Drawing Name: END-EFFECTORASSEMBLY2	Version:
	File:	Scale: 0.600
	Date: 25-May-05	Material:
	Drawn By:	Sheet No: 1 of 3

General Assembly

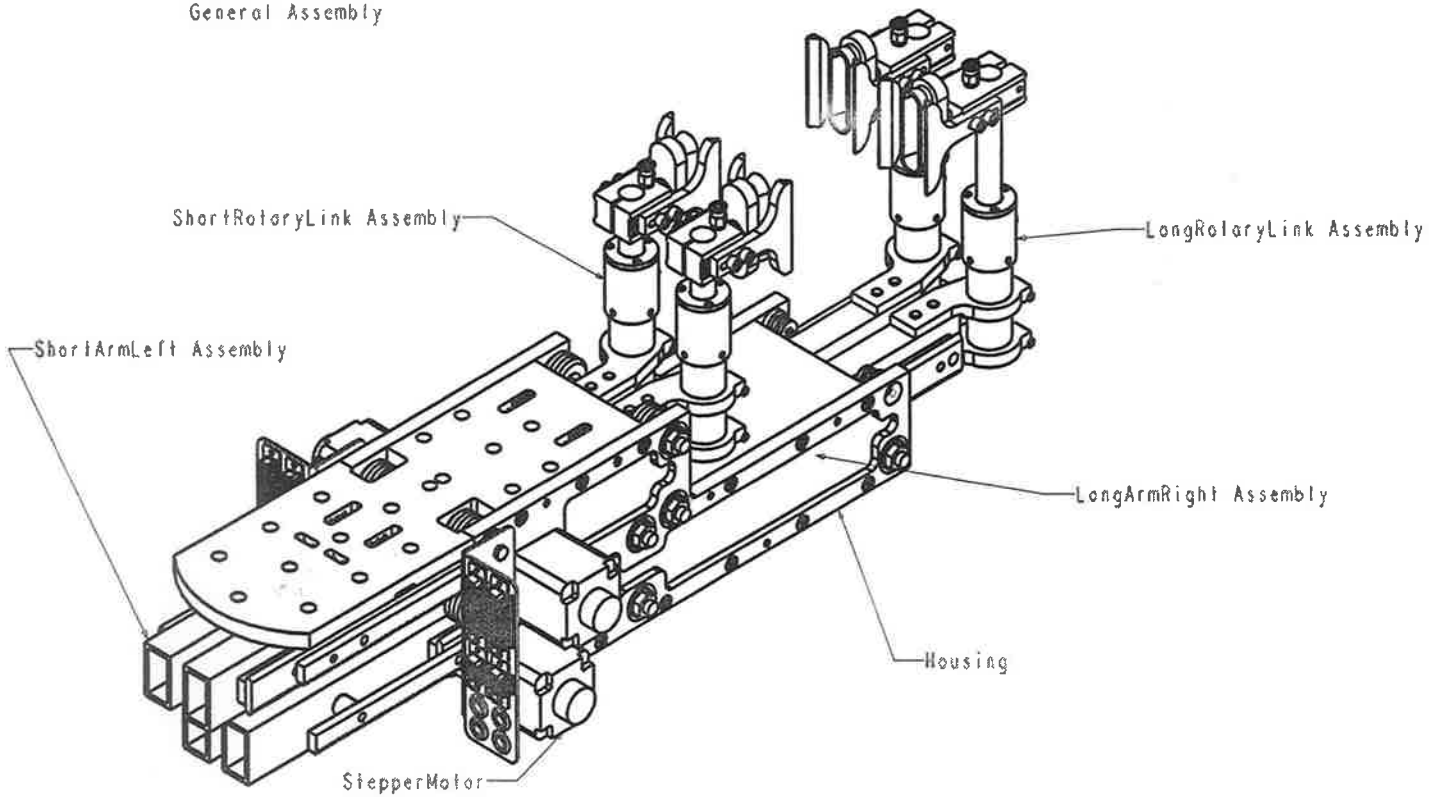

Notes:	Drawing Name: END-EFFECTORASSEMBLY2	Version:
	File:	Scale: 0.300
	Date: 25-May-05	Material:
	Drawn By:	Sheet No: 2 of 3

Left View Section, LeftSide of Housing Removed

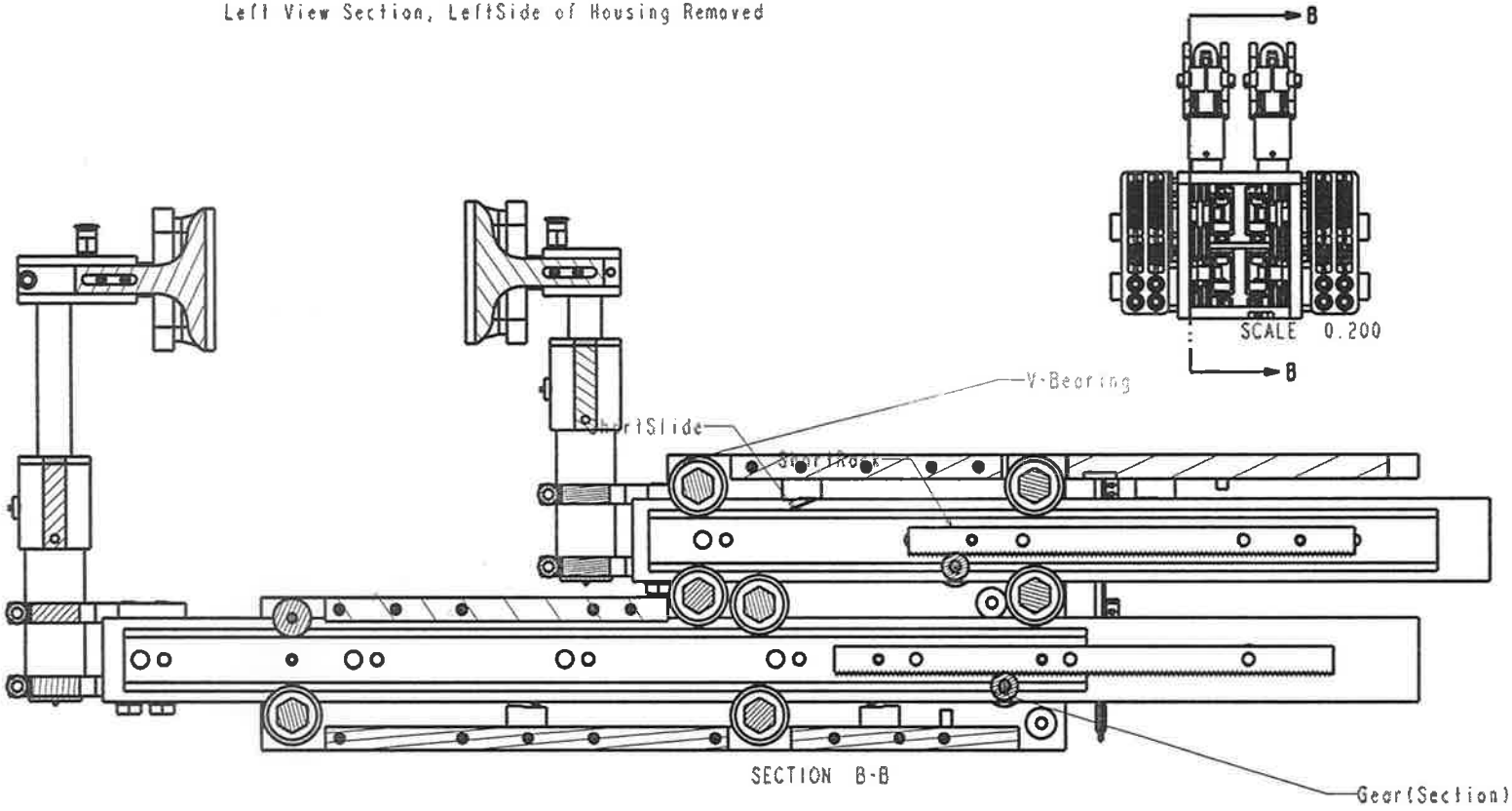

Notes:	Drawing Name: END-EFFECTORASSEMBLY2	Version:
	File:	Scale: 0.400
	Date: 25-May-05	Material:
	Drawn By:	Sheet No: 3 of 3

Short Arm Assembly Sections

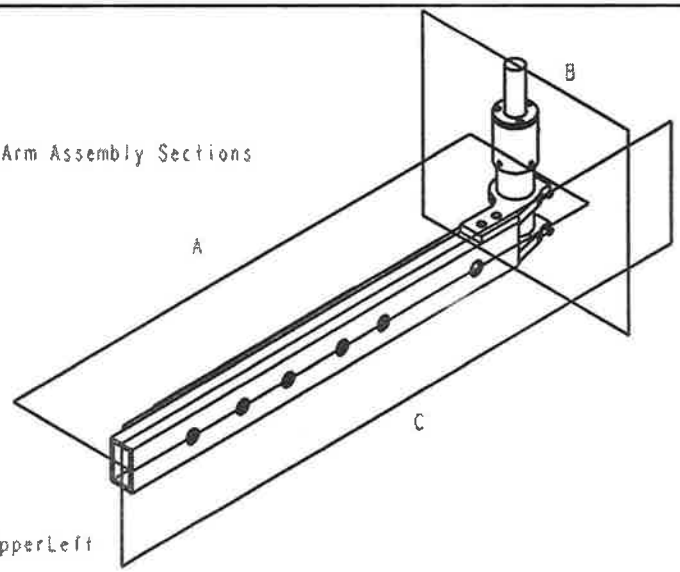

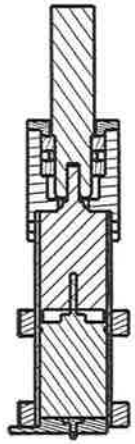

SECTION B-B

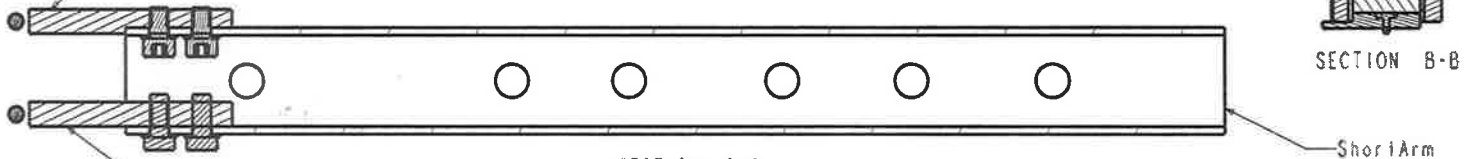

SECTION C-C

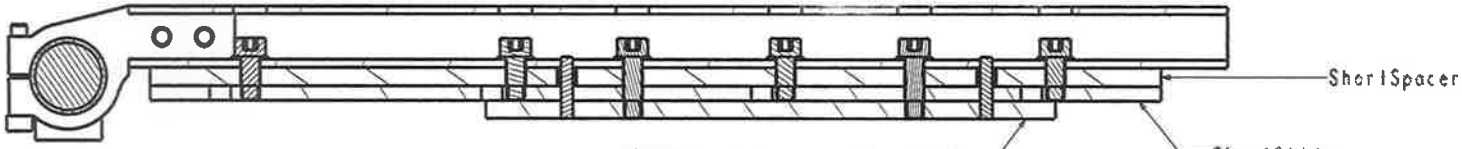

SECTION A-A

Notes:	Drawing Name: SHORTARMLEFT-SECTION	Version:
	File:	Scale: 0.500
	Date: 24-May-05	Material:
	Drawn By:	Sheet No: 1 of 1

Long Arm Assembly Sections

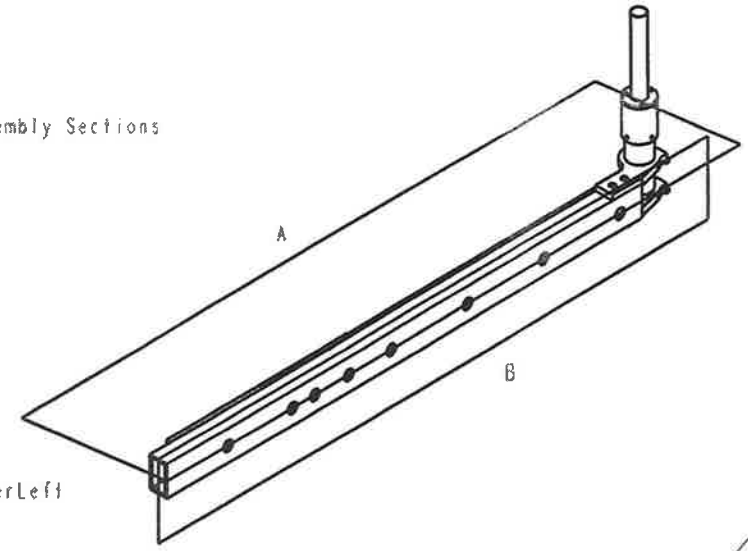

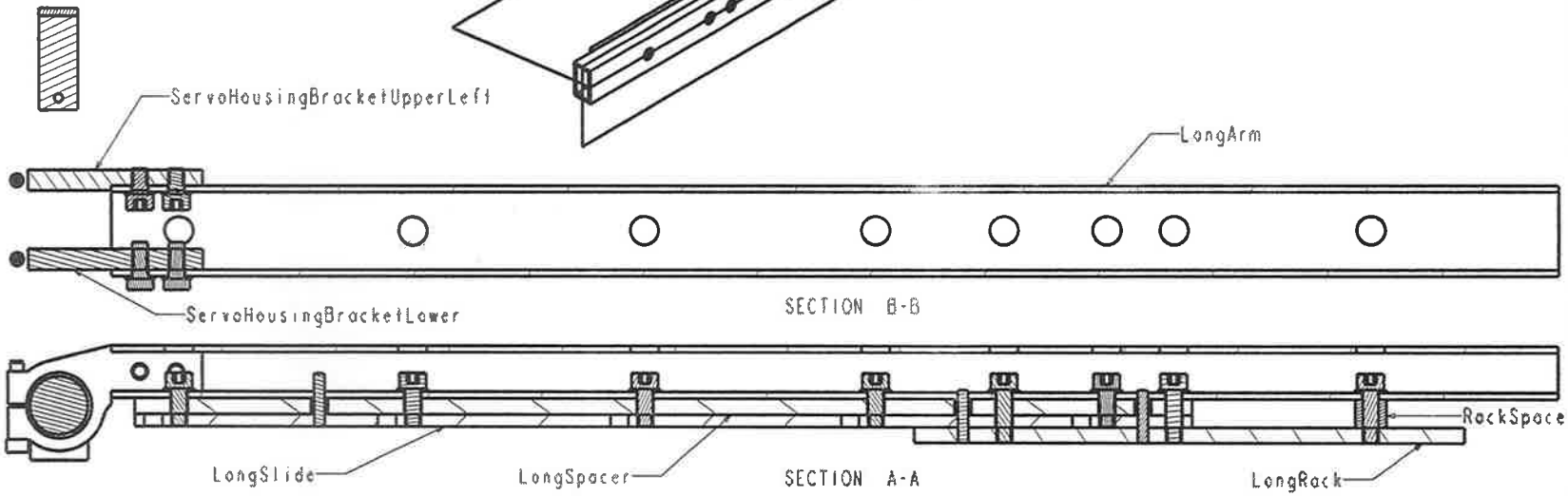

Notes:	Drawing Name: LONGARMLEFT-SECTION	Version:
	File:	Scale: 0.450
	Date: 25-May-05	Material:
	Drawn By:	Sheet No: 1 of 1

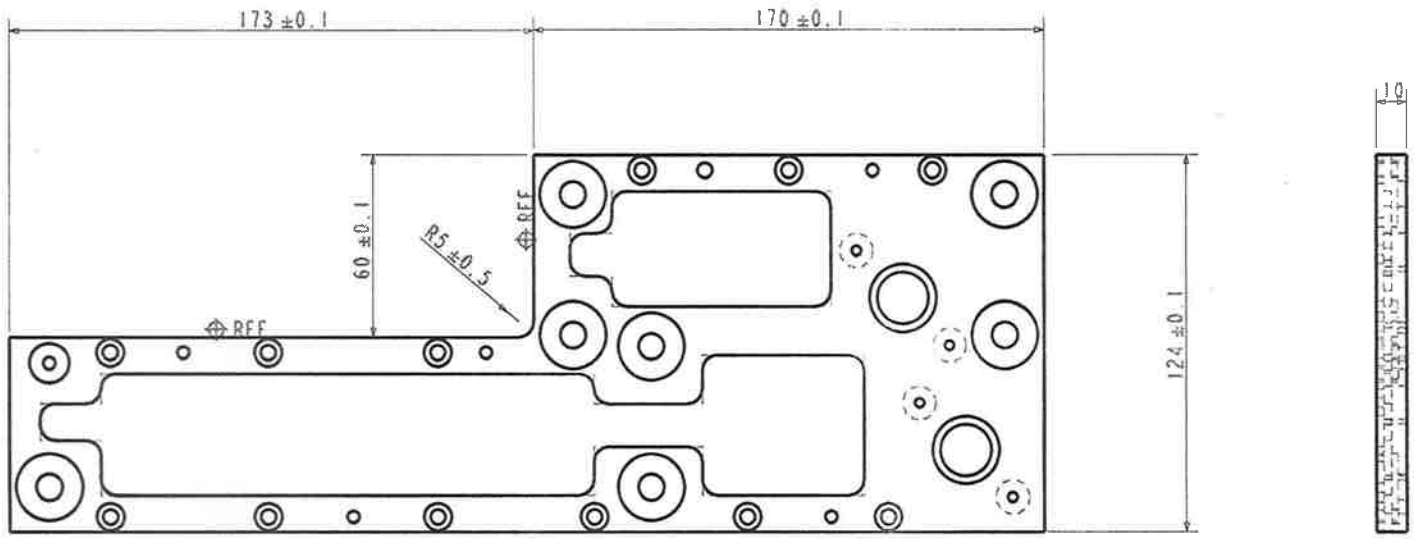

Plate Outline Dimensions

Notes:	Drawing Name: LEFTSIDE	Version: Working5
	File: ...\Working5\leftside.drw	Scale: 0.500
	Date: 27-Apr-05	Material: Aluminium MIC6, Tooling Plate
	Drawn By:	Sheet No: 1 of 5

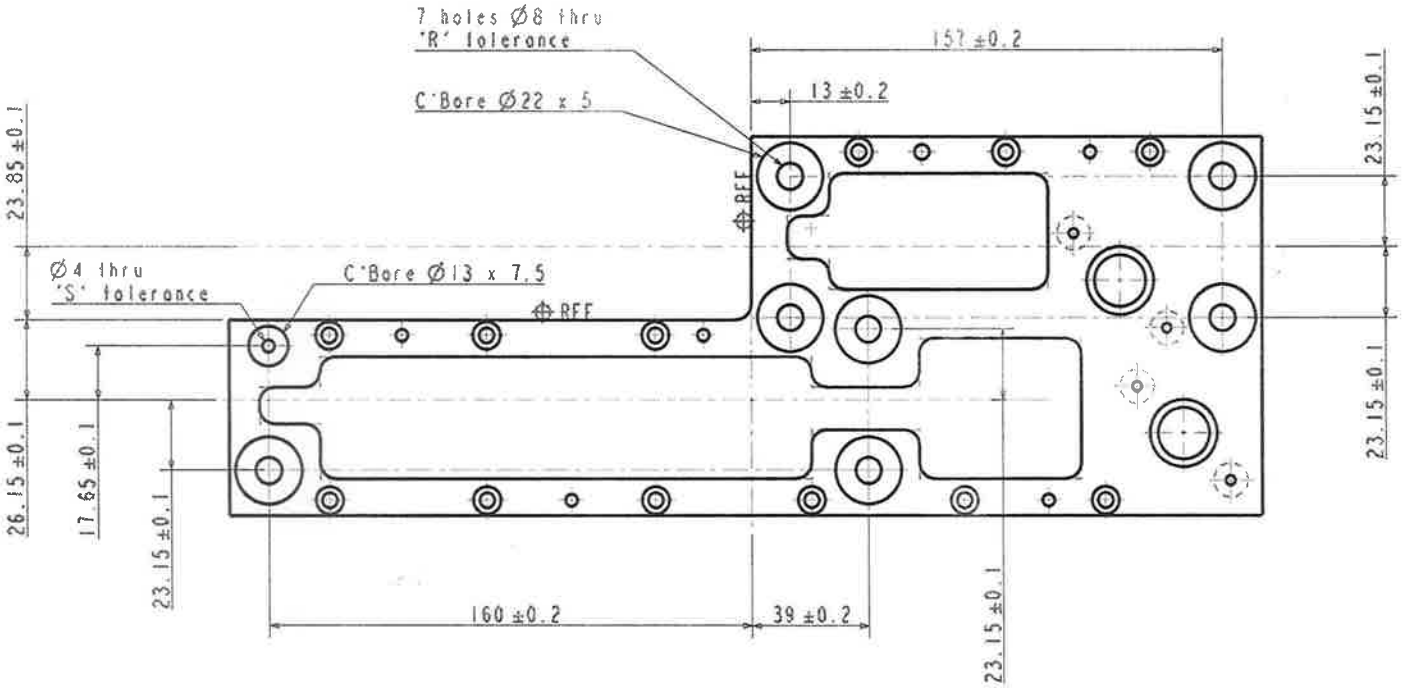

Bearing Assembly Locations

Notes: 1)Tolerances R = +0.010 +0.022 S = +0.008 +0.018 Unspecified tolerances to be taken as +/-0.2	Drawing Name: LEFTSIDE	Version:
	File: ...\Working 5\leftside.drw	Scale: 0.500
	Date: 27-Apr-05	Material:
	Drawn By:	Sheet No: 2 of 5

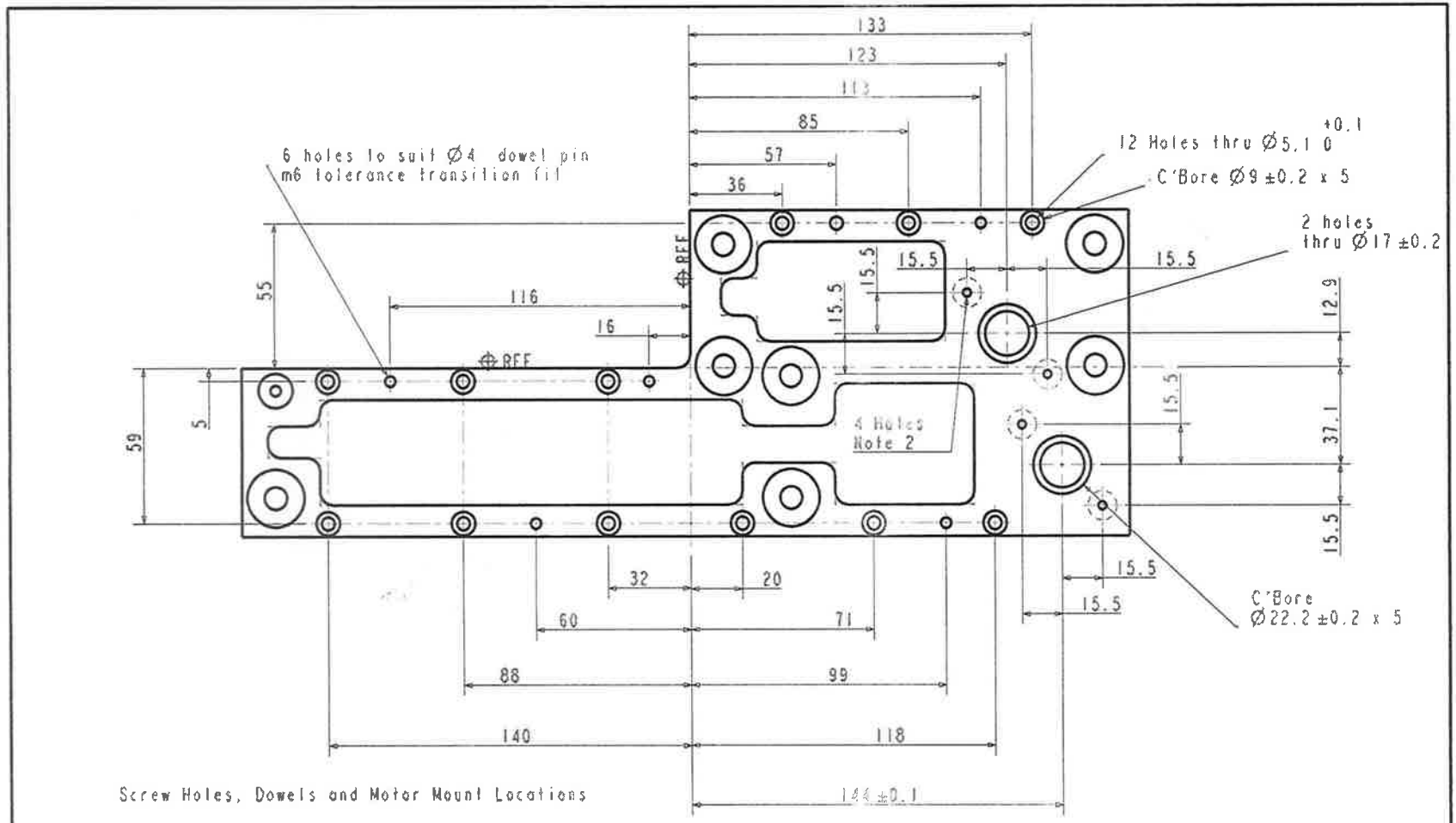

Notes: 1)Tolerances: All tolerances on this sheet +/-0.05mm unless stated 2)Hole Ø3 clearance Motor fixing hole	Drawing Name: LEFTSIDE	Version:
	File: ...\Working5\leftside.drw	Scale: 0.500
	Date: 03-May-05	Material:
	Drawn By:	Sheet No: 3 of 5

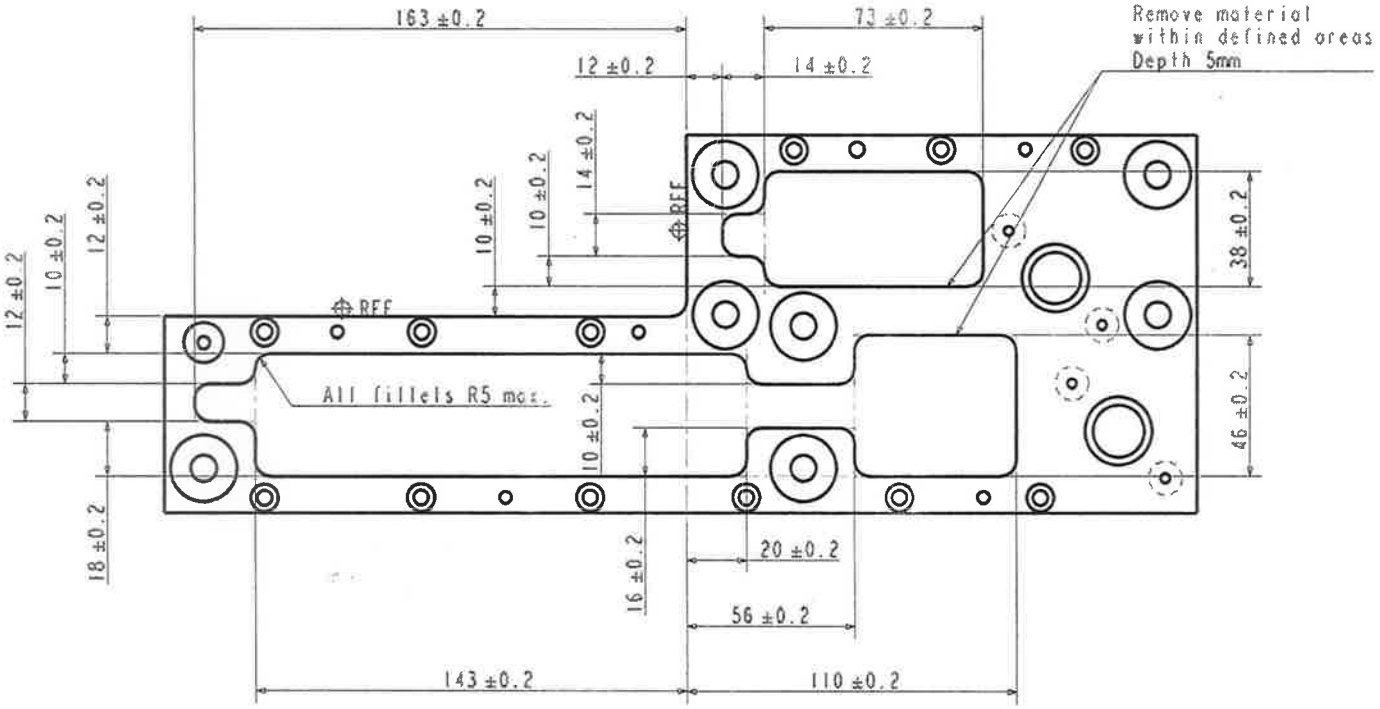

Material Removal

Notes:
1)Dimensions define rectangular area with filleted corners.
2)Dimensions may be altered to facilitate machine setup or provide additional clearance.
3)Fillet radius may be reduced, max.R5

Drawing Name: LEFTSIDE	Version:
File: ...\Working5\leftside.drw	Scale: 0.500
Date: 10-May-05	Material:
Drawn By:	Sheet No: 4 of 5

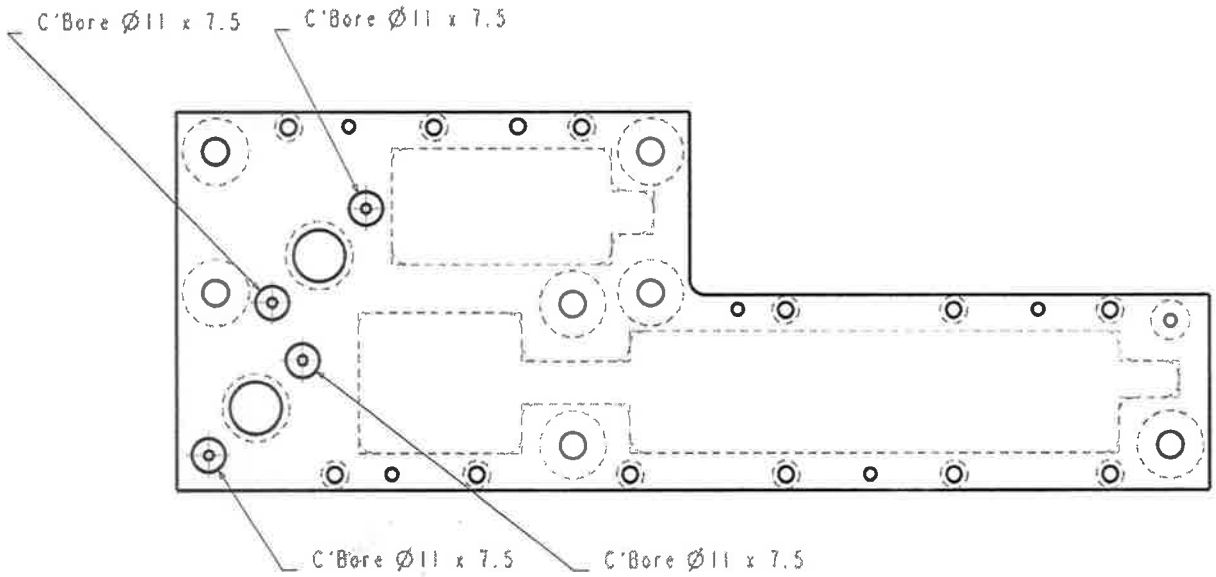

Rear View: Counterbores for motor fixing holes

Notes: 1)All tolerances on this sheet +/-0.2	Drawing Name: LEFTSIDE	Version:
	File: ...\Working5\leftside.drw	Scale: 0.500
	Date: 10-May-05	Material:
	Drawn By:	Sheet No: 5 of 5

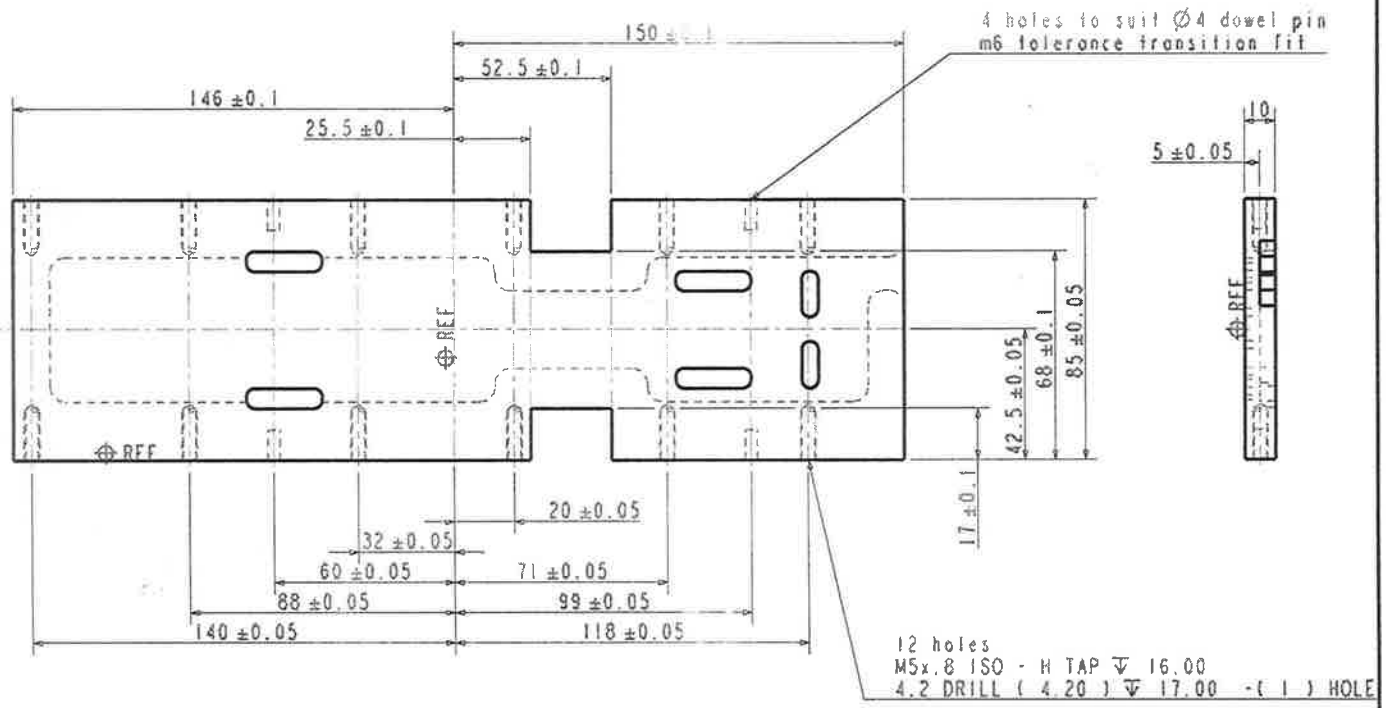

Notes: 1) The vertical reference line on this drawing coincides with the vertical reference surface on drawing LEFTSIDE	Drawing Name: BOTTOMPLATE	Version:
	File:	Scale: 0.500
	Date: 10-May-05	Material:
	Drawn By:	Sheet No: 1 of 3

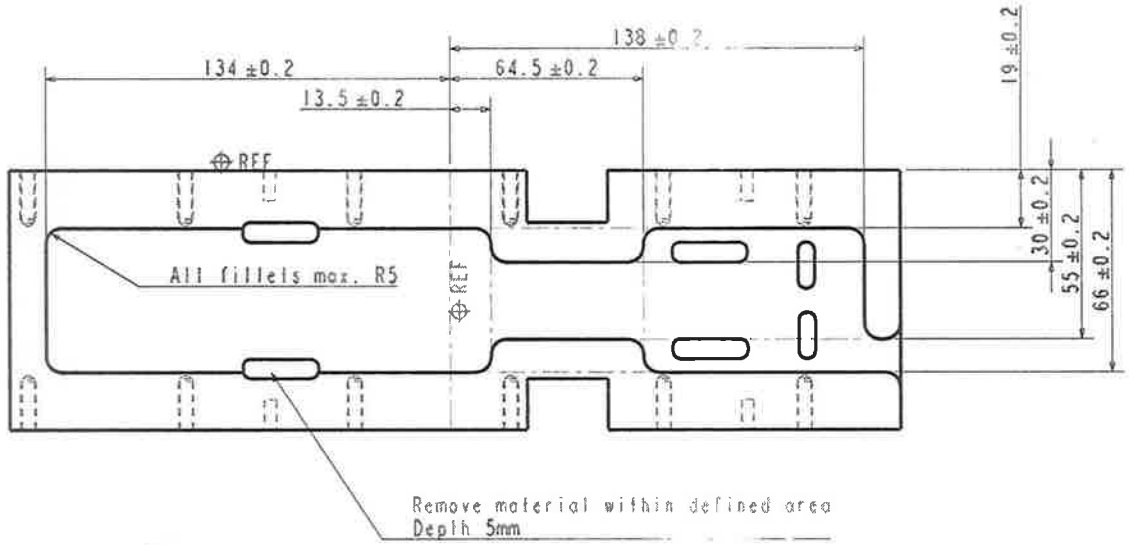

Material Removal

Notes: 1)Dimensions define rectangular area with filleted corners. 2)Dimensions may be altered to facilitate machine setup or provide additional clearance. 3)Fillet radius may be reduced, max.R5	Drawing Name: BOTTOMPLATE	Version:
	File:	Scale: 0.500
	Date: 11-May-05	Material:
	Drawn By:	Sheet No: 2 of 3

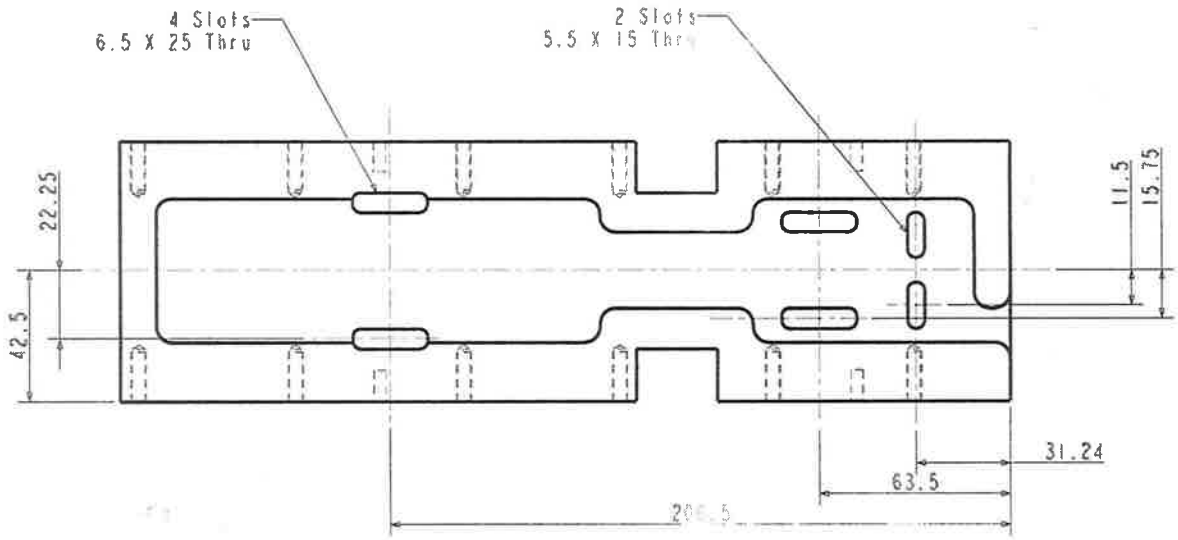

Notes: All fillets R2.5	Drawing Name: BOTTOMPLATE	Version:
	File:	Scale: 0.500
	Date: 11-Nov-05	Material:
	Drawn By:	Sheet No: 3 of 3

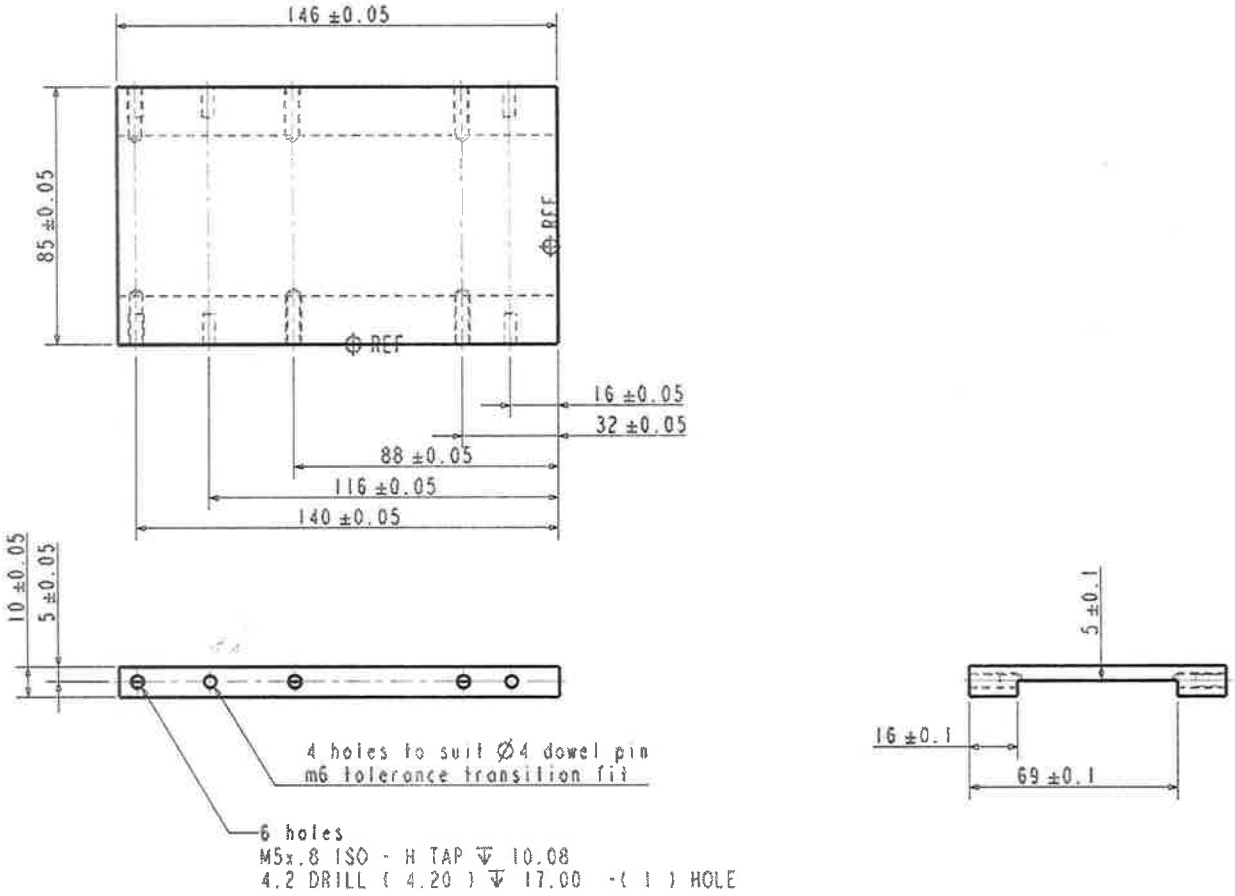

Notes:	Drawing Name: CENTREPLATE	Version:
	File:	Scale: 0.500
	Date: 13-May-05	Material:
	Drawn By:	Sheet No: 1 of 1

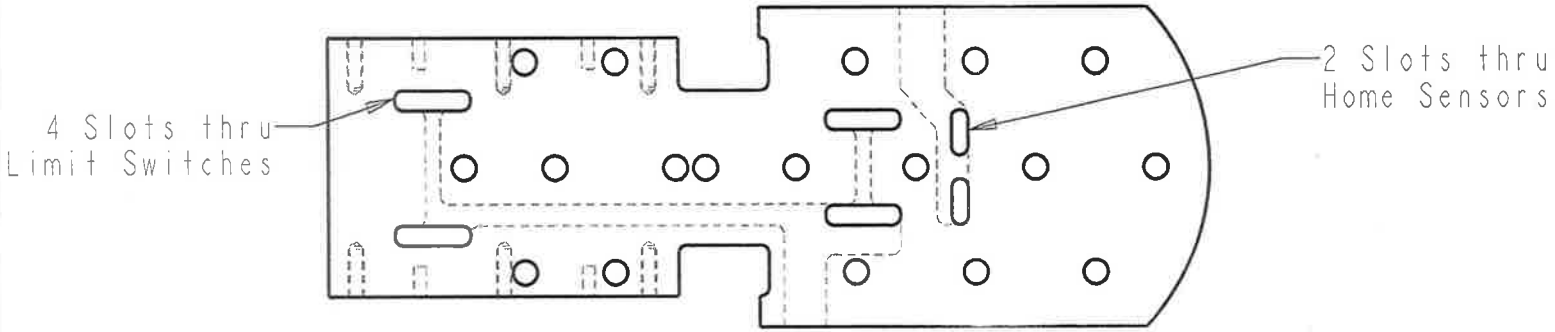

TOP VIEW

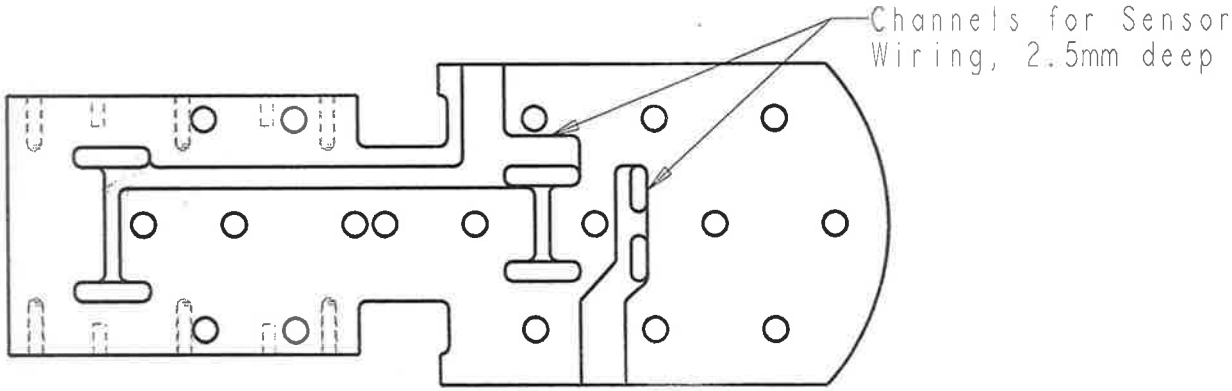

BOTTOM VIEW

Notes:	Drawing Name: TOPPLATE_V2_0	Version:
	File:	Scale: 0.500
	Date: 11-Nov-05	Material: Aluminiuim MIC 6
	Drawn By:	Sheet No: 1 of 6

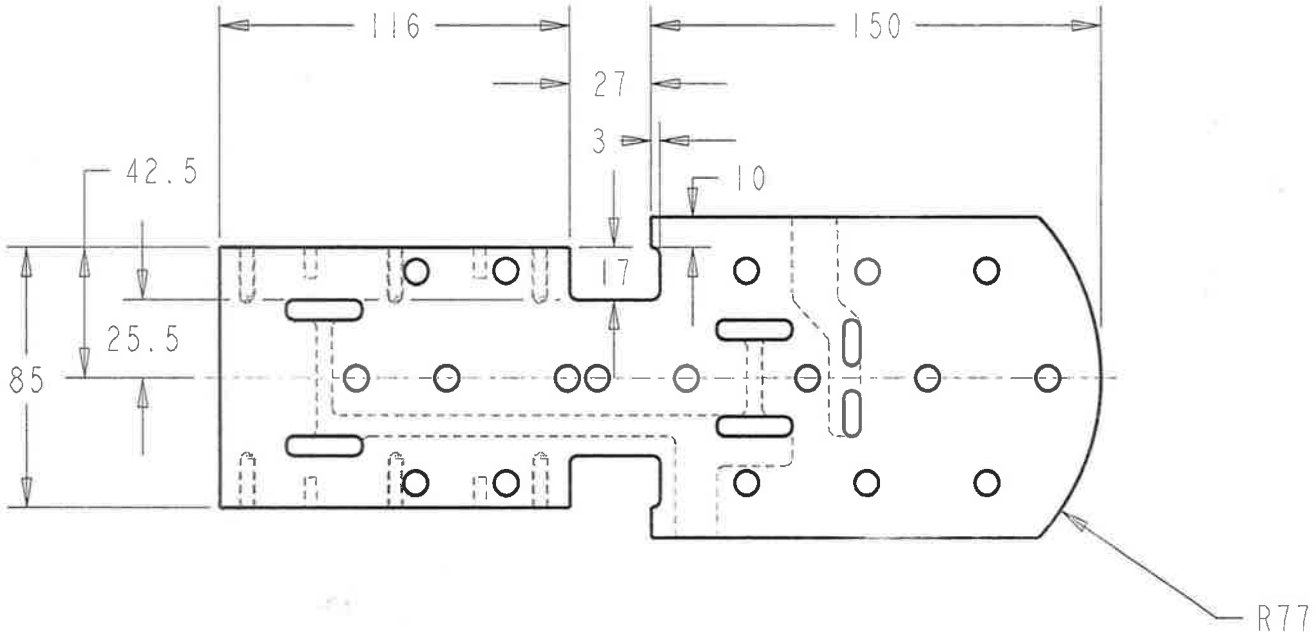

Notes: All Fillets R2.5	Drawing Name: TOPPLATE_V2_0	Version:
	File:	Scale: 0.500
	Date: 11-Nov-05	Material:
	Drawn By:	Sheet No: 2 of 6

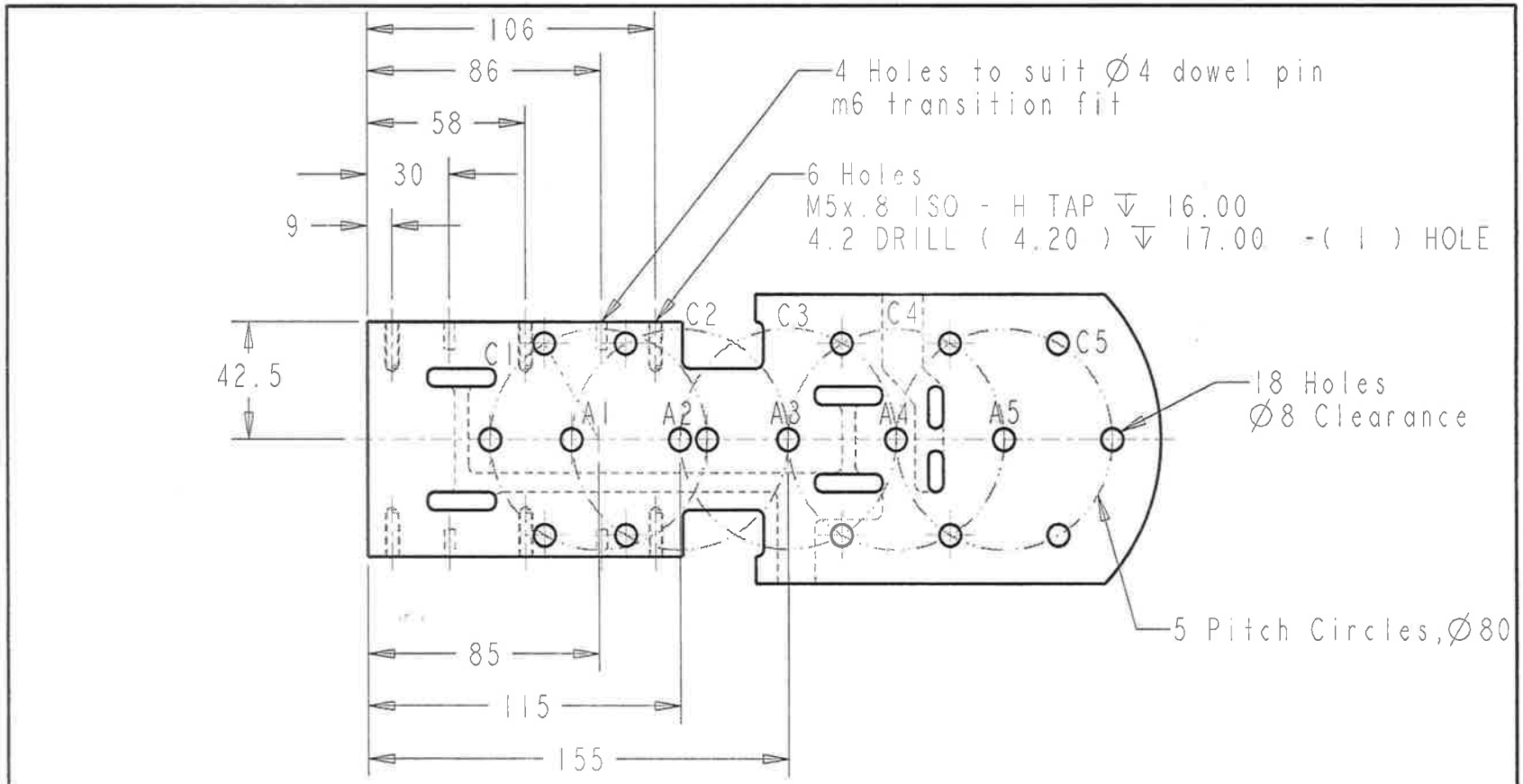

Note: All holes not on central axis are spaced at 60° on PCD

Notes: A1, A2, etc. indicate centres of construction circles C1, C2, etc.	Drawing Name: TOPPLATE_V2_0	Version:
	File:	Scale: 0.500
	Date: 11-Nov-05	Material:
	Drawn By:	Sheet No: 3 of 6

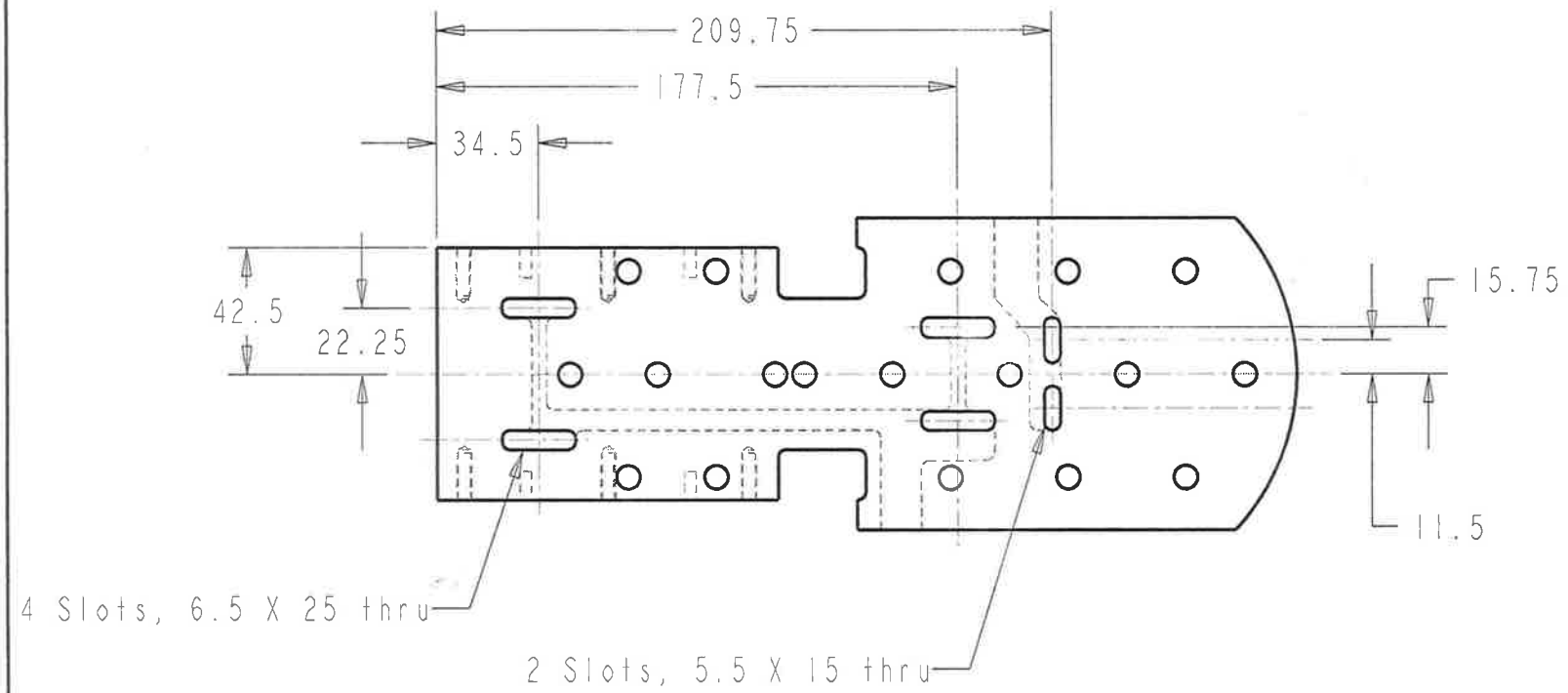

Notes: All Fillets R2.5	Drawing Name: TOPPLATE_V2_0	Version:
	File:	Scale: 0.500
	Date: 11-Nov-05	Material:
	Drawn By:	Sheet No: 4 of 6

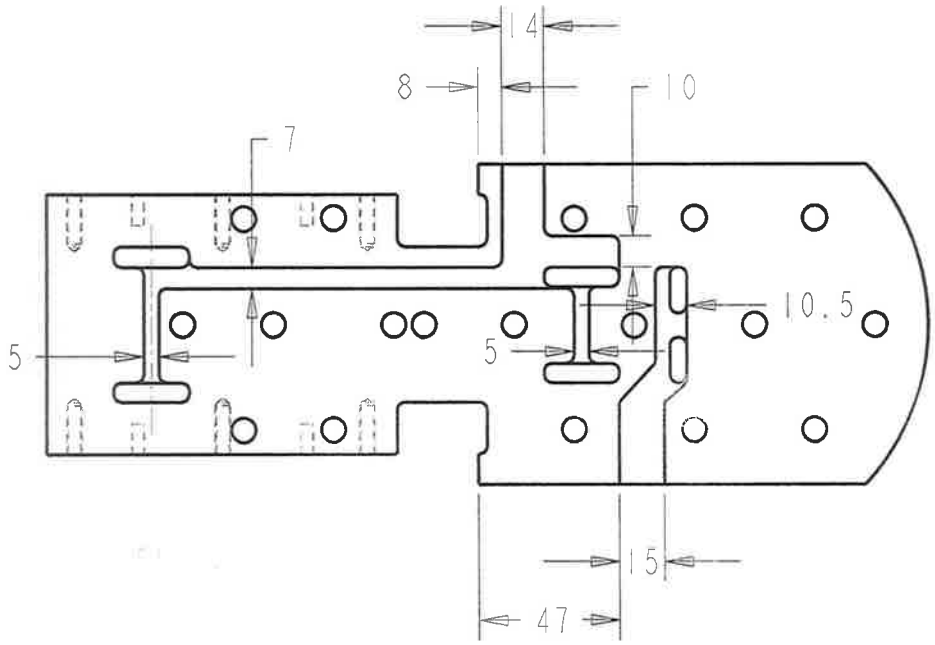

Notes: F&R R2.5	Drawing Name: TOPPLATE_V2_0	Version:
	File:	Scale: 0.500
	Date: 11-Nov-05	Material:
	Drawn By:	Sheet No: 5 of 6

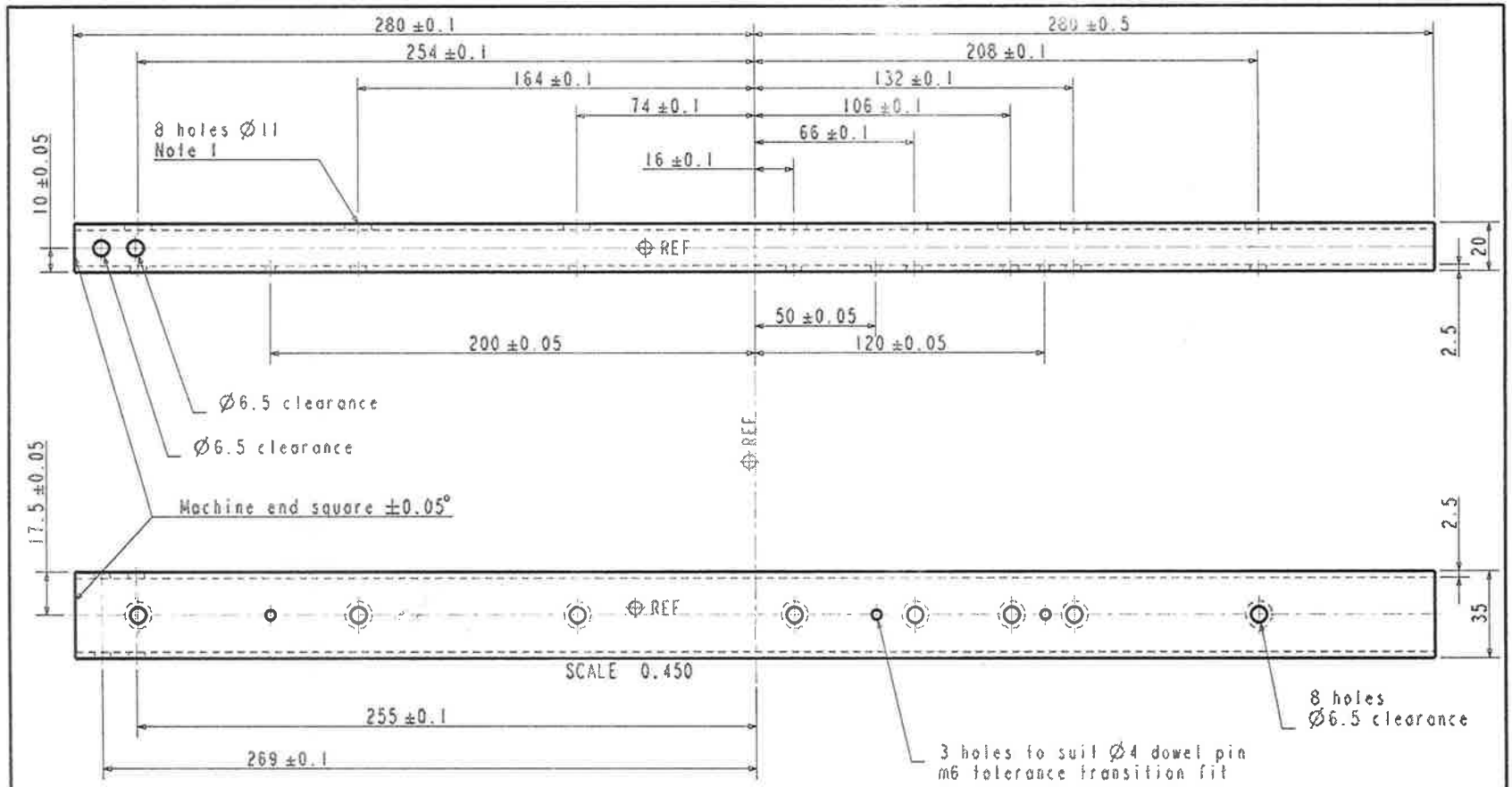

Notes: 1) These Ø11 holes give access for internal screw insertion thru Ø6.5 holes on opposite side. Drill on same axis. 2) Quantity: 2 off (LONGARMLEFT.PRT and LONGARMRIGHT.PRT)	Drawing Name: LONGARM	Version:
	File:	Scale: 0.500
	Date: 11-May-05	Material:
	Drawn By:	Sheet No: 1 of 1

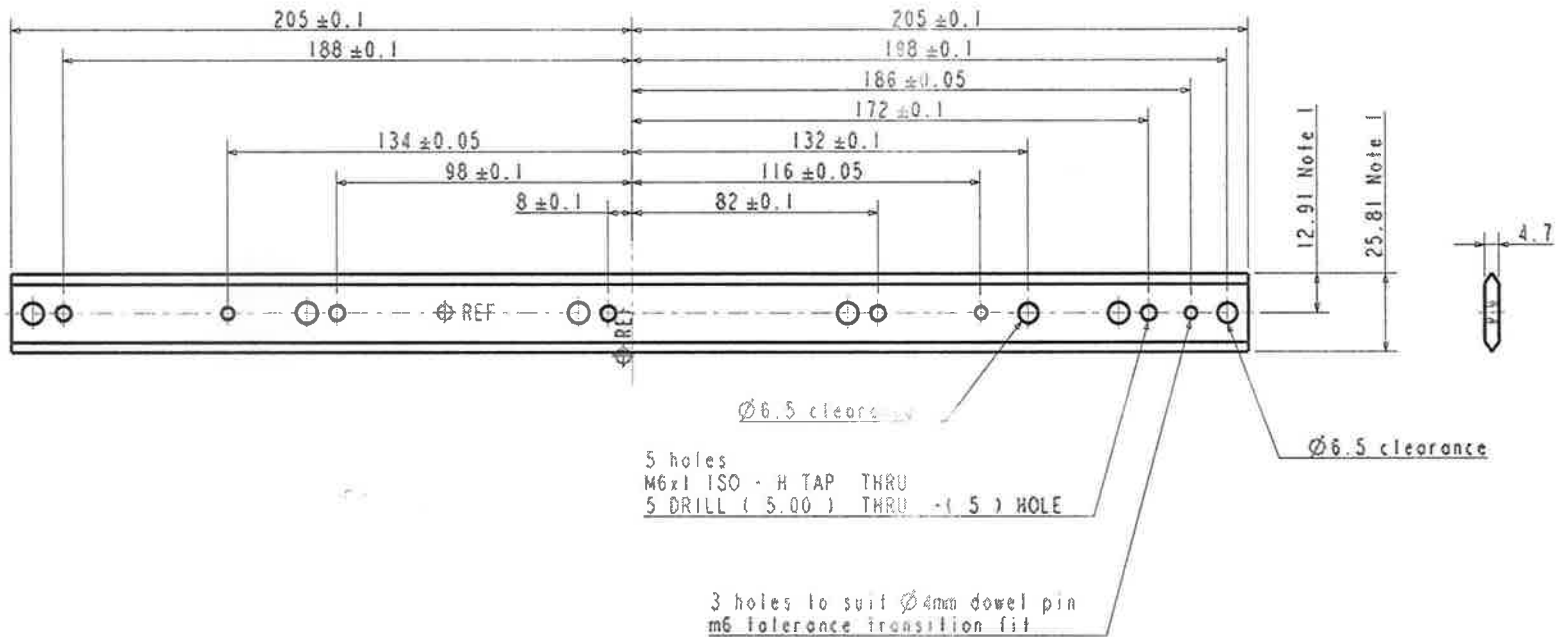

Notes: 1)Theoretical dimensions shown. Actual dimensions to be measured from stock as supplied. Centreline position tolerance: ±0.1 2) Non-dimensioned holes are pre-drilled in stock and not used 3)Quantity: 2	Drawing Name: LONGSLIDE	Version:
	File:	Scale: 0.500
	Date: 12-May-05	Material: Hepco SS25 V-slide
	Drawn By:	Sheet No: 1 of 1

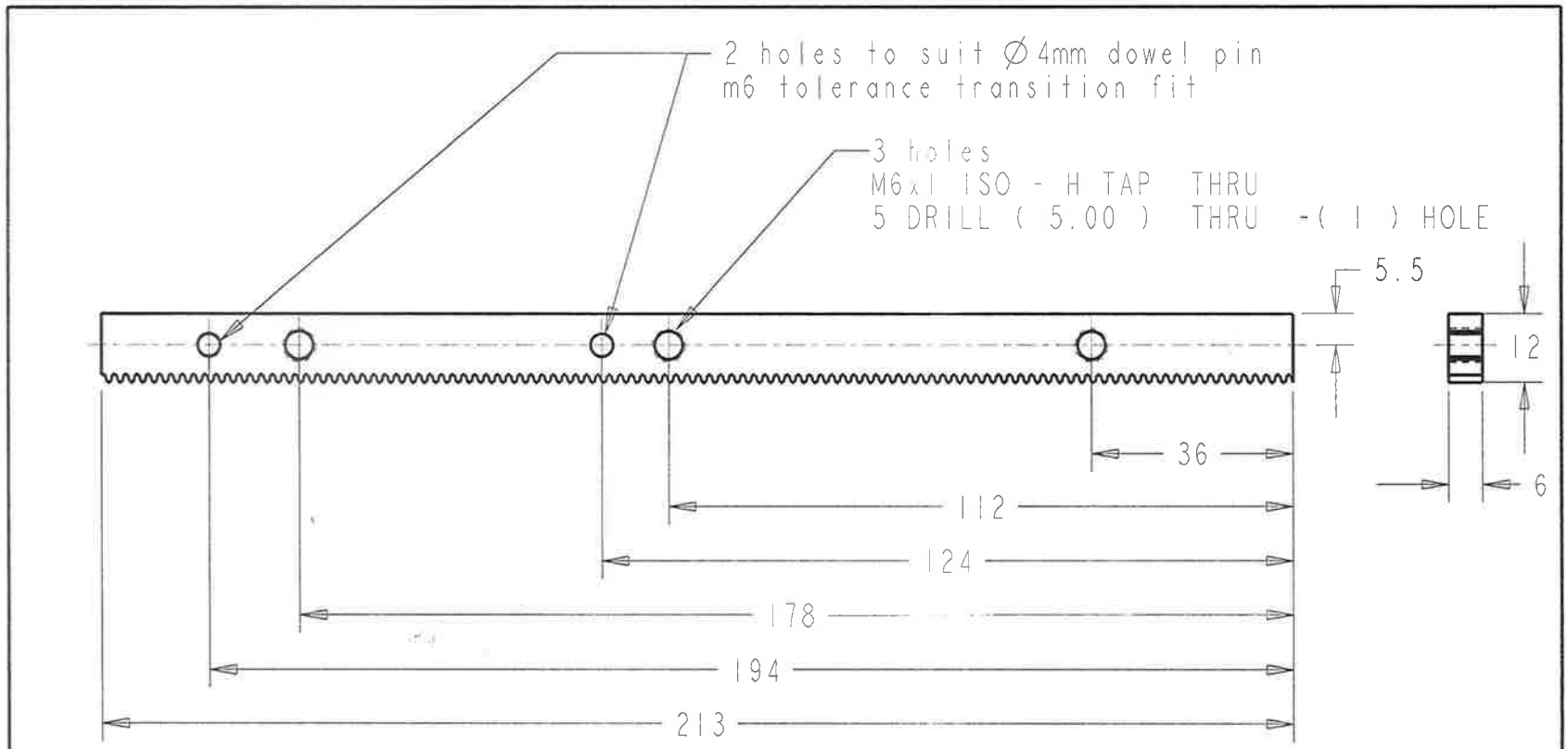

Notes: Quantity: 2 All tolerances ±0.1	Drawing Name: LONGRACK	Version:
	File:	Scale: 1.000
	Date: 05-Jul-05	Material:
	Drawn By:	Sheet No: 1 of 1

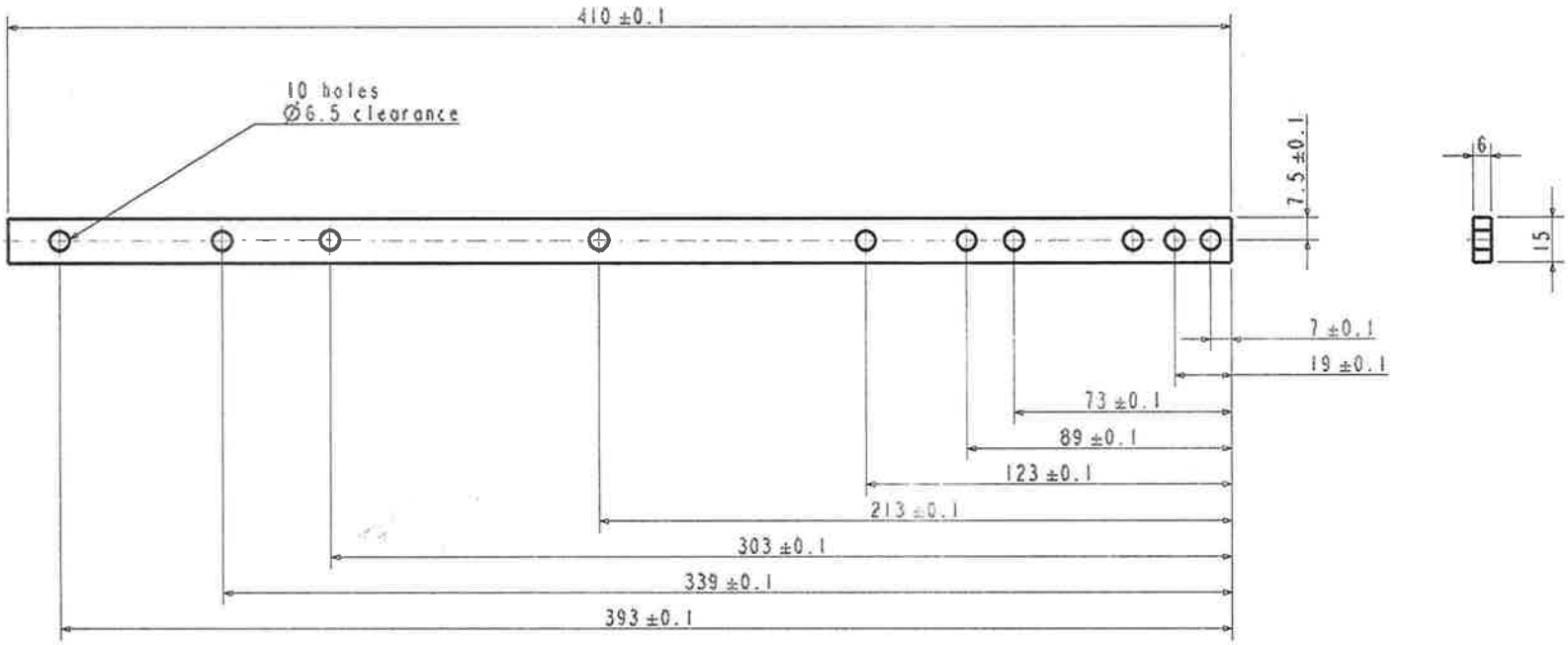

Notes: 1)Quantity: 2	Drawing Name: LONGSPACER	Version:
	File:	Scale: 0.500
	Date: 12-May-05	Material: Aliminium Bar. CSection 15x6
	Drawn By:	Sheet No: 1 of 1

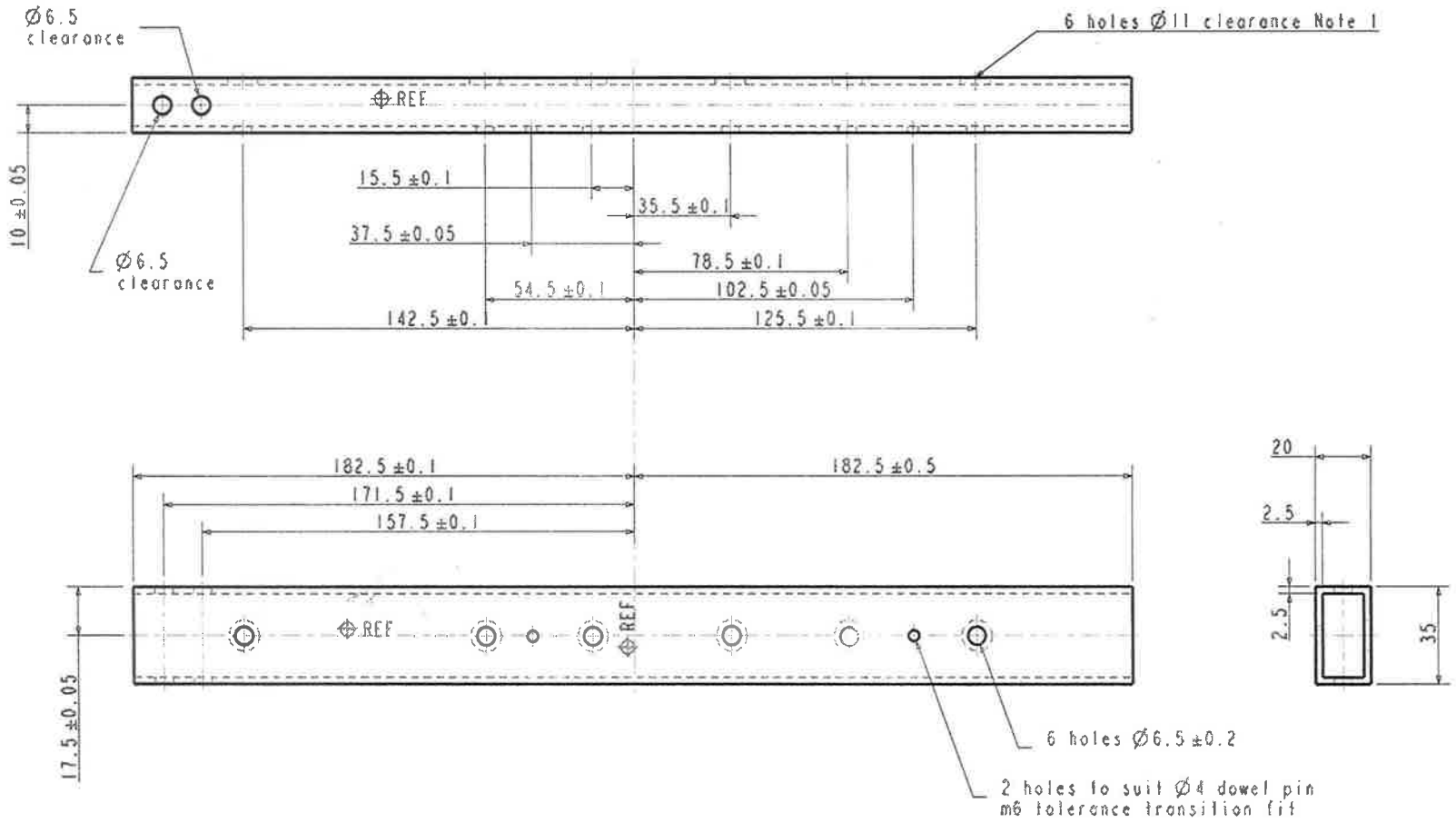

Notes: 1) These Ø11 holes give access for internal screw insertion thru Ø6.5 holes on opposite side. Drill on same axis. 2) Quantity: 2 off (SHORTARMLEFT.prt and SHORTARMRIGHT.prt)	Drawing Name: SHORTARM	Version:
	File:	Scale: 0.500
	Date: 11-May-05	Material: Aluminium, Rect.Tube, Section 35x20x2.5
	Drawn By:	Sheet No: 1 of 1

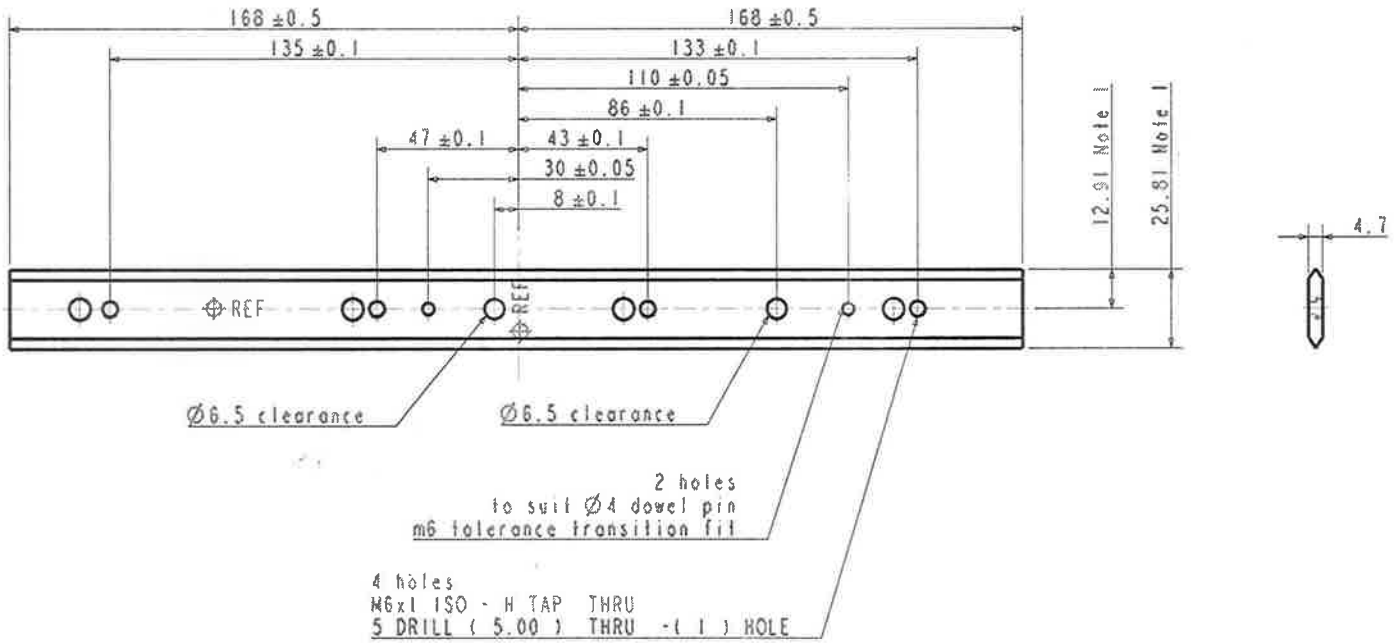

Notes: 1)Theoretical dimensions shown. Actual dimensions to be measured from stock as supplied. Centreline position tolerance: ±0.1 2) Non-dimensioned holes are pre-drilled in stock and not used 3)Quantity: 2	Drawing Name: SHORTSLIDE	Version:
	File:	Scale: 0.500
	Date: 12-May-05	Material: Hepco SS25 V-slide
	Drawn By:	Sheet No: 1 of 1

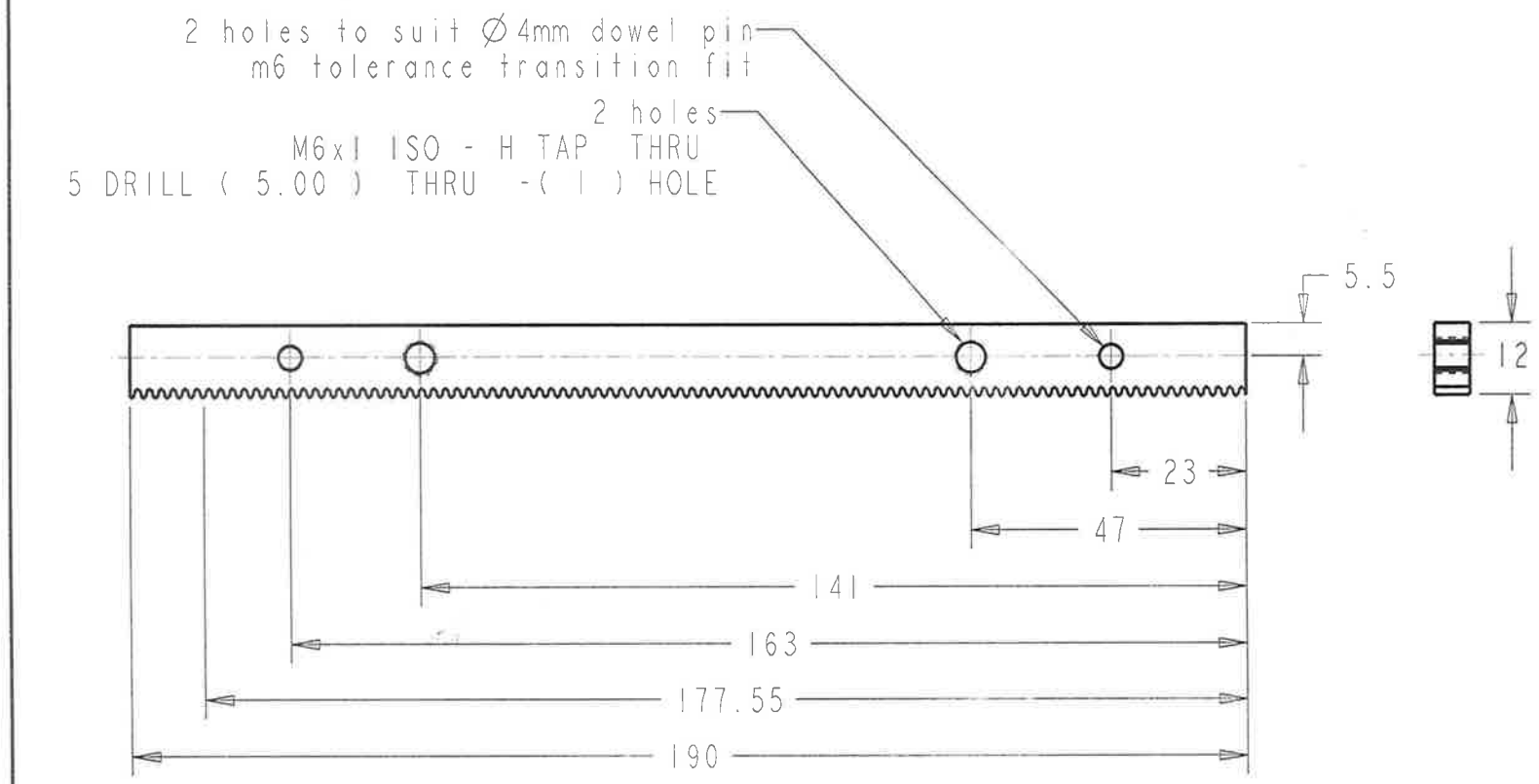

Notes: Quantity: 2 All tolerances ±0.1	Drawing Name: SHORTRACK	Version:
	File:	Scale: 1.000
	Date: 05-Jul-05	Material:
	Drawn By:	Sheet No: 1 of 1

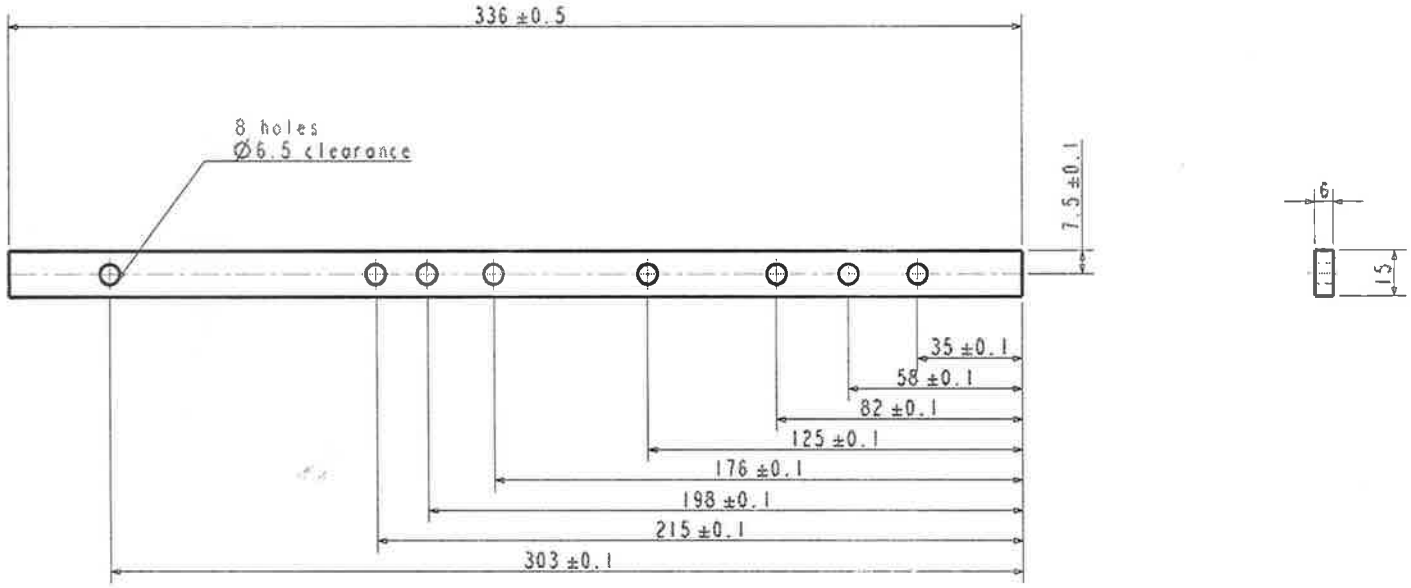

Notes: 1)Quantity: 2	Drawing Name: SHORTSPACER	Version:
	File:	Scale: 0.500
	Date: 12-May-05	Material: Aliminium Bar. CSection 15x6
	Drawn By:	Sheet No: 1 of 1

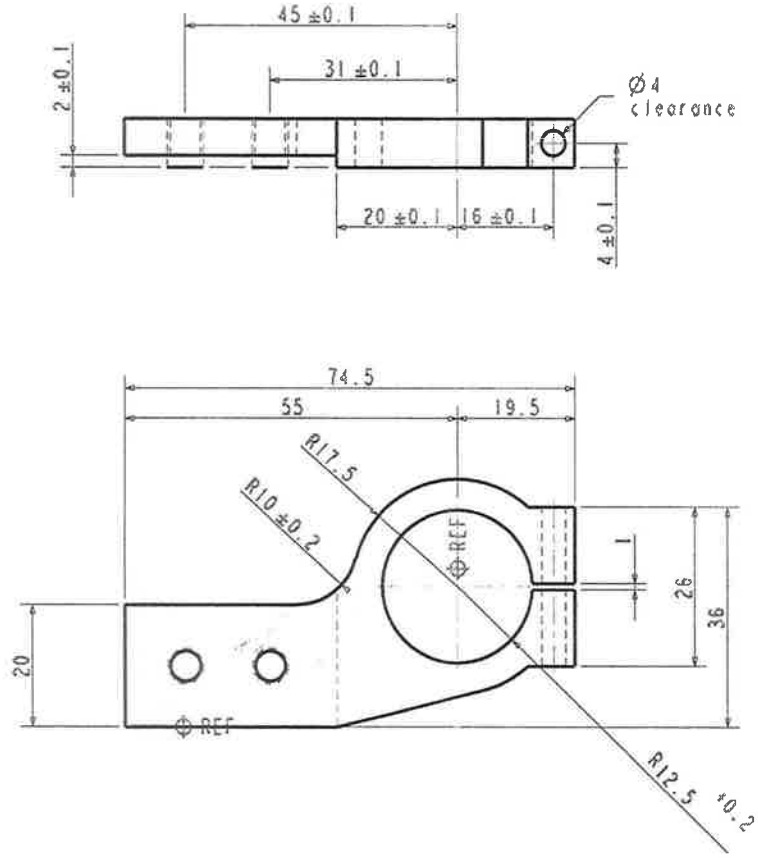

Notes: 1) Tolerances: All tolerances on this sheet ±0.2 unless specified 2)Quantity: 2 LEFT + 2 RIGHT	Drawing Name: SERVOHOUSINGBRACKETUPPERLEFT	Version:
	File:	Scale: 1.000
	Date: 12-May-05	Material: Aluminium MIC6, Tooling Plate
	Drawn By:	Sheet No: 1 of 1

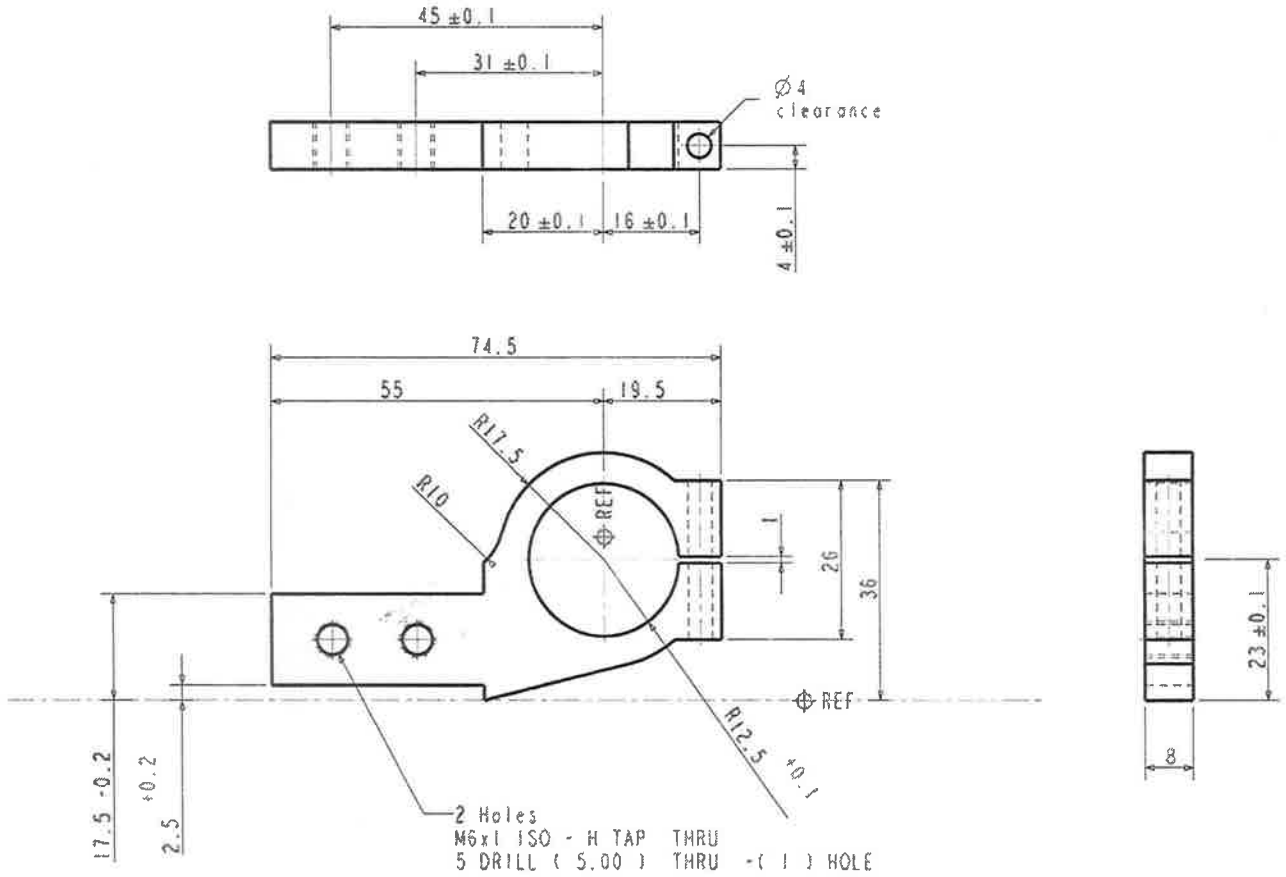

Notes: 1) Tolerances: All tolerances on this sheet ±0.2 unless specified 2) Quantity: 4	Drawing Name: SERVOHOUSINGBRACKETLOWER	Version:
	File:	Scale: 1.000
	Date: 12-May-05	Material: Aluminium MIC6, Tooling Plate
	Drawn By:	Sheet No: 1 of 1

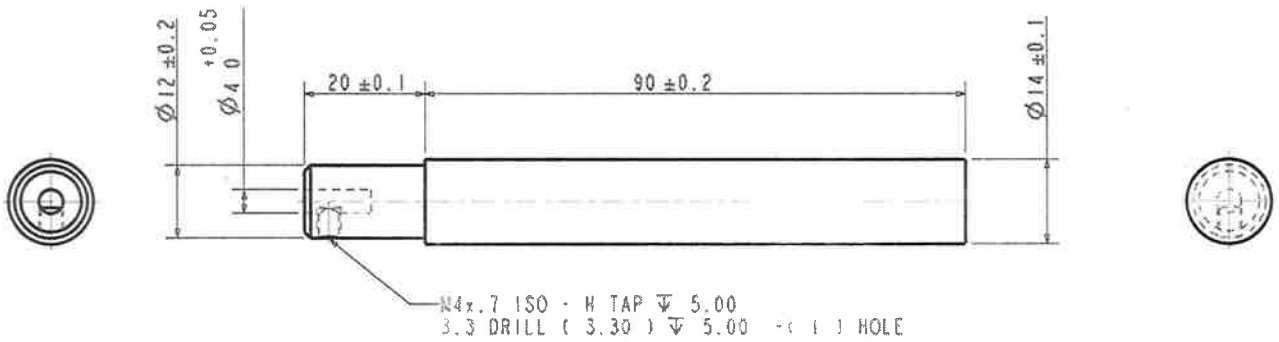

LONG SHAFT

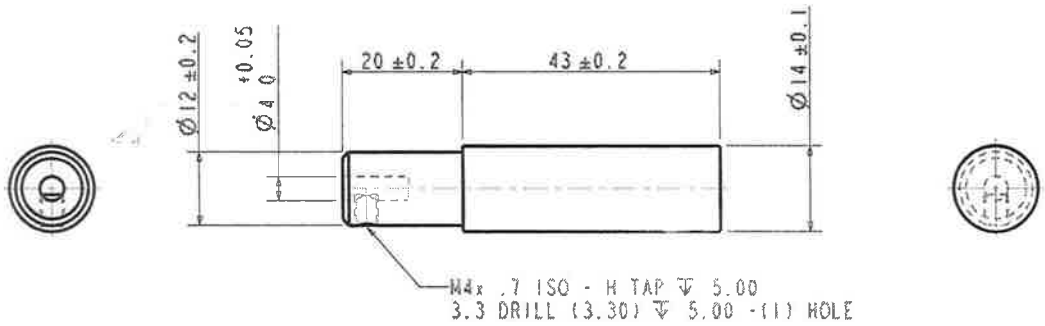

SHORT SHAFT

Notes: 1) Ø4 hole to accept gearhead shaft. Shaft size: Ø4 -0.007 -0.01	Drawing Name: SHAFTS	Version:
	File:	Scale: 1.000
	Date: 13-May-05	Material: Aluminium
	Drawn By:	Sheet No: 1 of 1

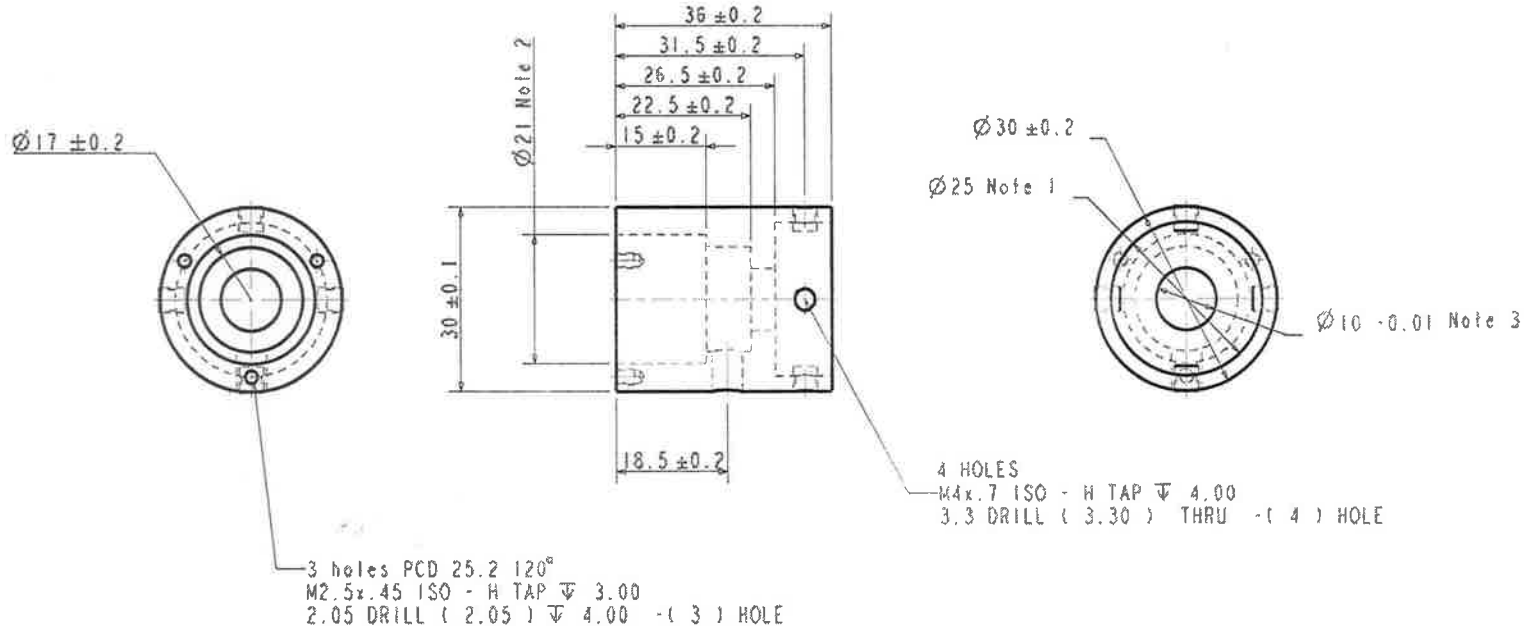

Notes: 1) Machine to close fit on part SERVOHOUSING 2) Tolerance to accept Ø21x5 deep groove roller bearing 3)Gearhead boss locates in this hole. Boss dimension: Ø10 +0.003 -0.01 4)Quantity: 4	Drawing Name: BEARINGHOUSING	Version:
	File:	Scale: 1.000
	Date: 12-May-05	Material: Aluminium
	Drawn By:	Sheet No: 1 of 1

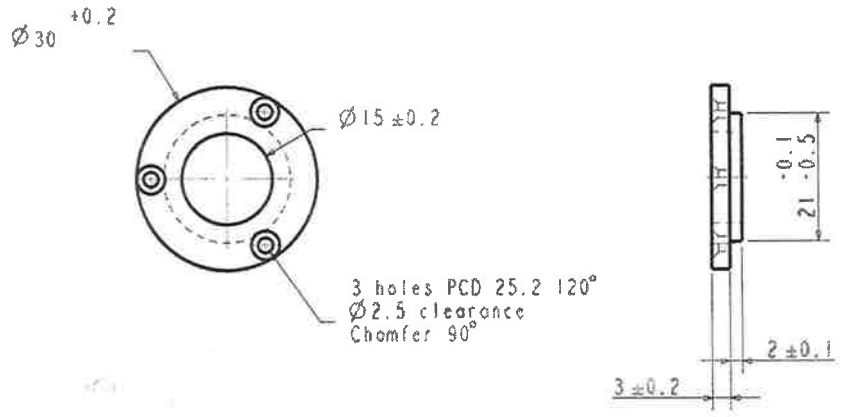

Notes:	Drawing Name: BEARINGCLAMPPLATE	Version:
	File:	Scale: 1.000
	Date: 13-May-05	Material: Aluminium
	Drawn By:	Sheet No: 1 of 1

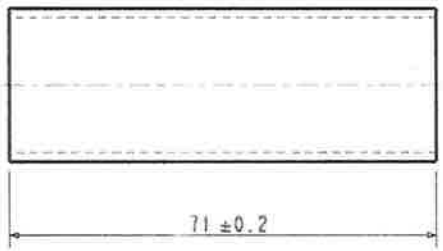

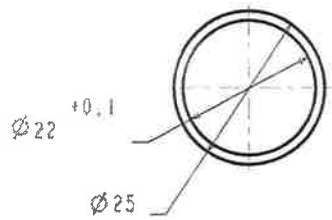

Notes: 1) Tube to accept gearhead. Gearhead dimension: Ø22 -0.1 Nominal ID of tube is 22mm. Machining may be necessary 2)Quantity: 4	Drawing Name: SERVOHOUSING	Version:
	File:	Scale: 1.000
	Date: 12-May-05	Material: Aluminium tube, 25x1.5
	Drawn By:	Sheet No: 1 of 1

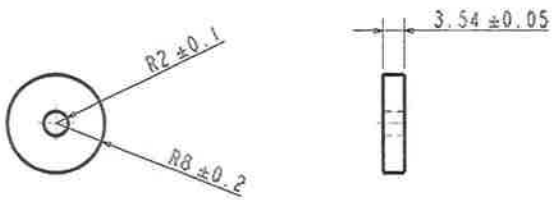

Spacer for 13mm Bearing Assembly. Quantity: 2

Bearing Spacer. Quantity: 4

Rock Spacer . Quantity: 2

Notes:	Drawing Name: SPACERS	Version:
	File:	Scale: 1.000
	Date: 13-May-05	Material: Aluminium
	Drawn By:	Sheet No: 1 of 1

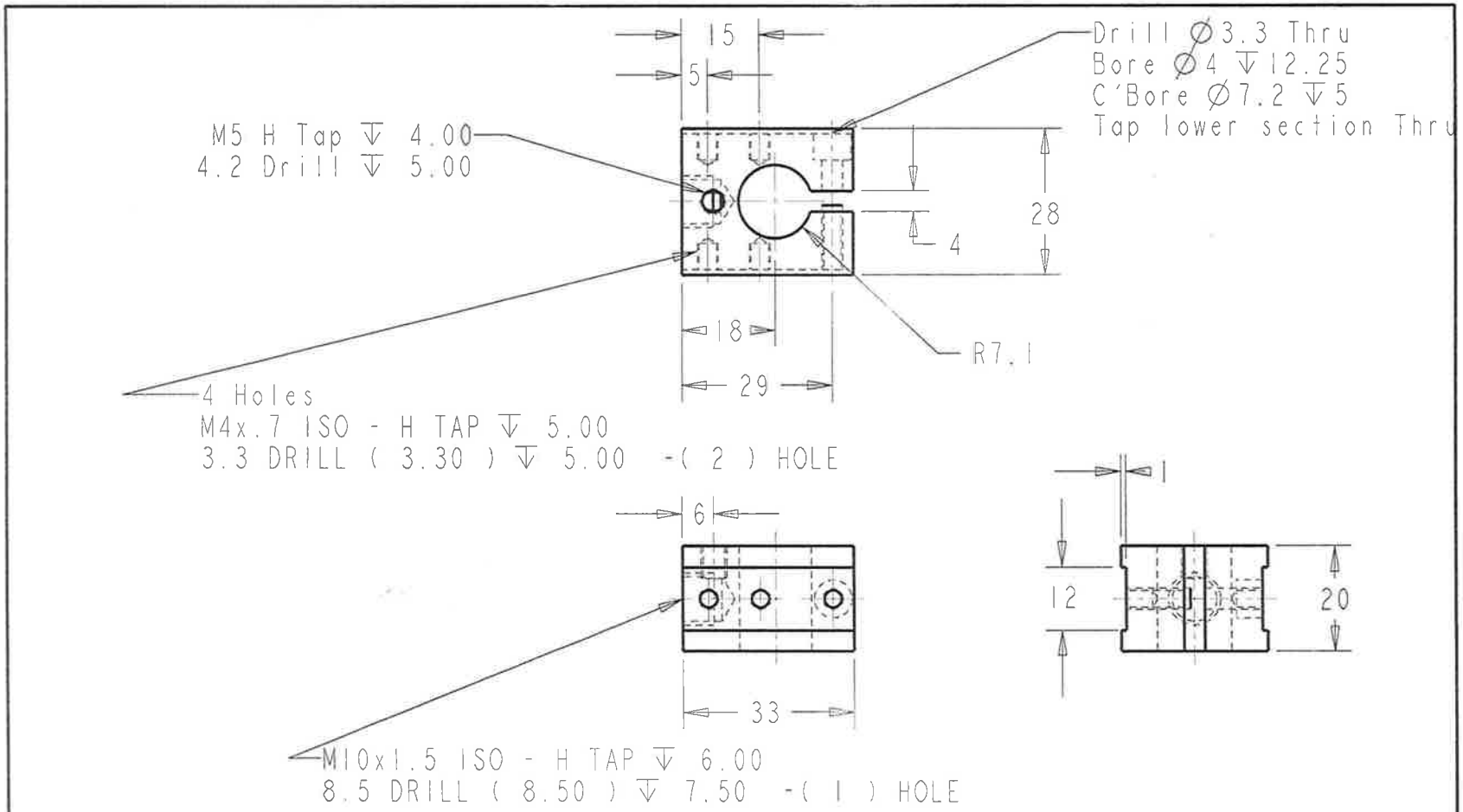

Notes: 1. QTY: 2 OFF	Drawing Name: SHORT_ARM04	Version:
	File:	Scale: 1.000
	Date: 20-Jan-06	Material: Aluminium
	Drawn By:	Sheet No: 1 of 1

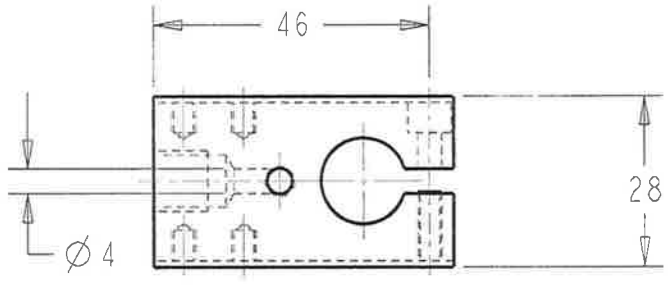

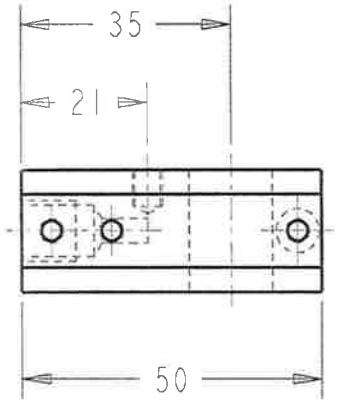

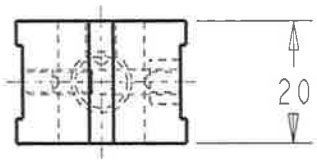

Notes: 1.Refer to drawing SHORT_ARM04 for dimensions not shown 2. QTY: 2 OFF	Drawing Name: LONG_ARM04	Version:
	File:	Scale: 1.000
	Date: 20-Jan-06	Material: Aluminium
	Drawn By:	Sheet No: 1 of 1

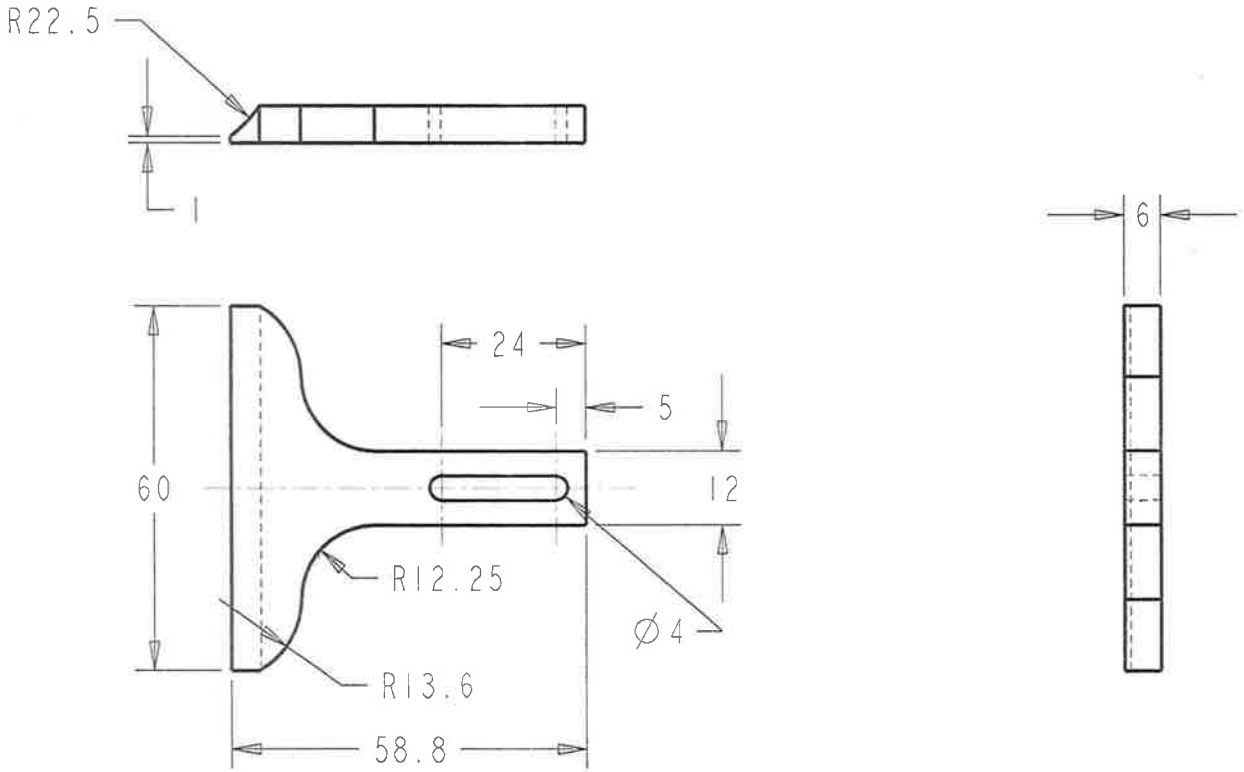

Notes:	Drawing Name: HARDSTOP01	Version:
	File:	Scale: 1.000
	Date: 13-Jan-06	Material:
	Drawn By:	Sheet No: 1 of 1

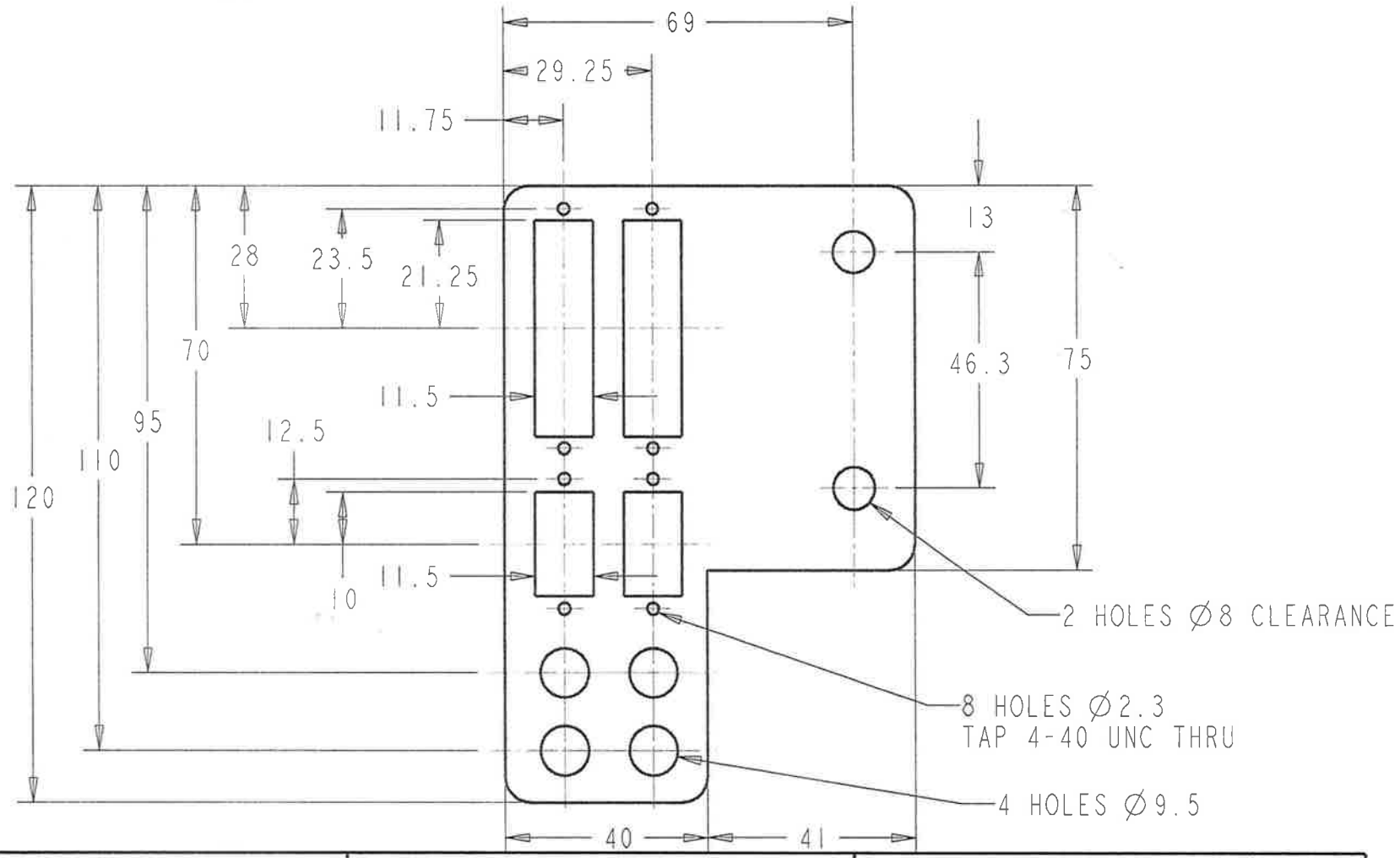

Notes: All rectangular cut-outs and Ø2.3 holes symmetrical about centre-lines	Drawing Name: CONNECTOR_BRACKETS	Version:
	File:	Scale: 1.000
	Date: 15-Sep-05	Material: 1.5mm SS Sheet
	Drawn By:	Sheet No: 3 of 4

Appendix C – Robot arm specifications

C1. SC35F-01 robot arm specifications

(reproduced courtesy of Nachi (UK) Ltd.)

Robot type : [SC35F-01] [SC50F-01]

[Table 1.2-3] Basic Specifications

Item				Specification	
Robot model				SC35F-01	SC50F-01
Construction				Articulated	
Number of axis				6	
Drive system				AC servo system	
Max. operating range	Arm	J1	Swivel	±2.79 rad *1	
		J2	Forward and backward	+2.62 to −1.40 rad	
		J3	Upward and downward	+2.30 to −2.44 rad	
	Wrist	J4	Rotation 2	±4.71 rad	
		J5	Bend	±2.18 rad	
		J6	Rotation 1	±7.85 rad	
Max. speed	Arm	J1	Swivel	2.79 rad/s	
		J2	Forward and backward	2.79 rad/s	
		J3	Upward and downward	2.79 rad/s	
	Wrist	J4	Rotation 2	3.93 rad/s	3.14 rad/s
		J5	Bend	3.93 rad/s	3.14 rad/s
		J6	Rotation 1	5.58 rad/s	4.47 rad/s
Pay load			Wrist	343 N	490 N
			Fore arm	294 N	147 N
Allowable static load torque		J4	Rotation 2	147 N·m	196 N·m
		J5	Bend	147 N·m	196 N·m
		J6	Rotation 1	78 N·m	98 N·m
Allowable moment of inertia *2		J4	Rotation 2	6.43 Kg·m^2	8 Kg·m^2
		J5	Bend	6.43 Kg·m^2	8 Kg·m^2
		J6	Rotation 1	1.83 Kg·m^2	2 Kg·m^2
Position repeatability				±0.1 mm (Applied by JIS B 8432)	±0.3 mm (Applied by JIS B 8432)
Installation parameter	Ambient temperature			0 to 45 °C	
	Ambient humidity			20 to 85 %RH (No dew formation)	
	Vibration value			under 0.5 G	
Robot type				Floor mount, Upside-down mount and Wall mount	
Robot mass				400 kg	

1[rad] = 180/π[°], 1[N·m] = 1/9.8[kgf·m]

*1 SC35F-01±0.61 rad in case of wall mount. SC50F-01±0.52 rad in case of wall mount.

*2 The wrist permission inertia moment depends on the wrist load condition.

C2. SC35F-01 robot arm dimensions and working envelope

(reproduced courtesy of Nachi (UK) Ltd.)

Robot Model : [SC35F-01] [SC50F-01]

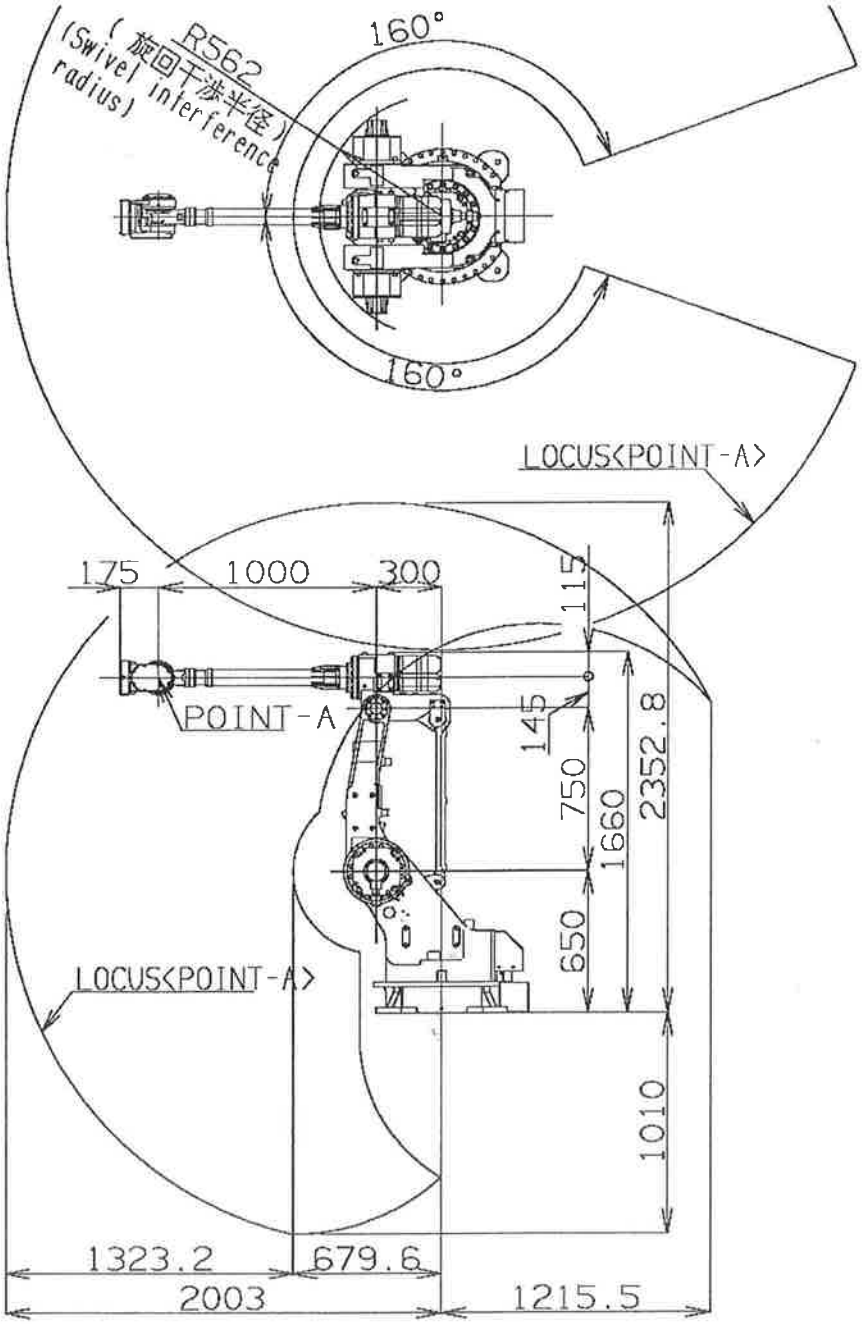

Fig. 1.3-3 Robot dimensions and working envelope

MSCE-144-001

Appendix D - Robot arm installation drawings and specifications

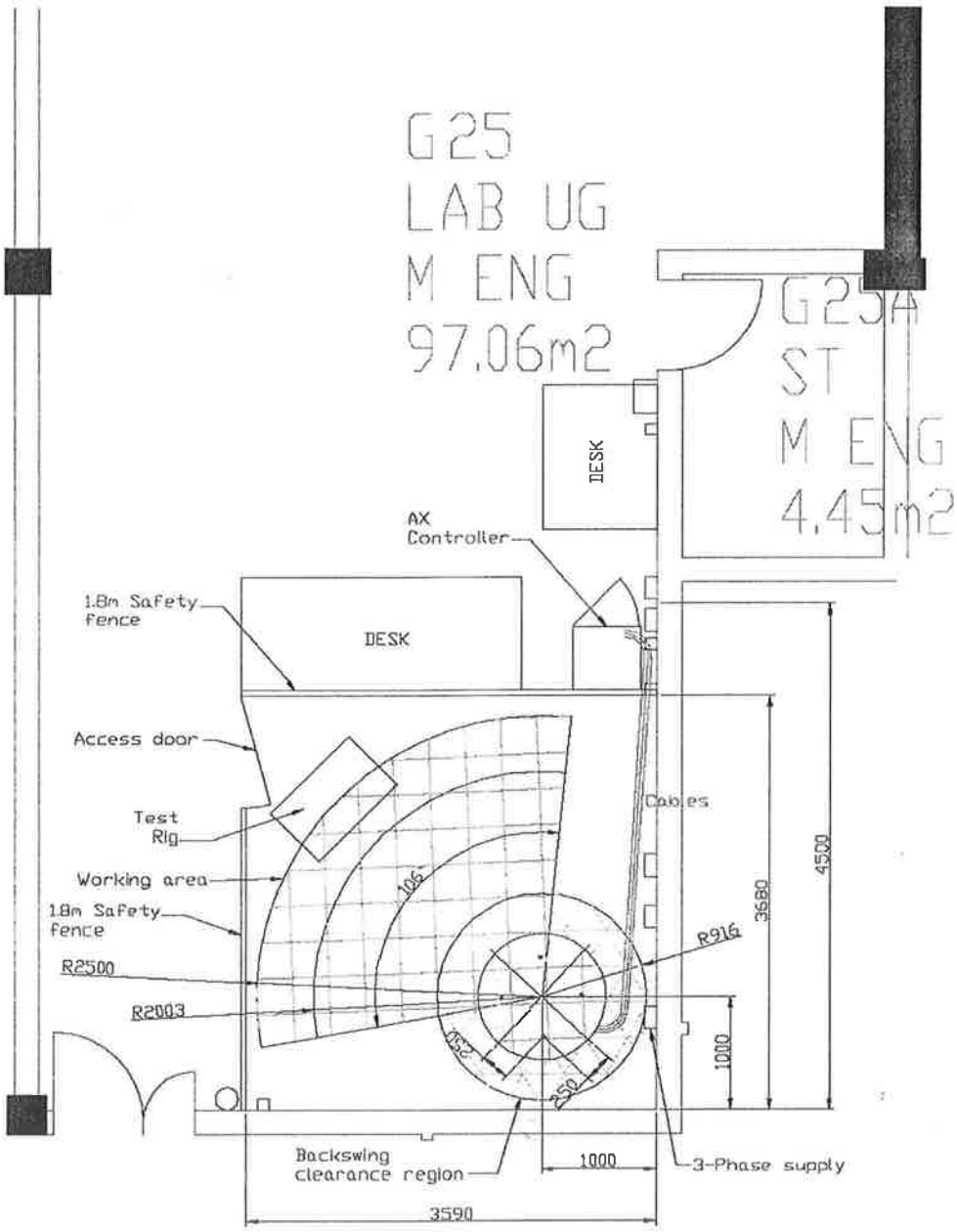

Fig. D1. Robot installation drawing

Requirements for robot installation

Source: *Nachi Robotics AX Controller and SC35 series Installation Manuals*

Electrical Supply

Robot load: max. 30A per phase, 380V

Required:
3ph + PE
32A 5-pin socket
(neutral not required, but robot controller is wired with 5-pin plug)

Control Hardware load: Power supplies, control PC, single phase 230V, <1kW

Required:
At least one double wall socket local to robot installation. Preferably 4 sockets, individually switched.

Air Supply

Current air demand is estimated at 180L/min at 6 bar (with duty cycle of approx 30%) to drive vacuum generators.

Required:
At least 45L/min @ 6 bar (can be supplied from stand-alone compressor)

Installation Area

- Robot work area is a hemisphere of approximately 2.4m radius. Not all of this area is utilised.
- The final work area will be 2.5m wide by 3.4m long, however for testing the width will be approximately 4m.
- Minimum vertical height (floor to ceiling) required is 2m.
- The barriers shown in Fig. D1 are compulsory machine guards and will be installed regardless of the final work area configuration.

Installation Surface

Basic requirements
Robot requires a solid concrete base, at least 150mm thick.

Surface finish
If robot is installed directly on floor, floor finish should be smooth within +/- 0.5mm over the installation area (0.6m x 0.6m). This tolerance is geometric; floor does not need to be level.

Appendix E – Elbow equipment housing layout

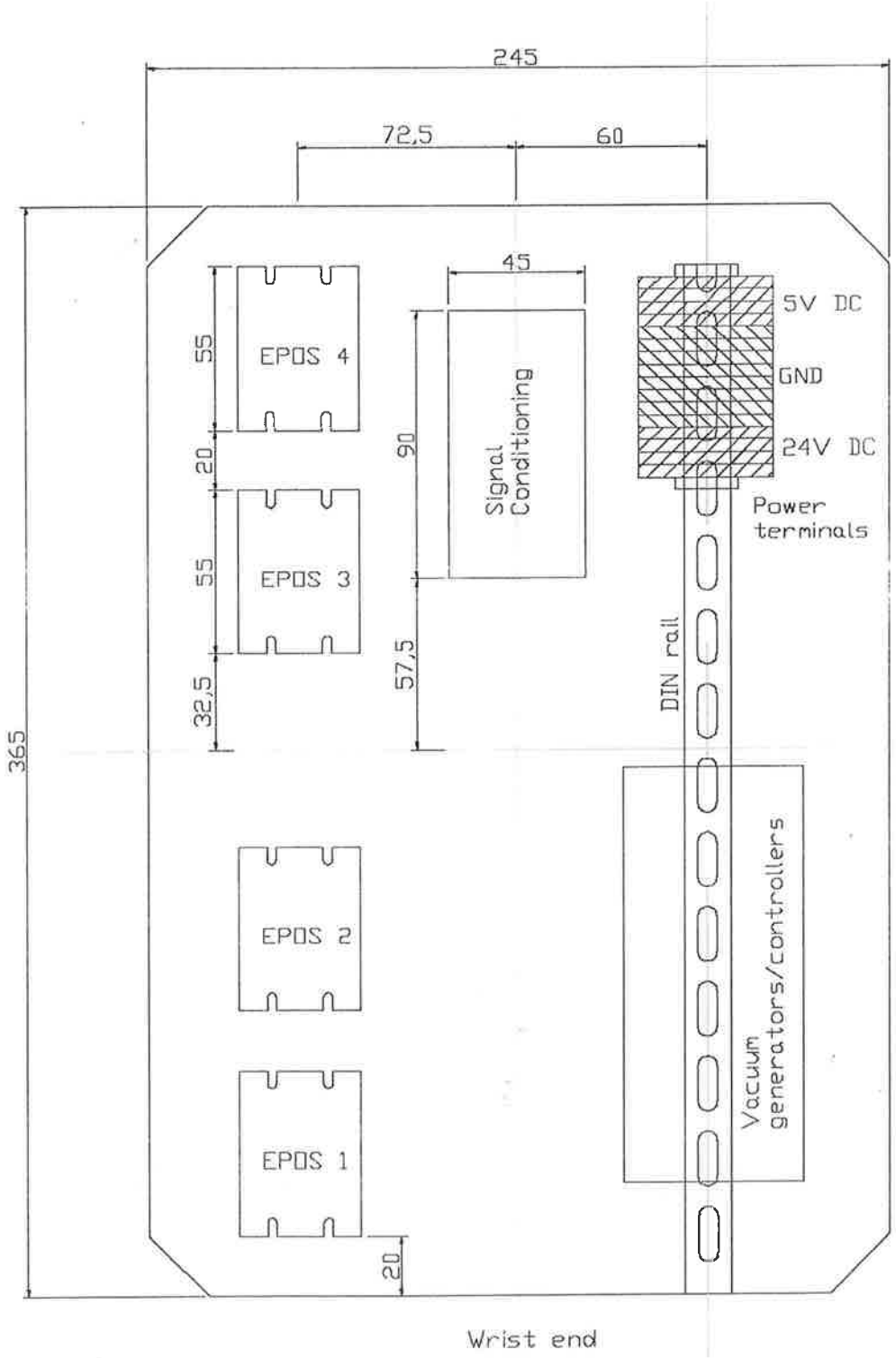

Fig. E1. Elbow equipment housing layout

Appendix F – Hardware I/O definition

Inputs

Group	Sub-Group	Source	Name	Type	I/O Device	I/O Port Name	Notes	Source Pin
End-effector	Servo Drives	EPOS 1	Data	Serial	QSU-100 RS232	Port 1 /COM 3	All Servo Signals,Vacuum Unit 1	See Epos
End-effector	Servo Drives	EPOS 2	Data	Serial	QSU-100 RS232	Port 2/COM 4	All Servo Signals,Vacuum Unit 2	Manual
End-effector	Servo Drives	EPOS 3	Data	Serial	QSU-100 RS232	Port 3/COM 5	All Servo Signals,Vacuum Unit 3	
End-effector	Servo Drives	EPOS 4	Data	Serial	QSU-100 RS232	Port 4/COM 6	All Servo Signals,Vacuum Unit 4	
End-effector	Stepper Drives	MSE570 1	Stepper Overload 1	Open Collector NPN	SCB-68	P1:0		Pin 20a
End-effector	Stepper Drives	MSE570 2	Stepper Overload 2	Open Collector NPN	SCB-68	P1:1		Pin 20a
End-effector	Stepper Drives	MSE570 3	Stepper Overload 3	Open Collector NPN	SCB-68	P1:2		Pin 20a
End-effector	Stepper Drives	MSE570 4	Stepper Overload 4	Open Collector NPN	SCB-68	P1:3		Pin 20a
End-effector	Stepper Encoders	Stepper Encoder 1	Stepper Encoder 1	Differential	UMI-7764	Axis 1		
End-effector	Stepper Encoders	Stepper Encoder 2	Stepper Encoder 2	Differential	UMI-7764	Axis 2		
End-effector	Stepper Encoders	Stepper Encoder 3	Stepper Encoder 3	Differential	UMI-7764	Axis 3		
End-effector	Stepper Encoders	Stepper Encoder 4	Stepper Encoder 4	Differential	UMI-7764	Axis 4		
End-effector	Linear Limits	Home & Limit Switches		Contact closure/TTL	UMI-7764	Axis 1		
End-effector	Linear Limits	Home & Limit Switches		Contact closure/TTL	UMI-7764	Axis 2		
End-effector	Linear Limits	Home & Limit Switches		Contact closure/TTL	UMI-7764	Axis 3		
End-effector	Linear Limits	Home & Limit Switches		Contact closure/TTL	UMI-7764	Axis 4		
AX Controller	Status Reporting	CNOUT 019	Unit Ready	Open Collector Opto	SCB-68	P2:0		Pin 21
AX Controller	Status Reporting	CNOUT 020	Program End	Open Collector Opto	SCB-68	P2:1		Pin 22
AX Controller	Status Reporting	CNOUT 021	Error	Open Collector Opto	SCB-68	P2:2		Pin 23
AX Controller	Status Reporting	CNOUT 023	Alarm	Open Collector Opto	SCB-68	P2:3		Pin 25
AX Controller	Status Reporting	CNOUT 024	Emergency Stopped	Open Collector Opto	SCB-68	P2:4		Pin 26
AX Controller	Status Reporting	CNOUT 026	Robot Running	Open Collector Opto	SCB-68	P2:5		Pin 34
AX Controller	Status Reporting	CNOUT 031	Work Home Position	Open Collector Opto	SCB-68	P2:6		Pin 39
AX Controller	Status Reporting	CNOUT 01	Controller Ready	Open Collector Opto	SCB-68	P2:7		Pin 1
AX Controller	Status Reporting	AX Serial	Data	Serial	COM 1 RS232			
AX Controller	Program Control	CNOUT 02	SREO Sent	Open Collector Opto	SCB-68	P3:0		Pin 2
AX Controller	Program Control	CNOUT 03	General (Position)	Open Collector Opto	SCB-68	P3:1	Output when target position reached	Pin 3
AX Controller	Program Control	CNOUT 04	ACK	Open Collector Opto	SCB-68	P3:2		Pin 4
Spare					SCB-68	P3:3	Spare Input	
Vision System		Vision Server	Data	Ethernet	Switch			

Outputs

Group	Sub-Group	Destination	Name	Type	I/O Device	I/O Port Name	Notes	Destination Pin
End-effector	Servo Drives	EPOS 1	Data	Serial	QSU-100 RS232	Port 1 /COM 3	All Servo Signals,Vacuum Unit 1	See Epos
End-effector	Servo Drives	EPOS 2	Data	Serial	QSU-100 RS232	Port 2/COM 4	All Servo Signals,Vacuum Unit 2	Manual
End-effector	Servo Drives	EPOS 3	Data	Serial	QSU-100 RS232	Port 3/COM 5	All Servo Signals,Vacuum Unit 3	
End-effector	Servo Drives	EPOS 4	Data	Serial	QSU-100 RS232	Port 4/COM 6	All Servo Signals,Vacuum Unit 4	
End-effector	Stepper Drives	MSE570 1	Direction	TTL	UMI-7764	Axis1		
End-effector	Stepper Drives	MSE570 1	Step	TTL	UMI-7764	Axis1		
End-effector	Stepper Drives	MSE570 2	Direction	TTL	UMI-7764	Axis2		
End-effector	Stepper Drives	MSE570 2	Step	TTL	UMI-7764	Axis2		
End-effector	Stepper Drives	MSE570 3	Direction	TTL	UMI-7764	Axis3		
End-effector	Stepper Drives	MSE570 3	Step	TTL	UMI-7764	Axis3		
End-effector	Stepper Drives	MSE570 4	Direction	TTL	UMI-7764	Axis4		
End-effector	Stepper Drives	MSE570 4	Step	TTL	UMI-7764	Axis4		
End-effector	Stepper Drives	MSE570 1	Reset	TTL	SCB-68	P1:4	O1 & O2 Common Reset Signal	16c
End-effector	Stepper Drives	MSE570 2	Reset	TTL			O1 & O2 Common Reset Signal	16c
End-effector	Stepper Drives	MSE570 1	Output Disable	TTL	SCB-68	P1:5	O1 & O2 Common O/P Disable Signa	18a
End-effector	Stepper Drives	MSE570 2	Output Disable	TTL			O1 & O2 Common O/P Disable Signa	18a
End-effector	Stepper Drives	MSE570 3	Reset	TTL	SCB-68	P1:6	O3 & O4 Common Reset Signal	16c
End-effector	Stepper Drives	MSE570 4	Reset	TTL			O3 & O4 Common Reset Signal	16c
End-effector	Stepper Drives	MSE570 3	Output Disable	TTL	SCB-68	P1:7	O3 & O4 Common O/P Disable Signa	18a
End-effector	Stepper Drives	MSE570 4	Output Disable	TTL			O3 & O4 Common O/P Disable Signa	18a
AX Controller	Program Control	CNIN 117	Program Select Bit 1	Opto, 24V	SCB-68	P3:4		Pin 19
AX Controller	Program Control	CNIN 118	Program Select Bit 2	Opto, 24V	SCB-68	P3:5		Pin 20
AX Controller	Program Control	CNIN 119	Program Select Bit 3	Opto, 24V	SCB-68	P3:6		Pin 21
AX Controller	Program Control	CNIN 120	Program Select Bit 4	Opto, 24V	SCB-68	P3:7		Pin 22
AX Controller	Program Control	CNIN 121	Program Select Bit 5	Opto, 24V	SCB-68	P4:0		Pin 23
AX Controller	Program Control	CNIN 125	Program Strobe	Opto, 24V	SCB-68	P4:1		Pin 33
AX Controller	Program Control	CNIN 126	Position Change	Opto, 24V	SCB-68	P4:2	Tell AX to SREO	Pin 34
AX Controller	Program Control	CNIN 130	External Play Start	Opto, 24V	SCB-68	P4:3		Pin 38
AX Controller	Status Control	CNIN 131	External Stop	Opto, 24V	SCB-68	P4:4		Pin 39
AX Controller	Status Control	CNIN 132	Motor Power OFF	Opto, 24V	SCB-68	P4:5		Pin 40
AX Controller	Status Control	TBEX2 E-MON	External Motors ON		SCB-68	P4:6		Pin 8
Spare					SCB-68	P4:7	Spare Output	

Fig. F1. Hardware I/O definition table

Appendix G – Electronics schematics

Contents:

Note: some detail may be lost in these schematics due to image compression and sizing limitations. Reference should be made to the original schematics for maintenance or rework.

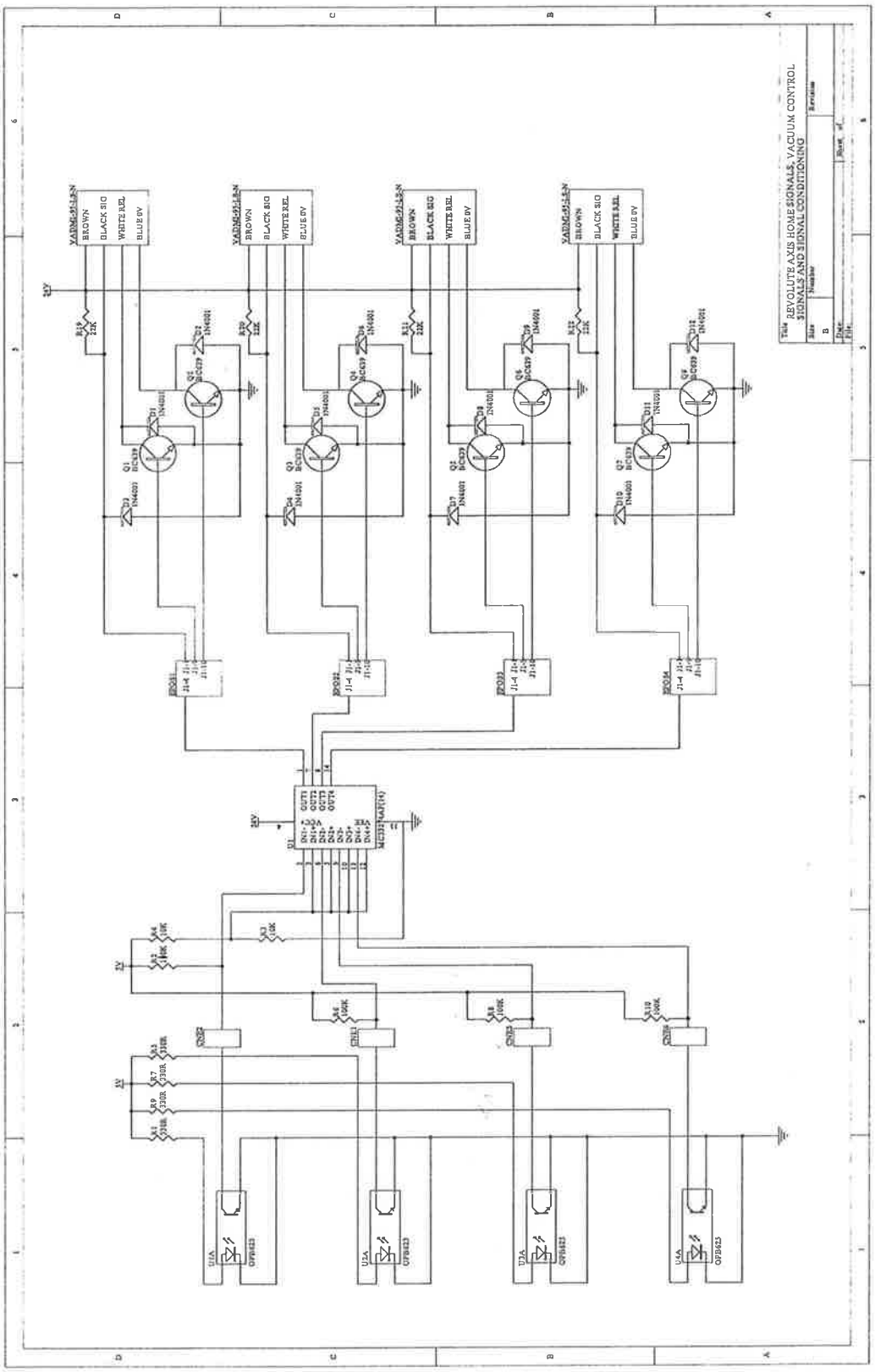
REVOLUTE AXIS HOME SIGNALS, VACUUM CONTROL
SIGNALS AND SIGNAL CONDITIONING

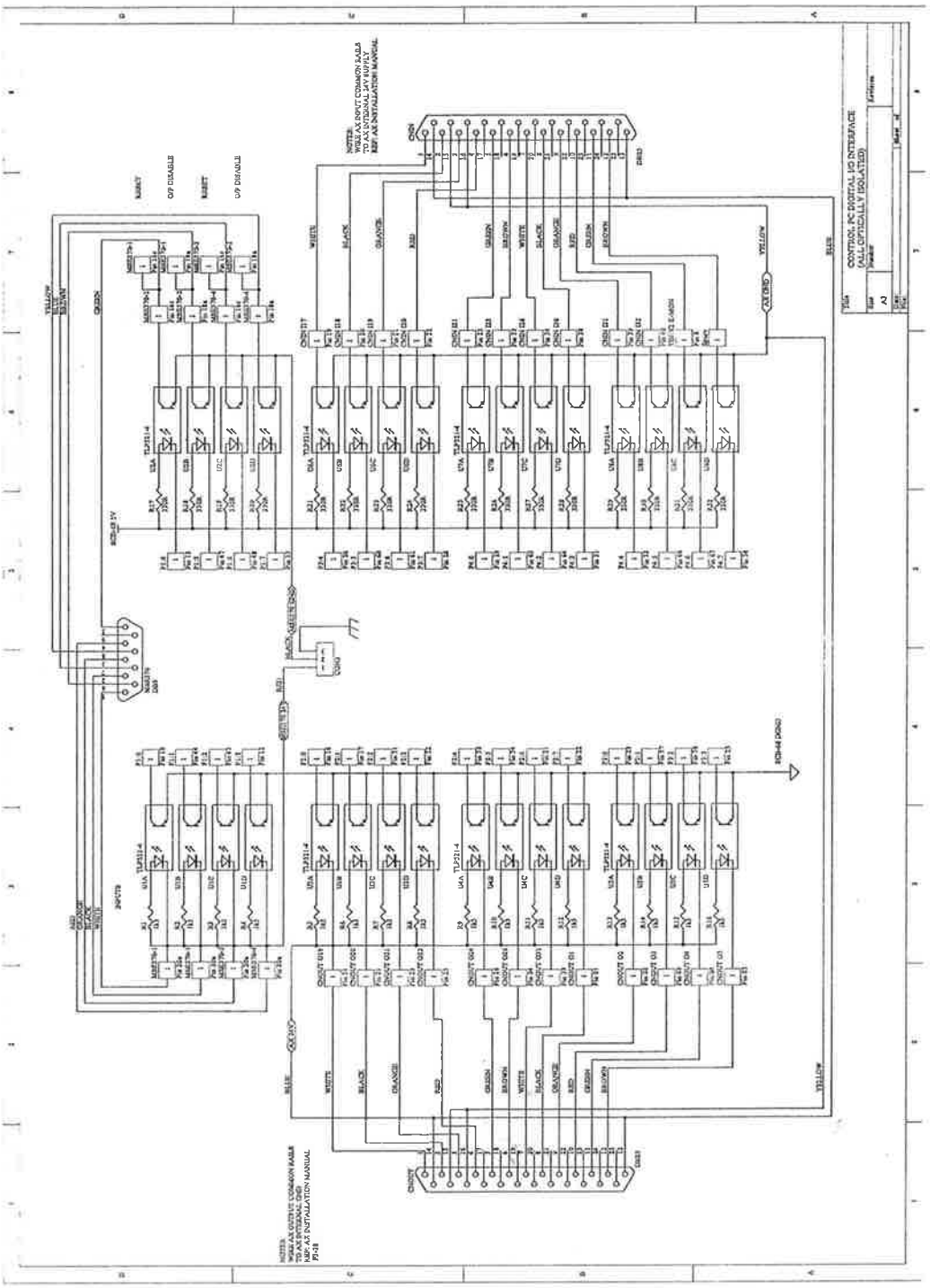

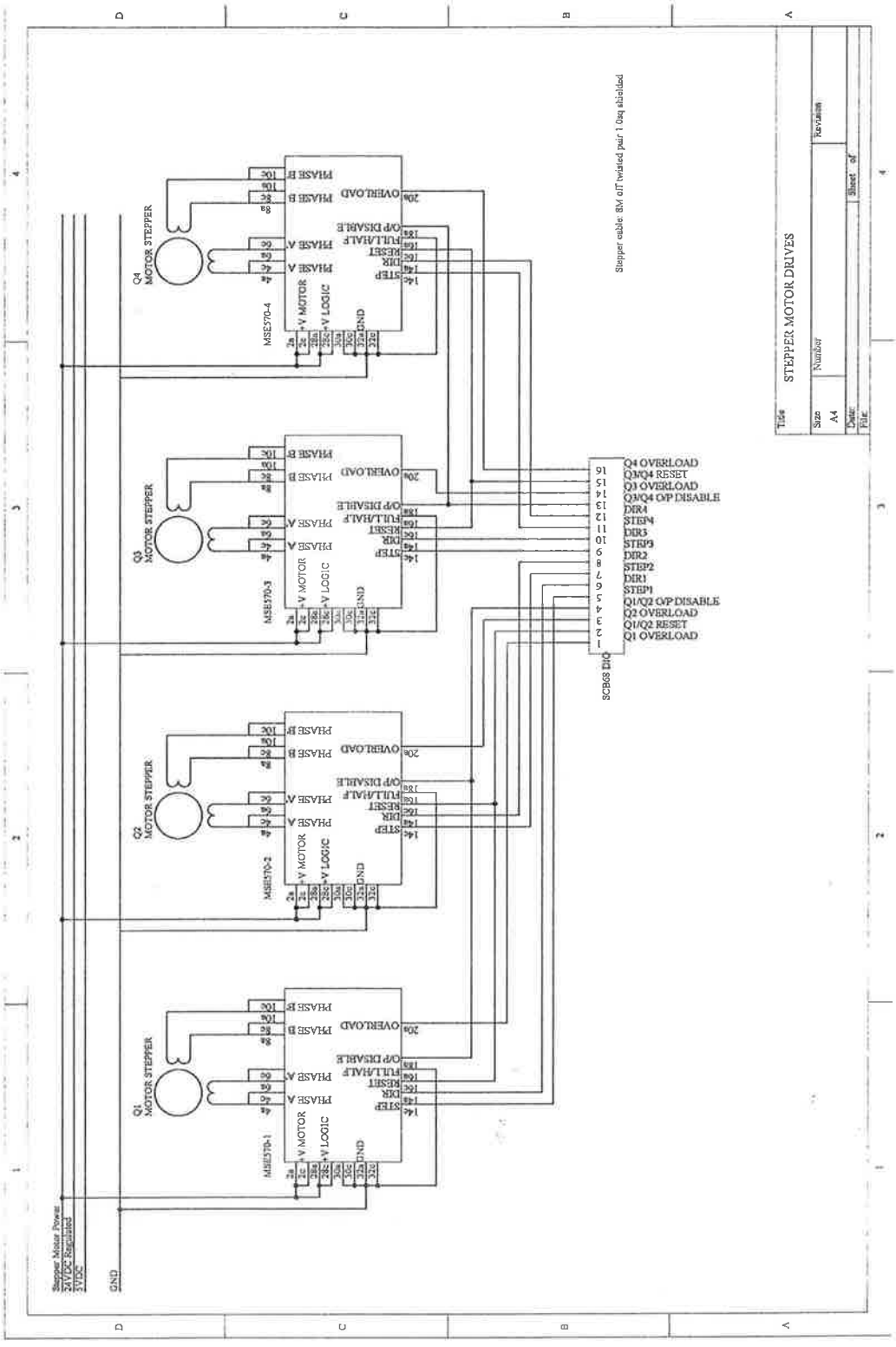
STEPPER MOTOR DRIVES
Title
Size
A4
Number
Revision
Sheet of
Date:
File:
Stepper cable: 8M oiT twisted pair 1 0aq shielded
Q4 MOTOR STEPPER
Q3 MOTOR STEPPER
Q2 MOTOR STEPPER
Q1 MOTOR STEPPER
MSE570-4
MSE570-3
MSE570-2
MSE570-1
+V MOTOR
+V LOGIC
GND
PHASE B
PHASE A
OVERLOAD
O/P DISABLE
FULL/HALF
RESET
DIR
STEP
SCB68 DIO
Q4 OVERLOAD
Q3/Q4 RESET
Q3 OVERLOAD
Q3/Q4 O/P DISABLE
DIR4
STEP4
DIR3
STEP3
DIR2
STEP2
DIR1
STEP1
Q1/Q2 O/P DISABLE
Q2 OVERLOAD
Q1/Q2 RESET
Q1 OVERLOAD
Stepper Motor Power
24VDC Regulated
5VDC
GND

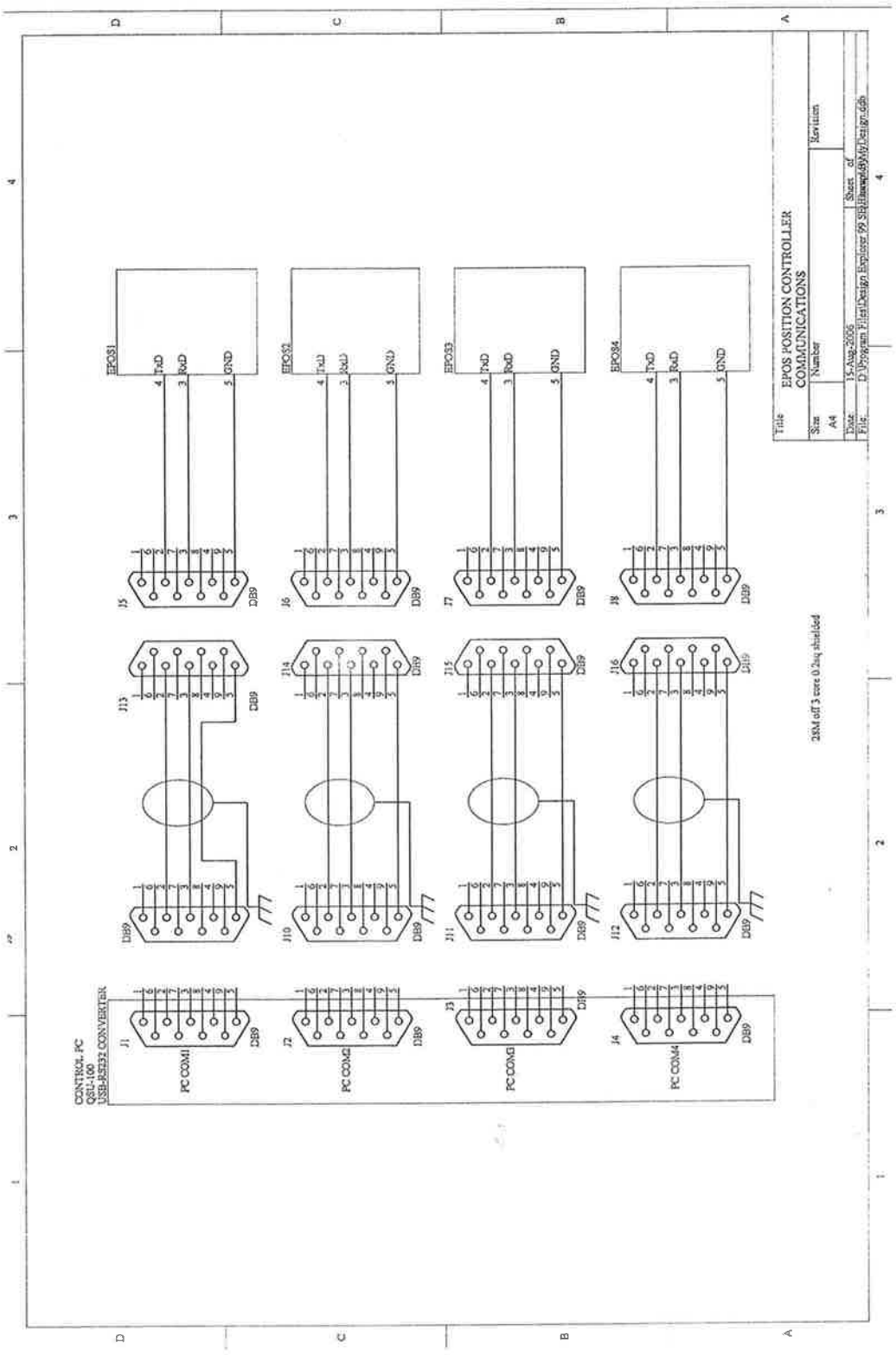
EPOS POSITION CONTROLLER
COMMUNICATIONS
Title
Size
A4
Number
Revision
Date: 15-Aug-2006
File: D:\Program Files\Design Explorer 99 SE\Designs\MyDesign.ddb
Sheet of
EPOS1
EPOS2
EPOS3
EPOS4
TxD
RxD
GND
J5
J6
J7
J8
J13
J14
J15
J16
J10
J11
J12
DB9
CONTROL PC
COM1 TO 4
USB-RS232 CONVERTER
J1
J2
J3
J4
PC COM1
PC COM2
PC COM3
PC COM4
28M off 3 core 0.2sq shielded

Layout and labelling of End-Effector Signals:

View from rear:

Left	Right
Quadrant 1	Quadrant 3
Quadrant 2	Quadrant 4

All components take the quadrant number, i.e. Servo 1 = Quadrant 1 servo motor

End-Effector Connector Layouts:

View from Rear:

Left (Quadrants 1&2)

CNE1	CNE2
CNE3	CNE4
Upper cable entry	Upper cable entry
Lower cable entry	Lower cable entry

Right (Quadrants 3&4)

CNE5	CNE6
CNE7	CNE8
Upper cable entry	Upper cable entry
Lower cable entry	Lower cable entry

Servo Motor 1						
Cable type	4 pair 0.2sq shielded					
No. Cables	2					
	Cable1			Cable 2		
Position	Upper		CNE2	Lower		CNE2
	Colour Code	Function	DB25 Pin		Function	DB25 Pin
Pair 1	Red	Dig +5V	1	Red	Vcc	9
	Black	Dig GND	2	Black	GND	10
Pair 2	White	Motor +	3	White	A	11
	Black	Motor -	4	Black	/A	12
Pair 3	Green	Home (-)	5	Green	B	13
	Black-(Yellow)	Spare	6	Black	/B	25
Pair 4	Blue	Limit (+)	7	Blue	I	24
	Black-(Orange)	Spare	8	Black	/I	23

Servo Motor 2						
Cable type	4 pair 0.2sq shielded					
No. Cables	2					
	Cable1			Cable 2		
Position	Upper		CNE1	Lower		CNE1
	Colour Code	Function	DB25 Pin		Function	DB25 Pin
Pair 1	Red	Dig +5V	1	Red	Vcc	9
	Black	Dig GND	2	Black	GND	10
Pair 2	White	Motor +	3	White	A	11
	Black	Motor -	4	Black	/A	12
Pair 3	Green	Home (-)	5	Green	B	13
	Black-(Yellow)	Spare	6	Black	/B	25
Pair 4	Blue	Limit (+)	7	Blue	I	24
	Black-(Orange)	Spare	8	Black	/I	23

Servo Motor 3						
Cable type	4 pair 0.2sq shielded					
No. Cables	2					
	Cable1			Cable 2		
Position	Upper		CNE5	Lower		CNE5
	Colour Code	Function	DB25 Pin		Function	DB25 Pin
Pair 1	Red	Dig +5V	1	Red	Vcc	9
	Black	Dig GND	2	Black	GND	10
Pair 2	White	Motor +	3	White	A	11
	Black	Motor -	4	Black	/A	12
Pair 3	Green	Home (-)	5	Green	B	13
	Black-(Yellow)	Spare	6	Black	/B	25
Pair 4	Blue	Limit (+)	7	Blue	I	24
	Black-(Orange)	Spare	8	Black	/I	23

Servo Motor 4						
Cable type	4 pair 0.2sq shielded					
No. Cables	2					
	Cable1			Cable 2		
Position	Upper			Lower		
	Colour Code	Function	DB25 Pin		Function	DB25 Pin
Pair 1	Red	Dig +5V	1	Red	Vcc	9
	Black	Dig GND	2	Black	GND	10
Pair 2	White	Motor +	3	White	A	11
	Black	Motor -	4	Black	/A	12
Pair 3	Green	Home (-)	5	Green	B	13
	Black-(Yellow)	Spare	6	Black	/B	25
Pair 4	Blue	Limit (+)	7	Blue	I	24
	Black-(Orange)	Spare	8	Black	/I	23

Stepper Motor 1			
Cable type	2 pair 0.65sq shielded		
No. Cables	1		
	Cable1		
Position	Upper		CNE4
	Colour Code	Function	DB9 Pin
Pair 1	White	A	1
	Yellow	/A	2
Pair 2	Red	B	3
	Blue	/B	4

Stepper Motor 2			
Cable type	2 pair 0.65sq shielded		
No. Cables	1		
	Cable1		
Position	Lower		CNE4
		Function	DB9 Pin
Pair 1	White	A	6
	Yellow	/A	7
Pair 2	Red	B	8
	Blue	/B	9

Stepper Motor 3			
Cable type	2 pair 0.65sq shielded		
No. Cables	1		
	Cable1		
Position	Upper		CNE7
	Colour Code	Function	DB9 Pin
Pair 1	White	A	1
	Yellow	/A	2
Pair 2	Red	B	3
	Blue	/B	4

Stepper Motor 4			
Cable type	2 pair 0.65sq shielded		
No. Cables	1		
	Cable1		
Position	Upper		CNE7
	Colour Code	Function	DB9 Pin
Pair 1	White	A	6
	Yellow	/A	7
Pair 2	Red	B	8
	Blue	/B	9

Linear Encoder 1			
Cable type	4 pair 0.2sq shielded		
No. Cables	1		
	Cable1		
Position			CNE2
	Colour Code	Function	DB25 Pin
Pair 1	Red	2 Vcc	22
	Black	3 GND	21
Pair 2	White	5 /A	20
	Black	6 A	19
Pair 3	Green	7 /B	18
	Black	8 B	17
Pair 4	Blue	NC	
	Black	NC	

Linear Encoder 2			
Cable type	4 pair 0.2sq shielded		
No. Cables	1		
	Cable1		
Position			CNE1
	Colour Code	Function	DB25 Pin
Pair 1	Grey	2 Vcc	22
	Grey	3 GND	21
Pair 2	Grey	5 /A	20
	Grey	6 A	19
Pair 3	Grey	7 /B	18
	Grey	8 B	17
Pair 4	Grey	NC	
	Grey	NC	

Linear Encoder 3			
Cable type	4 pair 0.2sq shielded		
No. Cables	1		
	Cable1		
Position			CNE5
	Colour Code	Function	DB25 Pin
Pair 1	Grey	2 Vcc	22
	Grey	3 GND	21
Pair 2	Grey	5 /A	20
	Grey	6 A	19
Pair 3	Grey	7 /B	18
	Grey	8 B	17
Pair 4	Grey	NC	
	Grey	NC	

Linear Encoder 4			
Cable type	4 pair 0.2sq shielded		
No. Cables	1		
	Cable1		
Position			CNE6
	Colour Code	Function	DB25 Pin
Pair 1	Grey	2 Vcc	22
	Grey	3 GND	21
Pair 2	Grey	5 /A	20
	Grey	6 A	19
Pair 3	Grey	7 /B	18
	Grey	8 B	17
Pair 4	Grey	NC	
	Grey	NC	

Linear Limits Q1, Q3						
Cable type	8 core 0.2sq shielded					
No. Cables	1					
	Cable1					
Position			CNE3		End-effector Colours	
	Colour Code	Function	Pin No.		Cable 1	Cable 2
Pair 1	White	Q1 Home	1			
	Black	Q1 +Limit	2			
Pair 2	Orange	Q1 -Limit	3			
	Red	Q3 -Limit	4			
Pair 3	Green	Q3 +Limit	5			
	Brown	Q3 Home	6			
Pair 4	Blue		7			
	Yellow		8			

Linear Limits Q2, Q4						
Cable type	8 core 0.2sq shielded					
No. Cables	1					
	Cable1					
Position			CNE8		End-effector Colours	
	Colour Code	Function	Pin No.		Cable 1	Cable 2
Pair 1	White	Q2 Home	1			
	Black	Q2 +Limit	2			
Pair 2	Red	Q2 -Limit	3			
	Black	Q4 -Limit	4			
Pair 3	Green	Q4 +Limit	5			
	Black	Q4 Home	6			
Pair 4	Blue		7			
	Black		8			

Stepper Drive 1-4				
Cable type	4 pair 0.2sq shielded			
No. Cables	1			
	Cable1			
Position				
	Colour Code	Function	Drive Pin No.	Control Pin No.
Pair 1	Red	STEP	14c	
	Black	NC		
Pair 2	White	DIR	14a	
	Black	GND		
Pair 3	Green	O/P DISABLE	18a	
	Black	GND		
Pair 4	Blue	RESET	16c	
	Black	GND		